LIÈGE université
Gembloux
Agro-Bio Tech

Deciphering the biology and chemistry of the mutualistic partnership between *Bacillus velezensis* and the mycorrhizal fungus *Rhizophagus irregularis*

Adrien Anckaert

COMMUNAUTÉ FRANÇAISE DE BELGIQUE
UNIVERSITÉ DE LIÈGE – GEMBLOUX AGRO-BIO TECH

Deciphering the biology and chemistry of the mutualistic partnership between *Bacillus velezensis* and the mycorrhizal fungus *Rhizophagus irregularis*

Adrien ANCKAERT

Dissertation originale présentée en vue de l'obtention du grade de doctorat en sciences agronomiques et ingénierie biologique

This thesis was supported by a FRS-FNRS Research Fellow (FRIA) grant.

Promoteur(s) : Dr. Marc Ongena
Année civile: 2025

Abstract

Plant protection has long relied on chemical pesticides, which has not only driven the evolution of resistant phytopathogens but also raised concerns about environmental and human health impacts. As an alternative, the use of beneficial microorganisms has emerged, mirroring the role of probiotics in human health. Plants, especially at the root level, host diverse microbial communities in the rhizosphere. Among them, the bacterium *Bacillus velezensis* and arbuscular mycorrhizal (AM) fungi, like *Rhizophagus irregularis* are two key plant-associated beneficial microbes. *B. velezensis* is particularly known for producing antibiotics active against bacteria, fungi, and even viruses, and for triggering induced systemic resistance in plants. In parallel, AM fungi contribute to plant protection, although their primary recognized benefit lies in enhancing plant nutrition. Nevertheless, the practical use of these microorganisms remains limited due to inconsistent efficacy across plant species and growing conditions, largely stemming from limited knowledge about the factors that govern their successful establishment on plant roots. Recent research has shown that combining different beneficial microbes can improve plant health and growth. However, the microbial ecology of the rhizosphere and the molecular mechanisms underlying these beneficial interactions remain poorly understood.

In this work, we found that *B. velezensis* and *R. irregularis* can coexist despite the bacterium production of antifungal compounds. This compatibility is enabled by chemical crosstalk between the two organisms, allowing mutualistic interaction. The bacterium recognizes fungal signals/cues and adapts its metabolism by modulating the production of antifungal metabolites. Notably, *B. velezensis* retains antimicrobial activity against potential fungal competitors, indirectly protecting its fungal partner and thus could contributed to the stability of the fungal population in the environment. The fungus, in turn, supports bacterial growth by providing nutrients and serves as a "highway," facilitating bacterial dispersal toward new plant hosts. Finally, we show that the association of *B. velezensis* and *R. irregularis* leads to stronger plant protection through enhanced activation of immune responses compared to either microorganism applied alone. Together, these findings highlight the potential of designing microbial consortia based on mechanistic understanding of their interactions to develop more effective and sustainable plant protection strategies.

Résumé

La protection des cultures repose depuis longtemps sur l'utilisation de pesticides chimiques. Cette stratégie a non seulement favorisé l'apparition d'agents phytopathogènes résistants, mais soulève également de sérieuses préoccupations pour la santé humaine et l'environnement. En alternative, l'utilisation de micro-organismes bénéfiques a émergé, à l'image du rôle des probiotiques en santé humaine. Les plantes, et en particulier leurs racines, abritent une grande diversité microbienne formant la rhizosphère. Parmi ces micro-organismes, la bactérie *Bacillus velezensis* et les champignons mycorhiziens à arbuscules (CMAs) tels que *Rhizophagus irregularis* occupent une place centrale. *B. velezensis* est notamment reconnue pour sa capacité à produire des antibiotiques actifs contre bactéries, champignons et virus, ainsi que pour sa faculté à induire une résistance systémique chez la plante. Parallèlement, les CMAs contribuent également à la protection des plantes, bien que leur principal atout reste historiquement lié à l'amélioration de la nutrition végétale. Cependant, leur utilisation par les agriculteurs demeure limitée en raison d'une efficacité variable, principalement due à une connaissance encore incomplète des facteurs qui conditionnent leur bonne implantation sur les racines. Des travaux récents ont montré que l'association de différents micro-organismes bénéfiques pouvait renforcer la croissance et la santé des plantes. Néanmoins, l'écologie microbienne de la rhizosphère et les mécanismes moléculaires sous-jacents à ces interactions restent encore largement méconnus.

Notre étude montre que *B. velezensis* et *R. irregularis* peuvent coexister malgré la production, par la bactérie, de composés antifongiques. Cette compatibilité repose sur un dialogue chimique entre les deux partenaires, permettant l'établissement d'une relation mutuellement bénéfique. La bactérie perçoit des signaux émis par le champignon et ajuste son métabolisme en modulant la production de ses métabolites antifongiques. De façon intéressante, *B. velezensis* conserve une activité antimicrobienne vis-à-vis de compétiteurs potentiels des CMAs, protégeant ainsi indirectement son partenaire fongique et contribuant potentiellement à la stabilité de la population fongique dans l'environnement. En retour, le champignon favorise la croissance bactérienne en fournissant des nutriments et en servant « d'autoroute », facilitant la dispersion bactérienne vers de nouveaux hôtes végétaux. Enfin, nous avons démontré que l'association de *B. velezensis* et *R. irregularis* confère aux plantes une protection renforcée grâce à une activation accrue des réponses immunitaires, comparée à l'application individuelle de chaque micro-organisme. Ces résultats soulignent le potentiel de concevoir des consortiums microbiens, fondés sur la compréhension de leurs interactions, afin de développer des stratégies de protection des plantes plus durables et plus efficaces.

Table of contents

List of figures

List of tables

List of videos

List of acronyms

AM	Arbuscular Mycorrhizal
AMF-EMM	AM fungus exudate mimicking medium
ANOVA	Analysis of variance
BAS	Branching-absorbing structure
BCA	Biocontrol agent
BGC	Biosynthetic gene cluster
BSM	Bioactive Secondary Metabolite
B.v.	*Bacillus velezensis*
CDPK	Calcium-dependent protein kinases
CFS	Cell-free supernatant
CFU	Colony forming unit
cLP	Cyclic lipopeptide
CMN	Common mycorrhizal network
CO	Chitooligosaccharide
CSSP	Common symbiosis signalling pathway
DAMP	Damage-associated molecular pattern
DNA	Deoxyribonucleic acid
DP	Degre of polymerization
dpi	Days post inoculation
EIC	Extracted ion chromatogram
EP	Exopolysaccharide
ERM	Extraradical mycelium
ETI	Effector-triggered immunity

EV	Extracellular vesicles	MHB	Mycorrhiza helper bacteria
GFP	Green fluorescent protein	MIR	Mycorrhizal-induced resistance
GIPC	Glucosyl inositol phosphoryl ceramide	MSI	Mass spectrometry imaging
GlcNAc	N-acetylglucosamine	MSR	Modified Strullu-Romand
GluCer	Glucosylceramide	NRPS	Non ribosomal peptide synthetase
HC	Hyphal compartment	OD	Optical density
HG	Homogalacturonan	OG	Oligogalacturonide
ISR	Induced Systemic Resistance	PAM	Periarbuscular membrane
LC-MS	Liquid chromatography coupled with mass spectrometry	PAMPs	Pathogen-associated molecular patterns
LCO	Lipochitooligosaccharide	PAS	Periarbuscular space
LysM-RLKs	Lysine motif receptor-like kinases	PGPR	Plant Growth-Promoting Bacteria
MAMP	Microbial-associated molecular pattern	PI	Propidium iodide
MAPK	Mitogen-activated protein kinase	PKS	Polyketide synthase

PM	Plasma membrane	RQ	Research Question
PRR	Pattern recognition receptor	RT-qPCR	Reverse transcription-quantitative polymerase chain reaction
PSB	Phosphate solubilizing bacteria	SAR	Systemic acquired resistance
PTI	Pattern-triggered immunity	SDH	Succinate dehydrogenase
qTOF	Quadrupole-time of flight	sRNA	small RNA
RC	Root Compartment	SYM pathways	Symbiosis signalling pathway
RE	Root mimicking exudates of Solanaceae	UPLC-MS	Ultrahigh performance liquid chromatography coupled with mass spectrometry
R.i.	*Rhizophagus irregularis*	VOC	Volatile organic compound
RLK	Receptor-like kinase	WAK	Wall associated kinase
RLP	Receptor-like protein		
RNA	Ribonucleic acid		
RNA-seq	RNA sequencing		
ROS	Reactive oxygen species		

Glossary

Air–liquid interface:
The interface between air and liquid where biofilms can form under static conditions.

AMF Exudate-Mimicking Medium (AMF-EMM):
A minimal medium containing only trace elements and the carbon sources typically detected in AM fungal exudates.

AM Fungal Exudates:
The totality of molecules actively or passively released by AM fungal hyphae into the soil.

Arbuscular Mycorrhizal Fungi (AM Fungi):
Ubiquitous soil fungi belonging to the phylum Glomeromycotina that form a mutualistic endosymbiotic association with the roots of approximately 80% of vascular plant species. They facilitate nutrient uptake (notably phosphorus) in exchange for plant-derived carbon.

Anastomosis:
The fusion or connection between fungal hyphae, allowing cytoplasmic continuity within or between hyphal networks. It enables nutrient redistribution, signalling, and network repair.

Arbuscules:
Finely branched, tree-like structures formed within plant root cortical cells by AM fungi. They are the primary sites of bidirectional nutrient exchange between the fungus and the host plant.

Branched Absorbing Structures (BAS):
Highly branched hyphal structures formed by AM fungi in the extraradical mycelium, specialized in nutrient uptake.

Bioactive Secondary Metabolites (BSMs):
Compounds produced by plants, fungi, or microbes that are not essential for growth or reproduction but play crucial roles in defence, communication, and ecological adaptation.

Biofilm:

A structurally and dynamically complex multicellular consortium in which microbial cells are embedded in a self-produced extracellular matrix. This matrix provides mechanical stability, protection, and cohesion to the community.

Biocontrol:
The use of living organisms or their natural products to suppress plant diseases, pests, or weeds through antagonism, competition, or induction of host resistance.

Chitin:
A conserved structural polysaccharide composed of β-1,4-linked *N*-acetyl-D-glucosamine (GlcNAc) residues. It constitutes the primary component of fungal cell walls and contributes to their mechanical strength and rigidity.

Chitosan:
A partially deacetylated derivative of chitin present in fungal cell walls. This chemical modification reduces the polymer susceptibility to chitinase degradation and helps fungi evade plant immune recognition.

Common Mycorrhizal Network (CMN):
An interconnected network of AM fungal hyphae linking multiple plant roots, allowing the transfer of nutrients, water, and signalling molecules between plants.

Cryptic metabolite:
A specialized metabolite whose biosynthesis is "silent" or weakly expressed under standard laboratory conditions.

Cyclic lipopeptides (cLPs):
Natural amphiphilic compounds composed of a cyclic peptide linked to a fatty acid chain. They exhibit important biological activities, including antibacterial, antifungal, and plant-immunity eliciting properties. Many bacteria, particularly those from the genera *Bacillus*, *Pseudomonas*, and *Streptomyces*, produce cLPs as part of their secondary metabolism.

Cytoplasmic Flow:
The bulk movement of cytoplasm within fungal hyphae, driven by cytoplasmic streaming and/or turgor pressure gradients. This flow enables long-distance transport of nutrients, organelles, and signalling molecules, essential for fungal growth and symbiotic functioning.

Electron tomography:
A 3D imaging technique that reconstructs a image volume by combining multiple 2D images taken from different angles with an electron microscope. It allows

visualization of organelles, cells, and tissues at nanometer resolution, providing detailed insights into cellular architecture.

Endocytosis:
The process by which a cell internalizes external substances by forming vesicles derived from its plasma membrane.

Effector-Triggered Immunity (ETI):
A robust and specific plant immune response activated by the recognition of pathogen effectors.

Extracellular Vesicles (EV):
Nano-sized, membrane-bound vesicles secreted by bacteria, fungi, or plants that transport proteins, lipids, and nucleic acids involved in intercellular communication, defence, and signalling.

Extraradical Mycelium (ERM):
A dense and far-reaching hyphal network that extends network of AM fungal hyphae extending from the root into the surrounding soil. It explores the soil matrix, absorbs nutrients (particularly phosphorus and nitrogen), and interacts with other soil microorganisms.

Hairy root:
A transformed root culture generated by infection of wounded plant tissues with *Agrobacterium rhizogenes*. This bacterium transfers a portion of its Ri (root-inducing) plasmid into the plant genome, causing the so-called "hairy root disease." The resulting roots are characterized by rapid, hormone-independent growth and high genetic and biochemical stability. Hairy root cultures are widely used as model systems for studying root–microbe interactions and for the production of secondary metabolites.

Homogalacturonan (HG):
The most abundant polysaccharide of the pectin in plant cell walls, composed of galacturonic acid residues that are partially esterified.

Hyphosphere:
The narrow soil zone influenced by AM fungal hyphae. It is enriched in fungal exudates and microbial activity.

Hyphosphere Microbiome:

The microbial community living in close association with the surface of AM fungal hyphae and within the hyphosphere. Its composition is shaped by fungal exudates and environmental conditions.

Induced Systemic Resistance (ISR):
A plant defence mechanism systemically activated (in all organs) by beneficial microbes or their metabolites. ISR primes the plant immune system, enhancing resistance against a broad spectrum of pathogens and pests.

Knock-Out Mutant:
A genetically engineered organism in which a specific gene has been deleted or inactivated (often via homologous recombination) to study its function by loss-of-function analysis.

LipoChitooligosaccharides (LCOs):
Signalling molecules secreted by rhizobia and AM fungi that trigger symbiotic responses in plants, such as activation of symbiosis-related genes and initiation of nodule or arbuscule formation.

Mass spectrometry imaging (MSI):
An analytical technique combining the high specificity of mass spectrometry with spatial information to create molecular maps of a sample, such as a biological tissue.

Microbiome:
The community of microorganisms (bacteria, fungi, archaea, protists, and viruses) living together and inhabiting a specific environment.

Minimum inhibitory concentration:
The lowest concentration of an antimicrobial agent that prevents visible growth of a microorganism *in vitro*. A lower MIC value indicates higher antimicrobial efficacy.

Mycelium:
The collective network of hyphae formed by fungi.

Myc-factor:
Signalling molecules, mainly lipochitooligosaccharides (LCOs) and chitooligosaccharides (COs), released by AM fungi and involved in early communicate with plant roots before colonization. Plants perceive these signals through specific receptors, triggering developmental and physiological responses such as lateral root formation.

Mycorrhiza Helper Bacteria (MHB):

Bacteria that enhance the establishment, functioning, or efficiency of mycorrhizal symbioses. They can stimulate spore germination, hyphal growth, or root colonization.

Mycorrhizal-induced resistance (MIR):
A systemic plant defence response activated by AM fungi, providing protection against a wide range of pathogens. MIR shares similarities with ISR triggered by beneficial rhizobacteria.

Non-Ribosomal Peptides (NRPs):
Bioactive molecules synthesized by microorganisms (e.g., *Bacillus*, *Pseudomonas*) through large enzyme complexes called non-ribosomal peptide synthetases (NRPS). They often possess antimicrobial, surfactant, or signalling activities.

Oligogalacturonides (OGs):
Oligomers of α-1,4-linked galacturonosyl residues released from partial degradation of homogalacturonan in plant cell walls. OGs act as elicitors of plant defence responses, including ROS accumulation and expression of pathogenesis-related proteins.

Polyketides (PKs):
A diverse group of secondary metabolites synthesized by polyketide synthases (PKS) in bacteria and fungi. Many PKs have antibiotic, antifungal, or signalling properties.

Pattern-Triggered Immunity (PTI) or Microbe-Associated Molecular Pattern Triggered Immunity (MTI):
The first layer of plant innate immunity triggered by the recognition of conserved microbial patterns (MAMPs/PAMPs) through pattern recognition receptors (PRRs) at the plant cell surface. PTI results in basal defence responses.

Quorum sensing:
A bacterial communication mechanism that coordinates gene expression in response to population density.

Rhizobacteria:
Root-associated bacteria that colonize the rhizosphere or root surface.

Rhizobiome:
The complex microbial community associated with the plant root surface and the rhizosphere. It consists of bacteria, fungi, and other microorganisms adapted to root exudates and plant-derived signals.

Rhizosphere:
The thin layer of soil surrounding plant roots, typically a few millimetres thick, directly influenced by root exudates. This area represents a hotspot for microbial activity with high abundance but lower species diversity than bulk soil.

Root Exudates:
The mixture of organic and inorganic molecules released by plant roots into the surrounding soil. These compounds shape the rhizosphere microbiome and influence nutrient cycling and plant–microbe interactions.

Strigolactone:
Plant hormones that regulate shoot branching and mediate interactions with soil microbes, including AM fungi.

Succinate dehydrogenase (SDH):
An enzyme complex of the mitochondrial respiratory chain often quantified to assess AM fungal viability.

4′-phosphopantetheinyl transferase enzyme (Sfp):
An enzyme essential for the activation of NRPS and PKS enzymes, enabling the biosynthesis of cyclic lipopeptides and polyketides in *Bacillus* spp.

Published content and contributions

First authorship

- **Book chapter: Anckaert, A**., Arias, A. A., Hoff, G., Calonne-Salmon, M., Declerck, S., & Ongena, M. (2021). The use of *Bacillus* spp. as bacterial biocontrol agents to control plant diseases. In R. W. Köhl J (Ed.), *Microbial bioprotectants for plant disease management* (pp. 247–300). Burleigh Dodds Science Publishing.
  https://doi.org/10.19103/AS.2021.0093.10

- **Article: Anckaert, A**., Declerck, S., Poussart, L.-A., Lambert, S., Helmus, C., Boubsi, F., Steels, S., Argüelles-Arias, A., Calonne-Salmon, M., & Ongena, M. (2024). The biology and chemistry of a mutualism between a soil bacterium and a mycorrhizal fungus. Current Biology, 34(21), 4934-4950.e8. **https://doi.org/10.1016/j.cub.2024.09.019**

This thesis is based on these two published papers. The book chapter was mainly used to build the state of the art for Chapters 2, 3, and 4 and the research article formed the core of the results presented in these same chapters.

Secondary authorship

- **Article:** Boubsi, F., Hoff, G., Arguelles Arias, A., Steels, S., Andrić, S., **Anckaert, A**., Roulard, R., Rigolet, A., van Wuytswinkel, O., & Ongena, M. (2023). Pectic homogalacturonan sensed by Bacillus acts as host associated cue to promote establishment and persistence in the rhizosphere. IScience, 26(10), 107925.
  https://doi.org/10.1016/J.ISCI.2023.107925

- **Article:** Rigolet, A., Argüelles Arias, A., **Anckaert, A.**, Quinton, L., Rigali, S., Tellatin, D., Burguet, P., & Ongena, M. (2024). Lipopeptides as rhizosphere public goods for microbial cooperation. Microbiology Spectrum, 12(1).
  https://doi.org/10.1128/spectrum.03106-23

- **Article:** Boubsi, F., **Anckaert, A**., Argüelles-Arias, A., & Ongena, M. (2025). Pectin-derived oligogalacturonides shape mutualistic interactions between *Bacillus* and its host plant. *The ISME Journal*. **https://doi.org/10.1093/ismejo/wraf232**

Attendance at Symposium

Poster presentation

- **miCROPe 2022:** July 11-14, 2022, Vienna, Austria, "UNTANGLING the unsuspected compatibility of the interaction between *Bacillus velezensis* and *Rhizophagus irregularis* with potential benefits for plant health".

- **Plant BioProTech symposium 2022:** June 28-30, 2022, Reims, France, "Combining *Rhizophagus irregularis* and *Bacillus velezensis*: Molecular aspects of a unconventional interaction.".

Oral presentation

- **EOS workshop Bacterial lipopeptides: from (physico)chemistry to ecology 2022:** 21-23 September, 2022, Liège, Belgium, "*Rhizophagus irregularis* tames *Bacillus velezensis* lipopeptidome to favor mutualism".

- **6th Plants Bacteria Meeting 2023 :** mars 20-24, 2023, Aussois, France, "Molecular crosstalk of the interkingdom interaction betwenn Rhizophagus irregularis and Bacillus velezensis".

- **4th Plant Microbiome Symposium 2023:** 31/07/2023 -05/08/2023, Quito, Ecuador, "The unsuspected mutualism between *Rhizophagus irregularis* and *Bacillus velezensis* confers enhanced biocontrol functionality".

Chapter 1

Introduction

1.1 Problem statement

Land health, defined by the interplay of its essential components, soils, vegetation, and inland water resources, is fundamental to sustainable and productive agriculture. However, land degradation remains a pressing issue, driven by factors such as water erosion, soil salinization, compaction, organic carbon loss, and pollution. These interconnected processes have far-reaching consequences, affecting agricultural productivity, food security, climate stability, environmental sustainability, and economic prosperity (Barbier & Hochard, 2018; Borrelli et al., 2022; Oakleaf et al., 2024; Olsson et al., 2019; Prăvălie, 2021; Prăvălie et al., 2021; Tilman et al., 2001).

On a global scale, approximately 23% of the world's soils are already degraded, significantly reducing the lands capacity to yield crops and threatening global food production. The economic repercussions of soil degradation, encompassing losses in productivity and biodiversity, are staggering, with estimates ranging from 6.3 to 10.6 trillion USD annually worldwide (Stewart et al., 2015; Tang et al., 2021). In Europe, the estimated cost of land degradation reaches approximately €1.25 trillion per year, resulting from decreased agricultural yields, water quality deterioration, and public health concerns (Beketov et al., 2013; Nicolopoulou-Stamati et al., 2016; Tilman et al., 2001). Furthermore, land degradation in Europe is not a unidimensional issue, agricultural lands face pressures from multiple processes, including soil pollution, nutrient imbalances, and contamination by heavy metals. Among these, pesticide pollution has the largest spatial footprint, impacting an estimated 52% of agricultural areas (Orgiazzi et al., 2022; Panagos et al., 2024a; Prăvălie et al., 2024). This issue is particularly critical in Belgium, which ranks as the fourth most pesticide-polluted country in Europe, with 93% of its arable land contaminated (Prăvălie et al., 2024). These alarming statistics underscore the urgent need for sustainable agricultural practices and alternative strategies to preserve soil and human health, reduce environmental footprints, and ensure resilience in a One Health approach (Banerjee & van der Heijden, 2023; D'Hondt et al., 2021). Notably, soil biodiversity loss further exacerbates the problem by weakening the ability of crops to resist diseases and climate-related stressors (Panagos et al., 2024b).

In response to these pressing challenges, biological control of plant diseases has emerged as a promising and sustainable alternative to chemical pesticides. **Biocontrol** leverages (micro-)organisms or biologically derived compounds to protect plants from pathogens while promoting growth (Compant et al., 2019, 2025; Raymaekers et al., 2020). This approach offers numerous advantages, including reduced environmental impact, fewer resistance issues in pathogens, and compatibility with sustainable agricultural practices. Consequently, the biocontrol market is expanding, with projected annual growth rates of 13.7%, and is expected to grow from approximately $5 billion today to $15 billion USD by 2029 (Compant et al., 2025; Marrone, 2024).

Microbial biocontrol agents (BCAs) are the cornerstone of this approach. Examples such as *Bacillus thuringiensis*, widely used as a bio-insecticide, demonstrate their potential (Aynalem et al., 2022). Similarly, plant growth-promoting **rhizobacteria** (PGPR), including species from genera such as *Pseudomonas*, *Streptomyces*, *Paenibacillus*, *Azospirillum*, and *Bacillus* play pivotal roles in biocontrol applications (Collinge et al., 2022; Compant et al., 2019, 2025; Köhl et al., 2019).

Despite their potential, the performance of microbial BCAs remains inconsistent across different agro-ecological environments and host plants. This variability is influenced by abiotic factors like temperature, humidity, and soil pH, as well as biotic factors such as plant species, pathogen interactions, and microbial community dynamics (Kaminsky et al., 2019; Mauch-Mani et al., 2017; Mayjonade et al., 2024; Qiu et al., 2019; Rouphael et al., 2015; Salvioli di Fossalunga & Bonfante, 2023; Sun & Shahrajabian, 2023). Furthermore, the specific traits and mechanisms underlying BCA efficacy remain poorly understood. Addressing these challenges requires further research to optimize biocontrol formulations, improve their stability in complex environments, and assess their long-term sustainability. The overarching challenge lies in uncovering the mechanisms through which microbial BCAs stimulate plant immune responses and interact with other microorganisms. A deeper understanding of these processes is critical for more rational implementation of BCAs and thereby for reducing chemical inputs, restoring soil biodiversity, and building resilient agricultural systems capable of supporting a growing global population.

1.2 Objectives

In recent years, the role of microbes in supporting ecosystem health has gained significant attention. However, the intricate processes occurring in the soil, particularly in the **rhizosphere**, remain poorly understood. Soil ecosystems play a key role in food production, climate regulation, and disease control, and their functions are closely linked to microbial community composition (Compant et al., 2025; Leach et al., 2017). Plants, as central components of these ecosystems, are influenced by a myriad of intraspecific, interspecific, and interkingdom interactions. While the potential of microbes to protect plants from pathogens is well-documented, the mechanisms by which these functional groups protect plants remain underexplored.

Beneficial microbes act within dynamic communities, forming complex intra- and interkingdom networks. Interactions among different beneficial species can synergistically promote plant growth and health (Lutz et al., 2023). Nevertheless, the microbial ecology of the rhizosphere, as well as the factors driving these beneficial interactions remain poorly understood (Collinge et al., 2022; Mitter et al., 2019; Trivedi et al., 2020). Harnessing such multitrophic interactions represents a promising approach to improve biological control, reduce chemical pesticide use, and promote sustainable agriculture, thereby restoring soil biodiversity and resilience. (Compant et al., 2025; French et al., 2021; Liu et al., 2023).

The overarching aim of this thesis is to investigate the potential synergistic interactions between plant-beneficial microbes and unravel the mechanisms underlying these partnerships. Focusing on a specific case study, the relationship between *Bacillus* spp. and arbuscular mycorrhizal (AM) fungi, this research seeks to demonstrate how these partnerships can be leveraged to enhance plant health and resilience. Among microbial BCAs, *Bacillus spp.*, particularly *Bacillus velezensis*, have shown remarkable potential for controlling plant diseases. These bacteria exhibit exceptional competitiveness in the rhizosphere, driven by their ability to colonize roots and secrete antimicrobial compounds and plant resistance elicitors. Such metabolites enable *Bacillus spp.* to combat a broad range of bacterial, viral, and fungal pathogens (Anckaert et al., 2021; Andrić et al., 2023; Rabbee et al., 2023). On the other hand, AM fungi, such as *Rhizophagus irregularis*, represent another key group of beneficial microorganisms. These fungi form symbiotic relationships with plant roots, mobilizing nutrients from the soil to the plant while reducing the need for synthetic fertilizers. Moreover, AM fungi enhance plant resilience to both biotic and abiotic stresses, contributing to the growing biofertilizer market (Owen et al., 2015; Parniske, 2008; Wipf et al., 2019). The synergy between *Bacillus spp.* and AM fungi holds promise for sustainable agriculture. While AM fungi mobilize nutrients and improve soil health, *Bacillus spp.* strengthen plant disease resistance. Understanding the interactions between these two key groups of microorganisms could pave the way for the development of effective microbial consortia.

To explore the potential interaction between *B. velezensis* and *R. irregularis*, this thesis focuses on three key research questions (RQs). By tackling these RQs, this research seeks to advance our understanding of microbial interactions in the rhizosphere and provide a foundation for the development of innovative and sustainable crop protection strategies. The goal of this thesis is to adopt a holistic approach for studying this relationship, combining molecular and microscopic investigations with macroscopic observations in greenhouse trials. The aim is to capture the relevance of this interaction at multiple scales, from the molecular to the ecosystem level.

RQ 1: Could fungal killers like *B. velezensis* and an AM fungus establish a stable cohabitation ? (Chapter 2)

RQ 2: What are the factors that drive this interkingdom interaction? (Chapter 3)

RQ 3: Is it advantageous to combine an AM fungus and a bacterial biocontrol agent for promoting plant health? (Chapter 4)

Chapter 2

When *B. velezensis* meets AM fungi

2.1 State of the art

The rhizosphere, a narrow region of soil shaped by root exudates, is a hotspot of microbial diversity and interactions. It hosts a complex microbial community comprising bacteria, fungi, archaea, and viruses, all engaging in intricate interactions with each other and their host plant (Philippot et al., 2013; Trivedi et al., 2020). Microbial interactions with plants in the rhizosphere can range from beneficial to pathogenic, with beneficial microorganisms playing pivotal role in plant health. They enhance nutrient acquisition, suppress plant pathogens, and mitigate abiotic stresses, significantly influencing plant growth and resilience (Leontidou et al., 2020; Liu et al., 2023; Mendes et al., 2011; Ribeiro et al., 2020).

2.1.1 Plant beneficial bacilli in the rhizosphere

Among the diverse beneficial microbes, members of the *Bacillus* genus have emerged as key players in the rhizosphere. In particular, species belonging to the *Bacillus subtilis* complex stand out from other *Bacillus* lineages such as the *B. flexus* and *B. cereus* groups (see Chapter 5 and Figure 5-2 for the phylogenetic tree). Species of the *subtilis* group are characterized by strong competitive abilities, versatile modes of action, and efficient root-colonizing capacity. The *B. subtilis* complex forms a phylogenetically coherent cluster within the *Bacillus* genus, comprising closely related species such as *B. subtilis*, *B. amyloliquefaciens*, *B. velezensis*, *B. licheniformis*, and *B. pumilus* (Asif et al., 2023; Balleux et al., 2025; Dunlap, 2019). These bacteria confer multiple benefits to their plant hosts through antibiosis, effective root colonization, and activation of **induced systemic resistance** (ISR) (see Chapter 4) (Anckaert et al., 2021; Blake et al., 2021; Rabbee et al., 2023). A major determinant of their ecological success is the production of **bioactive secondary metabolites** (BSMs). Within this complex, *B. velezensis* has become a model plant-associated species, distinguished by its capacity to synthesize a broad spectrum of BSMs (Molinatto et al., 2016; Pandin et al., 2018; Steinke et al., 2021). Comparative genomic analyses highlight the biocontrol potential of *B. velezensis*, which is notably rich in biosynthetic gene clusters (BGCs) (Grubbs et al., 2017; Harwood et al., 2018; Steinke et al., 2021), further establishing its role as a model species for microbial biocontrol (Andrić et al., 2020; Fan et al., 2018; Rabbee et al., 2019, 2023; Ye et al., 2018) (**Figure 2-1**).

Bacillus species produce both ribosomally synthesized and post-translationally modified peptides (RiPPs) and **non-ribosomal peptides** (NRPs). Among RiPPs, *B.*

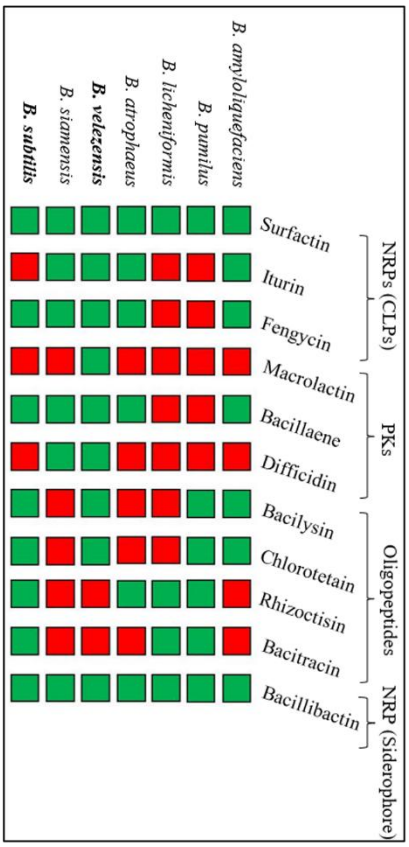

Figure 2-1: *B. velezensis* as the archetype of root-associated bacilli within the *B. subtilis* complex, characterized by its production of BSMs. *B. velezensis* is considered the archetypical plant-associated and plant-beneficial member of the *Subtilis* clade. It is estimated that up to 12% of its genome is dedicated to the biosynthesis of a wide diversity of BSMs. The figure illustrates the main non-ribosomal bioactive secondary metabolites produced by various species within the *B. subtilis* complex. *B. velezensis* has the highest number of different genes coding for BSMs. Adapted from Andric *et al.* (2020) and Steinke *et al.* (2021). Green squares indicate the presence of production, while red squares denote its absence.

subtilis and related species are known for producing bacteriocins, including lantibiotics such as plantazolicin, subtilin, ericin, mersacidin, amylolysin, subtilosin, and amylocyclicin (Caulier et al., 2019; Harwood et al., 2018). In contrast, NRPs are more conserved across species (**Figure 2-1**) and are synthesized by large multimodular enzyme complexes, non-ribosomal peptide synthetases and polyketide synthases, that assemble metabolites from amino acids (for **cyclic lipopeptides**, cLPs) or carboxylic acids (for **polyketides**, PKs) (Caulier et al., 2019; Duban et al., 2022; Kaspar et al., 2019; Kiesewalter et al., 2021; Théatre et al., 2021). Some oligopeptides such as bacilysin are also produced through non-ribosomal pathways but not via NRP synthetase machinery; they are therefore classified as "unusual peptides" (Ming & Epperson, 2002; Rajavel et al., 2009). Within the *B. subtilis* group, three main PK families, bacillaene, difficidin, and macrolactin, are typically produced (Caulier et al., 2019; Chen et al., 2006).

Among NRPs, cLPs from the iturin, surfactin, and fengycin families are the most extensively studied for their potent antimicrobial properties (Structure and synthesis, **Figure 2-2**) (Caulier et al., 2019; Cawoy et al., 2015; Miljaković et al., 2020; Rabbee et al., 2023). These amphiphilic molecules consist of a peptide moiety (seven amino acids for iturins and surfactins, ten for fengycins) linked to a fatty acid chain of 12–19 carbons, which allows them to insert into and disrupt pathogen membranes, leading to pore formation and cell lysis (Bakker et al., 2024; Deleu et al., 2008, 2014; Wise et al., 2014; Yang et al., 2024a; Zakharova et al., 2019). Their activity is often enhanced through synergistic interactions between different families (Luna-Bulbarela et al.,

2018; Tanaka et al., 2015a). cLP biosynthesis involves multimodular NRPSs that incorporate both L- and D-amino acids, generating homologues (differing in fatty acid length or branching) and variants (differing in peptide sequence) (Antonioli Júnior et al., 2022; Caulier et al., 2019; Duban et al., 2022; Théatre et al., 2021). This structural diversity broadens their antimicrobial spectrum and enhances ecological adaptability (Balleza et al., 2019; Deleu et al., 2005; Leconte et al., 2024; Luna-Bulbarela et al., 2018; Wang et al., 2025a).

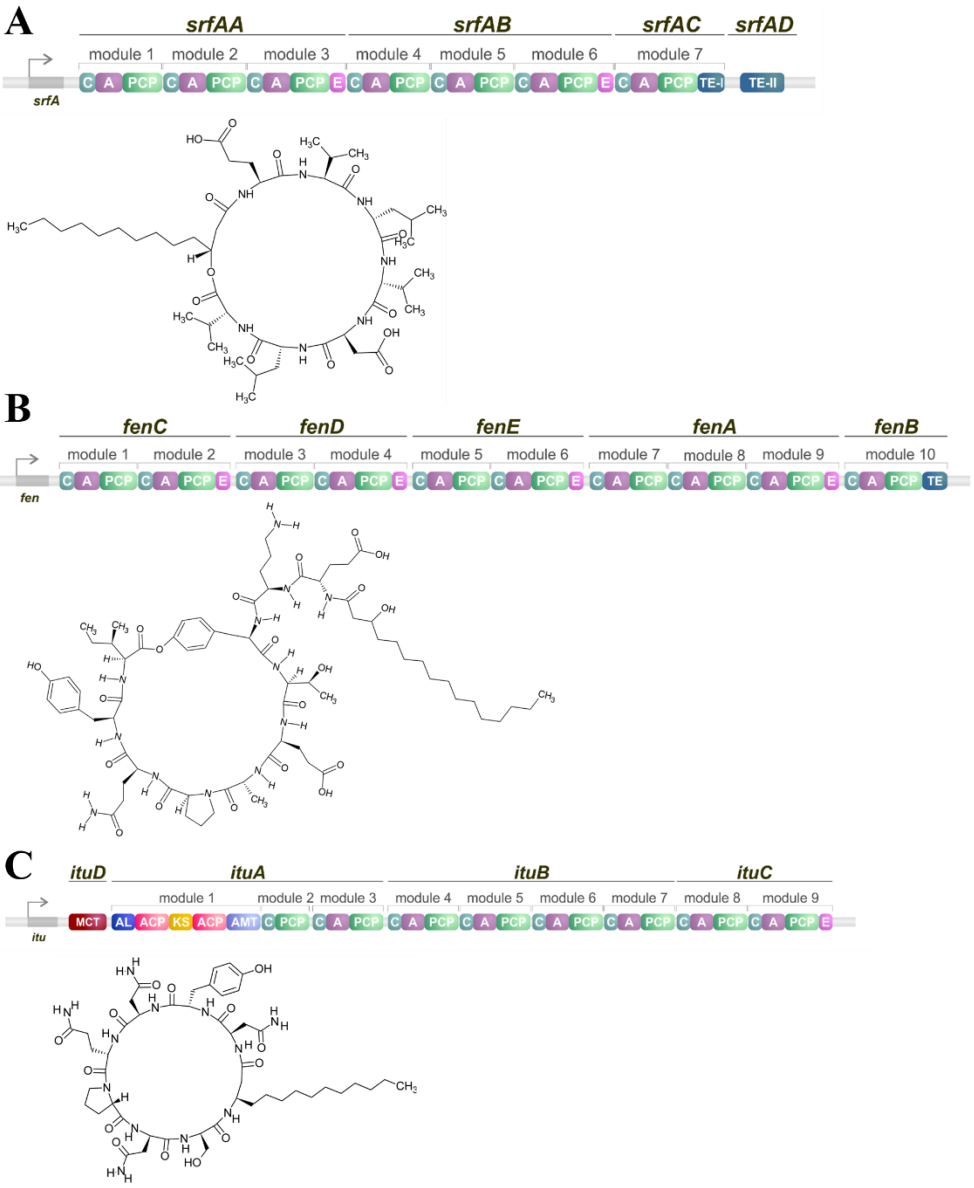

Figure 2-2: Synthesis of surfactin (A), fengycin (B) and iturin (C). For surfactin synthesis, the *srfAA–D* genes of the *srfA* operon encode four proteins (SrfAA–SrfAD) that form the NRP synthetase complex responsible for surfactin production. The *fenA–E* genes of the *fen* operon encode five proteins (FenA–FenE) that form the NRP synthetase complex responsible for fengycin synthesis. Each protein contain several modules encompassing A, C, PCP domains and E. The *ituA–C* and *ituD* genes of the *itu* operon encode four proteins (ItuA–ItuD) involved in iturin biosynthesis. Iturins are synthesized by a PK synthetase – NRP synthetase hybrid complex. The first protein (encoded by *ituD* in the *itu* operon) contains a malonyl-CoA transacylase (MCT) domain. The second protein (encoded by *ituA*) includes ACP and KS domains, as well as AL (acyl-CoA ligase) and AMT (aminotransferase) domains typical of PK synthetase enzymes. The subsequent proteins (ItuB and ItuC) are NRP synthetase-type enzymes responsible for the sequential addition of amino acids in the peptide assembly line. Each operon is illustrated with a representative molecular structure: surfactin (A), fengycin (B), and iturin (C). Abbreviations: condensation (C), adenylation (A), carrier protein (CP), epimerization (E), and thioesterase (TE) domains. Illustration adapted from Antonioli Júnior et al. (2022) and Anckaert et al. (2021).

Iturins and fengycins are particularly effective against fungal pathogens (Anckaert et al., 2021; Cawoy et al., 2015; Rabbee et al., 2023). Iturins have also demonstrated strong antimicrobial activity against oomycetes such as *Phytophthora infestans* (Wang et al., 2020b), while fengycins are known to suppress mycotoxin production in *Fusarium graminearum* (Hanif et al., 2019). Although surfactins are generally less potent as standalone antimicrobial agents, they can synergistically enhance the efficacy of other cLPs (Mihalache et al., 2018; Tanaka et al., 2015a; Wang et al., 2020a). Interestingly, recent studies have revealed that surfactins can also impair fungal cell walls, as observed in *Aspergillus niger*, inducing significant cellular stress (Richter et al., 2024). Unlike iturins and fengycins, which primarily disrupt the plasma membrane, surfactins may exert their effects more through membrane perturbation than direct permeabilization (Gilliard et al., 2024).

Beyond lipopeptides, bacilysin, targets also bacterial, fungal, and oomycete pathogens (Caulier et al., 2018; Chen et al., 2009a; Nannan et al., 2021; Wu et al., 2015), and the polyketide difficidin, has demonstrated activity against plant pathogens like *Erwinia amylovora* and *Xanthomonas oryzae* (Chen et al., 2009b; Wu et al., 2015). Collectively, these metabolites represent a robust arsenal for pathogen suppression.

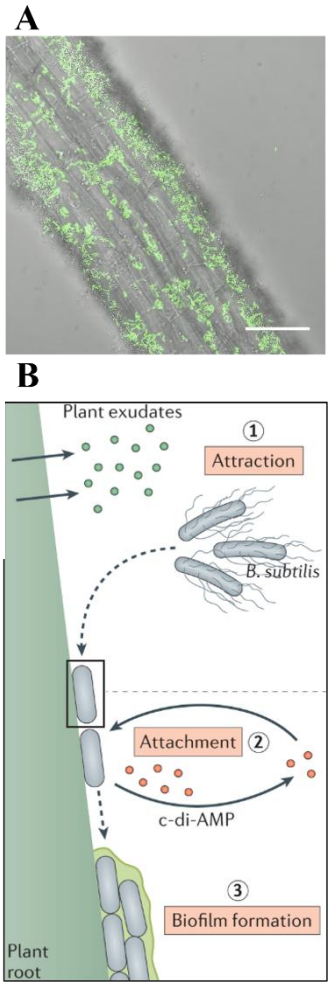

Figure 2-3: *Bacillus* as an efficient root-associated bacterium. A, *Bacillus subtilis* colonization of plant roots. In addition to being a model organism for studying secondary metabolite production, *Bacillus* spp. are widely used as models for sporulation, biofilm development, and root attachment. Image adapted from Blake *et al.* (2020). Scale bar = 50 µm. **B,** Behaviours of *B. subtilis* during root colonization. This illustration represents the three steps of *Bacillus* spp. root colonization: attraction (1), attachment (2), and biofilm formation (3). In step 1, root exudates or plant-derived compounds are perceived by the bacterium, triggering chemotactic attraction. Signals originating from root exudates or the plant cell wall, as well as bacterial self-produced molecules such as cyclic di-adenylate monophosphate (c-di-AMP) and surfactin, play key roles in attraction, attachment, and ultimately biofilm formation. Illustration adapted from Arnaouteli *et al.* (2021).

The ability of *Bacillus* spp. to thrive in the rhizosphere is not solely attributed to their antagonistic traits but also to their unique survival strategies and multifunctional roles such as chemotaxis, **biofilm** formation, and spore production (Arnaouteli et al., 2021; Blake et al., 2021; Kovács, 2019). Chemotaxis enables bacteria to detect and move toward root exudates, facilitating root colonization through a flagellum-mediated movement (Blake et al., 2021; Feng et al., 2021; Liu et al., 2024a). Once established, they form biofilms, which are multicellular communities embedded in a self-produced matrix of exopolysaccharides (EPs), proteins (e.g., TasA, BsIA), and DNA (Arnaouteli et al., 2021; Flemming et al., 2023; Knights et al., 2021; Liu et al., 2024a) (**Figure 2-3 B**). Within biofilms, phenotypic heterogeneity enables bacteria to adopt coordinated responses and adaptive strategies, including motility, spore formation, and BSM production (Arnaouteli et al., 2021; Romero, 2013; Vlamakis et al., 2013). Moreover, the biofilm seems to be disparate along the roots and not uniform, *Bacillus* forming macrocolonies preferentially in the elongation zone (Massalha et al., 2017; Stoll et al., 2021) (**Figure 2-3 A**). These biofilms provide multiple benefits, including protection against environmental stresses, enhanced nutrient acquisition, and resistance to biotic threats (Arnaouteli et al., 2021; Flemming et al., 2016; Molina-Santiago et al., 2019). Surfactin, a key lipopeptide, reduces surface tension and acts as a wetting agent, facilitating the structural organization of biofilms (Jautzus et al., 2022). Mutants of *B. velezensis* deficient in surfactin production exhibit impaired biofilm formation and reduced the ability to colonize efficiently plant roots, underscoring its importance for

this species (Al-Ali et al., 2018; Stoll et al., 2021). While surfactin plays a primary role in biofilm establishment, the other lipopeptides iturins and fengycins may also contribute to this process, though in a more strain-specific way (Cao et al., 2018; Luo et al., 2015). Biofilm formation also enables *Bacillus* spp. to colonize fungal hyphae (Benoit et al., 2015; Kjeldgaard et al., 2019; Richter et al., 2024; Xie et al., 2024). The ability to grow along fungal structures allows *Bacillus* to persist in the rhizosphere, potentially improving its ability to counteract fungal growth while ensuring its own survival (Zhou et al., 2024, 2022). Spore formation is another critical survival strategy in *Bacillus* spp., as spores confer resistance to environmental stressors such as nutrient depletion and drought. Within biofilms, a subset of bacterial cells differentiate into spores, ensuring long-term persistence strategy (Charron-Lamoureux & Beauregard, 2019; Nicholson et al., 2000; Tan & Ramamurthi, 2014; Wahlen et al., 2018). *Bacillus* spp. root colonization and biofilm formation play thus pivotal roles for rhizosphere persistence and for promoting plant health, emphasizing its role in maintaining robust plant-microbe interaction (Al-Ali et al., 2018; Blake et al., 2021; Liu et al., 2024a).

Although *Bacillus* spp. are widely recognized for their strong antagonistic potential, their relationship with fungi are more nuanced than previously assumed. Under specific conditions, *Bacillus* species can coexist with certain fungi, such as *A. niger* and *nidulans* (Abeysinghe et al., 2020; Kjeldgaard et al., 2019; Xu et al., 2025) and *Trichoderma guizhouense* (Xie et al., 2024). These interactions are often dependent on experimental factors, including the composition of the culture medium used for co-cultivation. This versatility highlights the ability of *Bacillus* spp. to engage in both competitive and synergistic microbial interactions.

2.1.2 Arbuscular Mycorrhizal (AM) fungi: Plant symbiont of the soil

AM fungi form symbiotic associations with over 70% of vascular plant species, making them one of the most ubiquitous and influential soil microorganisms (Brundrett & Tedersoo, 2018; Genre et al., 2020; Strullu-Derrien et al., 2018; van der Heijden et al., 2015). These fungi account for 20–30% of the total soil microbial biomass (Leake et al., 2004), playing a pivotal role in nutrient cycling and plant health (Chialva et al., 2022; van der Heijden et al., 2015). As obligate root symbionts, AM fungi are heterotrophic and depend on their host plants for carbon and lipids (Roth & Paszkowski, 2017; Tanaka et al., 2022; Tang et al., 2016; Venice et al., 2020; Wewer et al., 2014). This mutualistic relationship involves bidirectional exchange of nutrients (Choi et al., 2018; Duan et al., 2024), while plants provide carbohydrates to the fungi, AM fungi facilitate the transfer of macronutrients, micronutrients, and water to their plant hosts (Averill et al., 2019; Banasiak et al., 2021; Smith et al., 2003). Thus, through this symbiosis at the root level, AM fungi enhanced nutrient uptake, increased tolerance to biotic and abiotic stresses, and improved plant growth (Augé et al., 2015; Genre et al., 2020; Jeffries et al., 2003; Shi et al., 2023). Furthermore, some AM fungi induce systemic resistance in plants, known as **Mycorrhiza-Induced Resistance**

(MIR), which provides protection against below- and above-ground pathogens through mechanisms similar to ISR triggered by plant growth-promoting rhizobacteria like *Bacillus* spp. (See Chapter 4) (Cameron et al., 2013; Durant et al., 2023; Jung et al., 2012).

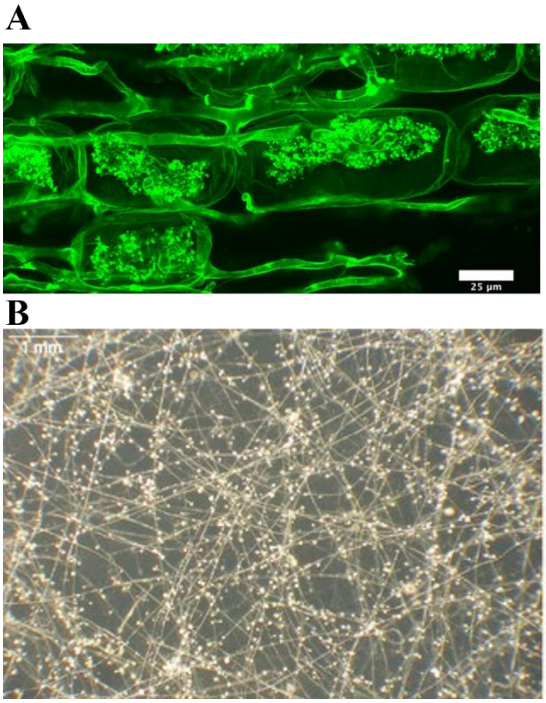

Figure 2-4: AM fungi as symbiotic microorganisms beneficial to plants. A, Confocal image of arbsucules in *Lotus japonicus* root. Image credit to Pimprikar et al.(2016). **B,** Image of the dense ERM formed by *Glomus intraradices*. Images from Juge et al. (2009).

The symbiosis between AM fungi and their plant hosts is characterized by the formation of highly branched structures, known as **arbuscules**, within the root cortex (**Figure 2-4 A**). These arbuscules serve as specialized interfaces for the bidirectional exchange of nutrients (Duan et al., 2024; Genre et al., 2020; Lanfranco et al., 2016). Following symbiosis establisment, AM fungi develop an extensive network of hyphae. Thus, the primary benefit of AM fungal symbiosis lies in improved plant nutrition. AM fungi achieve this through their extensive **extraradical mycelium** (ERM), a dense and far-reaching hyphal network that extends several centimetres from the root surface (**Figure 2-4 B**). These hyphae, with diameters significantly smaller than root hairs, efficiently explore soil pores, extracting nutrients and water that would otherwise remain inaccessible to plant roots (Brundrett & Tedersoo, 2018; Cargill et al., 2025; Parniske, 2008; Wipf et al., 2019).

Thus, the symbiosis between plants and AM fungi is characterized by the exchange of nutrients, facilitated by a **cytoplasmic flow** within the hyphae of the ERM (Bago et al., 2002; Hammer et al., 2024; Whiteside et al., 2019). Through the fungal network, micronutrients such as nitrogen and phosphorus, as well as carbon, water, vacuoles, mitochondria, lipid droplets and fungal nuclei, move bidirectionally (Cargill et al., 2025; Jany & Pawlowska, 2010; Roper et al., 2015). AM fungi actively regulate network-level structure and resource flows to meet both their own metabolic demands and those of their host plants (Oyarte Galvez et al., 2025). To optimize their network

and enhance soil colonization, AM fungi manage key structural components, including runner hyphae and **anastomosis**. The AM fungal network included also **branching-absorbing structures** (BAS), and spores (Jany & Pawlowska, 2010; Kameoka et al., 2019) (**Figure 2-5 A**). Previous studies suggest that BAS structures play a crucial role in nutrient absorption and are present in high density within AM fungal networks, underscoring their significance in mediating nutrient exchange (Bago et al., 1998; Oyarte Galvez et al., 2025). The intraradical cytoplasmic flow within the hyphal network has been shown to be bidirectional, with varying speeds across different parts of the network (**Figure 2-5 B**). (Oyarte Galvez et al., 2025). Moreover, the velocity of cytoplasmic flow increases in response to phosphorus-rich patches, with the highest flow rates occurring within hyphae corresponding to these phosphorus-enriched zones (Whiteside et al., 2019). AM fungi regulate network formation and nutrient transport. Some hyphae act as main "trunk routes", thicker, reinforced pathways that connect distant parts of the network and support the flow of nutrients and cytoplasm. These trunk routes are complemented by smaller, branching

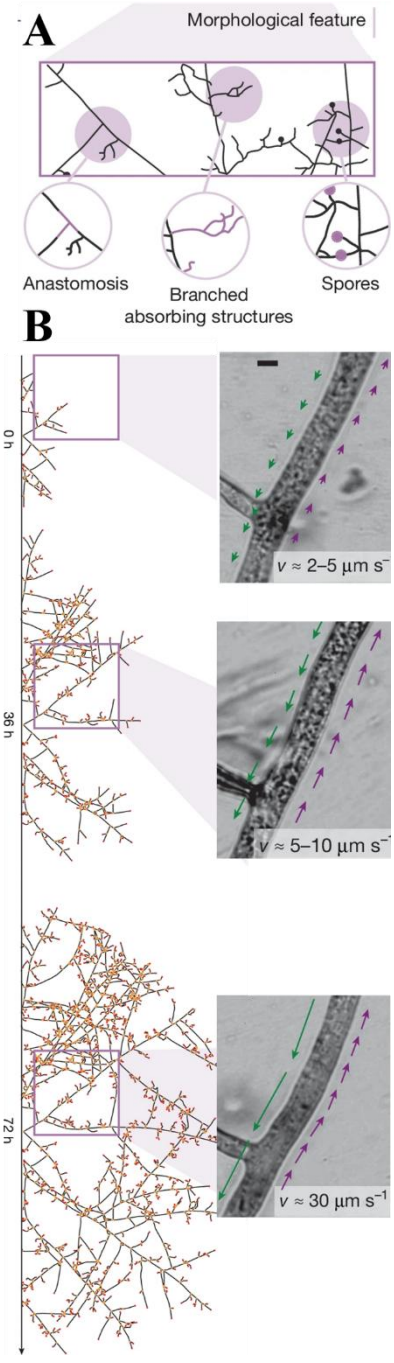

Figure 2-5: Features of the network of AM Fungi.. **A,** Structural diversity within the ERM, including branching patterns, anastomosis, branching-absorbing structures (BAS), spores and main "runner" hyphae that support the overall structure and enable environmental exploration. **B,** Evolution of network architecture and cytoplasmic flow dynamics during hyphal expansion. Representative image frames show bidirectional cytoplasmic flows recorded over 72 hours, with arrows indicating the direction and relative velocity of flow: larger arrows represent faster speeds; green arrows point toward the root; purple arrows point away from the root. These observations suggest that AM fungi regulate both hyphal diameter and flow velocity according to network topology. Enhanced flow occurs along "trunk" hyphae, major transport routes with a high density of connections to the root, allowing the colony to efficiently distribute lipids toward growing tips and nutrients toward the root interface. Scale bars = 10 µm. Adapted from Oyarte Galvez et al. (2025)

hyphae that explore the soil for new resources. Together, they form dynamic networks that function as self-sustaining systems. The continuous growth of hyphal tips drives nutrient absorption and distribution, optimizing the exchange of resources with the host plant (Oyarte Galvez et al., 2025).

Additionally, the ERM forms **common mycorrhizal networks** (CMNs) that interconnect multiple plants, even between different species (Barto et al., 2012; Wipf et al., 2019). These networks not only facilitate nutrient exchange (He et al., 2003; Johnson & Gilbert, 2015) but also enable the transmission of warning signals in response to pest and pathogen attacks (Alaux et al., 2020; Babikova et al., 2013; Duhamel et al., 2013), further enhancing plant resilience. By supporting both individual plant health and the stability of entire plant communities, AM fungi play a pivotal role in ecosystem dynamics (Simard et al., 2012; Wipf et al., 2019).

2.1.3 The hyphosphere microbiome

Plants allocate approximately 4–20% of their photosynthetically fixed carbon to support AM fungi. AM fungi use this carbon to sustain their own metabolic activities and release portion of this carbon as exudates into the surrounding soil to form the **hyphosphere** (Jakobsen & Rosendahl, 1990; Shi et al., 2023; Zhou et al., 2025). Similar to how carbon-rich rhizodeposits in the rhizosphere recruit bacterial communities, these fungal exudates attract a diverse array of bacteria to the hyphosphere (Faghihinia et al., 2022; Jin et al., 2025; Zhang et al., 2022; Zhou et al., 2025). Phylogenetic and functional analyses have shown that these bacterial communities often include genera such as *Pseudomonas*, *Bacillus*, *Rhodococcus,* and *Streptomyces* (Agnolucci et al., 2015; Basiru et al., 2023; Duan et al., 2024; Emmett et al., 2021; Scheublin et al., 2010; Xu et al., 2023b; Zhang et al., 2022; Zhou et al., 2020b). The composition of the **hyphosphere microbiome** is influenced by a range of factors, including the identity of the AM fungal species, the host plant species, and abiotic conditions such as nutrient availability (Jin et al., 2024, 2025; Luthfiana et al., 2021; Toljander et al., 2007; Wang et al., 2025b; Zhang et al., 2022; Zhou et al., 2020b). Consequently, microbial communities in the hyphosphere can vary

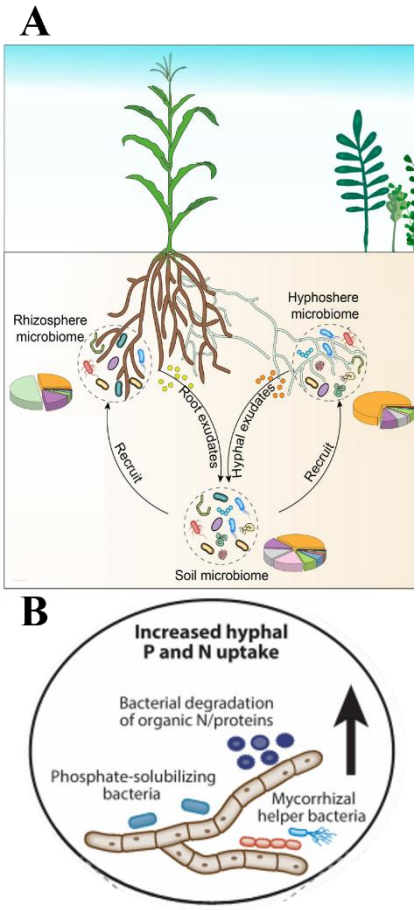

significantly depending on these environmental and biological parameters. Interestingly, the microbial assemblages in the rhizosphere and hyphosphere are distinct, suggesting that plants and AM fungi deploy different strategies for recruiting beneficial microbes (**Figure 2-6 A**) (Jin et al., 2025; Wang et al., 2025b; Zhang et al., 2022).

Figure 2-6: Features of the hyphosphere and benefits of bacterial recruitment by AM fungi. A, The composition of the hyphosphere microbiome differs markedly from that of bulk soil and rhizosphere microbiomes. AM fungal hyphae utilize plant-derived carbon to produce specific exudates that shape and recruit their associated hyphosphere microbiome. Illustration from Zhang et al. (2022). **B,** Schematic representation of the main benefits associated with bacterial recruitment by AM fungi. The hyphosphere microbiome compensates for the fungal inability to access organic nutrient sources by producing extracellular enzymes and stimulating the mineralization of organic nitrogen and phosphorus. This functional cooperation within the mycorrhizal microbiome enhances nutrient availability for both the fungus and the host plant. Adapted from Bennett et al. (2022).

The AM fungal-bacteria collaboration benefits both partners, bacteria improve nutrient availability for AM fungi owing to their limited saprotrophic capability (**Figure 2-6 B**) (Duan et al., 2024; Rozmoš et al., 2022; Zhang et al., 2018a), while the fungi feed and enhance bacterial dispersal and colonization (Jiang et al., 2021; Wang et al., 2016, 2023a). For instance, phosphate solubilizing bacteria (PSB) moving along fungal hyphae can solubilize phosphorus or nitrogen, which the AM fungi can then assimilate and transport to their host plants (Jiang et al., 2021; Jin et al., 2024; Nacoon et al., 2020; Rozmoš et al., 2022; Sharma et al., 2020b; Zhang et al., 2024a). This dynamic cooperation forms a continuum between plants, AM fungi, and bacteria, based on a nutrient exchange system underpinned by a top-down carbon flow (from plants to AM fungi and bacteria) and a bottom-up mineral flow (from bacteria and AM fungi to plants). This intricate interplay exemplifies the ecological interconnectedness and mutual benefits among these organisms, reinforcing their critical roles in enhancing plant health and ecosystem stability (Duan et al., 2024, 2025). Nevertheless, our understanding of AM fungal–bacterial interactions remains limited, particularly concerning variability between AM fungal lineages within the phylum Glomeromycotina (Lee et al., 2013; Montoliu-Nerin et al., 2021; Tedersoo et al., 2024). Most studies have concentrated on a few model species, mainly *Rhizophagus intraradices* and *Rhizophagus irregularis*, with little attention given to other genera (**Figure 2-7**) (Basiru et al., 2023; Faghihinia et al., 2022; Vieira et al., 2025).

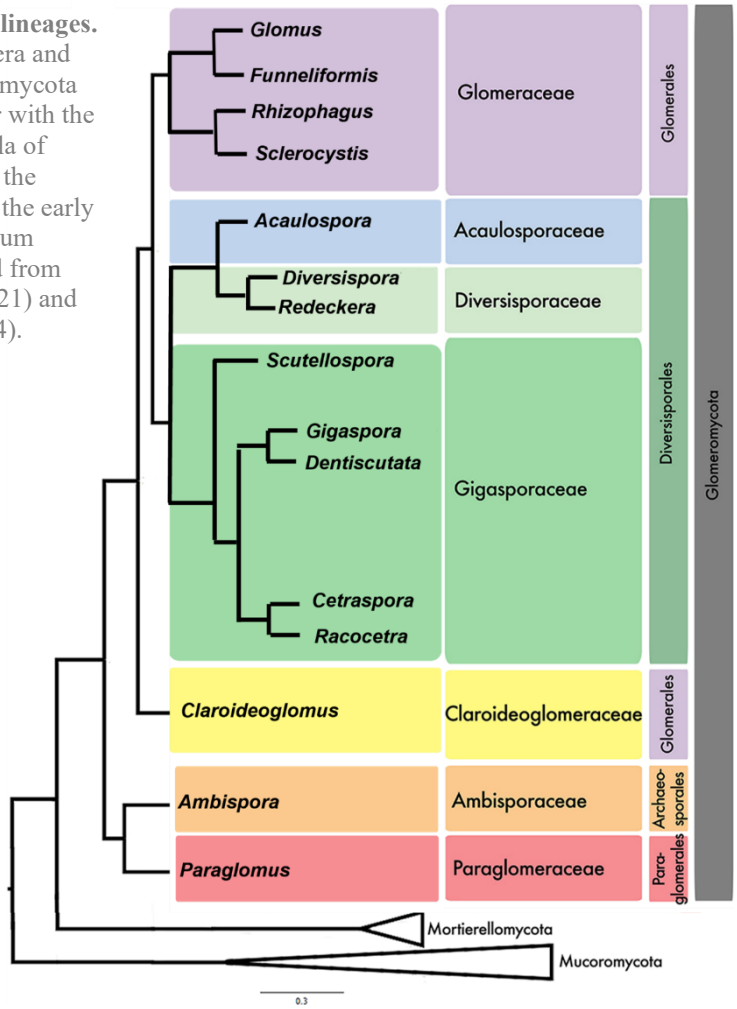

Figure 2-7: AM Fungal lineages. Phylogenetic tree of genera and order within the Glomeromycota subphylum, which together with the closely related subphyla of Mucoromycotina and the Mortierellomycotina, form the early divergent fungal phylum Mucoromycota Adapted from Montoliu-Nerin et al. (2021) and Tedersoo et al. (2024).

2.2 Gap of knowledge and Research Question outline

The concept that AM fungi recruit specific bacterial species into their hyphosphere is well established. However, the dynamics and the abilities of hyphal colonization by beneficial bacteria, remain poorly understood (Faghihinia et al., 2022; Vieira et al., 2025; Zhang et al., 2022). This gap is particularly pronounced when it comes to associations between AM fungi and rhizobacteria such as *B. velezensis* known for their strong antimicrobial activity and plant-protective potential (Faghihinia et al., 2022). Although these microorganisms coexist in the same ecological niche, almost no information is available about how they might interact or potentially establish partnerships. To address this knowledge gap, our work explores the interkingdom interactions through the following research question:

RQ 1: Could fungal killers like *B. velezensis* and an AM fungus establish a stable cohabitation?

The first objective was to determine whether *B. velezensis*, could colonize the ERM of *R. irregularis*. To explore this, we used a custom-designed *in vitro* cultivation system that enables live-cell, time-lapse microscopy imaging of microbial interactions in a controlled and sterile environment (**Figure 2-8**) (Cranenbrouck et al., 2005; St-Arnaud et al., 1996; Toljander et al., 2007; Whiteside et al., 2019). This setup allowed us to monitor

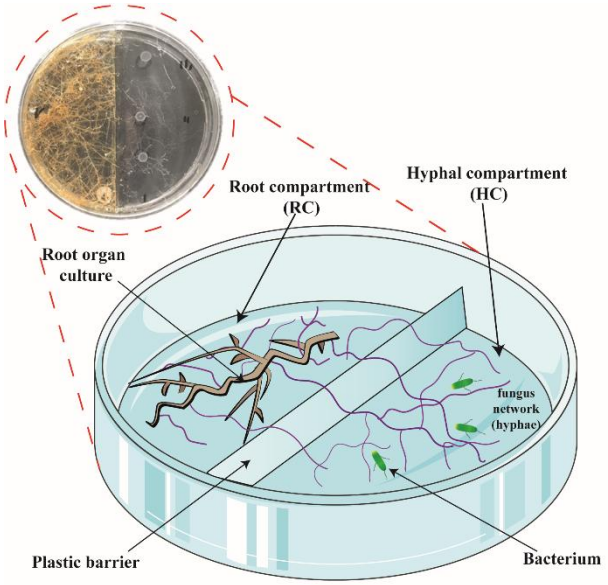

Figure 2-8: Tripartite *in vitro* cultivation system to study interkingdom interactions. Picture (red circle) and schematic representation of the *in vitro* bi-compartmented Petri plate system used for live-cell microscopy. The system consists of two compartments separated by a plastic barrier: the root compartment (RC), which contains *Daucus carota* DC2 root clone transformed with *Rhizobium rhizogenes* T-DNA (Ri T-DNA) and colonized by *R. irregularis*, and the hyphal compartment (HC), which supports growth of extraradical hyphae of *R. irregularis*. Once hyphal growth is established in the HC, *B. velezensis* is inoculated directly onto the hyphae to study their interaction. Brown – transformed *D. carota* roots; Purple – *R. irregularis* hyphae; Green – *B. velezensis* cells.

the spatial and temporal colonization dynamics and the functional relationships between GFP-tagged *B. velezensis* and the ERM of *R. irregularis* without interference from other microorganisms. Equally important, we assessed whether colonization by *B. velezensis* compromises fungal viability, using both respiratory activity measurements and greenhouse experiments to evaluate potential negative impacts on fungal growth and symbiotic function.

2.3 *B. velezensis* efficiently colonizes the hyphae of *R. irregularis* and expands rapidly along the ERM network

We first studied the spatio-temporal dynamics of the physical interaction between *B. velezensis* and *R. irregularis* in the hyphal zone of bi-compartmented plates as illustrated in **Figure 2-9**. The *B. velezensis* strain GA1 was selected due to its well-established biocontrol potential, its fully characterized genome and detailed secondary metabolome (Andrić et al., 2020, 2023; Boubsi et al., 2023; Hoff et al., 2021). To facilitate the monitoring of bacterial development and colonization on fungal structures, a GFP-tagged derivative of GA1 was constructed. The *gfp* gene was placed under the control of the constitutive *Pveg* promoter and integrated into the *amyE* locus, which is commonly used as a stable genomic integration site in *Bacillus* species. The *Pveg* promoter enables robust GFP expression, ensuring clear visualization of bacterial cells (Ferro et al., 2018; Fukushima, 2003; Laforge et al., 2025; Mortier et al., 2023; Overkamp et al., 2013). The *R. irregularis* strain MUCL 41833 was selected for its use in the understanding of AM fungal interaction with rhizobacteria (Loján et al., 2017; Zhang et al., 2018a) and its well-known beneficial effects on plant growth and resistance against biotic stresses (Alaux et al., 2020; Gbongue et al., 2019).

We used mature systems with well-developed ERM network obtained approx. three months after initial mycorrhization of roots. Time lapse microscopy imaging revealed that GFP-tagged *B. velezensis* cells inoculated at short distance (~20 µm) from the hyphae of *R. irregularis* moved to and established on the hyphal surface within 48h (**Figure 2-8**), suggesting a behaviour similar to the chemotaxis observed with plant roots (Allard-Massicotte et al., 2016; Arnaouteli et al., 2021) and observed in some bacterial-fungal interactions (Haq et al., 2016; Li et al., 2023; Zhou et al., 2022).

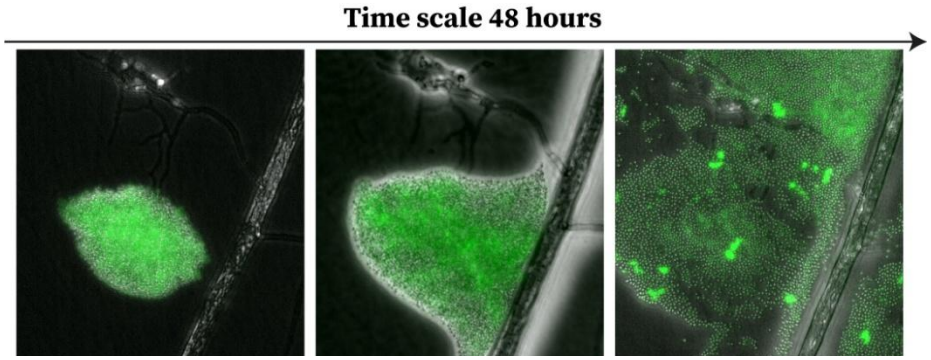

Figure 2-9: Chemotactic behaviour of *B. velezensis* toward *R. irregularis* hyphae. Microscopic picture of *B. velezensis* GA1 labelled with GFP, attracted and established on the hyphae of *R. irregularis* by chemotaxis (time scale of 48 hours).

Following initial attachment, bacteria spreads along the *R. irregularis* hyphae as motile cells but quickly switch within hours into a sessile state, leading to the formation of multicellular colonies (**Video 1** and **2**). Both videos were recorded at the same location within the *R. irregularis* hyphal network, at 24 and 48 hours post-inoculation of *B. velezensis*, respectively.

[1]

Video 1: Motile phase of *B. velezensis* along *R. irregularis* hyphae, 24 hours post-inoculation (hpi). Time-lapse microscopy showing motile *B. velezensis* cells moving along the surface of *R. irregularis* hyphae during the early stage of colonization. **https://youtu.be/OBZW3WR9JlU**

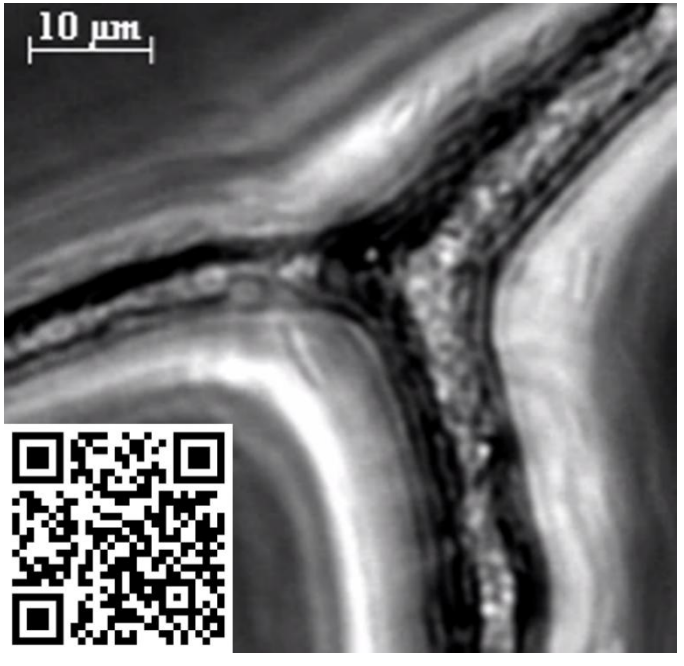

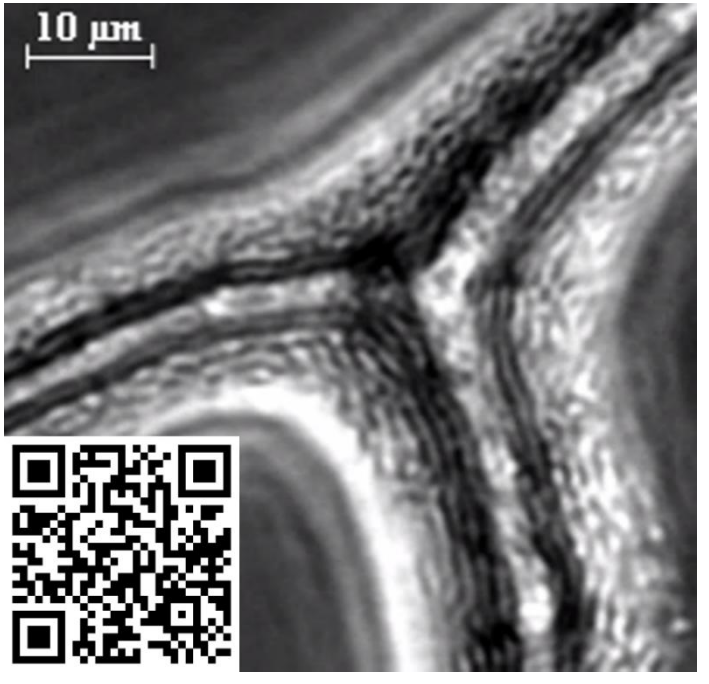

Video 2: **Sessile phase and biofilm formation of *B. velezensis* along *R. irregularis* hyphae, 48 hpi.** Time-lapse microscopy showing the transition of *B. velezensis* from a motile to a sessile lifestyle, leading to the formation of a biofilm-like layer along *R. irregularis* hyphae. **https://youtu.be/lv03SB3fn0E**

[1] Click on the link or scan the QR Code to see the video

This process leads to the development of a homogeneous bacterial cell layer along the hyphae, as illustrated by the significant increase in colony thickness within the first days post-inoculation (dpi) of the bacterium on short segments of runner hyphae (**Figure 2-10**). The expansion and thickness of this biofilm-like layer were quantified using ImageJ/FIJI (Schindelin et al., 2012), by measuring biofilm thickness over time at identical positions along one side of *R. irregularis* hyphae within the ERM. This biofilm-like layer rapidly expanded along the runner hyphae and colonized other ERM structures, such as spores and branched absorbing structures specialized in nutrient uptake (**Figure 2-11**) (Bago et al., 1998; Oyarte Galvez et al., 2025).

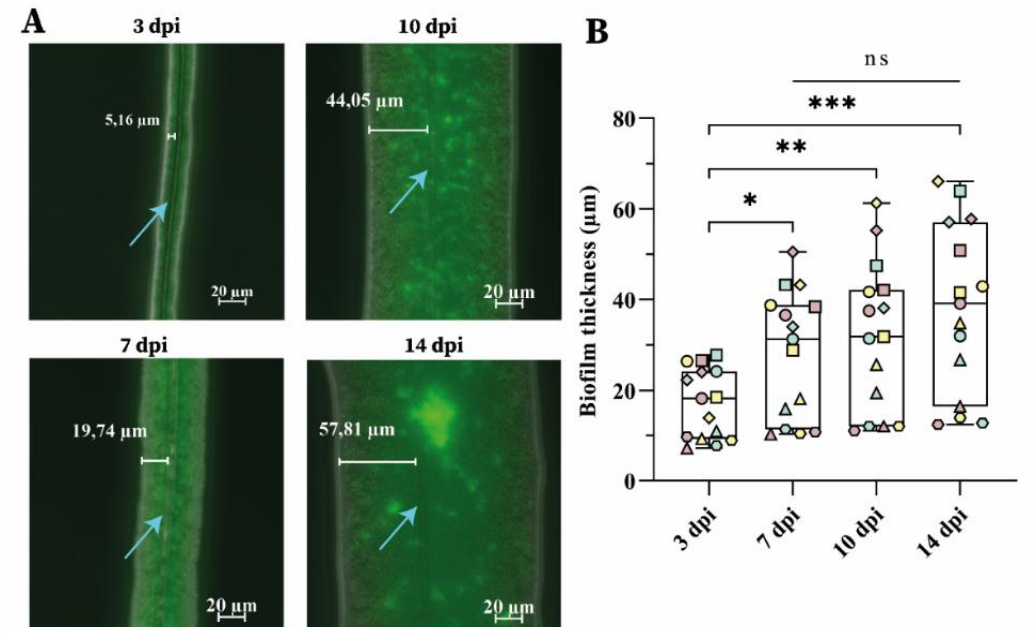

Figure 2-10: Expansion of *B. velezensis* cell layer along *R. irregularis* hyphae over time. **A**, Epifluorescence pictures of *B. velezensis* biofilm development along *R. irregularis*. Epifluorescence pictures were taken by microscopy 3, 7, 10 and 14 days post-inoculation (dpi) of *B. velezensis* GA1 expressing GFP (green colour) on 3-month-old *R. irregularis* hyphae (Blue arrow). By Fiji image processing, measurement of biofilm-like thickness was achieved on one side of the hyphae. Five co-culture systems were used (biological replicates), and 4 images per co-culture system were taken at different locations over time (technical replicates). Representative pictures are shown in the figures. **B**, Evolution of *B. velezensis* biofilm thickness along *R. irregularis* hyphae, 3, 7, 10 and 14 dpi. The boxes encompass the 1st and 3rd quartiles, the whiskers extend to the minimum and maximum points, and the midline indicates the median. The individual points represent 5 biological replicates (different shapes) and 3 technical replicates (3 different colours in the same shape). The evolution of the biofilm thickness over time can be followed for each replicate by the same shape and colour. n = 15; one-way analysis of variance (ANOVA) and Tukey's HSD test ($\alpha = 0.05$): ns = not significant; * $0.01 < p < 0.05$; ** $0.001 < p < 0.01$; *** $0.0001 < p < 0.001$.

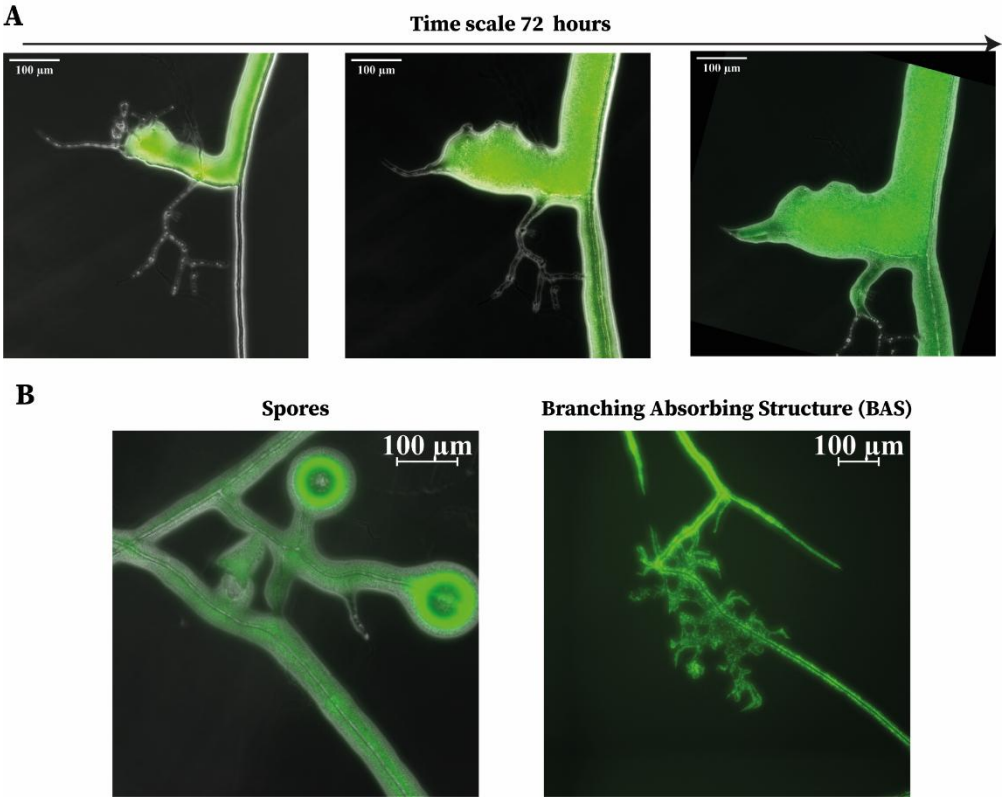

Figure 2-11: *B. velezensis* colonization of the AM fungal network architecture. A, Epifluorescence pictures of *B. velezensis* colonization along hyphae of a 3 month-old culture of *R. irregularis* during a time scale of 72 hours showing the development of a biofilm and colonization of new sections of the hyphae. **B,** Epifluorescence pictures of *B. velezensis* biofilm development along *R. irregularis* hyphae and spores. Right: *B. velezensis* development along branched absorbing structures. Left, *B. velezensis* growth on the surface of spores. Epifluorescence pictures were taken by microscopy respectively 3 and 7 dpi of *B. velezensis* GA1 expressing GFP (green colour).

To demonstrate that the observed bacterial cell layer corresponds to a *stricto sensu* biofilm, additional experiments were performed using *B. velezensis* **knock-out** mutants defective in biofilm matrix synthesis. Specifically, the Δ*epsA-O* and Δ*tasA* mutants, impaired in the production of exopolysaccharides and the TasA protein, respectively, both essential components of the *Bacillus* biofilm matrix, were tested. Growth assays confirmed that both mutants exhibited comparable biomass accumulation and growth kinetics to the wild-type strain when cultivated in liquid medium (**Figure 2-12**).

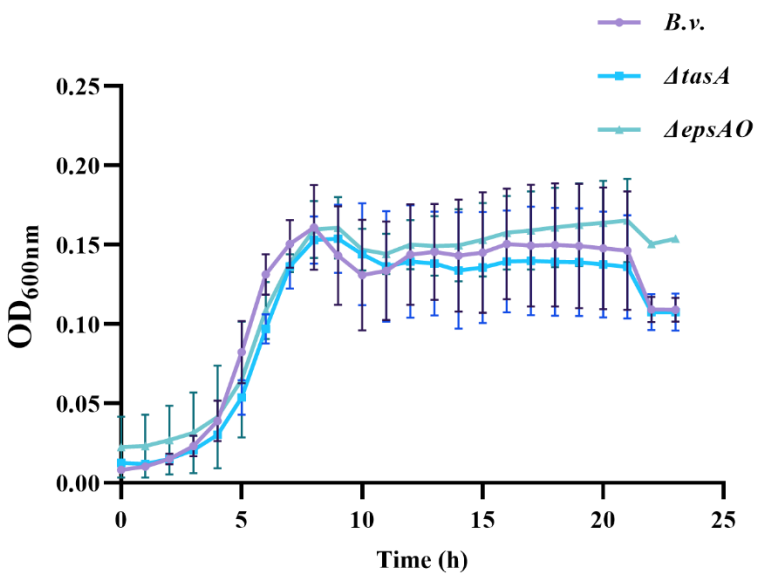

Figure 2-12: Growth of *B. velezensis* (*B.v.*) GA1 wild type or mutants in liquid medium. The optical density (OD_{600}nm) of the bacteria were measured during 24h of growth. Lines represent the means ± SD of 3 biological replicates and 8 technical replicates.

However, compared to the wild type, the formation of the thick bacterial layer and the extent of hyphal colonization were significantly reduced in both Δ*epsA-O* and Δ*tasA* mutants (**Figure 2-13**) (Arnaouteli et al., 2021; Karygianni et al., 2020). Imaging with the mCherry-tagged Δ*tasA* mutant revealed a disrupted biofilm phenotype, characterized by the presence of isolated cell aggregates rather than a continuous and cohesive biofilm along the *Rhizophagus* mycelium, as observed for the wild type (**Figure 2-13 B**). These findings confirm that the observed bacterial cell layer indeed represents a *stricto sensu* biofilm.

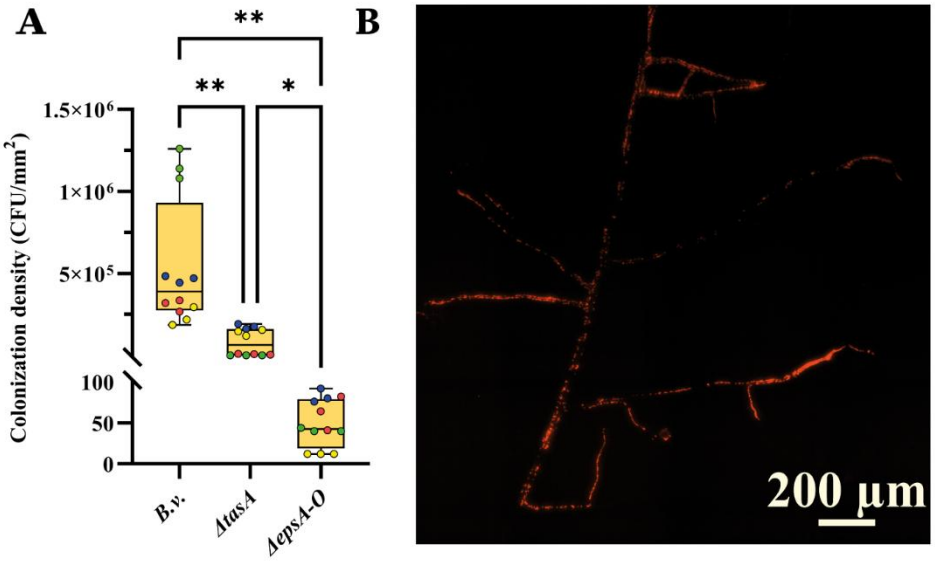

Figure 2-13: Ability of *B. velezensis* to form biofilm along AM fungal hyphae of *R. irregularis*. **A**, Colonization density (CFU/mm^2) of hyphae of 3-month-old *R. irregularis*, 7 days post inoculation (dpi) of *B. velezensis* tagged GFP (*B.v.*) or knock-out mutants unable to produce exopolysaccharide(*ΔepsA-O*) or proteins TasA (*ΔtasA*). The boxes encompass the 1st and 3rd quartiles, the whiskers extend to the minimum and maximum points, and the midline indicates the median. The individual points represent 4 at 5 biological replicates (different colour) and 3 technical replicates (same colour). $12 \leq n \leq 15$; one-way analysis of variance (ANOVA) and Tukey's HSD test ($\alpha = 0.05$). **B**, picture of *B. velezensis* knock-out mutants unable to produce proteins TasA (*ΔtasA*) and mCherry-tagged. Epifluorescence pictures of the biofilm development of this mutant along 3-month-old *R. irregularis* hyphae were taken by microscopy 7 days after inoculation (dpi) of *B. velezensis* GA1 *ΔtasA* (red color).

Further imaging at a larger scale showed that *B. velezensis* spread over the major part of the dense ERM network within three days (**Figure 2-14**).

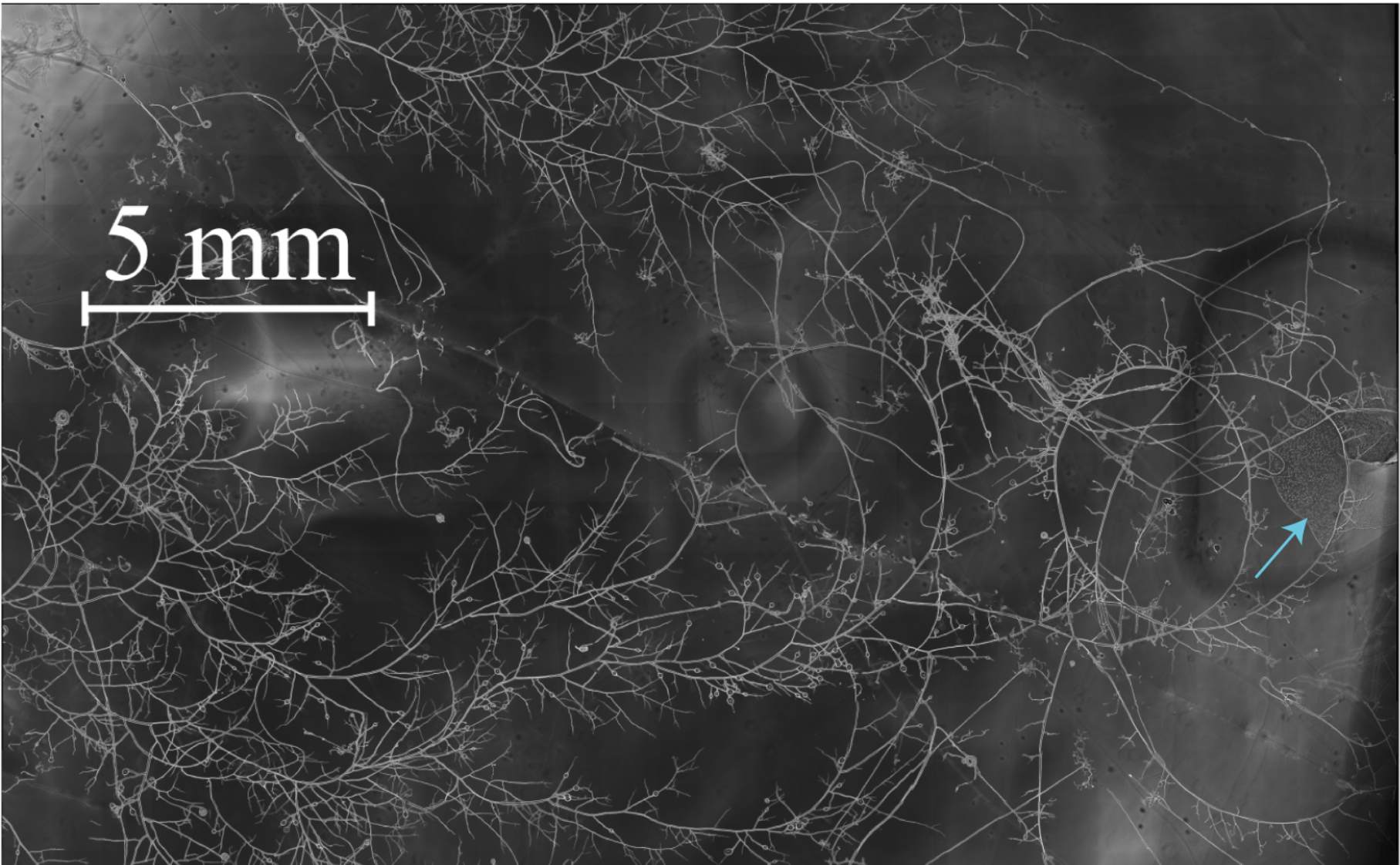
5 mm

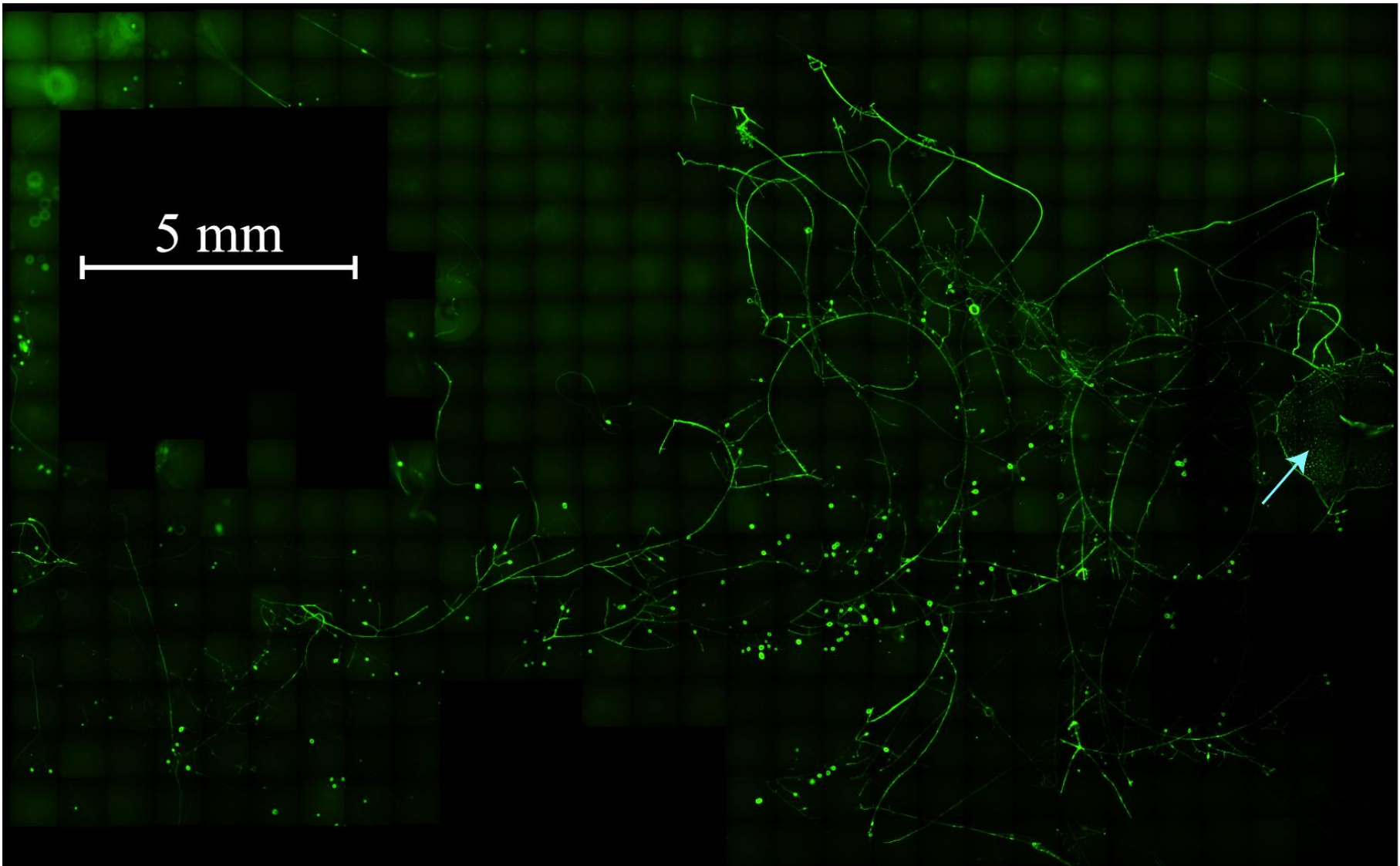
5 mm

Figure 2-14: Colonization of *B. velezensis* along the entire network of *R. irregularis.* Macroscopic view of the colonization of GFP tagged strain *B. velezensis* GA1 (Green colour in epifluorescence) along the hyphal network of *R. irregularis* 3 dpi of *B. velezensis*. Microscopic composite pictures were taken in bright field channel (**A**) and in epifluorescence (**B**) The blue arrow shows the inoculation drop area on the AM fungal hyphal network.

Given that *B. velezensis* is traditionally considered an archetypal root-associated *Bacillus*, we aimed to determine whether its colonization dynamics and efficiency differ between root tissues and AM fungal hyphae. To address this, two complementary experiments were conducted. In the first experiment (**Figure 2-15 A, B**), we assessed the expansion rate, or colonization speed, of *B. velezensis* on both *D. carota* **hairy roots** and *R. irregularis* hyphae using time-lapse microscopy. The objective was to evaluate the bacterium ability to rapidly spread along the complex ERM network. For this analysis, we measured the distance travelled by fluorescently labeled (GFP-tagged) bacterium along hyphae or roots over time, irrespective of direction, to capture the overall expansion potential across the available surface. The total length of colonized hyphae or root (in green) was quantified and divided by the number of days post-inoculation (dpi) to obtain a colonization speed (mm/day). We calculated an average expansion rate for the bacterium (colonization speed) of 5.6 mm/day on the surface of hyphae, which was significantly higher than observed for the colonization of *D. carota* hairy roots (1.2 mm/day) (**Figure 2-15 A**). It thus revealed a quite fast invasion of distal parts of the ERM by *B. velezensis* (**Figure 2-15 B**) compared to roots (**Figure 2-16 A**). In the second experiment (**Figure 2-15 C**), we evaluated bacterial colonization density by CFU (colony-forming unit) counting at 3, 7, and 14 dpi. Colonization was quantified on the first 2 cm of roots or AM fungal hyphae proximal to the inoculation site. To normalize between hosts, the data were expressed relative to the colonizable surface area, considering both the sampling length (2 cm) and the average diameter of roots and hyphae (Colonization density, CFU/mm^2) (**Figure 2-17**). To verify that this pattern was not specific to *D. carota* hairy roots, we also analysed root colonization of *Solanum tuberosum* plants. Data showed 20-fold higher populations at the surface of *R. irregularis* hyphae compared with *D. carota* roots (**Figure 2-15 C**) and *S. tuberosum* roots (**Figure 2-16 B**), further indicating that *B. velezensis* is more prone to colonize *R. irregularis* hyphae than roots in the early stage of interaction.

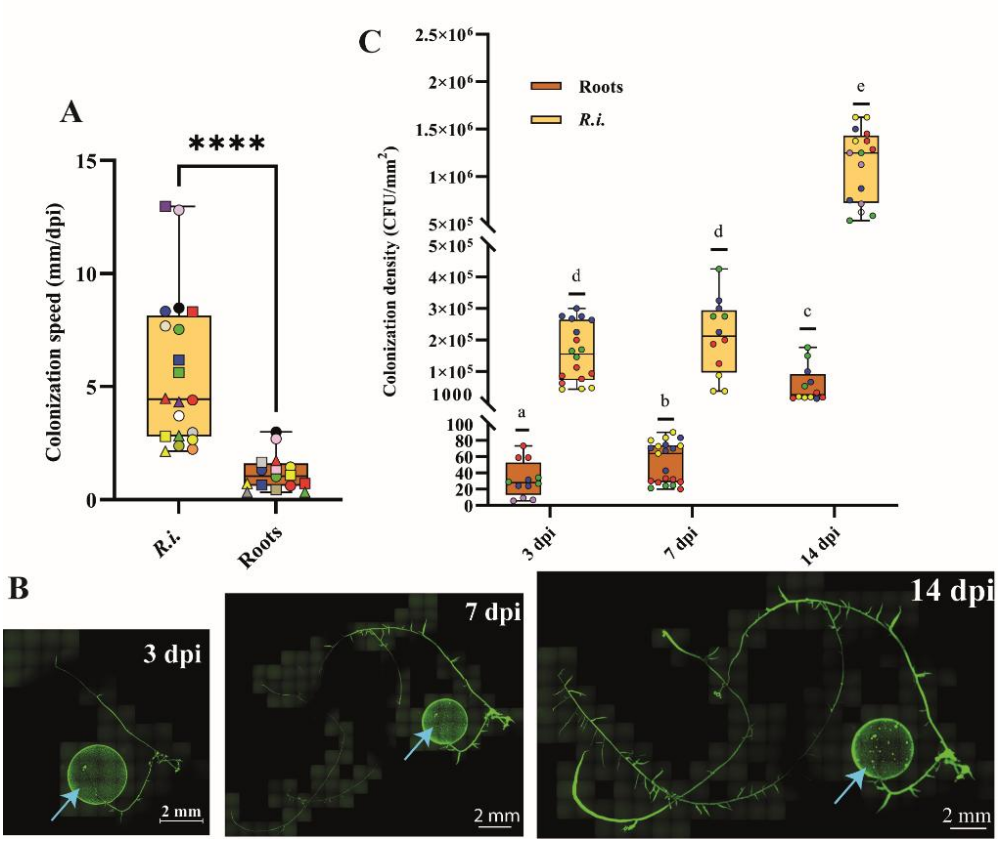

Figure 2-15: *B. velezensis* colonize effectively AM fungal hyphae compared to root. A, Colonization speed of *B. velezensis* along hyphae of 3 months-old cultures of *R. irregularis* (*R.i.* - yellow) and along *D. carota* hairy roots without *R. irregularis* (Roots – brown) during a time lapse of 14 days. The boxes encompass the 1st and 3rd quartiles, the whiskers extend to the minimum and maximum points, and the midline indicates the median. The individual points represent 7 to 11 biological replicates (different colour) and 1-3 technical replicates corresponding to the speed of colonization taken at different time point (measured 3 dpi = circle shape, 7 dpi = square shape and 14 dpi = triangle shape)(dpi = days post inoculation). The evolution of the speed of colonization over time can be followed for each replicate with the same colour. $12 \leq n \leq 24$; Student's t-test ($\alpha = 0.05$): **** = $p < 0.0001$. **B**, *B. velezensis* colonization along hyphae of 3 months-old cultures of *R. irregularis* overtime. Microscopic composite pictures were taken in epifluorescence. The blue arrow shows the inoculation drop area on the AM fungus hyphal network. The speed colonization is quantified by the measurement of the distance travelled by *B. velezensis* (green colour) from the inoculation drop (Blue arrow) divided by the dpi. **C**, Colonization density of hyphae of 3 months-old *R. irregularis* cultures (*R.i.*- yellow) or transformed roots of *D. carota* cultures (Roots - brown) 3, 7 and 14 dpi of *B. velezensis* The boxes encompass the 1st and 3rd quartiles, the whiskers extend to the minimum and maximum points, and the midline indicates the median. The individual points represent 4 at 6 biological replicates (different colour) and 1 at 6 technical replicates (same colour). $12 \leq n \leq 21$; one-way analysis of variance (ANOVA) and Tukey's HSD test ($\alpha = 0.05$). Groups with different letters differed significantly from each other.

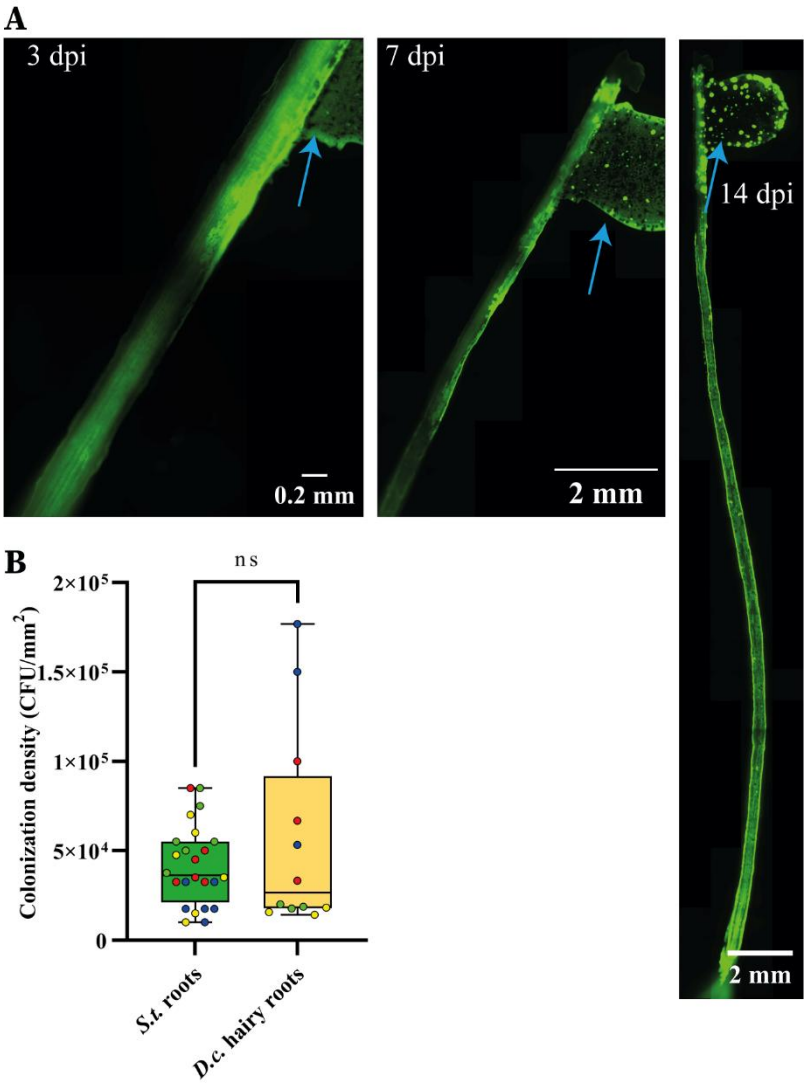

Figure 2-16: *B. velezensis* colonization along roots. A, *B. velezensis* colonization along a *D. carota*. transformed root. Microscopic composite pictures were taken in epifluorescence. The blue arrow show the inoculation drop area on the root. **B,** Colonization density of 3 months old cultures of *Solanum tuberosum* (*S.t.*) roots or transformed roots of *Daucus carota* (*D.c.*) 14 dpi of *B. velezensis.* The boxes encompass the 1st and 3rd quartiles, the whiskers extend to the minimum and maximum points, and the midline indicates the median. The individual points represent 4 biological replicates (different colours) and 3 at 6 technical replicates (same colours). $12 \leq n \leq 24$; student's t test ($\alpha = 0.05$): ns = not significant.).

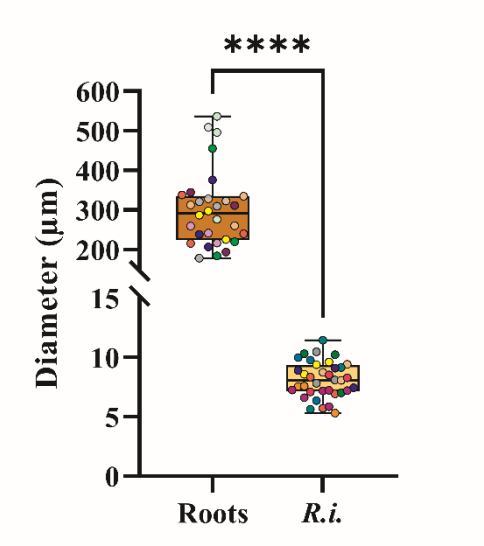

Figure 2-17: Determination of the available surface provide by *D. carota* and *R. irregularis* for the bacterial colonization. Diameter of *D .carota* roots or *R. irregularis* hyphae quantified by ImageJ Fiji. The boxes encompass the 1st and 3rd quartiles, the whiskers extend to the minimum and maximum points, and the midline indicates the median. The individual points represent 10 to 12 biological replicates (different colours) and 3 technical replicates (same colours). $30 \leq n \leq 36$. student's t test ($\alpha = 0.05$): **** = $p < 0.0001$.

Additionally, we assessed the colonization rate across different *Rhizophagus* species to determine whether the colonization potential of *B. velezensis* depends on the specific AM fungal partner considering the intrinsic genomic heterogeneity among AM fungal species and their differences in exudate profiles (Chen et al., 2018; Luthfiana et al., 2021; Zhou et al., 2025). Our results indicated that the bacterium was more prone to colonize the hyphae of *R. irregularis* compared to *R. clarus*, *R. aggregatus* and *R. intraradices*. (**Figure 2-18**). Even considering the lowest colonization rates on *R. aggregatus* and *R. intraradices*, bacterial populations on hyphae (644 ± 176.5 and 240.2 ± 49.95 CFU/mm², respectively; mean ± SD) were still at least 2.5 times higher than on roots (53.12 ± 24.98 CFU/mm²). These results underscore the influence of genetic diversity within the *Rhizophagus* genus on the interaction dynamics with *B. velezensis* and support the general trend of higher bacterial colonization on AM fungal hyphae compared to plant roots. This may be due to the formation of an homogeneous biofilm along hyphae while colonization of roots is known to occur at preferential zones via the formation of bacterial macrocolonies (Massalha et al., 2017; Stoll et al., 2021).

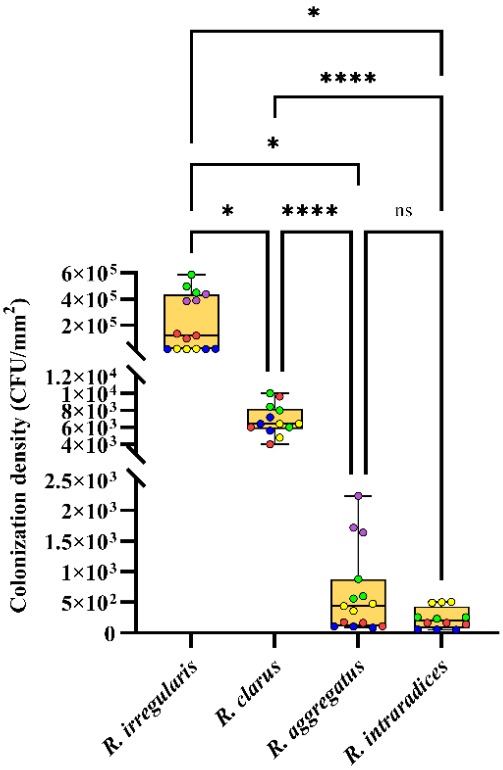

Figure 2-18: *B. velezensis* colonize effectively species of the *Rhizophagus* genus with a preference for *R. irregularis*. Colonization density of hyphae of 3-month-old *R. irregularis* MUCL 41833, *R. Clarus* MUCL 46238, *R. aggregatus* MUCL 49408 or *R. intraradices* 49410 cultures 7 dpi of *B. velezensis* The boxes encompass the 1st and 3rd quartiles, the whiskers extend to the minimum and maximum points, and the midline indicates the median. The individual points represent 4 at 5 biological replicates (different colour) and 3 technical replicates (same colour). $12 \leq n \leq 15$; one-way analysis of variance (ANOVA) and Dunnett test ($\alpha = 0.05$): ns = not significant; * $0.01 < p < 0.05$; ** $0.001 < p < 0.01$; *** $0.0001 < p < 0.001$; **** = $p < 0.0001$.

The difference in biofilm development observed between roots and AM fungal hyphae may result from variations in the bacterial subpopulations constituting the biofilm depending on the host. To explore this possibility, we quantified the proportion of spores within the biofilm formed on each host surface. Within a biofilm, a subpopulation of *B. velezensis* cells differentiates into spores, ensuring long-term persistence but also indicating that the bacterial community experiences environmental or physiological stress leading to sporulation (Charron-Lamoureux & Beauregard, 2019; Nicholson et al., 2000; Tan & Ramamurthi, 2014; Wahlen et al.,

2018). To estimate spore abundance, heat-treatment assays were performed to selectively quantify spores within the *B. velezensis* biofilm. Thus, we also observed that the relative proportion of spores compared to vegetative cells within the *B. velezensis* population colonizing the hyphae of *R. irregularis* was significantly lower (1.6 fold at 7 dpi) than the one colonizing *D. carota* roots (**Figure 2-19**). This high proportion of metabolically active cells in the AM fungal-associated biofilm may thus also reflect a bacterial community more prompt to colonize the fungal host than plant roots.

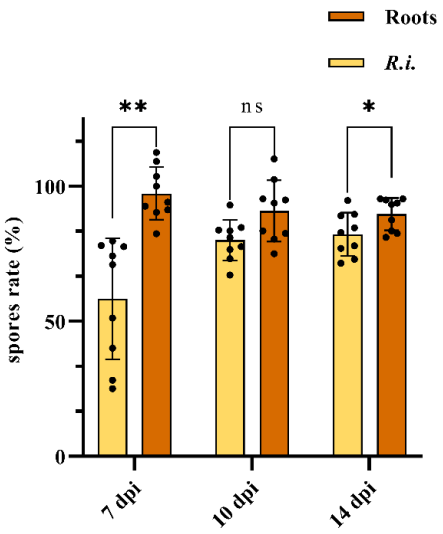

Figure 2-19: Proportion of *B. velezensis* spores within biofilms formed along AM fungal hyphae and plant roots. Spore proportion relative to the total bacterial population during colonization of *R. irregularis* hyphae and *D. carota* hairy roots (3 months old) at 7, 10, and 14 days post-inoculation (dpi). Bars represent the means ± SD of 9 biological replicates. n =9; ns = not significant; Mixed-effects model and Šídák's multiple comparisons test ($p < 0.05$): * $0.01 < p < 0.05$; ** $0.001 < p < 0.01$.

To further investigate the ecological significance of the *R. irregularis* ERM colonization by *B. velezensis*, we examined whether the fungus enhances the ability of *B. velezensis* to explore and colonize the surrounding environment. Given that the ERM forms CMNs interconnecting different plants, we specifically assessed whether these fungal structures facilitate bacterial colonization toward new hosts. This allowed us to explore potential ecological advantages for *B. velezensis* in colonizing the hyphosphere.

To evaluate *B. velezensis* colonization under more realistic conditions, we established a dual-compartment system using mycorrhized *S. tuberosum* plants in greenhouse conditions. We used a custom made setup with two pots (Basiru et al., 2023; Emmett et al., 2021; Wang et al., 2023a), each containing a single plant, connected by a plastic tube covered at both ends with a thin nylon mesh (50 µm diam. porosity) allowing only hyphae of *R. irregularis* to connect both plants (**Figure 2-20 A**). In that system, the bacterium inoculated on the mycorrhized plant was able to reach the plant in the other pot only by colonizing the hyphae connecting the two plants (**Figure 2-20 B**). Selective plate counting of *B. velezensis* among the bacterial community naturally present in the substrate was based on antibiotic resistance and fluorescence of GFP-tagged GA1. The abundance of *R. irregularis* was quantified by qPCR targeting a strain-specific housekeeping gene (**Figure 2-20 C**). To convert qPCR copy numbers into fungal biomass, we established a calibration curve correlating known AM fungal dry weight with qPCR signal (**Figure 2-21**). For calibration, extraradical mycelium of *R. irregularis* was harvested from the hyphal compartment of *in vitro* bi-compartmental cultures (**Figure 2-8**). Measured amounts of this material were added to 500 mg of soil substrate before DNA extraction, allowing the conversion of qPCR copy numbers to milligrams of fungal biomass (mg *R.i.* g^{-1} sample) (Buysens et al., 2017; Whiteside et al., 2019). Standard curves were generated using DNA extracted from *in vitro* grown *R. irregularis* spores and mycelium (**Figure 2-21**). Data first revealed that plant roots associated with *R. irregularis* (Pot 1+R.i.) exhibited a significantly higher number of GA1 CFUs compared with non-mycorrhized plants (Pot 1-R.i.), indicating that the presence of *R. irregularis* favours *B. velezensis* root colonization also in these conditions (**Figure 2-20 B**). Moreover, our results showed that *B. velezensis* inoculated on a plant associated with *R. irregularis* (Pot 1+R.i.), was able to colonize a non-bacterized neighbouring plant (Pot 2+R.i.) via the CMN connecting both plants. In the control system without *R. irregularis* (Pot 1-R.i.), no bacterial cells were detected on the plant in Pot 2, 20 dpi (**Figure 2-20 B**). These findings indicate that the association with *R. irregularis* facilitates the transfer of *B. velezensis* cells from one root system to another much faster than expected via passive diffusion.

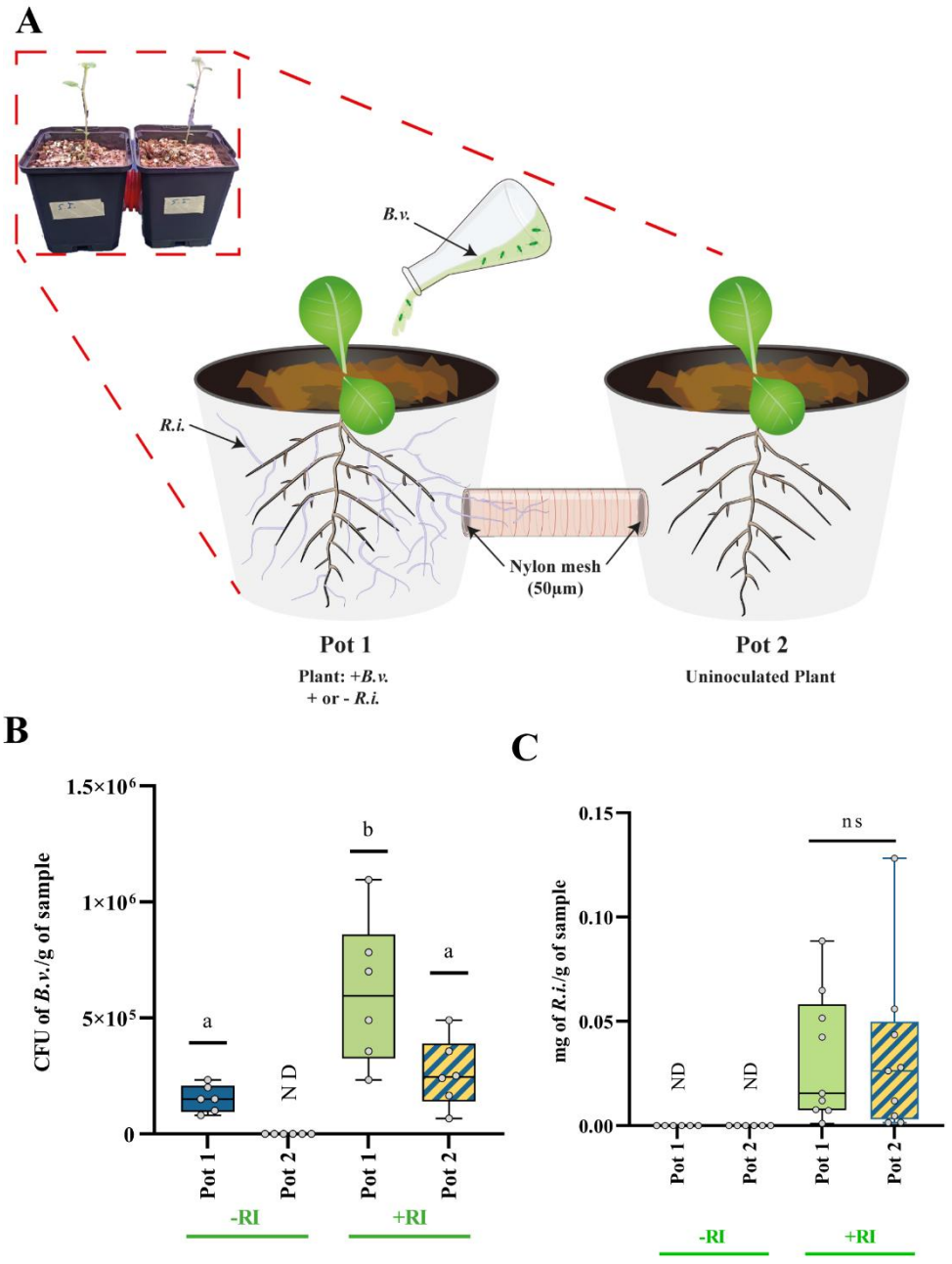
A
B.v.
R.i.
Nylon mesh
(50µm)
Pot 1
Plant: +B.v.
+ or - R.i.
Pot 2
Uninoculated Plant
B
CFU of B.v./g of sample
1.5×10⁶
1×10⁶
5×10⁵
0
a
N D
b
a
Pot 1
Pot 2
Pot 1
Pot 2
-RI
+RI
C
mg of R.i./g of sample
0.15
0.10
0.05
0.00
ND
ND
ns
Pot 1
Pot 2
Pot 1
Pot 2
-RI
+RI

Figure 2-20: Common Mycorrhizal Network-mediated dissemination of *B. velezensis* between plants. **A**, Picture (red square) and schematic view of the experimental design in which two plants of *Solanum tuberosum* (Pot 1 and Pot 2) were connected by a tube with both ends closed with a nylon mesh of 50 µm porosity. The nylon barrier prevented the passage of roots. During the planting, the Pot 1 was inoculated (+ R.i.) or not (-R.i.) with *R. irregularis*. After 5 month of growth, the plants associated or not with *R. irregularis* in Pot 1 were inoculated with *B. velezensis*. The Plants in Pot 2 were not inoculated with any microorganisms. **B**, Bacterial population of GFP tagged strain *B. velezensis* GA1 quantified by plate-counting of colony forming units (CFU) by gram of sample, 10 dpi. All the plants in pot 1 associated (+R.i.) or not (-R.i.) with *R. irregularis* were inoculated with *B. velezensis*. Plants in pot 2 were not inoculated with any microorganisms. The boxes encompass the 1st and 3rd quartiles, the whiskers extend to the minimum and maximum points, and the midline indicates the median. The individual points represent 6 biological replicates (6 different systems). n = 6; one-way analysis of variance (ANOVA) and Tukey's HSD test (α = 0.05). Groups with different letters differed significantly from each other. ND = no detected. **C,** Fungal population of *R. irregularis* quantified by qPCR reported by gram of sample (mg of R.i. /g of sample). All the plants in pot 1 associated (+R.i.) or not (-R.i.) with *R. irregularis* were inoculated with *B. velezensis*. Plants in pot 2 were not inoculated with any microorganisms. The individual points represent 9 biological replicates (9 systems). n =9; one-way analysis of variance (ANOVA) and Tukey's HSD test (Honestly significantly different, α = 0.05): Groups with different letters differed significantly from each other at an α of 0.05.ND= no detected.

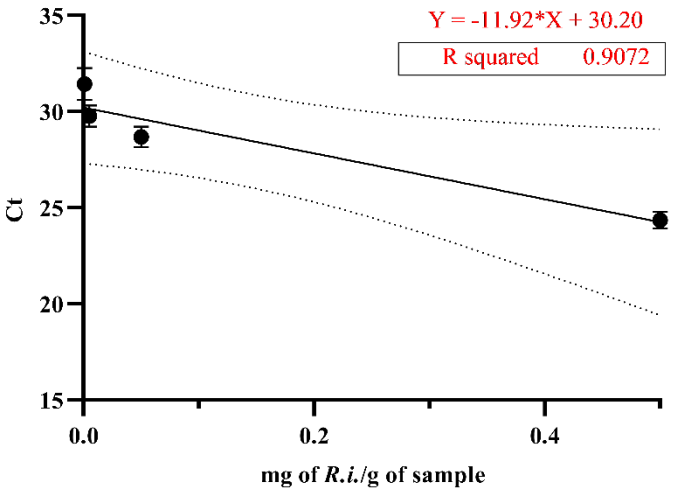

Figure 2-21: Calibration curve used for the quantification of AM fungal biomass in the greenhouse experiment. Relationship between AM fungal biomass and Cycle threshold (Ct) value. n=9.

2.4 The surfactin lipopeptide contributes to *B. velezensis* colonization of the hyphosphere

Bacterial fitness can be influenced by secondary metabolites playing key roles in various developmental processes including motility and biofilm formation (Balleux et al., 2025; Cao et al., 2018; Ghelardi et al., 2012; Luo et al., 2015). Thus, a range of mutants specifically repressed in the synthesis of BSMs were tested in order to determine their role in the AM fungal colonization potential of *B. velezensis.* The bacterial population at the surface of hyphae 7dpi was significantly reduced for all the knockout mutants unable to produce surfactin (**Figure 2-22**). No other non-ribosomal BSMs were involved in hyphal colonization as indicated by the similar loss in colonization ability observed for the Δ***sfp*** mutant (repressed in **4′-phosphopantetheinyl transferase** which is essential for the proper functioning of non-ribosomal peptide biosynthesis machineries), and other double or triple mutants unable to produce at least surfactin (**Figure 2-22 A**). In *B. velezensis*, it has been shown that surfactin deficiency causes impaired biofilm formation, the strains becoming unable to colonize roots (Al-Ali et al., 2018; Stoll et al., 2021). Based on these data, we wanted to confirm the production of surfactin by *B. velezensis* upon AM fungal colonization. Thus, we generated hyphosphere extracts obtained upon *B. velezensis* colonization of the hyphae in *in vitro* system that were analysed next by UPLC-qTOF-MS optimized for detection of nanomolar amounts, quantification and structural characterization of non-ribosomal BSMs. Based on exact mass and retention time compared with standards, we observed substantial amounts of surfactin (as a mixture of homologues that differ in the length of the fatty acid chain, **Figure 2-22 B**) at concentrations close to the micromolar range (0.605 µM in average at 9 dpi). This confirmed that *B. velezensis* cells in biofilm associated with *R. irregularis* readily secrete this cLP, which significantly contributes to colonization.

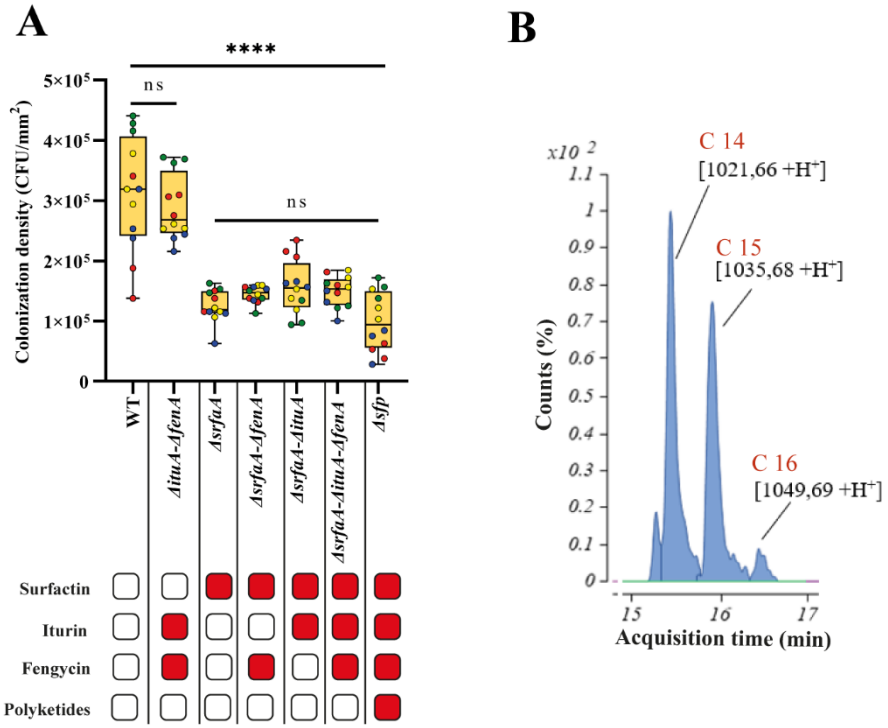

Figure 2-22: Surfactin production by *B. velezensis* is essential to have an optimal AM fungal colonization. A, Colonization density of hyphae of 3 months-old *R. irregularis* cultures 7 dpi of *B. velezensis* wild type (WT) and mutants unable to produce one or several bioactive secondary metabolites (BSMs). Metabolites not produced by the different mutants are illustrated with red boxes in the table below. The boxes encompass the 1st and 3rd quartiles, the whiskers extend to the minimum and maximum points, and the midline indicates the median. The individual points represent 4 biological replicates (different colour) and 3 technical replicates (same colour). n = 12; one-way analysis of variance (ANOVA) and Tukey's HSD test ($\alpha = 0.05$). ns = not significant; **** $p < 0.0001$. **B,** UPLC-MS extract ion chromatogram (EIC) illustrating the relative abundance of surfactin (blue) secreted by *B. velezensis* 9 dpi on hyphae of a 3 months-old *R. irregularis* culture. The different peaks correspond to the structural variants differing in fatty acid chain length (Surfactin, C14 to C16), the number in red represent the length of the fatty acid tail.

2.5 *B. velezensis* associates with *R. irregularis* in a compatible interaction

B. velezensis efficiently colonized the hyphae of *R. irregularis* but this bacterium is a strong producer of antimicrobials that may affect the fungus. We thus next wanted to evaluate the impact of *B. velezensis* on hyphae viability. We first measured succinate dehydrogenase (SDH) activity as an indicator of AM fungal viability by histochemical staining (Schaffer & Peterson, 1993) (**Figure 2-23 A**). Image analysis revealed that the enzymatic activity did not differ between non-colonized and colonized hyphae (**Figure 2-23 B**) indicating that the presence of the bacterium did not influence adversely the respiratory metabolism of *R. irregularis*. We also monitored by time lapse microscopy imaging, the impact of *B. velezensis* on the cytoplasmic flow within hyphae which is considered as functional trait of AM fungi, allowing the translocation of resources from plant to fungus and vice-versa and somehow reflecting fungal vitality (**Videos 4** and **5**) (Bago et al., 2002; Hammer et al., 2024; Oyarte Galvez et al., 2025; Whiteside et al., 2019).

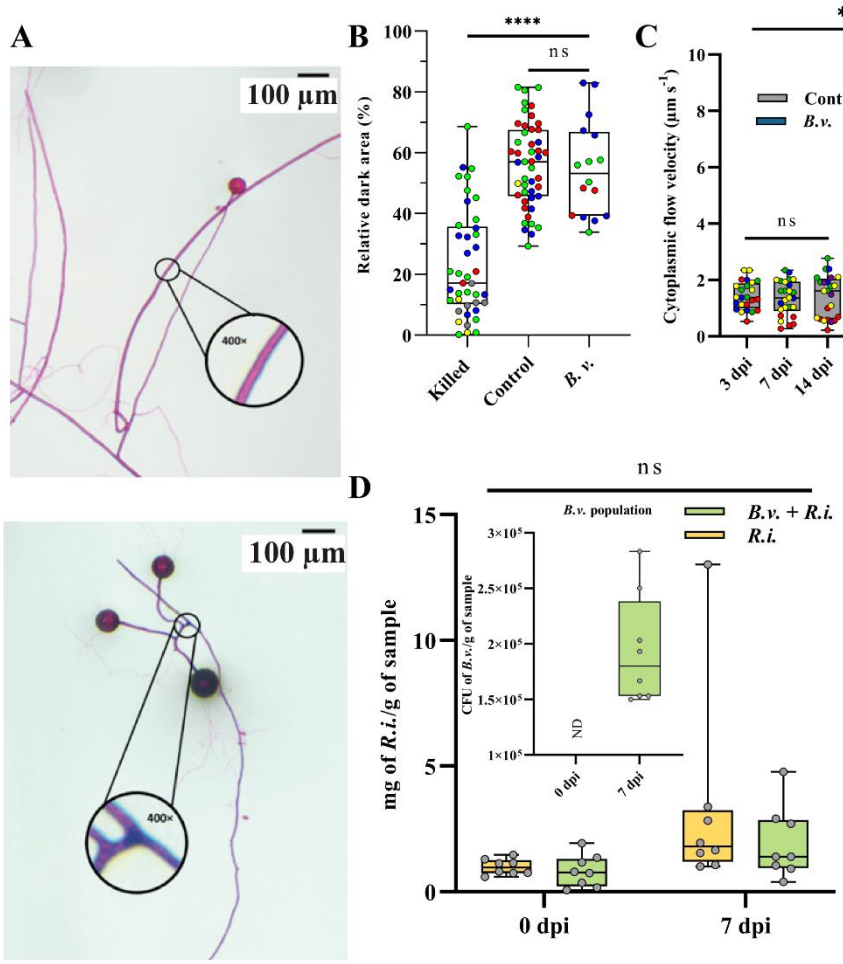
A
100 µm
400×
100 µm
400×
B
****
ns
Relative dark area (%)
Killed
Control
B. v.
C
****
ns
Control
B.v.
ns
Cytoplasmic flow velocity (µm s-1)
3 dpi
7 dpi
14 dpi
3 dpi
7 dpi
14 dpi
D
ns
B.v. population
B.v. + R.i.
R.i.
CFU of B.v./g of sample
ND
0 dpi
7 dpi
mg of R.i./g of sample
0 dpi
7 dpi

Figure 2-23: *B. velezensis* colonization does not impair *R irregularis* viability. A, Histochemical determination of succinate dehydrogenase (SDH) activity indicating respiratory metabolism of *R. irregularis* hyphae. (Bottom) Control (with physiological water) showing dark blue-violet zones corresponding to SDH activity. (Top) killed hyphae (with formaldehyde) showing pink colour corresponding to dead hyphae. Pictures of stained hyphae of a 3 months-old culture of *R. irregularis* were taken with the stereomicroscope. The images presented are representative examples selected from independent samples repeated on minimum 3 biological replicates. **B**, Relative dark area corresponds to potential SDH activity of *R. irregularis.* colonized by *B. velezensis* (*B.v.*) 14 dpi along hyphae of 3 months-old cultures of *R. irregularis*, compared to killed hyphae (with formaldehyde 2%) and the control (treated with physiological water). The boxes encompass the 1st and 3rd quartiles, the whiskers extend to the minimum and maximum points, and the midline indicates the median. The individual points represent 3 to 5 biological replicates (different colours) and 1 to 20 technical replicates (same colours). $16 \leq n \leq 47$; one-way analysis of variance (ANOVA) and Tukey's HSD test ($\alpha = 0.05$): ns = not significant; **** = $p < 0.0001$. **C**, Cytoplasmic flow velocity in hyphae of *R. irregularis* in presence or absence of GFP-tagged *B. velezensis.* measured 3, 7 and 14 dpi. The boxes encompass the 1st and 3rd quartiles, the whiskers extend to the minimum and maximum points, and the midline indicates the median. The individual points represent 4 to 8 biological replicates (different colours) and 4 to 6 technical replicates (same colours). $18 \leq n \leq 24$; one-way analysis of variance (ANOVA) and Tukey's HSD test ($\alpha = 0.05$): ns = not significant; **** $p < 0.0001$. **D**, Fungal population of *R. irregularis* (*R.i.*) quantified by quantitative PCR reported by gram of roots sampled with attached substrate/rhizopsheric soil (mg of *R.i.* /g of sample), 0 and 7 dpi of plants treated with inoculum of *B. velezensis* (*B.v.+R.i.*, green) or with a solution without any microorganism (*R.i.*, yellow). The boxes encompass the 1st and 3rd quartiles, the whiskers extend to the minimum and maximum points, and the midline indicates the median. The individual points represent 8 biological replicates (8 different plants). $n = 8$; one-way analysis of variance (ANOVA) and Tukey's HSD test ($\alpha = 0.05$): ns = not significant between each time and each condition. Inside the graph is included the bacterial population of *B. velezensis* in the treatment combining *B. velezensis* and *R. irregularis* (*B.v.+R.i.*, green), before the inoculation of the bacterium and 7 dpi of *B. velezensis*

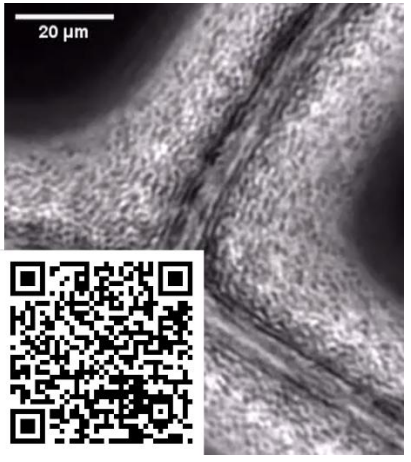

Video 3: Live imaging of the cytoplasmic flow velocity inside *R. irregularis* hyphae colonized by *B. velezensis* 3 days post-inoculation of the bacterium. **https://youtube.com/shorts/jI4bMXfH_2Q?feature=share**

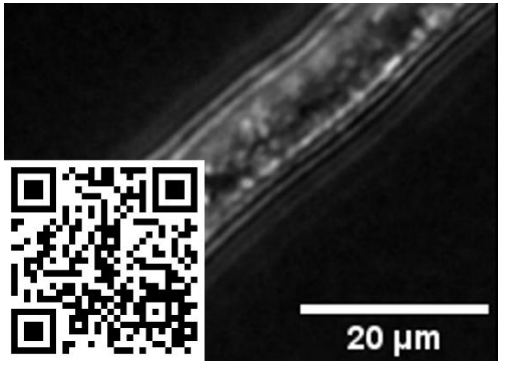

Video 4: Live imaging of the cytoplasmic flow velocity inside *R. irregularis* hyphae before processed using Manual tracking plug-in within the Tracking tool in the Plug-in menu in Fiji. **https://youtu.be/MqO17p40cfE**

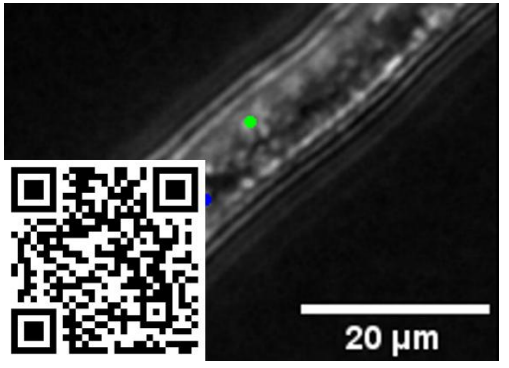

Video 5: Live imaging of the cytoplasmic flow velocity inside *R. irregularis* hyphae processed using Manual tracking plug-in within the Tracking tool in the Plug-in menu in Fiji. The video illustrates the tracking of two particle chosen in Video S4, moving in both direction of the flow. The overlay dots and lines (green and blue) show the manual tracking performed to follow each particle. **https://youtu.be/bH9psdjD22w**

As previously reported by Whiteside et al. (2019) and more recently by Hammer et al. (2024) and Oyarte Galvez et al. (2025), we observed bidirectional cytoplasmic flows within the hyphae of *R. irregularis*, with different velocities depending on the direction of movement (**Figure 2-24**). However, due to the large and mature ERM networks used in our system, it was not possible to accurately determine the directionality of flow (e.g., from root to hyphal tip or vice versa), as was done in studies using young networks (Oyarte Galvez et al., 2025; Whiteside et al., 2019). For this reason, we chose to express our data as the average of velocities measured in both directions. Interestingly, the cytoplasmic flow velocities measured in our setup were lower than those reported in previous studies. For example, Whiteside et al. (2019) documented an average speed of 18.8 µm/s using a similar *in vitro* system. Multiple factors may account for these differences:

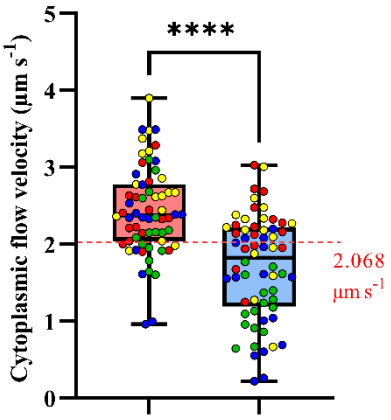

Figure 2-24: Bidirectional cytoplasmic flow in hyphae of *R. irregularis* (3-month-old ERM systems). In all measurements, the flow in one direction was faster (red box) compared to the other direction (blue box). The red line indicates the median from all the data grouped. The boxes encompass the 1st and 3rd quartiles, the whiskers extend to the minimum and maximum points, and the midline indicates the median. The individual points represent 4 biological repetitions (different colours) and 16 technical replicates (same colour). n=64; Unpaired t test: **** = $p < 0.0001$.

First, the method of measurement differs. We initially attempted to use the TrackMate plugin in Fiji, as described by Whiteside et al. (2019). However, this automated approach proved difficult to apply under bacterial co-culture conditions. TrackMate misidentified bacterial cells as fungal organelles leading to erroneous velocity estimates in early post-inoculation stages. Consequently, we opted for manual tracking using the Fiji plugin "Manual Tracking" (Tinevez et al., 2017). In each video, at least 8 fungal particles were tracked for a minimum of 10 frames (at 10 fps over 10 seconds). The velocity was calculated individually for each object. Our

methodology is consistent with that of Hammer et al. (2024), who reported comparable flow velocities (average 3.7 µm/s, maximum 5.3 µm/s) (Cargill et al., 2025; Oyarte Galvez et al., 2025).

Second, the medium used in the hyphal compartment may play a role. Phytagel supplemented with sucrose was used in the root compartment to ensure optimal development of roots and their mycorrhization. In the other compartments, we used high-purity agarose with no added sugar to avoid the residual growth of the bacterium observed on phytagel and agar-solidified media. In this way, we ensured that the bacterial growth on hyphae was exclusively due to exudate consumption. To evaluate the impact of the medium, we tested phytagel in the hyphal compartment (as in Whiteside et al. 2019) and observed a two times higher velocity of the cytoplasmic flow compared with agarose (see **Figure 2-25 A**). Thus, the nature of the gelling agent used in our systems represents an additional factor that may explain the low flow velocities observed.

A third possible explanation can be related to our specific setup using mature and fully developed ERM networks. We performed bacterial inoculation and thus speed measurements in the most distal parts of the network relative to the RC. We used this setup to accurately follow bacterial spatio-temporal colonization first, on isolated hyphal segments (in not overcrowded zones) and second, to make measurements over 7-14 days with no risk that the bacterium invades the root compartment. Thus, the lower flow we observed can be explained by the fact that we performed our analyses on runner hyphae, not close to spores and distant from roots in a mature network presenting BAS and spores (Oyarte Galvez et al., 2025). However, we used plates presenting spores and a well-established hyphal network because we wanted to evaluate the development of the bacterium in a complex ERM. To test the possible influence of distance from the roots, we performed additional measurements of cytoplasmic flow velocity in runner hyphae developing in two different zones in the hyphal compartment. We observed a significantly slower (2 times) flow in area at approx. 2.5 cm from the RC compared to hyphae closer to the RC (1.5 cm) (**Figure 2-25 B**). We observed that at the distance where the measurements were performed (2.5 cm from the RC), the velocity is two times lower than the flow measured close to the root compartment (1.5 cm from the RC). Thus, the distance from the roots is important and influences the velocity of the flow measured in the ERM, which may explain the differences reported in various studies like observed in Oyarte Galvez et al. (2025).

The last potential explanation for the difference in velocity is intrinsic to our strain. Indeed, when we compared the cytoplasmic flow velocity of *R. irregularis* MUCL 41833 with other species inside the *Rhizophagus* genus, we observed that this strain had the lowest flow among the four AM fungal species used (**Figure 2-19**). Thus, the difference in velocity within the *Rhizophagus* genus and between studies like Whiteside et al. (2019), Oyarte Galvez et al. (2025) and Hammer et al, (2024) using other strains of *R. irregularis*, can be explained by possible intraspecies and interspecies variations.

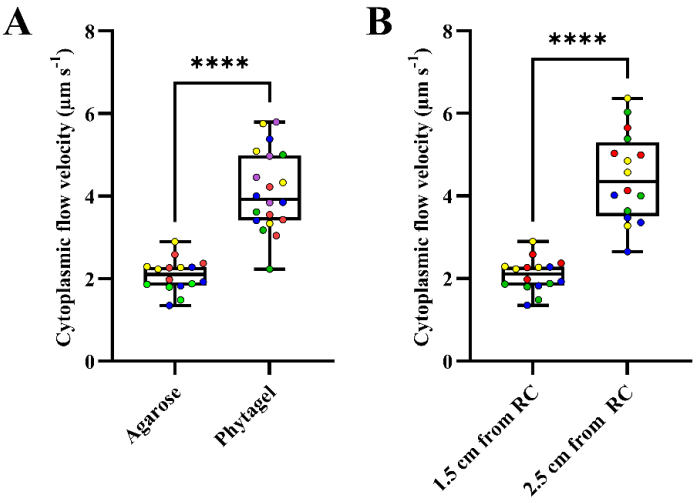

Figure 2-25: Impact of the experimental set-up on the cytoplasmic flow velocity inside hyphae of 3-month-old *R. irregularis* culture. A, Impact of the medium used in the HC compartment. The boxes encompass the 1st and 3rd quartiles, the whiskers extend to the minimum and maximum points, and the midline indicates the median. The individual points represent 4 at 5 biological replicates (different colors) and 4 technical replicates (same color). 16≤ n ≤ 20; Unpaired t test: **** = $p < 0.0001$. **B,** Impact of area selected for measurements at two distances from the RC. n =16; Unpaired t test: **** = $p < 0.0001$.

However, flow velocity inside non-colonized (**Video 4**) or colonized hyphae (**Video 3**) remained stable over time, as observed at 3 and 14 dpi. However, the presence of the bacterium increased the cytoplasmic flow velocity compared to non-colonized hyphae whatever the time of observation (**Figure 2-23 C**). This indicates that bacterial colonization enhances cytoplasmic dynamics without impairing fungal fitness. To confirm this under more realistic conditions, we evaluated whether *B. velezensis* affected AM fungal colonization of tomato roots in a greenhouse assay. The results

showed no reduction in *R. irregularis* colonization in the presence of the bacterium. (**Figure 2-23 D**).

To determine whether cytoplasmic flow dynamics influence or correlate with bacterial colonization efficiency, we compared flow velocities across four *Rhizophagus* species using the same experimental system employed for colonization assays (**Figure 2-18**). Interestingly, we found that *R. irregularis* exhibited the lowest baseline flow velocity (2.080 ± 0.3947 µm/s), at least 1.6 times slower than the other species tested, *R. aggregatus* (3.493 ± 0.6364 µm/s), *R. intraradices* (3.608 ± 1.075 µm/s), and *R. clarus* (4.460 ± 1.597 µm/s) (**Figure 2-26 A**). However, this lower basal velocity did not translate into reduced bacterial colonization, *B. velezensis* colonized *R. irregularis* hyphae more efficiently than the other AM fungal species.

These results indicate that a higher initial cytoplasmic flow velocity is not predictive of enhanced bacterial colonization. Instead, we observed that the most substantial increase in cytoplasmic flow velocity occurred specifically in *R. irregularis* upon colonization by *B. velezensis* (**Figure 2-26 B**), correlating with the highest bacterial colonization rates (**Figure 2-18**). Conversely, species that exhibited higher basal flow velocities supported lower levels of bacterial colonization and showed only moderate increases in flow velocity upon *Bacillus* interaction (**Figure 2-26 B**).

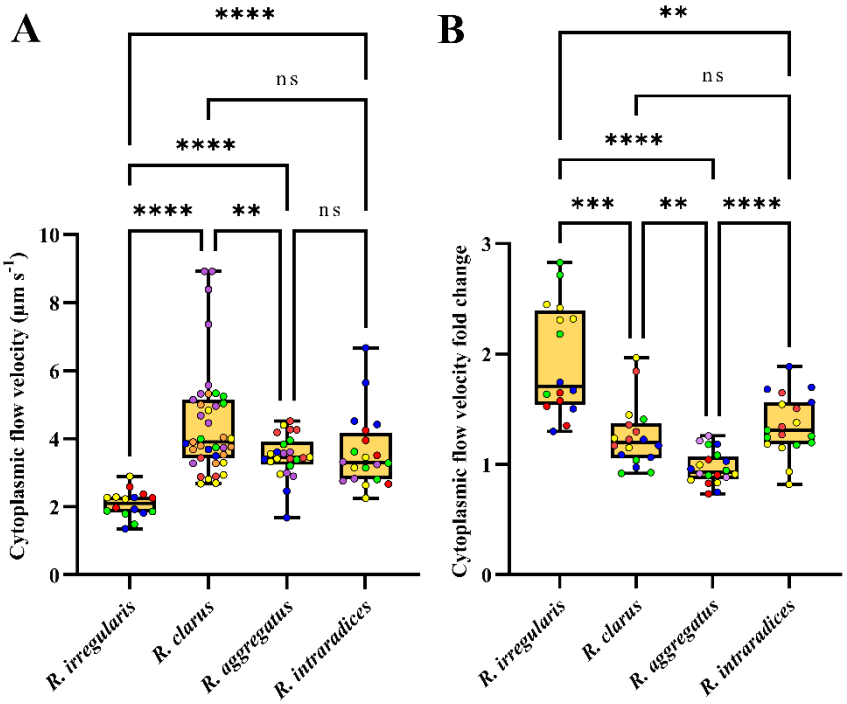

Figure 2-26: Cytoplasmic flow velocity in AM fungi and its modulation following *B. velezensis* colonization. A, Basal cytoplasmic flow velocity of four *Rhizophagus* species, Cytoplasmic flow velocity in hyphae of 3-month-old *R. irregularis* MUCL 41833, *R. intraradices* MUCL 49410, *R. clarus* MUCL 46238 and *R. aggregatus* 49408. **B,** Fold change in cytoplasmic flow velocity at 7 dpi with *B. velezensis*, normalized to the baseline (pre-inoculation) velocity for each fungal species. Fold change values indicate the relative increase in streaming velocity induced by bacterial colonization. The boxes encompass the 1st and 3rd quartiles, the whiskers extend to the minimum and maximum points, and the midline indicates the median. The individual points represent 4 to 5 biological replicates (different colours) and 4 to 6 technical replicates (same colours). $16 \leq n \leq 20$; one-way analysis of variance (ANOVA) and Brown-Forsythe ANOVA test ($\alpha = 0.05$): ns = not significant; * $0.01 < p < 0.05$; ** $0.001 < p < 0.01$; *** $0.0001 < p < 0.001$; **** = $p < 0.0001$

2.6 Summary: *B. velezensis* and AM fungi an unsuspected partnership

RQ 1: Could fungal killers like *B. velezensis* and an AM fungus establish a stable cohabitation? YES.

We demonstrate that the AM fungus *R. irregularis* provides carbon-rich resources that support the growth and persistence of *B. velezensis* in the hyphosphere (**Figure 2-27**). Our data show that *B. velezensis* promptly colonizes the ERM of AM fungi with a higher efficiency than plant roots, strongly suggesting that this bacterium preferably associates with AM fungi than with plants. Remarkably, the bacterium exploits the fungus as "highways" for soil exploration, enabling its dispersal across the hyphal network and facilitating the colonization of neighbouring plants via the CMN that interconnects root systems. We also identified that surfactin, a major lipopeptide produced by *B. velezensis*, plays a critical role in its successful colonization of the hyphosphere,

Despite its antifungal potential, *B. velezensis* establishes a non-destructive and compatible interaction with *R. irregularis*. The fungus maintains viability in the presence of the bacterium, as evidenced by sustained cytoplasmic flow, a marker of metabolic activity often associated with nutrient transport efficiency. Greenhouse experiments further confirmed that co-inoculation with *B. velezensis* does not impair AM fungal colonization of plant roots, indicating functional compatibility *in planta*.

Together, these results reveal an unexpected compatibility between the two microorganisms, suggesting potential mutual ecological advantages but also raising intriguing questions about the mechanisms underlying such cohabitation.

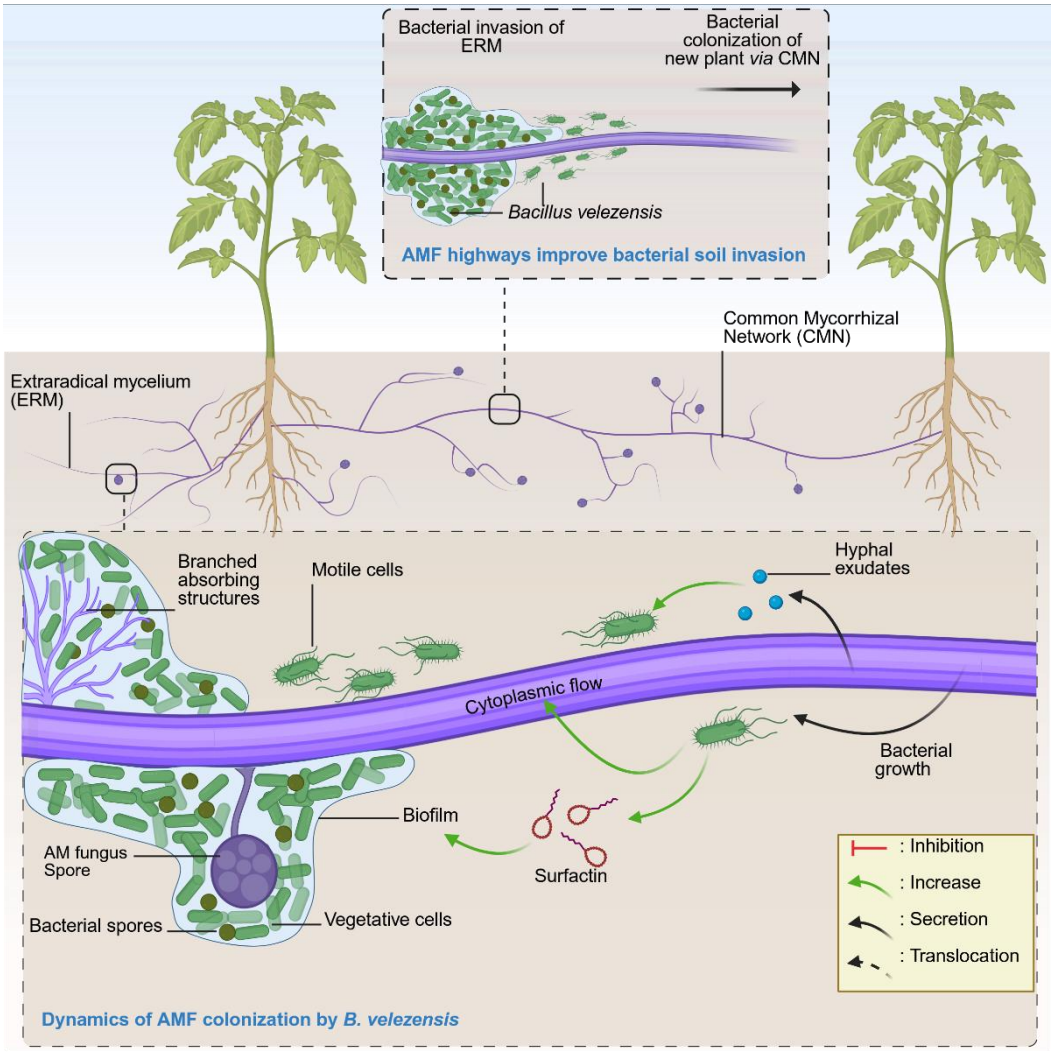

Figure 2-27: Schematic summary of the unsuspected partnership between *B. velezensis* and *R. irregularis*. Illustration of the colonization dynamics of *B. velezensis* in association with *R. irregularis*, emphasizing key stages in bacterial attachment, biofilm formation, and dispersal along the ERM. It highlights the hyphae-mediated spread of *B. velezensis* through the soil and across the CMN, facilitating the colonization of neighboring plants. The schematic also outlines the ecological advantages conferred to the bacterium, including access to fungal-derived carbon sources. This interaction exemplifies an unsuspected, yet functionally compatible, interkingdom association between a known antifungal bacterium and an AM symbiotic fungus. Figure was created with Biorender.com.

Chapter 3

Molecular dialogue across kingdoms

3.1 State of the art

The soil, especially the rhizosphere, is an ecological hotspot where a multitude of (micro)organisms coexist and interact (Nayfach et al., 2021). Competition in this context is traditionally defined as the struggle between organisms sharing the same ecological niche for resources such as space and nutrients. To thrive in this competitive environment, microorganisms have evolved diverse strategies. Among these microbes, *Bacillus* species stand out due to their adaptability underpinned by sophisticated mechanisms of environmental sensing and communication (Andrić et al., 2020; Arnaouteli et al., 2021; Balleux et al., 2025; Boubsi et al., 2023; Jautzus et al., 2022; Kalamara et al., 2018; Xie et al., 2024).

3.1.1 Environmental sensing and behavioural plasticity in *Bacillus* spp.

By detecting environmental signals, *Bacillus* modulates its behaviour and phenotypic responses through global regulatory networks (Bischofs et al., 2009; Gallegos-Monterrosa & Kovács, 2023; Grau et al., 2015; Romero, 2013). A pivotal communication mechanism employed by *Bacillus* species is **quorum sensing**, which enables bacterial populations to coordinate physiological processes based on cell density (Babel et al., 2020; Bareia et al., 2017; Bischofs et al., 2009; Kalamara et al., 2018). Through quorum sensing, *Bacillus* stabilizes cooperative behaviour during biofilm formation among genetically identical ("self") or closely related ("kin") individuals by recognizing shared cooperative traits (Jautzus et al., 2022; Kalamara et al., 2018; Oslizlo et al., 2014; Romero, 2013). Surfactin is a central fitness factor in *Bacillus* spp., functioning as a self-signalling molecule that induces matrix production in biofilm-forming subpopulations (Oslizlo et al., 2014; Romero, 2013). It also enhances biofilm motility by promoting swarming and upregulating *hag* expression, a gene involved in flagellin synthesis (Ghelardi et al., 2012) . However, the role of surfactin in biofilm formation is not universal. For instance, *Bacillus subtilis* 3610 can form biofilms without surfactin (Thérien et al., 2020), suggesting alternative biofilm regulatory pathways in certain strains.

The competitive ability of *Bacillus* spp. is further enhanced by its arsenal of BSMs, which help combat competitors, often phytopathogens, and secure ecological niches through antibiosis or by modifying the surrounding environment to facilitate colonization (Andrić et al., 2020; Blake et al., 2021; Rabbee et al., 2019, 2023). However, the production of BSMs incurs a fitness cost, reducing growth rate particularly under nutrient-limited conditions (Hiller et al., 2024; Jautzus et al., 2022; Kafri et al., 2016; Sexton & Schuster, 2017). To balance these costs and benefits, *Bacillus* regulates BSM production through global regulatory networks, tailoring responses to environmental cues such as the presence of competitors, host plants, or its own population dynamics (**Figure 3-1**) (Kalamara et al., 2018; Théatre et al., 2021;

Zhu et al., 2023a). For instance, in response to other bacteria such as *Ralstonia solanacearum* and *Pseudomonas fuscovaginae*, *Bacillus* spp. overexpresses cLP and bacilysin BGCs (Almoneafy et al., 2014; Cao et al., 2018; Kakar et al., 2016). Likewise, the cocktail of BSMs is modulated when *Bacillus* is in interaction with *Pseudomonas* competitors (Andrić et al., 2023; Lyng & Kovács, 2023). The siderophore produced either by *Bacillus* (baccilibactin) and *Pseudomonas* have been shown to drive antagonistic interaction (Andrić et al., 2023; Lyng & Kovács, 2023). In *Bacillus,* the production of BSM has been shown to be induced upon the perception of peptidoglycan from competing bacteria, in a process mediated by the global regulator of cellular competence, ComA (Maan et al., 2022). This study further revealed that *B. subtilis* resolves the conflict between antibiotic production and growth by increasing transcription of NRPs/PKS only when competing against phylogenetically distant species. In few case, *Bacillus*

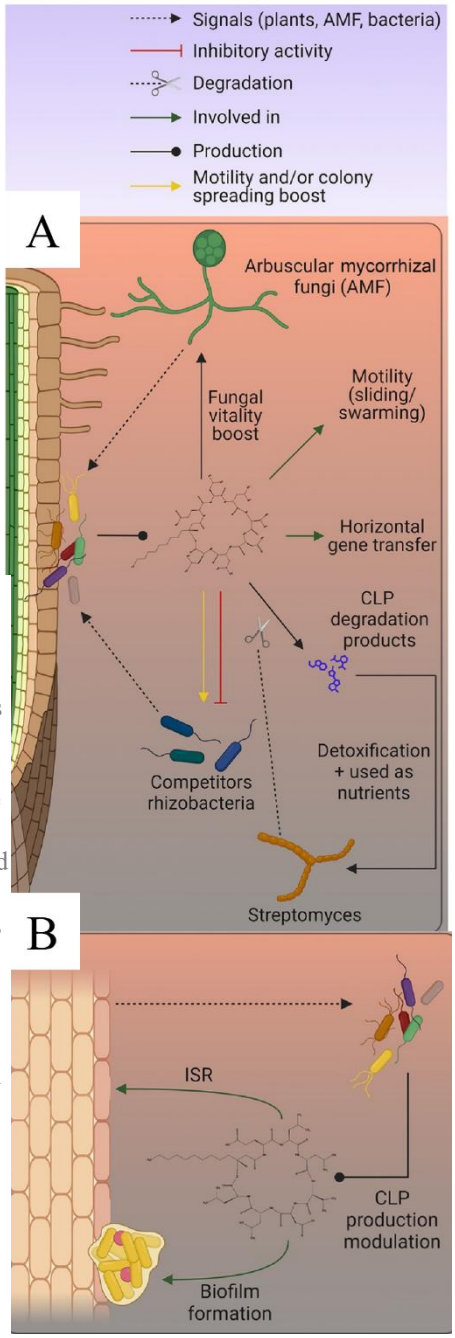

Figure 3-1: *Bacillus* adaptation, phenotypic plasticity, and BSMs production in response to surrounding organisms. A, BSMs in social and interspecies interactions. In response to exogenous cues, BSMs mediate commensal or mutualistic associations with other soil microorganisms. Beyond their roles in motility, certain cLPs can be biotransformed and utilized by *Streptomyces* species to sustain growth. Surfactin is also involved in horizontal gene transfer by modulating membrane permeability in closely related bacteria, leading to extracellular DNA (eDNA) release and enhanced genetic competence. By facilitating horizontal gene transfer, surfactin contributes to genetic diversification and ecological adaptability in *Bacillus* populations. **B,** Perception of plant cell wall polymers and root exudates by *Bacillus* triggers the production of cLPs, which act as elicitors of plant immunity and induce systemic resistance against pathogens. CLPs also promote biofilm formation on root surfaces, enhancing microbial colonization and plant protection. Illustration from Balleux et al. (2025).

exhibits **cryptic** compound production, synthesizing metabolites exclusively during specific interactions (Ochi, 2017; Put et al., 2024; Tojo et al., 2015). Bacterial competitors can also stimulate *B. subtilis* motility and biofilm formation (Bleich et al., 2015; Liu et al., 2018). Beyond BSM production, *Bacillus* spp. employ defensive mechanisms, including early sporulation, biofilm formation, and quorum-quenching enzymes, such as those that disrupt *Pseudomonas* quorum-sensing signals (Molina-Santiago et al., 2019; Pandin et al., 2019).

When interacting with fungal pathogens, *Bacillus spp.* modulate their metabolic activity and secretome composition. Fungal cell wall components, such as **chitin** and β-glucan, induce the production of cell wall-degrading enzymes, including chitinases and glucanases (Alamri, 2015; Pérez-Lorente et al., 2025; Vela-Corcia et al., 2025). Additionally, antifungal cLPs, such as iturin and fengycin, are produced in higher quantities during interactions with fungal pathogens such as *Pythium aphanidermatum*, *Fusarium oxysporum*, and *Sclerotinia sclerotiorum* (Cawoy et al., 2015; Farzand et al., 2020; Luna-Bulbarela et al., 2024; Xu et al., 2023a; Zihalirwa Kulimushi et al., 2017). The production of these compounds is often accompanied by adjustments in the blend of cLP variants, suggesting a highly specific adaptation to fungal signals (Cao et al., 2018; DeFilippi et al., 2018). Thus, different homologues of iturin family have different antimicrobial activities against the same pathogen according to the fungal physiological stage (Luna-Bulbarela et al., 2018; Tanaka et al., 2015a). Surfactin production is also increased in the presence of fungi (Singh et al., 2022; Xie et al., 2024) like *Phytophthora parasitica*, *Rhizoctonia solani*, and *S. sclerotiorum*, contributing to biofilm production, motility, and root colonization, which are essential for host plant protection (Chowdhury et al., 2013; Pandin et al., 2019). In contrast, when *B. subtilis* was co-cultured with *A. niger* in a mutualistic interaction, the production of surfactin was reduced (Benoit et al., 2015). However, evolutionary experiments with *B. subtilis* co-cultured with *A. niger* revealed enhanced surfactin production, which counteracted fungal development by inducing dysmorphisms (Richter et al., 2024). Interactions with fungi also thus result in phenotypic changes in *Bacillus* with an increase of biofilm formation. For instance, the presence of *Fusarium culmorum* modulates the master regulator, *sinR*, leading to enhanced biofilm formation (Khezri et al., 2016). Furthermore, co-cultivation studies have shown that *Bacillus* can produce cryptic metabolites under ecologically relevant conditions. For instance, *B. subtilis*, when co-cultured with *Trichoderma atroviride*, produced previously unidentified compounds, highlighting the potential for novel metabolite discovery (Li et al., 2020; Liu et al., 2022). Some competitors of *Bacillus* spp. have evolved strategies to counteract the antagonistic effects of cLPs. Studies have shown that competitors like *Streptomyces* spp. degrade cLPs through the secretion of an enzymatic arsenal (Hoefler et al., 2012; Rigolet et al., 2024). The resulting degradation products may support the competitor growth, but they could also generate novel compounds with unexpected bioactivities (Balleux et al., 2025; Rigolet et al., 2024). Interestingly, in response to *Bacillus* colonization and its harmful effects,

Botrytis cinerea has been shown to produce enzymes that degrade fengycin, neutralizing its toxicity (Pérez-Lorente et al., 2025) (**Figure 3-2**).

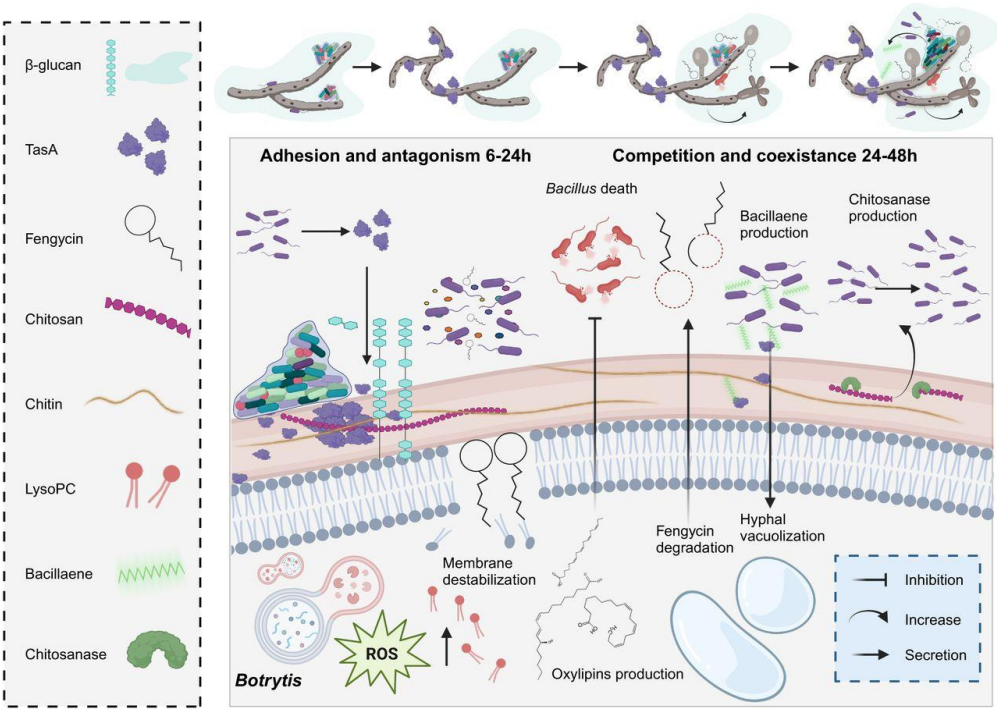

Figure 3-2: Adapt to survive: The battle between *Bacillus subtilis* and *Botrytis cinerea*. Schematic representation of the antagonistic interaction between *B. subtilis* and *B. cinerea*, highlighting the adaptive strategies of *Bacillus* for survival and competitiveness. Upon co-cultivation, *B. subtilis* upregulates genes involved in biofilm formation and secondary metabolite production, promoting attachment to *Botrytis* hyphae. The extracellular matrix components TasA and fengycin act synergistically to induce reactive oxygen species (ROS) and accumulation of lysophosphatidylcholine (lyso-PC) in *Botrytis*. Lyso-PC acts as a lipid signaling molecule associated with ROS generation and membrane damage, while TasA disrupts the fungal β-glucan layer. In response, *B. cinerea* remodels its membrane, alters its metabolome, and produces antibacterial oxylipins. Over time, *Botrytis* develops resistance by degrading fengycin, leading *Bacillus* to shift from a fungicidal to a fungistatic mode of action via bacillaene (a PKS-derived metabolite). *Bacillus* also metabolizes chitosan, a deacetylated form of chitin from the fungal cell wall, as a nutrient source to sustain fengycin synthesis. This dynamic interaction illustrates the continuous co-adaptation and metabolic plasticity underlying bacterial–fungal competition.. Illustration from Pérez-Lorente et al. (2025).

3.1.2 Plant host sensing by *Bacillus* spp.

Beyond its antagonistic interactions, *Bacillus* spp. must also secure nutrients to sustain its growth. In nutrient-poor soil environments, *Bacillus* relies on root exudates

from plants. These exudates serve not only as nutrient sources but also as chemical cues that *Bacillus* interprets to adjust its behaviour. *Bacillus* spp. exhibit increased motility, chemotaxis, and biofilm formation in response to root exudates (Kierul et al., 2015; Pandin et al., 2017). Chemotaxis allows *Bacillus* to detect exudate gradients, facilitating root colonization (Jin et al., 2019; Liu et al., 2020b; Sourjik & Wingreen, 2012; Yssel et al., 2011). This process is mediated by chemoreceptors that detect specific exudate compounds, such as amino acids, organic acids or sugars, triggering changes in flagellar movement (Allard-Massicotte et al., 2016; Brunet et al., 2025; Feng et al., 2018, 2021; Sharma et al., 2020a; Zhang et al., 2015). Root exudate composition varies according to plant genotype and growth stage (Berruto & Demirer, 2024; Chaparro et al., 2014; Sasse et al., 2018; Van Overbeek & Van Elsas, 2008; Zhang et al., 2014). Consequently, *Bacillus* species display host-specific chemotactic responses, as demonstrated by *B. subtilis* N11 (from banana rhizosphere) and *B. amyloliquefaciens* SQR9 (from cucumber rhizosphere), which show stronger attraction to their respective hosts (Zhang et al., 2014).

Plant sensing is also essential for *Bacillus* attachment to roots, involving a phenotypic shift from planktonic cells to biofilm formation (Arnaouteli et al., 2021; Blake et al., 2021). This phenomenon is driven by the recognition of signals provided by the plant. The switch between these physiological states leads to a downregulation of flagellar gene expression and an upregulation of genes involved in extracellular matrix production. Various root exudate compounds and polysaccharides derived from the plant cell wall stimulate biofilm formation in *Bacillus* spp. For example, root exudates from maize and cucumber, or individual exudate compounds such as glucose, fructose, citric acid, malic acid, and fumaric acid, trigger biofilm formation in two *B. velezensis* strains (Jin et al., 2019; Liu et al., 2020a; Zhang et al., 2015). Perception of the pectin backbone **homogalacturonan** (HG) and its degraded products, **oligogalacturonides** (OGs), stimulates key developmental traits via a dynamic process involving two conserved pectinolytic enzymes in *B. velezensis*. This response integrates transcriptional changes, leading to the switch from planktonic to sessile cells, a strong increase in biofilm formation, accelerated sporulation dynamics and while boosting the potential to efficiently produce some BSMs (Beauregard et al., 2013; Boubsi et al., 2023; Hoff et al., 2021). Thus, plants also modulate the production of *Bacillus* BSMs (**Figure 3-1 B**). Organic acids present in root exudates trigger the production of surfactin. Moreover, the relative proportion of surfactin homologues varies depending on carbon source availability (Nihorimbere et al., 2012). Likewise, the gene expression of lipopeptides (fengycin and surfactin) and polyketides is upregulated in the presence of rocket salad, cucumber, or maize root exudates (Ogran et al., 2019; Qiu et al., 2014; Zhang et al., 2015).

Following pathogen attack, plants recruit microbial species in their root-associated **microbiome** to complement or enhance their defence, a phenomenon known as "cry for help." (Liu et al., 2024b; Spooren et al., 2024). The presence of pathogens modifies root exudates, increasing their attractiveness for *Bacillus* spp. (Liang et al., 2024;

Rudrappa et al., 2008). In cucumber plants infected by *F. oxysporum* f. sp. cucumerinum, the proportion of chemoattractant compounds (citric acid and fumaric acid) is higher compared to non-infected plants, resulting in enhanced root colonization by *B. velezensis* SQR9 (Liu et al., 2014, 2020b). Similarly, improved colonization of *B. velezensis* 32 on *Agrobacterium tumefaciens*-infected tomato roots has been observed, correlating with changes in root exudate composition (Abdallah et al., 2020). Thus, *Bacillus* effectively "eavesdrops" on its host, establishing and proliferating in the rhizosphere. The interaction between *Bacillus* spp. and plants is mediated through molecular crosstalk, which is essential for *Bacillus* root associated species to sense the plant, attach to it, and persist on root surfaces.

3.1.3 Host recognition by AM fungi

Similarly, AM fungi recognize host plants through plant-exuded metabolites, known as branching factors, which activate fungal growth and serve as directional cues (**Figure 3-3**). **Strigolactones**, a class of phytohormones derived from carotenoids, stimulate hyphal branching by AM fungi (Akiyama et al., 2010; Besserer et al., 2006, 2008; Kodama et al., 2022) but also serve as germination stimulants for parasitic plants, sensors of neighbouring vegetation, and key regulators of microbiome composition (Kee et al., 2023; Kodama et al., 2022; Naz et al., 2025). This raises the question of whether specific structural features of strigolactones dictate their function, with emerging evidence suggesting such a structure-function relationship (Kee et al., 2023). Plants produce structurally diverse strigolactones, including canonical and non-canonical variants, which vary among species. A single plant often synthesizes multiple strigolactone structures, which function in diverse ecological interactions beyond AM symbiosis (Kee et al., 2023; Lanfranco et al., 2018; Nomura et al., 2024; Yoneyama & Brewer, 2021). Regarding AM fungi, both canonical and non-canonical strigolactones have been reported as hyphal branching factors, though non-canonical forms generally exhibit weaker activity (**Figure 3-3 A**) (Akiyama et al., 2010; Tominaga et al., 2023; Xie et al., 2019). Interestingly, different strigolactone structures appear to modulate distinct branching patterns,

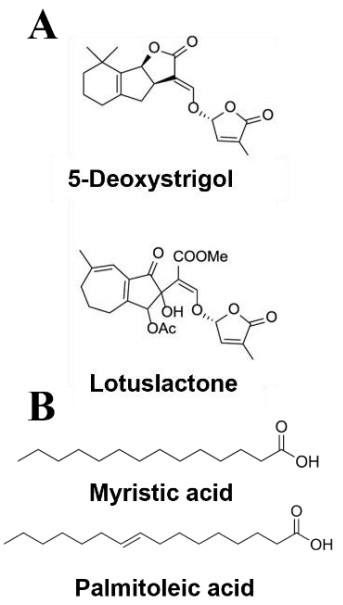

Figure 3-3: Example of compounds considered as branching factors. A. Examples of canonical (5-Deoxystrigol) and non-canonical (Lotuslactone) strigolactones produced by *Lotus japonicus*, acting as signalling molecules for AM fungi. Structures taken from Mori et al. (2020). **B**. Example of fatty acid inducing hyphal growth in *R. irregularis* (Palmitoleic acid), *R. clarus* and *G. margarita* (Myristic acid). Adapted from Sugiura et al., (2020) and Kameoka et al. (2019).

suggesting that a specific cocktail of strigolactones may influence hyphal development (Akiyama et al., 2010).

Strigolactones are not the sole plant-derived signals which may affected AM fungal growth, certain root-exuded fatty acids also modulate hyphal development (Nagahashi & Douds, 2011). In *Gigaspora gigantea*, several fatty acids differentially induce small hyphal branches and stimulate overall hyphal growth. Notably, branched-chain fatty acids such as hydroxytetradecanoic acid and 2-hydroxydodecanoic acid promote hyphal branching in *G. gigantea* but inhibit responses in *R. irregularis* (Kameoka et al., 2019; Kameoka & Gutjahr, 2022; Nagahashi & Douds, 2011). Conversely, different fatty acids selectively trigger hyphal branching *in R. irregularis* and *R. clarus* (members of the Glomerales order), but not in *Gigaspora* species (Diversisporales member order), highlighting genus-specific responses within AM fungal lineages (Delaux & Gutjahr, 2024; Kameoka et al., 2019; Sugiura et al., 2020; Tanaka et al., 2022). However myristate has been showed to promote the growth of *R. clarus, R. irregularis* and *Gigaspora margarita* (**Figure 3-3 B**) (Sugiura et al., 2020).

3.1.4 Root-beneficial microbes evade plant immunity

Communication between beneficial microbes and plants is likely the result of co-evolution, fostering mutualism and symbiosis. Microorganisms need to sense their host to move toward it and adapt their behaviour for efficient colonization (Liu et al., 2024a). Simultaneously, they must either be recognized as beneficial or mask themselves to avoid triggering plant immune responses (Mauch-Mani et al., 2017).

Plants have evolved sophisticated defence mechanisms activated upon the perception of specific molecular patterns, leading to **pattern-triggered immunity** (PTI) or **Microbe-Associated Molecular Pattern Triggered Immunity** (MTI). This first line of defence is initiated by the recognition of either microbe-associated molecular patterns (MAMPs) or damage-associated molecular patterns (DAMPs). MAMPs are conserved microbial signatures such as flg22 (the N-terminal epitope of bacterial flagellin), chitin, peptidoglycan, and lipopolysaccharides. In parallel, DAMPs are endogenous molecules released upon cellular damage caused by pathogen attack. These include oligogalacturonides (OGs), which derive from the degradation of homogalacturonan (HG), a major component of pectin in plant cell walls, by pathogen-secreted hydrolytic enzymes (Bacete et al., 2018; Voxeur et al., 2019; Yu et al., 2017; Zhang & Kong, 2022). The recognition of MAMPs and DAMPs is mediated by cell-surface pattern recognition receptors (PRRs) belonging to two main families: receptor-like kinases (RLKs) and receptor-like proteins (RLPs). Numerous RLKs and RLPs have been identified as receptors for MAMPs or DAMPs from both bacterial and fungal origins (Bacete et al., 2018; DeFalco & Zipfel, 2021; Desaki et al., 2018; Peng et al., 2018; Schellenberger et al., 2019; Zipfel & Oldroyd, 2017). Recognition of these patterns triggers a cascade of coordinated defence responses, including ion

fluxes (notably H^+ and $Ca2^+$), production of reactive oxygen species (ROS), activation of mitogen-activated protein kinase (MAPK) cascades, upregulation of defence-related genes, modulation of plant hormone signalling, callose deposition, and synthesis of antimicrobial compounds (Bigeard et al., 2015; Yuan et al., 2021; Zhang et al., 2021; Zipfel & Oldroyd, 2017). A paradox in mutualistic interactions arises because the recognition of pathogens is based on universal/conserved MAMPs, such as flagellin (flg22) and chitin, which are also present in beneficial microorganisms like *Bacillus* and AM fungi. Therefore, beneficial microbes have evolved strategies, like some phytopathogens, to mask these patterns or to produce alternative signals that suppress/reduce root immune responses (Liu et al., 2024a; Zhang & Kong, 2022; Zhou et al., 2020a).

3.1.5 Symbiotic signalling and immune modulation by AM fungi

The establishment of molecular dialogue in plant-microbe interactions is crucial in symbiotic relationships such as mycorrhizae (see review Delaux & Gutjahr, 2024). In AM fungal symbiosis, fungi release diffusible signals that trigger specific genetic reprogramming in plant roots, enabling fungal accommodation. These signalling molecules were initially hypothesized to resemble the Nod factors of nitrogen-fixing bacteria. AM fungi produce analogous compounds known as **Myc-factors**, which include sulfated and non-sulfated **lipochitooligosaccharides** (LCOs) detected in fungal exudates of various AM fungi. The main LCOs produced by *R. irregularis*, designated LCO-V (C18:1, Fuc/MeFuc), contain a C18:1 fatty acid chain and fucosyl or methylfucosyl decorations on the chitooligosaccharide backbone (**Figure 3-4**) (Rush et al., 2020). In addition to LCOs, chitin-derived short-chain chitooligosaccharides (CO_4 and CO_5) also act as Myc-factors. Both LCOs and short COs are composed of four to five N-acetylglucosamine (GlcNAc) residues, with LCOs additionally carrying a lipid moiety on the terminal non-reducing sugar species and various chemical decorations on this backbone (Feng et al., 2019; Genre et al., 2013; Giovannetti et al., 2024a; Khokhani et al., 2021; Maillet et al., 2011; Rush et al., 2020; Sun et al., 2015).

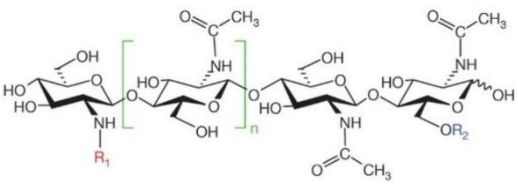

Figure 3-4: Structure of Myc-LCOs. *n* = 1 or 2, R2 = H or SO_3H. For Myc-LCOs, R1 = C16, C16:1, C16:2, C18:0 or C18:1Δ9Z (oleic acid), and for rhizobial Myc-LCO analogues, R1 = C16:0 or C18:1 Δ11Z (*cis*-vaccenic acid). Adapted from Maillet et al. (2011).

Similar to beneficial bacteria, AM fungi harbour conserved MAMPs, which may trigger plant immunity such as chitin, a conserved structural polymer of β-1,4-linked GlcNAc in their fungal cell walls (Geoghegan et al., 2017; Gow et al., 2017). To counteract fungal infections, plants secrete chitinases that hydrolyse chitin and release COs with different degree of polymerization (DP) (Gow et al.,

2017; Vaghela et al., 2022). While short COs (CO4/CO5) and LCOs promote symbiosis, longer COs (CO6–CO8) are potent immune elicitors (Molina et al., 2024; Pinto et al., 2025; Yu et al., 2017). Therefore, AM fungi must balance immune evasion and symbiotic recognition to enable successful colonization (Russo et al., 2019). Both short and long COs can activate symbiosis-related genes, though long COs induce stronger immune responses. These GlcNAc-containing molecules are perceived by LysM receptor-like kinases (LysM-RLKs) or LysM receptor-like proteins (LysM-RLPs), subfamilies of RLKs/Ps located at the plant plasma membrane (Buendia et al., 2018; He et al., 2019). These receptors thus play a dual role in symbiotic and immune signalling. Recent studies suggest that many of them exhibit broad functional specificity, reflecting a complex regulatory network. Some LysM-RLK/Ps display higher specificity toward COs or LCOs, activating distinct downstream pathways linked to either symbiosis or immunity (Buendia et al., 2018; Fukuda et al., 2024; Girardin et al., 2019; He et al., 2019; Miyata et al., 2014, 2022; Tan et al., 2025; Teyssier et al., 2025; Zhang et al., 2025, 2021, 2024c). Double mutants in *Medicago truncatula* (Zhang et al., 2024c) and *Lotus japonicus* (Fukuda et al., 2024) lacking key LysM-RLK/Ps exhibit nearly complete loss of colonization, underscoring their crucial role (Desaki et al., 2018; Girardin et al., 2019; Stracke et al., 2002). However, most angiosperms display only partial defects in single or double mutants, suggesting strong genetic redundancy within this expanded family (Buendia et al., 2018; Ding et al., 2024, 2025; Feng et al., 2019; He et al., 2019; Miyata et al., 2022; Rasmussen et al., 2016).

Thus, LCOs, short-chain (CO4/CO5), and long-chain (CO7) COs can be perceived by plants, with CO7 preferentially activating immune responses while CO4/CO5 and LCOs induce symbiotic signalling. Interestingly, short COs and LCOs are not exclusive to AM fungi; several other fungi can synthesize them (Rush et al., 2020). Remarkably, CO_4 and LCOs can suppress long CO-triggered immunity, suggesting that Myc-factors may mask MAMPs and thereby modulate plant immune perception (Feng et al., 2019; Tan et al., 2025). The production of Myc-factors by AM fungi is closely linked to the nutritional status of the host. Under phosphorus or nitrogen limitation, plants release strigolactones, which stimulate fungal hyphal branching and enhance LCO and short CO production, reinforcing a reciprocal signalling loop that promotes symbiosis (Khokhani et al., 2021; Li et al., 2022; Pimprikar et al., 2016; Tan et al., 2025) (**Figure 3-5**). Yet, only AM fungi show strigolactone-induced enhancement of LCO or short CO production, indicating that symbiotic signalling specificity may arise from chemical decorations of Myc-LCOs, release concentration and localized secretion at the root interface (Ding et al., 2025; Genre et al., 2013; Kumar et al., 2025a; Li et al., 2022; Tan et al., 2025; Zhang et al., 2025). Recent findings suggest that short COs and LCOs may not be universal signal leading to the AM fungal symbiosis across land plants. The bryophyte *Marchantia paleacea*, a non-vascular liverwort with only four LysM-RLKs, offers a simplified model to test these mechanisms. Teyssier et al. (2025) demonstrated that *Marchantia* mutants defective in CO/LCO perception still established AM symbiosis, implying that additional or

ancestral signalling molecules beyond COs and LCOs can mediate fungal recognition. This highlights the evolutionary plasticity of symbiotic communication and suggests that the CO/LCO pathway may have diversified later in land plant evolution (Zhang et al., 2025).

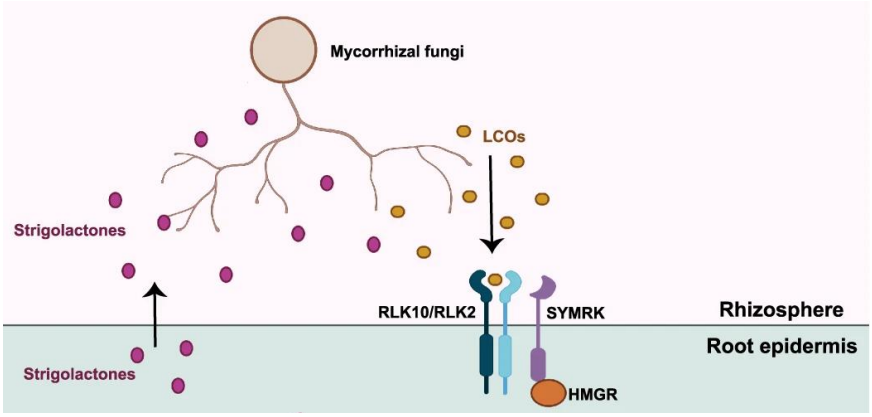

Figure 3-5: Plants integrate environmental nutrient cues to regulate costly symbiotic associations. Under P-starvation conditions, promotion of gene expression associated with the biosynthesis of strigolactones. Strigolactones are exuded to the rhizosphere to activate hyphal branching of mycorrhizal fungi and stimulate the production of fungal signals, including LCOs. The LysM-RLK, *RLK10/RKL2* in barley and *NFR5* in rice, allowing LCO recognition and activation of symbiosis signaling,. Illustration adapted from Li et al. (2022).

Upon perception of these GlcNAc-containing molecules, plants activate the common symbiosis signalling (SYM) pathway or common symbiosis signalling pathway (CSSP) (Zhang et al., 2025). Studies on symbiotic pathways in model plants such as *M. truncatula* have led to the discovery of genes and proteins regulating different stages of AM symbiosis (Bravo et al., 2016; Delaux & Gutjahr, 2024). These findings demonstrate that plants actively control fungal progression and colonization. The understanding of AM symbiosis largely been derived from research on root nodule symbiosis with nitrogen-fixing bacteria (Kistner & Parniske, 2002; Martin et al., 2017). In host plants, AM fungi also activate the SYM pathway, triggering a signalling cascade that reprograms gene expression to establish symbiosis. This cascade involves lysin motif receptor-like kinases (LysM-RLKs and SYMR/DIM2), nuclear envelope-localized cation channels (CASTOR and POLLUX/DMI1 and CNGC15), nuclear calcium and calmodulin-dependent protein kinases (CCaMK/DMI3) and transcription factors (**Figure 3-6**) (Genre & Russo, 2016; Lanfranco et al., 2016; MacLean et al., 2017; Oldroyd, 2013; Zipfel & Oldroyd, 2017).

Mutations in any CSSP gene abolish AM symbiosis (Jin et al., 2018; Lam et al., 2024; Miyata et al., 2023; Stracke et al., 2002; Vernié et al., 2025). Early responses to symbiotic or immune signals include rapid ion fluxes (H^+, Ca^{2+}) and transient ROS bursts (Arthikala et al., 2013; Fester & Hause, 2005; Liu et al., 2024a). Calcium oscillations ("spiking") around the nucleus constitute a hallmark of CSSP activation (Giovannetti et al., 2024b; a; Köster et al., 2022; Peng et al., 2018). Notably, the calcium signatures induced by CO_4, CO_5, and LCOs (sulfated or non-sulfated) differ in frequency and amplitude from those triggered by CO_7–CO_8 or pathogen-derived molecules, reflecting distinct recognition mechanisms (**Figure 3-7**) (Feng et al., 2019; Genre et al., 2013; Sun et al., 2015). Moreover, calcium responses vary among fungal species, e.g., *Rhizophagus* vs *Gigaspora*, suggesting that distinct signal combinations are used by different AM fungi to engage their hosts (Binci et al., 2024; Genre et al., 2013; Giovannetti et al., 2024a; b; Khokhani et al., 2021).

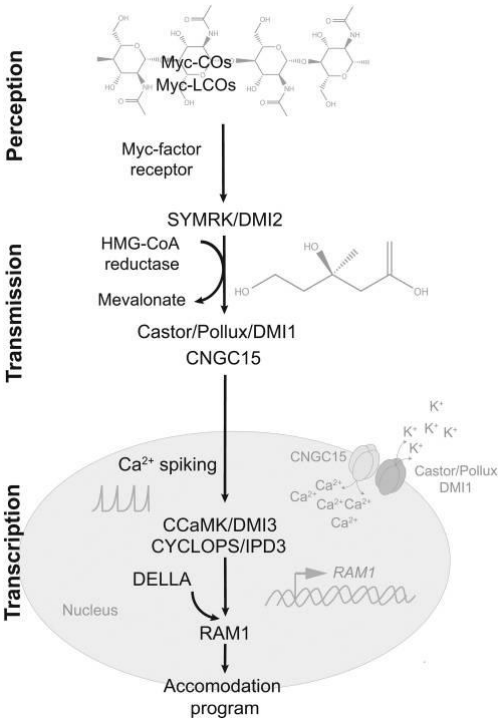

Figure 3-6: The symbiosis (SYM) signalling pathway activated in plants following the recognition of Myc-factors. Recognition of Myc-factors triggers a cascade of intracellular signalling events that facilitate cellular remodelling and metabolic changes necessary to accommodate the fungal endosymbiont. Distinct RLK/Ps, Ca^{2+} signatures, and ROS production govern both symbiotic accommodation and immune defence. Adapted from MacLean et al., (2017).

Short COs and LCOs also show cell-type- and species-specific plant activity (Cao et al., 2024). Comparative studies between *M. truncatula* and rice further confirm species- and cell-type-specific variations in CO/LCO signalling (Sun et al., 2015). In legumes, COs and LCOs activate symbiosis signalling in epidermal cells to facilitate AM fungal entry, whereas in rice, primarily COs drive recognition, with limited LCO involvement (He et al., 2019; Sun et al., 2015). Notably, chitin-derived molecules, including short COs and LCOs, induce also lateral root formation in both monocots and dicots. Since lateral roots are preferred entry sites for AM fungi, these findings suggest a link between developmental reprogramming and symbiotic readiness (Bonhomme et al., 2021; Buendia et al., 2019; Chiu et al., 2022; Gutjahr et al., 2008; Khokhani et al., 2021; Mukherjee & Ané, 2011; Tanaka et al., 2015b). Collectively, these findings underscore the complexity of chitin-based signalling in

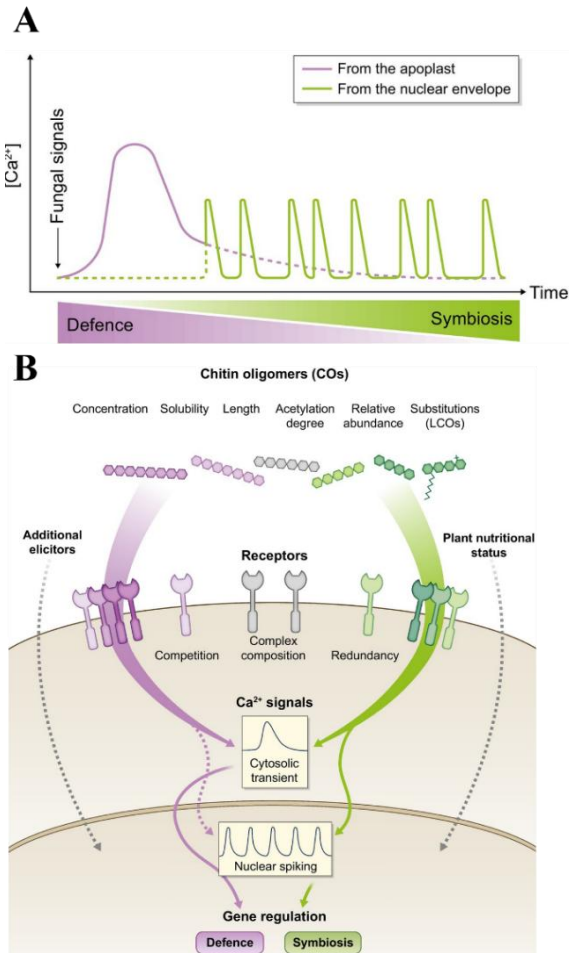

AM symbiosis, where plants must decode overlapping immune and symbiotic cues. The evolutionary diversification of LysM-RLKs/Ps and the chemical flexibility of GlcNAc-containing signals likely underlie the broad host range and adaptive success of AM fungi across land plants.

Figure 3-7: Ca^{2+} Signatures as a central hub in defence and symbiotic signalling. This figure highlights that chitin-derived signals operate within a broader communication network in which the plant nutritional status and associated microbiota determine whether the host supports or resists fungal colonization. It illustrates the nonbinary nature of chitin oligomer (CO) recognition, reflected by the partial overlap between defence- and symbiosis-related Ca^{2+} signalling, which share similar yet distinct Ca^{2+} signatures. The figure also underscores the challenges of studying Ca^{2+} dynamics, emphasizing the need for integrative approaches combining multiple genetically encoded Ca^{2+} indicators to obtain a comprehensive view of Ca^{2+} signalling in plant–microbe interactions (apoplastic or/and nuclear response/signature). **A**, Distinct Ca^{2+} signalling patterns between defence and symbiosis: rapid, high-amplitude Ca^{2+} influx from the apoplast is characteristic of defence activation, while symbiotic signalling involves oscillatory, nuclear-centred Ca^{2+} spiking originating from the nuclear envelope. **B,** Chitin oligomers (COs) elicit Ca^{2+}-mediated responses associated with both immunity and symbiosis, depending on factors such as their concentration, relative abundance, length, solubility, and degree of acetylation. Adapted from Giovanetti et al. (2024).

3.1.6 AM fungal immune evasion: beyond chitin-derived signals

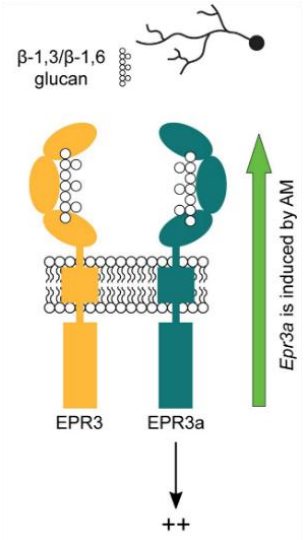

Figure 3-8: Immune evasion and root colonization by *Rhizophagus intraradices* through β-1,6-glucan recognition. In *Lotus japonicus*, Epr3a, a LysM-RLK, was identified as a key component of a AM fungal colonization. *Epr3a* expression is strongly upregulated in arbusculated cells and is essential for proper arbuscule development. *Epr3a* mutants display reduced arbuscule formation and increased vesicle accumulation, reflecting an altered fungal developmental program. *Epr3a* specifically recognizes branched β-1,6-glucan but not linear β-1,6- or β-1,3-glucans. This specificity suggests that branched β-1,6-glucan acts as a distinctive AM fungal signal perceived by the host to facilitate symbiosis and immune evasion. The role of *Epr3a* in AM fungal symbiosis contrasts with that of *Epr3*, which responds to rhizobial EPS during root nodule formation and is not involved in AM symbiosis. Adapted from Kelly et al. (2023).

β-glucans are the main polysaccharides in fungal cell walls, where they provide structural integrity and rigidity. Composed of β-1,3 and β-1,6 linkages, these polymers form a fibrillar network whose synthesis and remodelling are tightly regulated by fungal β-glucanases and other enzymes (Gow et al., 2017; Pinto et al., 2025). Importantly, β-glucans are also recognized by plant PRRs as MAMPs because they are ubiquitous components of fungal cell walls (Bacete et al., 2018). However, a plant receptor involved in the perception of a specific β-1,3/β-1,6 decasaccharide, originating from exopolysaccharides of both endophytic and pathogenic fungi, was upregulated in roots colonized by AM fungi (**Figure 3-8**) (Kelly et al., 2023). Furthermore, this receptor was shown to be essential for efficient fungal infection and for the proper formation of intracellular arbuscules. Thus, β-1,3/β-1,6 glucans with specific degrees of polymerization may function as potential symbiotic signals, contributing both to immune evasion and to the successful colonization of host roots by AM fungi (van Boerdonk et al., 2024).

Effector production is a widely used strategy among microbial pathogens to evade plant immunity (Lopez-Gomollon & Baulcombe, 2022; Thieron et al., 2021; Xu et al., 2022; Zhu et al., 2022). For instance, pathogenic *Pseudomonas syringae* and *R. solanacearum* deliver effectors into plant cells via the type III secretion system to suppress immune responses and facilitate colonization (Liu et al., 2024b; Yun et al., 2023). Similarly, rhizobia use effectors, including small RNAs (sRNAs), through the same system to interfere with plant immunity, enabling symbiotic interactions (Baldrich & Meyers, 2019; Ren et al., 2019). Both symbiotic and pathogenic bacteria interact with the plant immune system, with resistance (R) genes playing a crucial role in disease resistance by encoding R proteins. Genome mining analysis suggest that AM fungi

produce also effectors, potentially modifying host cells, suppressing defences, and facilitating nutrient exchange (Betz et al., 2024; Chen et al., 2018; Kloppholz et al., 2011; Vasistha et al., 2025). Some effector-related genes are upregulated by strigolactones (Tsuzuki et al., 2016), while others may be involved in chitin degradation and modification, suggesting that AM fungi dynamically remodel their cell wall in response to environmental and host-specific conditions (Sędzielewska Toro & Brachmann, 2016). Thus, effectors likely play a key role in maintaining AM fungal symbiosis. Although bioinformatics predicts a diverse repertoire of effectors secreted during symbiosis across multiple AM fungal species (Zeng et al., 2018), the number of functionally characterized effectors remains limited and, so far, exclusively described in *R. irregularis* (Aparicio Chacón et al., 2023; Betz et al., 2024; Silvestri et al., 2024; Teulet et al., 2023; Tsuzuki et al., 2016; Zeng et al., 2020). Still, it indicates that mycorrhizal fungi effector molecules are involved in host immunity suppression (Betz et al., 2024; Xie & Fan, 2025) .

Arbuscule formation in root cortical cells involves plant-mediated cell wall remodelling, (Balestrini & Bonfante, 2014; Chialva et al., 2019; Su, 2023), which may release OGs known to act as strong immunity elicitors (Bacete et al., 2018; Rui & Dinneny, 2020; Voxeur et al., 2019). Indeed, fungal pathogens use enzymatic arsenals to degrade plant cell walls, either to penetrate plant tissues or as a nutrient source, producing DAMPs that trigger immune responses in plants (Pinto et al., 2025; Voxeur et al., 2019; Yu et al., 2017). Thus, OGs and other HG-derived oligomers are perceived by plant cells as signals of fungal attack, triggering immune responses (Rui & Dinneny, 2020; Yu et al., 2017). The perception of OGs has been attributed to Wall-Associated Kinases (WAKs), which are RLKs. However, recent evidence suggests that other receptors may also be involved in OG perception triggering immune response in plants (Herold et al., 2024). Regarding AM fungi, despite their genomes being larger than those of fungal pathogens, large-scale genome sequencing has revealed that their arsenal of plant cell wall-degrading enzymes is relatively limited compared to phytopathogenic fungi. This limitation is thought to reflect the evolutionary trajectory of AM fungi along the saprotrophy-to-symbiosis continuum, with arbuscular mycorrhizal symbiosis emerging in the early Devonian period (393–419 Mya) (Miyauchi et al., 2020). Consequently, the majority of cell wall-modifying enzymes involved in this process are highly upregulated in the host plant during symbiosis with AM fungi (Luginbuehl et al., 2017; Luginbuehl & Oldroyd, 2017; Su, 2023). Interestingly, work by Zhang et al., (2024) suggests that WAKs regulate AM symbiosis. The activation of a specific WAK receptor appears to play a pivotal role in immune suppression, thereby facilitating AM fungal colonization. Conversely, exogenous application of OGs suppressed AM symbiosis through the activation of another WAK receptor (**Figure 3-9**). These findings suggest that the mechanism facilitating AM fungal symbiosis is highly localized to inner root tissues, where signals derived from the plant cell wall are transduced within cortical cells (Giovannetti & Genre, 2024). While WAK receptors appear to play a role in AM symbiosis, it remains unclear which specific molecules drive WAK receptor

activation, leading the plant to distinguish between symbiotic and immune-related responses (Su, 2023). Nevertheless, the immune suppression mechanism appears to be conserved and similar to that observed in plant-pathogen interactions (Giovannetti & Genre, 2024; Zhang et al., 2024d).

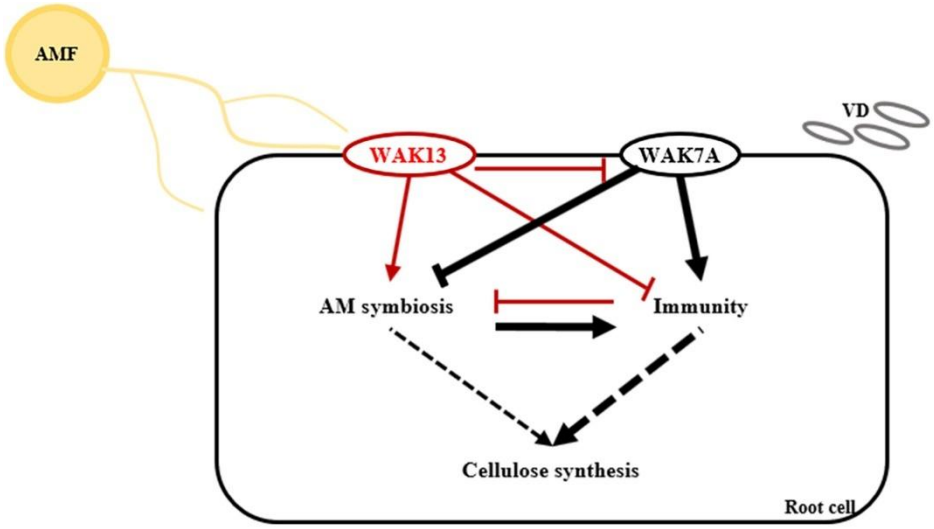

Figure 3-9: Oligogalacturonides and wall-associated kinases (WAKs) balance immunity and AM symbiosis in *Gossypium hirsutum*. In cotton, the cell wall-associated receptor kinase *GhWAK13* acts as an immune suppressor required for efficient AM fungal colonization by *R. irregularis*. *GhWAK13* expression is induced during colonization by both AM fungi and the pathogen *Verticillium dahliae*. Silencing *GhWAK13* impairs AM symbiosis and downregulates genes of the mycorrhizal signalling pathway, while simultaneously enhancing resistance to *Verticillium* and activating defence-related genes. Conversely, GhWAK7A, a positive regulator of *Verticillium* resistance, is upregulated in *GhWAK13*-silenced plants, and its silencing promotes AM symbiosis. Application of OGs suppresses AM colonization, suggesting that OG perception through WAKs modulates the trade-off between immunity and symbiosis. Together, these results indicate that *GhWAK13* and *GhWAK7A* act antagonistically to balance plant defence and symbiotic compatibility. Adapted from Zhang et al. (2023).

3.1.7 The hyphosphere: a hotspot of bacteria-AM fungi interactions

The ERM is colonized by surrounding bacteria, forming the so-called hyphosphere microbiome. The few studies exploring the molecular crosstalk between AM fungi and hyphosphere-associated bacteria have primarily focused on nutrient exchange, particularly interactions with PSB (**Figure 3-10**). AM fungi are inefficient in mineralizing organic phosphorus into its inorganic, assimilable form, relying instead on PSB for this process (Bennett & Groten, 2022; Duan et al., 2024; Zhang et al., 2022). Studies have shown that AM fungal exudates can recruit PSB or bacteria selecting them and even induce phosphatase expression in these bacteria based on carbon-phosphorus exchange (Jiang et al., 2021; Jin et al., 2024; Li et al., 2023; Nacoon et al., 2020; Zhang et al., 2016). For example, Zhang et al. (2018) identified fructose in AM fungal exudates as a dual-purpose compound, serving as both a carbon source and a signalling molecule that promotes organic phosphorus mineralization by the PSB *Rahnella aquatilis*. However, under phosphorus-limited conditions, AM fungi and PSB shift from cooperation to competition for available inorganic phosphate, highlighting the dynamic nature of their relationship depending on environmental nutrient availability (Duan et al., 2024).

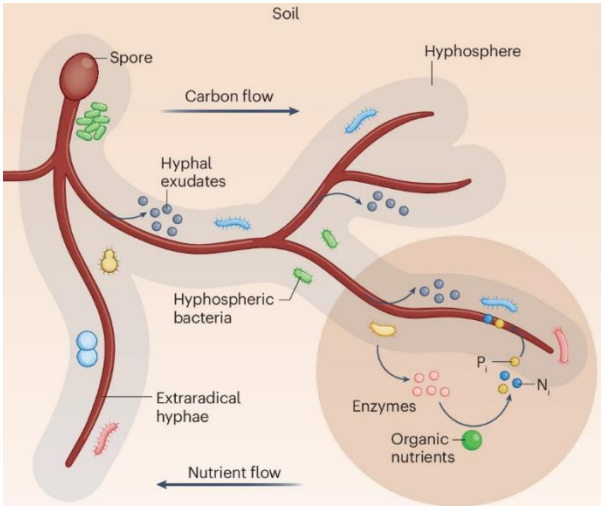

Figure 3-10: Limited knowledge on the crosstalk between AM fungi and associated bacteria in the hyphosphere. Interactions and nutrient exchanges between AM fungi and bacteria at the hyphosphere interface. Together with the plant, these three partners influence each other and modulate nutrient fluxes, shaping their mutualistic relationships into a plant–AM fungus–bacterium continuum. Adapted from Duan et al. (2024).

3.2 Gap of knowledge and Research Question outline

The molecular dialogue underlying direct cross-kingdom communication between AM fungi and bacteria remains largely unexplored. Most research to date has focused on reciprocal nutrient exchanges, such as those occurring between PSB and AM fungi like *R. irregularis*. However, the chemical interactions and specific signaling molecules that might mediate cooperation between AM fungi and rhizobacteria, particularly species with strong antimicrobial activity such as *B. velezensis*, are still unknown. Building on the findings from Chapter 2 (RQ 1), which showed that *B. velezensis* can actively migrate along AM fungal hyphae and may even boost the fungal cytoplasmic streaming, a new question emerge.

RQ 2: What are the factors that drive this interkingdom interaction?

The objective of this chapter was to investigate why *Bacillus* inhibits fungal pathogens but not AM fungi. Our experimental approach involved two complementary strategies. First, we evaluated whether purified antifungal cLPs, especially fengycins and iturins, exhibit intrinsic toxicity against *R. irregularis* to test if the fungus shows natural resistance to these compounds. Second, we monitored the production of antifungal cLPs and other secondary metabolites by *B. velezensis* when the bacterium growth along AM fungal hyphae. Through this approach, we aimed to better understand the molecular mechanisms that drive the interaction between *B. velezensis* and *R. irregularis*.

.

3.3 Attenuated fengycin production in the hyphosphere prevents *B. velezensis* from antagonizing *R. irregularis*

B. velezensis is a strong producer of antifungal BSMs including iturin- and fengycin-type cLPs which are well described for their activity against a wide range of fungal plant pathogens (Anckaert et al., 2021; Andrić et al., 2020; Ongena & Jacques, 2008). In order to understand how *R. irregularis* may co-exist with this antagonistic bacterium, we tested the toxicity of pure cLPs on the fungus. We used propidium iodide (PI) staining as indicator of membrane integrity since toxicity of the cLPs mainly relies on their pore-forming activity in biological membranes causing cytosolic leakage and death of target cells (**Figure 3-11 A)** (Balleza et al., 2019; Mantil et al., 2019; Nasir et al., 2010). PI cannot penetrate intact membranes of living cells, but readily enters damaged cells, where it intercalates with nucleic acids (DNA and RNA), resulting in a red fluorescence signal (Cargill et al., 2025; Hijri & Sanders, 2005; Zhang et al., 2018b). The mean red fluorescence intensity (MeanRed), corresponding to the arithmetic mean of pixel intensities, was quantified in treated hyphae using microscopy and ImageJ analysis. Hyphae were exposed to purified cLPs at different concentrations and compared with two controls, a negative control treated with physiological water (Na Cl 9 g L^{-1}, w/v), used for solubilized the pure cLPs, and a positive control ("killed hyphae") treated with a mixture of Triton X-100 and formaldehyde (1% and 2%, v/v) to induce plasma membrane permeabilization (Calonne et al., 2014; Mattei et al., 2017; Mazheika et al., 2024). Fengycin and iturin did not affect hyphal membrane integrity at 2 µM. At 20 and 50 µM, fengycin markedly destabilized the membranes, whereas iturin caused significant membrane damage only at the highest concentration (50 µM). In contrast, surfactin did not affect membrane integrity over the tested concentration range (**Figure 3-11 B**).

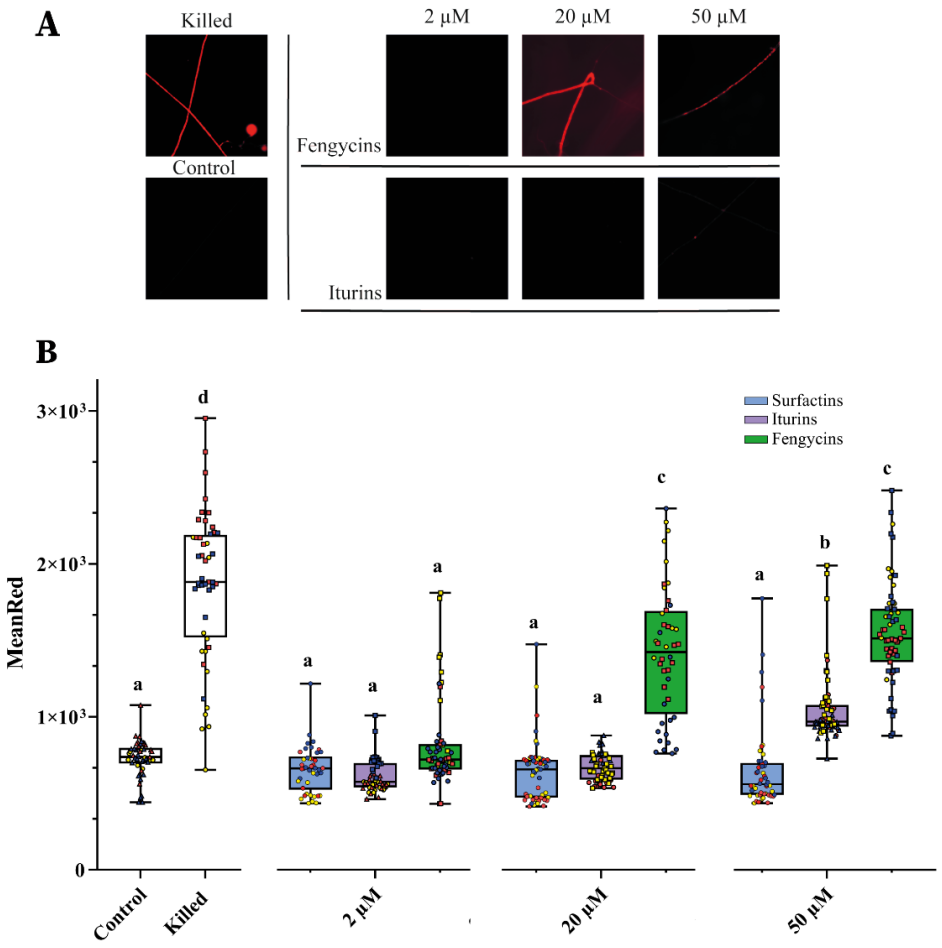

Figure 3-11: Effect of *B. velezensis* antifungal compounds on *R. irregularis*. **A** and **B**, *R. irregularis* hyphae stained with 50 µg ml^{-1} Propidium Iodide after treatment with 2 µM, 20 µM or 50 µM of fengycin, iturin or surfactin. AM fungal hyphae treated with PBS solution (Control) and mixed solution of Triton X-100 and formaldehyde (Killed) were used as controls. **A**, Propidium iodide cell staining of *R.i.* hyphae observed by fluorescence microscopy. **B**, Dose effect of pure fengycin (green), iturin (purple) and surfactin (blue) produced by *B. velezensis* on membrane integrity of 3 months-old (triangle shape), 5 months-old (square shape) or 6 months-old (circle shape) hyphae of *R. irregularis* cultures measured by fluorescence upon staining with propidium Iodide. High MeanRed values mean high membrane permeabilization. The boxes encompass the 1st and 3rd quartiles, the whiskers extend to the minimum and maximum points, and the midline indicates the median. The individual points represent 3 biological replicates (different colours) and 9 to 26 technical replicates (same colours). The dose effect of fengycin, iturin and surfactin has been evaluated according to different ages of *R. irregularis* cultures (different shapes). $43 \leq n \leq 65$; Letters a to d indicate statistically significant differences according to one-way analysis of variance (ANOVA) and Tukey's HSD test ($\alpha = 0.05$).

We observed that *B. velezensis* interacts with *R. irregularis* without causing detrimental effects on fungal integrity, despite producing compounds previously shown to be harmful to *R. irregularis*. To further explore this apparent compatibility, we next examined the production of these antifungal metabolites within the hyphosphere during AM fungal colonization. Profiling of *B. velezensis* secondary metabolites by UPLC-qTOF-MS revealed the presence of substantial amounts of surfactin, iturin and bacilysin, as well as detectable but limited quantities of fengycin (**Figure 3-12 A)** , the latter being observed for their antifungal activity against AM fungus. These observations suggested a potential modulation of cLP production patterns in the hyphosphere, particularly a reduction in fengycin biosynthesis.

To identify the factors responsible for this modulation, we compared the CLPs profiles of *B. velezensis* grown under different nutritional conditions. The results revealed a distinct pattern compared to the one observed upon growth in lab media or in a medium mimicking plant exudates (Nihorimbere et al., 2012) (**Figure 3-12 A**). Upon growth in rich optimized lab media, *B. velezensis* typically secretes cLPs in relative proportions of approx. 50% surfactin, 25% iturin and 25% fengycin (Nihorimbere et al., 2012). However, the hyphosphere samples exhibited different ratios, with surfactin accounting for 60% (± 11.21%) and iturin for 36.5% (± 10.20%), while fengycin was present in minimal amounts of only 1.5% (± 0.78%) (**Figure 3-12 B**). The amounts recovered corresponded approximately to 0.61 µM ± 0.21 for surfactin, 0.48 µM ± 0.016 for iturin and 0.03 µM ± 0.001 for fengycin. Similar relative cLPs proportions were observed when *B. velezensis* planktonic cells were cultured in presence of exudates collected from AM fungal hyphae as sole nutrient source (surfactin: 2.73 µM ± 1.04; iturin: 1.86 µM ± 1.06; fengycin: 0.0478 µM ± 0.0325), indicating that the reduced fengycin production is not related to biofilm formation and is not contact-dependent (**Figure 3-12 B**). Also data presented in **Figure 3-11** show that at these concentrations, fengycin is not cytotoxic for the fungus.

Since the nature of available carbon sources can influence cLP production in *Bacillus* spp. (Lu et al., 2016; Medeot et al., 2017; Nihorimbere et al., 2012), we hypothesized that the modulation of cLP production in the hyphosphere might be driven by the specific nutritional context provided by AM fungal exudates. To test this hypothesis, we assessed the potential influence of carbon compounds commonly reported in AM fungal hyphal exudates (Luthfiana et al., 2021; Toljander et al., 2007; Zhang et al., 2022), on the secondary metabolite production of *B. velezensis*. For this purpose, *B. velezensis* was cultivated under agitation in liquid M9 minimal salts medium supplemented with individual carbohydrates representative of those found in AM fungal exudates. This approach allowed us to assess the specific impact of each carbon source on the production of individual cLPs as well as bacilysin (**Figure 3-13**). In addition, we evaluated the combined influence of these carbohydrates to determine whether the cLP pattern observed in the hyphosphere could result from their collective action. To further simulate the nutritional conditions of the AM fungal

environment, we developed a minimal medium termed **AMF Exudate-Mimicking Medium** (AMF-EMM), containing only oligo-elements and the carbon sources typically detected in AM fungal exudates. Cultivating *B. velezensis* in this medium resulted in a significant increase in the relative proportions of fengycin and surfactin compared with natural exudates (**Figure 3-12 B**). Therefore, we assume that the cLP pattern produced by *B. velezensis* upon interaction with *R. irregularis* and characterized by very low amounts of harmful fengycin is not due to specific nutritional context but is formed in response to the perception of some unidentified signal(s) secreted by the AM fungus.

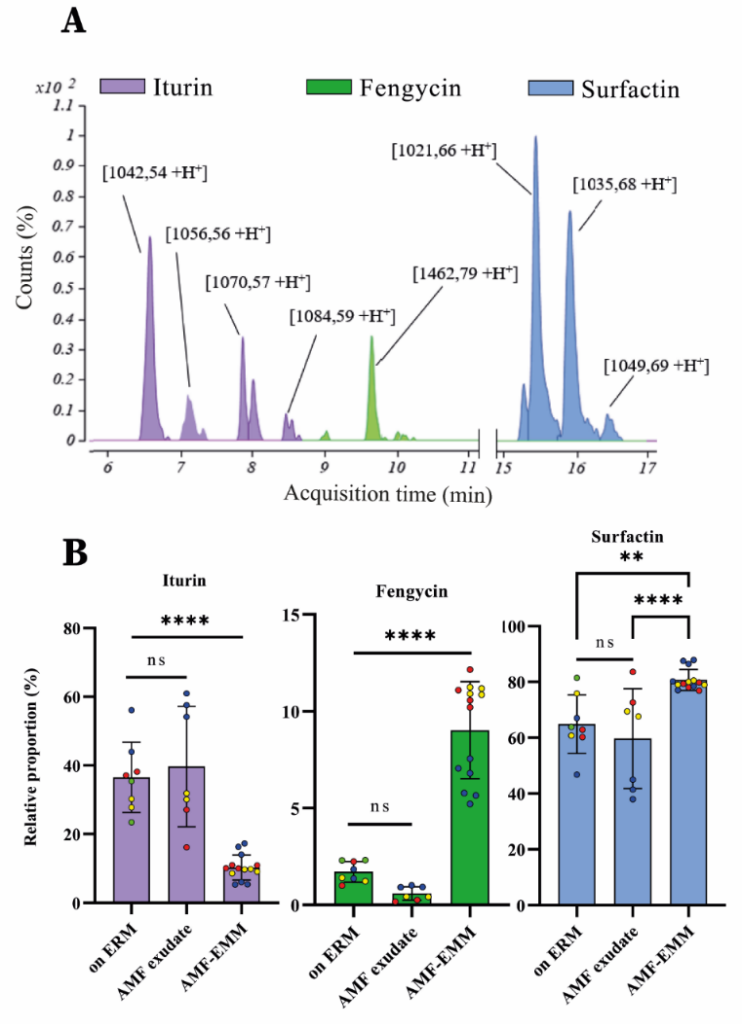

Figure 3-12: *B. velezensis* antifungal compounds modulation through *R. irregularis* exudates. **A**, UPLC-MS extract ion chromatogram (EIC) illustrating the relative abundance of surfactin (blue), iturin (purple) and fengycin (green) family secreted by *B. velezensis* 9 dpi on hyphae of 3 months-old cultures of *R. irregularis*. The different peaks for each cLPs correspond to the structural variants differing in fatty acid chain length. **B**, Relative surfactin (blue), iturin (purple), fengycin (green) proportion corresponding to the detected peaks areas of each cLP compared to the total amount of the 3 families of cLPs following growth condition. cLPs relative proportion when B. velezensis evolved along AM fungal hyphae (on ERM), on exudates collected from AM fungal hyphae (AM fungal exudate), on AM fungal exudates mimicking medium (AMF-EMM). Bars represent the means ± SD of 3 to 4 biological replicates (different colours) and 2 to 4 technical replicates (same colours). $7 \leq n \leq 14$; Letters a to d indicate statistically significant differences according to one-way analysis of variance (ANOVA) and Tukey's HSD test ($\alpha = 0.05$): ns = not significant; ** $0.001 < p < 0.01$, **** $p < 0.0001$.

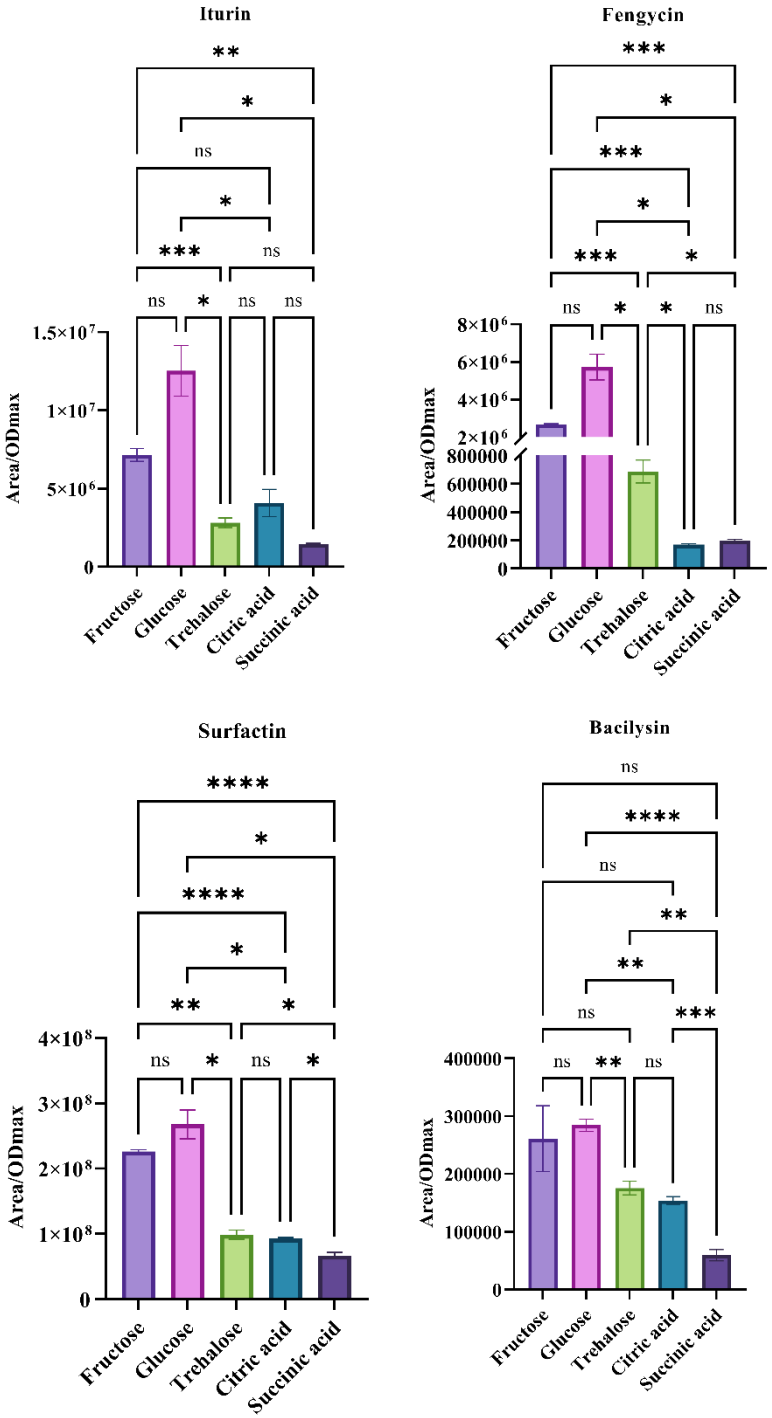
Iturin
Area/ODmax
1.5×10⁷
1×10⁷
5×10⁶
0
Fructose
Glucose
Trehalose
Citric acid
Succinic acid
Fengycin
Area/ODmax
8×10⁶
6×10⁶
4×10⁶
2×10⁶
800000
600000
400000
200000
0
Surfactin
Area/ODmax
4×10⁸
3×10⁸
2×10⁸
1×10⁸
0
Bacilysin
Area/ODmax
400000
300000
200000
100000
0

Figure 3-13: Influence of each carbon source found in hyphal exudate of *R. irregulairs* on the metabolome of *B. velezensis*. The carbon sources of AM fungus exudates individually (10 mM of fructose, glucose, inositol, citric acid, 5 mM trehalose or 15 mM succinic acid) were solubilized in M9 minimal salts medium and buffered at pH 6.8 with MOPS (10.5 g l-1). Bars represent the means ± SD of 3 biological replicates and 3 technical replicates. n=9, one-way analysis of variance (ANOVA) and Tukey's HSD test ($\alpha = 0.05$): ns = not significant; * $0.01 < p < 0.05$; ** $0.001 < p < 0.01$; *** $0.0001 < p < 0.001$; **** = $p < 0.0001$.

3.4 Myc-LCOs impact *B. velezensis* metabolite production and phenotype

The symbiotic relationship between plants and AM fungi relies on a sophisticated molecular dialogue, in which LCOs play a central role (Feng et al., 2019). These signaling molecules are not only essential for initiating symbiosis with plants but have also been shown to influence fungal development (Rush et al., 2020, 2022). To gain deeper insight into the molecular basis of the compatibility between *B. velezensis* and *R. irregularis*, we investigated whether AM fungal-derived LCOs could modulate the metabolome and behaviour of *B. velezensis*.

To test this hypothesis, we used a synthetic equimolar mixture of the main LCOs typically found in AM fungal exudates (**Figure 3-14**), applied at a final concentration of 10^{-11} M, a concentration previously shown to be biologically active in the context of plant–AM fungal symbiosis (Feng et al., 2019; Khokhani et al., 2021; Rush et al., 2020, 2022; Sun et al., 2015). *B. velezensis* planktonic cultures were grown in the presence of this LCO mix to evaluate potential effects on metabolite production and on biofilm formation. After 24 h of cultivation, both optical density and overall cLP production appeared similar between LCO-treated and control conditions, suggesting a transient effect under liquid culture conditions. Therefore, we monitored the kinetics of cLP production over time, focusing on the onset of surfactin (after 9 h) and iturin/fengycin (after 10 h) biosynthesis.

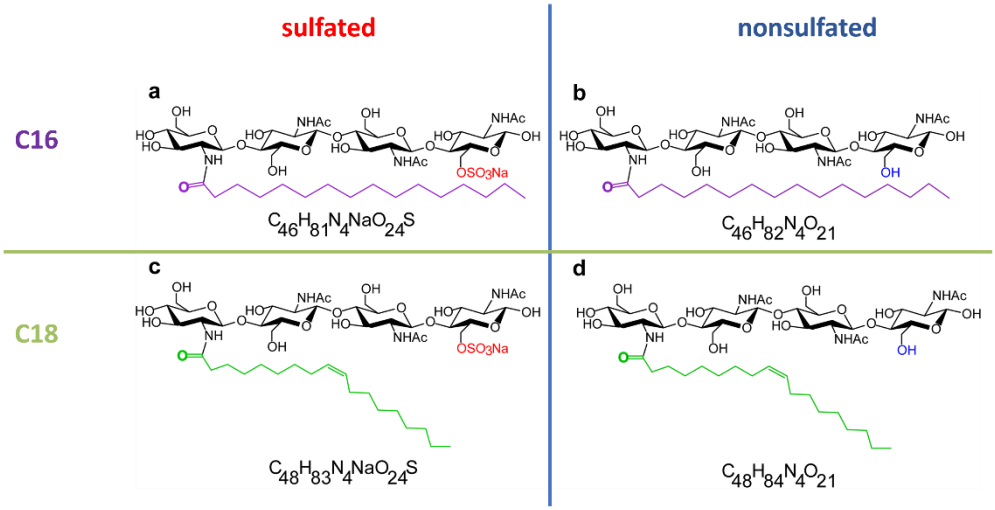

Figure 3-14: Main Myc-LCOs produced by AM fungi and used in this study.
Illustration of the four mycorrhizal LCOs (Myc-LCOs) selected for this study. Adapted from Rush et al. (2022).

We first observed that exposure to LCOs led to a significant shift in the production of cLPs by *B. velezensis*. In particular, fengycin levels were reduced, while surfactin levels increased, mimicking the metabolic profile observed during direct contact with AM fungal hyphae and in the presence of fungal exudates (**Figure 3-15 A**). Given that surfactin has been shown to promote bacterial colonization of *R. irregularis*, whereas fengycin exhibits toxic effects on the AM fungus at higher concentrations, these results suggest that *B. velezensis* responds to AM fungal LCOs by modulating its secondary metabolism to favor coexistence.

To further examine the influence of LCOs on bacterial lifestyle, biofilm formation was evaluated under static conditions that promote pellicle development at the **air–liquid interface**. Under such conditions, without agitation, *Bacillus* forms a biofilm on the liquid surface, accessing both gaseous and aqueous phases for nutrients and oxygen. *B. velezensis* cultures were grown in AMF-EMM medium supplemented with 1% (v/v) of a 10^{-8} M LCO mixture, AM fungal exudates, or PBS as a control. After 24 h at 30 °C, the biofilm pellicle was quantified by crystal violet staining, and absorbance was measured at 595 nm. The addition of LCOs led to a clear reduction in pellicle formation when *B. velezensis* was grown at the air–liquid interface in static liquid medium. This result suggests that LCOs interfere with biofilm development (**Figure 3-15 B**). However, optical density measurements taken after 11 h of culture revealed increased growth in the presence of LCOs (**Figure 3-15 C**). This may reflect a physiological shift from a sessile to a more proliferative state, favouring vegetative cell multiplication over sporulation or structured biofilm development along fungal

hyphae, an observation consistent with the early colonization dynamics described in Chapter 2.

Altogether, these results indicate that LCOs act as interkingdom signalling molecules capable of modulating bacterial behaviour and metabolism. By reshaping cLP production and growth strategies, AM fungal LCOs may promote a physiological state in *B. velezensis* conducive to a cooperative, non-antagonistic interaction with R. irregularis.

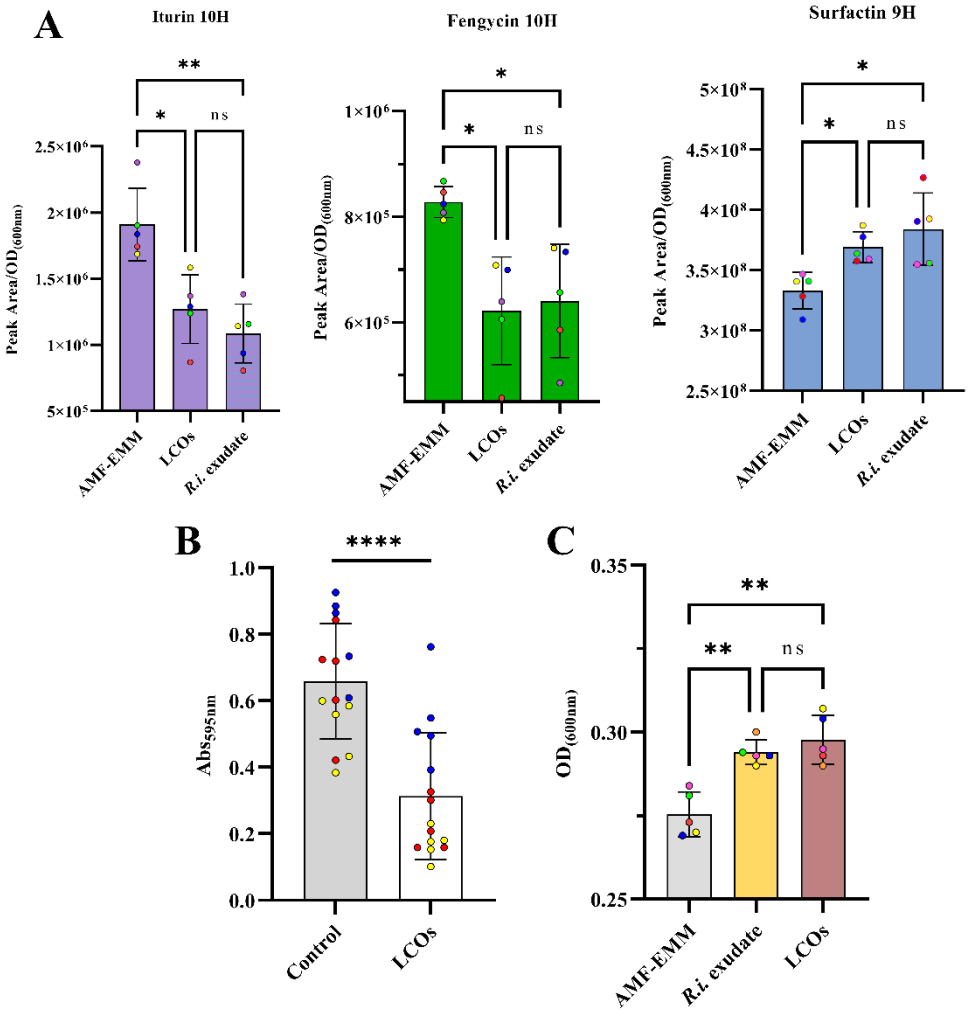

Figure 3-15: Effect of LCOs produced by *R. irregularis* on *B. velezensis* behaviour and metabolite production. A, Relative production (Peak Area/OD) of surfactins, fengycins and iturins (from left to right) in planktonic cultures of *B. velezensis* on AM fungal exudates mimicking medium (AMF-EMM) and upon supplementation with 1% (v/v) of AM fungal exudates (*R.i.* exudate) or with with LCOs at the concentration of 10^{-11} M (Mean ± SD, n = 5, and Dunnett test ($\alpha = 0.05$); ns, non-significative; ∗, $p < 0.05$; ∗∗, $p < 0.01$; ∗∗∗, $p < 0.001$). **B,** Assessment of biofilm formation at the air-liquid interface by *B. velezensis* in the control medium and upon supplementation with LCOs at the concentration of 10^{-11} M in a 96-well microplate by crystal violet staining. **C**, Growth of *B. velezensis* in AMF-EMM liquid medium and upon supplementation with LCOs at the concentration of 10^{-11} M or with 1% of AM fungal exudate. The optical density (OD600nm) of the bacterium was measured after 11h of growth in presence or in absence (control) of LCOs or exudate . Bars represent the means ± SD of 6 biological replicates (different colours). ; one-way analysis of variance (ANOVA) and Dunnett test ($\alpha = 0.05$).

3.5 *B. velezensis* produces antimicrobials inhibiting soilborne AM fungal competitors

Our data in **Figure 3-12 A** indicates that *B. velezensis* developing as biofilm on AM fungal hyphae still efficiently produces cLPs and potentially other antimicrobial secondary metabolites. Therefore, we next wanted to assess if some compounds actively secreted by the bacterium could protect AM fungus against potentially harmful competitors such as *Trichoderma harzianum* and *Collimonas fungivorans* (De Jaeger et al., 2010; Purin & Rillig, 2008).

We first evaluated the growth inhibitory activity of the crude cell free supernatant (CFS) obtained after growth of *B. velezensis* in AM fungal exudates towards *T. harzianum* and *C. fungivorans.* The CFS was prepared by centrifugation of bacterial cultures followed by filtration through 0.22 µm filters to remove cells. To assess the effect of the CFS, we cultured the competitors in PDB medium supplemented with 20% (v/v) of the CFS. Controls were supplemented with physiological water (20% v/v). In parallel, we tested the impact of AM fungal exudates alone on the growth of both competitors and observed no significant effect (**Figure 3-17**). In contrast, the CFS from the *B. velezensis* wild-type (WT) strain exhibited a strong antagonistic effect on both *T. harzianum* and *C. fungivorans* (**Figure 3-16**).

To identify the metabolites responsible for these antimicrobial activities, we performed the same experiment using *B. velezensis* mutants defective in the biosynthesis of specific BSMs typically produced by the wild-type strain in the hyphosphere. All mutants were tested simultaneously under identical conditions. For clarity, results are presented separately according to the targeted competitor and the set of mutants analysed. In **Figure 3-16**, we show the effects of mutants impaired in

the synthesis of NRPs due to deletion of the *sfp* gene, which disrupts both cLP and polyketide biosynthesis. Additionally, we included a *bacA* mutant, unable to produce bacilysin, a NRP synthesized independently of the *sfp*-dependent machinery. In **Figure 3-17**, we present the activity profiles of mutants selectively deficient in one or several cLP families (iturin, fengycin, or surfactin), while retaining the ability to produce polyketides and bacilysin. This design allowed us to evaluate the specific contribution of each cLP family and the possible involvement of polyketides in the observed antimicrobial activity.

A complete loss of anti-*Trichoderma* activity was observed by testing CFS extracts obtained from the mutants *ΔbacA* and *ΔsfpΔbacA* repressed in the synthesis of the non-ribosomal SFP-independent di-peptide bacilysin (**Figure 3-16 A**). The crucial role of bacilysin in the antifungal activity developed by *B. velezensis* against *T. harzianum* was further supported by the similar activity of the *Δsfp* mutant unable to form the other non-ribosomal products cLPs and polyketides (**Figure 3-16 A**). Significant amounts of bacilysin were detected in hyphosphere extracts from AM fungus colonized by *B. velezensis* (**Figure 3-16 C**) indicating that this compound was readily formed by the bacterium while growing on the fungus. Results with other mutants repressed in the synthesis of antifungal cLPs known for their individual or synergistic antifungal activity, demonstrated the reduced role of these metabolites against *T. harzianum* within the hyphosphere context (**Figure 3-17 A**).

The interaction between *Trichoderma sp.* and *B. velezensis* can be context dependent from mutualism to antagonism (Li et al., 2025; Mohd Din et al., 2025; Xie et al., 2024). Previous research has highlighted the significance of iturin production by *B. velezensis* in inhibiting the growth of *Trichoderma* spp. (Fifani et al., 2022). However, we assume that in our conditions, the concentration of iturin in the hyphosphere did not reach the level necessary to affect the development of this mycoparasite. Regarding *C. fungivorans*, none of the knockout mutants showed a significant loss in the antibacterial activity observed for the wild type (**Figure 3-16 B** and **Figure 3-17 B**). Conserved anti-*Collimonas* activity in Δ*sfp* and Δ*sfp*Δ*bacA* extracts suggests the involvement of additional ribosomal compound(s) that remains to be identified.

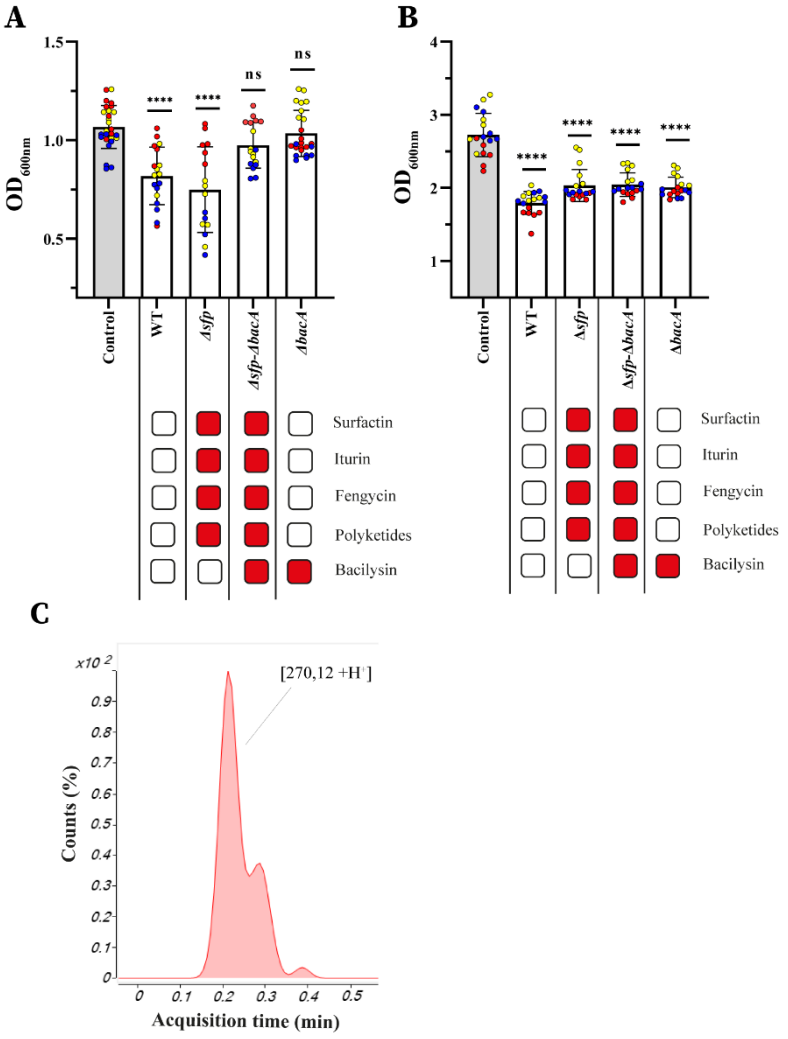
A
B
C
OD600nm
Control
WT
Δsfp
Δsfp-ΔbacA
ΔbacA
Surfactin
Iturin
Fengycin
Polyketides
Bacilysin
****
ns
[270,12 +H+]
x10 2
Counts (%)
Acquisition time (min)

Figure 3-16: BSMs produced by *B. velezensis* in the hyphosphere of *R. irregularis* allowing an antagonism activity against *Trichoderma harzianum* and *Collimonas fungivorans*. **A**, Effect of *B. velezensis* GA1 wild type or mutant cell-free supernatants (CFS), produced on exudates of *R.irregularis* cultures, on the growth of *Trichoderma harzianum* Rifai MUCL 29707. The optical density (OD_{600nm}) of the fungi was measured after 36 h of growth in presence or in absence (control) of CFS. Metabolites not produced by the different mutants are illustrated with red boxes in the table below. Bars represent the means ± SD of 3 biological replicates (different colours) and 4 to 9 technical replicates (same colours). $16 \leq n \leq 27$, one-way analysis of variance (ANOVA) and Dunnett's test ($\alpha = 0.05$): ns = not significant; **** = $p < 0.0001$. **B**, Effect of *B. velezensis* GA1 wild type or mutant cell-free supernatants (CFS) produced on exudates of *R.irregularis* cultures on the growth of *Collimonas fungivorans* LMG 21973. The optical density (OD_{600nm}) of the bacterium was measured after 24 h of growth in presence or in absence (control) of CFS. Metabolites not produced by the different mutants are illustrated with red boxes in the table below. Bars represent the means ± SD of 3 biological replicates (different colours) and 6 technical replicates (same colours). $16 \leq n \leq 27$, one-way analysis of variance (ANOVA) and Dunnett's test ($\alpha = 0.05$) compared to the control: ns = not significant; **** = $p < 0.0001$. **C**, UPLC-MS extract ion chromatogram (EIC) illustrating the relative abundance of bacilysin (red), secreted by *B. velezensis* 9 dpi on 3 months-old *R.irregularis* cultures.

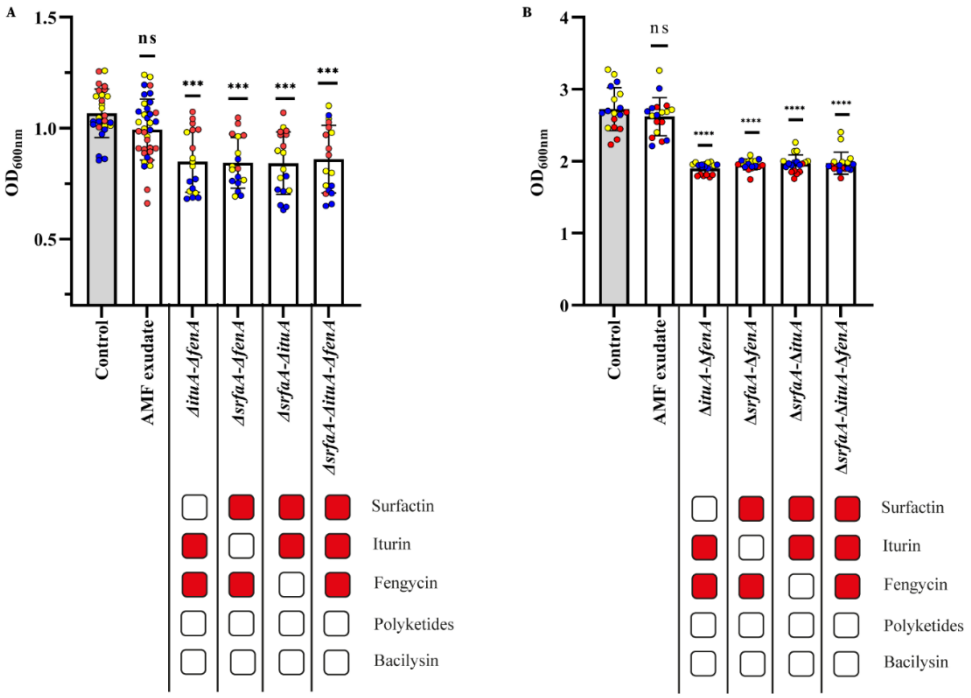

Figure 3-17: BSMs produced by *B. velezensis* on AM fungal exudates allowing an antagonism activity against *Trichoderma harzianum* and *Collimonas fungivorans.* A, Effect of *B. velezensis* GA1 mutant cell-free supernatants (CFS), produced on exudate of *R. irregularis*, on the growth of *Trichoderma harzianum* Rifai MUCL 29707. The optical density (OD_{600}) of the mycoparasite fungus was quantified after 36 h of growth in presence or in absence (control) of CFS. Metabolites not produced by the different mutants are illustrated with red boxes in the table above. Bars represent the means ± SD of 3 biological replicates (different colours) and 4 to 9 technical replicates (same colours). $16 \leq n \leq 27$, one-way analysis of variance (ANOVA) and Tukey's HSD test ($\alpha = 0.05$): ns = not significant; **** = $p < 0.0001$. **B,** Effect of *B. velezensis* GA1 wild type or mutant cell-free supernatants (CFS), produced on exudate of *R. irregularis*., on the growth of *Collimonas fungivorans* LMG 21973. The optical density (OD_{600}) of the bacteria was quantified after 36 h of growth in presence or in absence (control) of CFS. Metabolites not produced by the different mutants are illustrated with red boxes in the table above. Bars represent the means ± SD of 3 biological replicates (different colours) and 6 technical replicates (same colours). $16 \leq n \leq 27$, one-way analysis of variance (ANOVA) and Tukey's HSD test ($\alpha = 0.05$): ns = not significant.

3.6 Surfactin as a key molecule in the interaction with *R. irregularis*

Secondary metabolites and more particularly cLPs are key components involved in multitrophic interactions established by *Bacillus* spp. in the rhizosphere (Andrić et al., 2020; Balleux et al., 2025; Traxler & Kolter, 2015). We thus investigated their possible role in the increase of cytoplasmic flow velocity triggered by the bacterium in *R. irregularis* hyphae (Chapter 2). We first analysed *B. velezensis* mutants deleted in cLP-biosynthesis genes. Co-cultivation with *R. irregularis* of all mutants impaired in surfactin production did not result in increased flow velocity, providing first evidence for the crucial role of this cLP but not iturin, fengycin or any other non-ribosomal compounds (**Figure 3-18 A**). We next added purified surfactin to monocultures of *R. irregularis* associated to *D. carota* and observed a similar trend on flow velocity upon treatment with concentrations as low as 2 µM, which is in the range of the amounts detected in the hyphosphere (**Figure 3-18 B**).

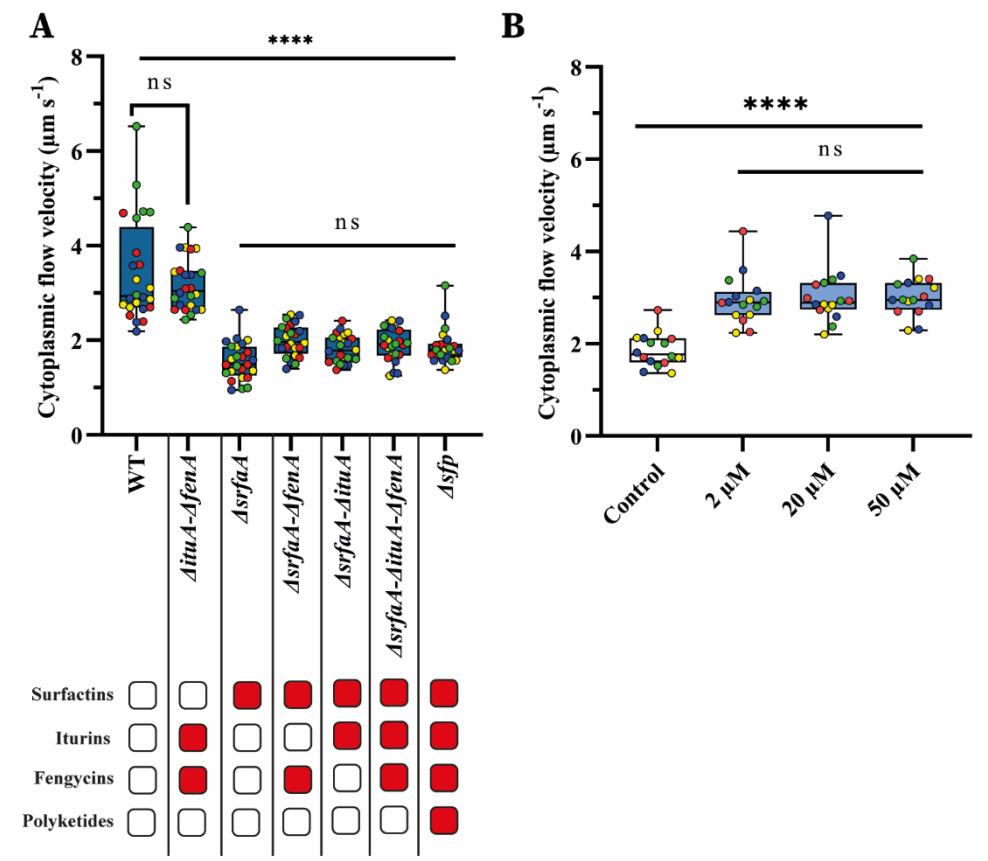

Figure 3-18: Surfactin increase cytoplasmic streaming within AM fungal hyphae. A, Cytoplasmic flow velocity in hyphae of *R. irregularis*. in presence of *B.velezensis* wild type (WT) or knock out mutants, 7 dpi along hyphae. Metabolites not produced by the different mutants are illustrated with red boxes in the table below. The boxes encompass the 1st and 3rd quartiles, the whiskers extend to the minimum and maximum points, and the midline indicates the median. The individual points represent 4 biological replicates (different colours) and 6 to 7 technical replicates (same colours). $24 \leq n \leq 25$; one-way analysis of variance (ANOVA) and Tukey's HSD test ($\alpha = 0.05$): ns = not significant; **** $p < 0.0001$. **B**, Cytoplasmic flow velocity in hyphae of *R. irregularis* in contact with increasing concentrations of pure surfactin (2 µM, 20 µM or 50 µM) compared to a PBS control. The boxes encompass the 1st and 3rd quartiles, the whiskers extend to the minimum and maximum points, and the midline indicates the median. The individual points represent 4 biological replicates (different colours) and 4 technical replicates (same colours). $n = 16$; one-way analysis of variance (ANOVA) and Tukey's HSD test ($\alpha = 0.05$): ns = not significant; **** $p < 0.0001$.

To determine if this response is restricted to hyphae segments in contact with the lipopeptide or not, we next used a tri-compartmented culture system in which the hyphal network but not the root, is allowed to cross into two different hyphal compartments physically separated by a plastic barrier (Whiteside et al., 2019), thereby preventing surfactin from diffusing between the compartments (**Figure 3-19**). With this set-up, we observed the diffusion of the response within the ERM and across the root compartment. The effects of surfactin were not limited to hyphae in the treated compartment (HCsolid+Ri+srf) but also influenced distal regions (**Figure 3-20**), resulting in an overall increase in cytoplasmic flow observed in the untreated compartment (HCsolid+Ri-srf) at 48 hours post inoculation (**Figures 3-20**). These data strongly suggest that surfactin acts as a trigger driving the AM fungus to systemically boost its cytoplasmic translocation.

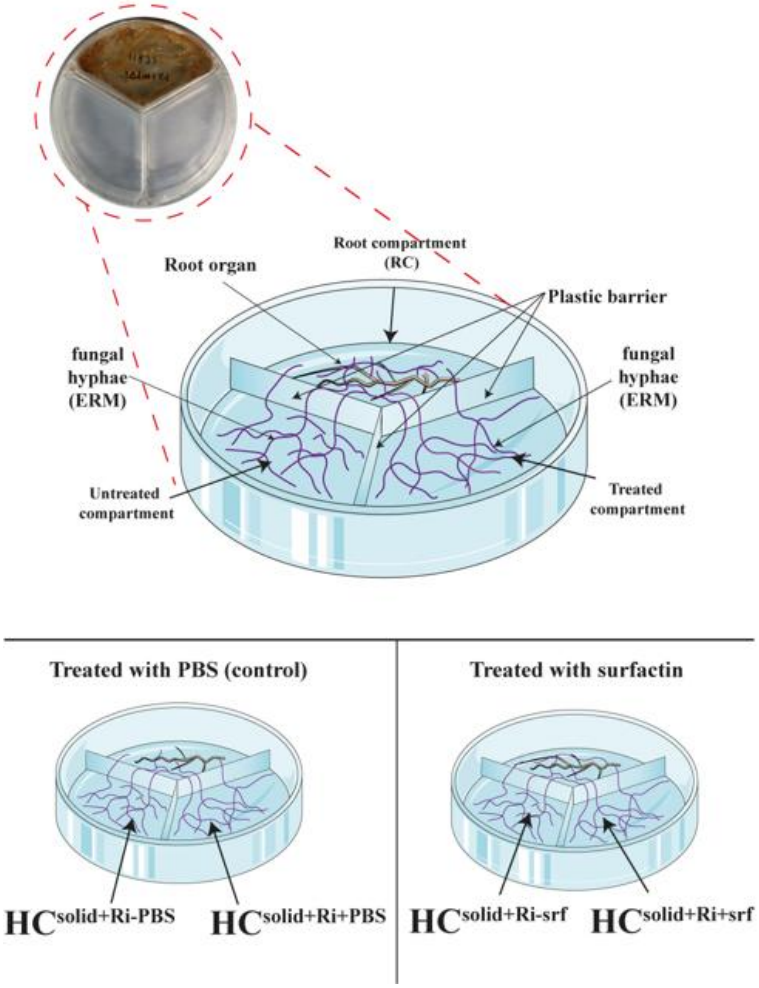

Figure 3-19:Surfactin systemically boost the cytoplasmic streaming inside *R. irregularis* hyphae. Picture (red circle) and illustration of a tri-compartmented experimental setup. In one compartment (root compartment – RC) roots of *D. carota* are associated to *R. irregularis*, from which the hyphae colonize two side compartments. One side compartment contained either pure surfactin at a concentration of 2µM ($HC^{solid+Ri+srf}$) or PBS ($HC^{solid+Ri+PBS}$). The other side compartment non supplemented with surfactin or PBS was annotated as follows ($HC^{solid+Ri-srf}$ or $HC^{solid+Ri-PBS}$). A plastic barrier prevents surfactin from diffusing between compartments.

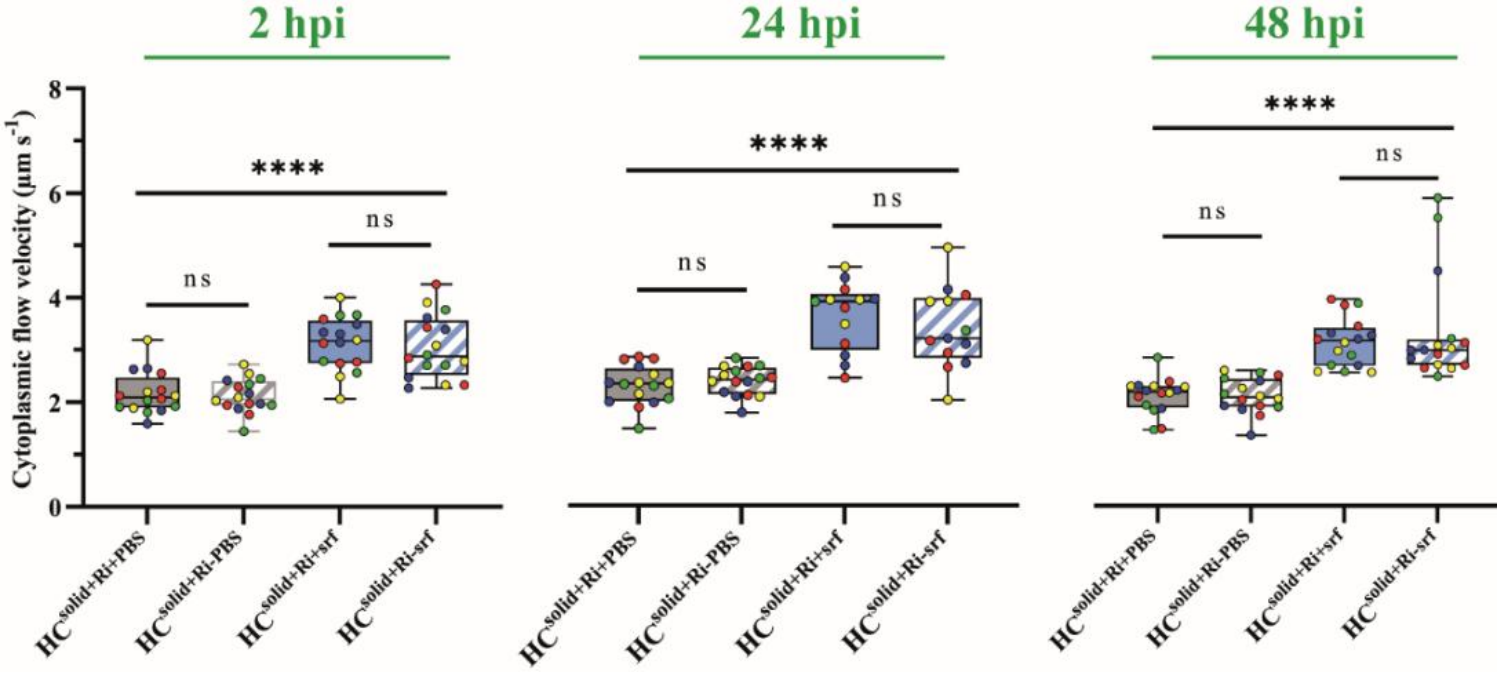

Figure 3-20: Dynamics of *R. irregularis* cytoplasmic flow velocity in presence of surfactin. The velocity of the cytoplasmic flow in the compartment treated with surfactin ($HC^{Solid+Ri+srf}$, blue) or PBS ($HC^{Solid+Ri+PBS}$, gray) and in the untreated compartment following the treated compartment either with surfactin ($HC^{Solid+Ri-srf}$, blue stripes) or with PBS ($HC^{Solid+Ri-PBS}$, gray stripes) after 2, 24 and 48 hours of treatment. The boxes encompass the 1st and 3rd quartiles, the whiskers extend to the minimum and maximum points, and the midline indicates the median. The individual points represent 4 biological replicates (different colours) and 4 technical replicates (same colours). n=16; one-way analysis of variance (ANOVA) and Tukey's HSD test ($\alpha = 0.05$): ns = not significant; **** $p < 0.0001$.

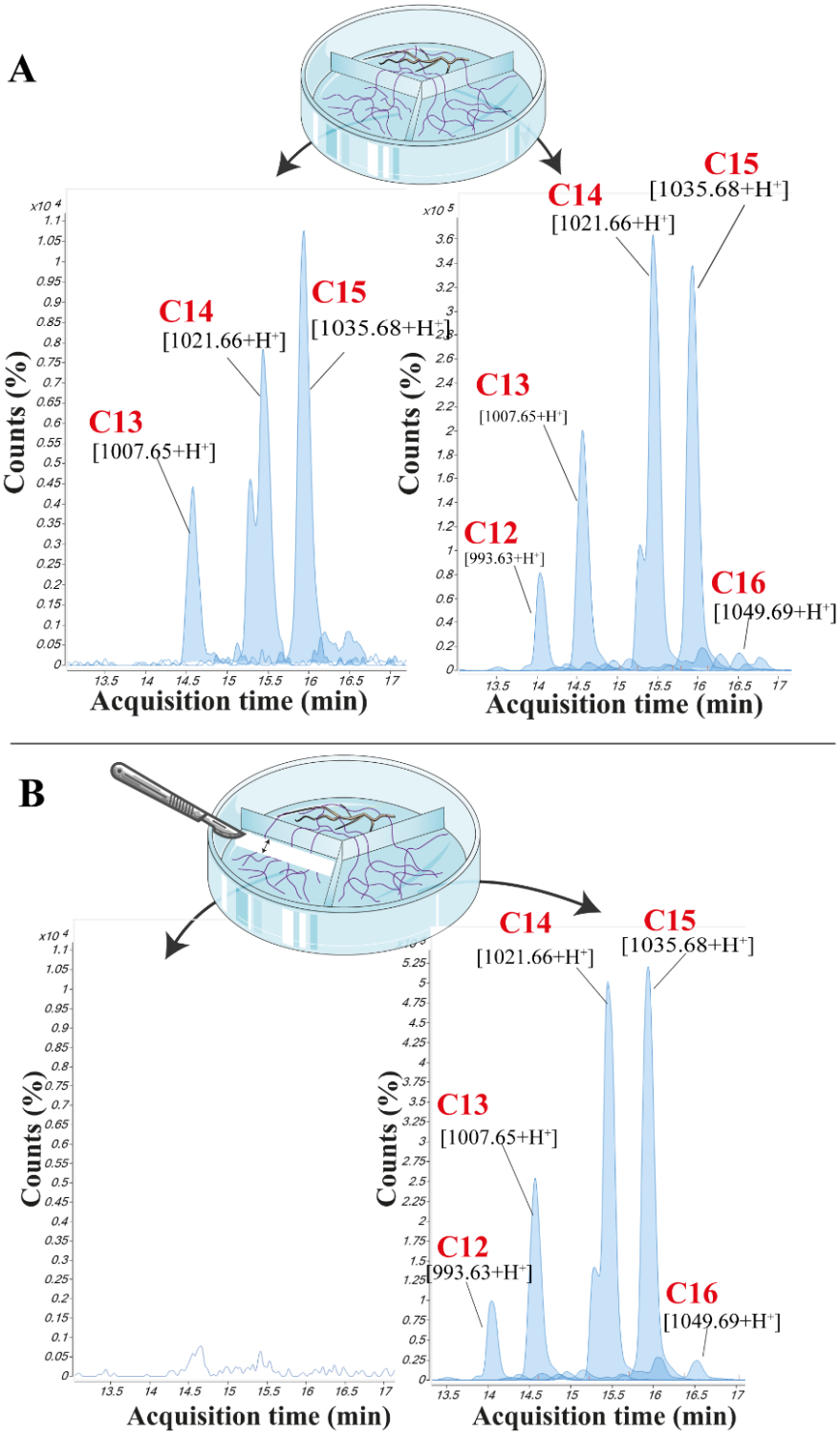
A
C13
[1007.65+H+]
C14
[1021.66+H+]
C15
[1035.68+H+]
C12
[993.63+H+]
C16
[1049.69+H+]
Counts (%)
Acquisition time (min)
B
C13
[1007.65+H+]
C14
[1021.66+H+]
C15
[1035.68+H+]
C12
[993.63+H+]
C16
[1049.69+H+]
Counts (%)
Acquisition time (min)

Figure 3-21: Translocation of surfactin through the network of *R. irregularis*. Illustration of the tri-compartmented experimental setup in which surfactin was added to one hyphal compartment (Treated compartment), keeping the same amount of surfactin 19.16 µM in average (n = 3) than the concentration used to the treatment (20 µM). In the second compartment, the amount of surfactin was quantified when the ERM was intact (**A**) or when the network was cut by a band of 0.5 cm width (**B**) to evaluate if surfactin may be translocated by *R. irregularis*. Representative UPLC-MS extract ion chromatogram (EIC) illustrating the relative abundance of surfactin (blue) in each compartment, the number in red represent the length of the fatty acid tail. *D. carota* transformed roots were confined to the root compartment (RC), but the fungus was able to cross the plastic barrier, entering the hyphal compartments (HC). Another plastic barrier prevented the transfer of surfactin between the two HC.

Interestingly, UPLC-qTOF MS analyses of hyphosphere extracts prepared from the untreated compartment (HCsolid+Ri-srf) revealed that surfactin was translocated at distal zone through the ERM (**Figure 3-21**) since significant amounts (corresponding to 0.32 µM in average) were recovered from the HCsolid+Ri-srf when the ERM was intact but no trace of the lipopeptide could be detected when the mycelium network was cut. These results underlined the potential of the AM fungus to transport this bacterial secondary metabolite through its network. We hypothesize that surfactin translocation may occur either by diffusion along the water films covering the hyphal surface or via internalization within fungal hyphae.

We also used **mass spectrometry imaging** (MSI) to spatially map surfactin localization along the fungal network. A section of *R. irregularis* hyphae from the untreated compartment was mounted on a microscope slide and analysed by MSI following composite bright-field imaging (**Figure 3-22 A**). Surfactin ion signatures were clearly detected in the distal zone of the fungal network, confirming its long-distance translocation through the ERM (**Figure 3-22 B**). Interestingly, surfactin localization appeared more intense in regions with dense hyphal branching or where spore are present, although the resolution of the MSI technique did not allow us to distinguish whether the compound was internalized or surface-associated.

To address this, we adapted our setup using Phytagel instead of agarose, which allows for easier hyphae collection and dissolution of the medium. Hyphae from both compartments (HCsolid+Ri+srf and HCsolid+Ri-srf) were harvested and washed twice with water. In the treated compartment, surfactin was detectable in the first wash but absent in the second, suggesting successful surface removal. In the untreated compartment, no surfactin was detected in either wash. Next, the rinsed hyphae were subjected to sonication in 70% acetonitrile to extract internal or membrane-associated compounds. Surfactin was consistently recovered from both compartments, at average concentrations of 0.29 µM (treated) and 0.27 µM (untreated), showing no statistically significant difference between the two. These values were also comparable to the total

recovered concentration from whole-compartment extractions (0.32 µM) of the untreated compartment.

Altogether, these findings strongly suggest that surfactin produced by *B. velezensis* is not only perceived by *R. irregularis* but also actively translocated through its hyphal network, where it modulates physiological traits such as cytoplasmic streaming.

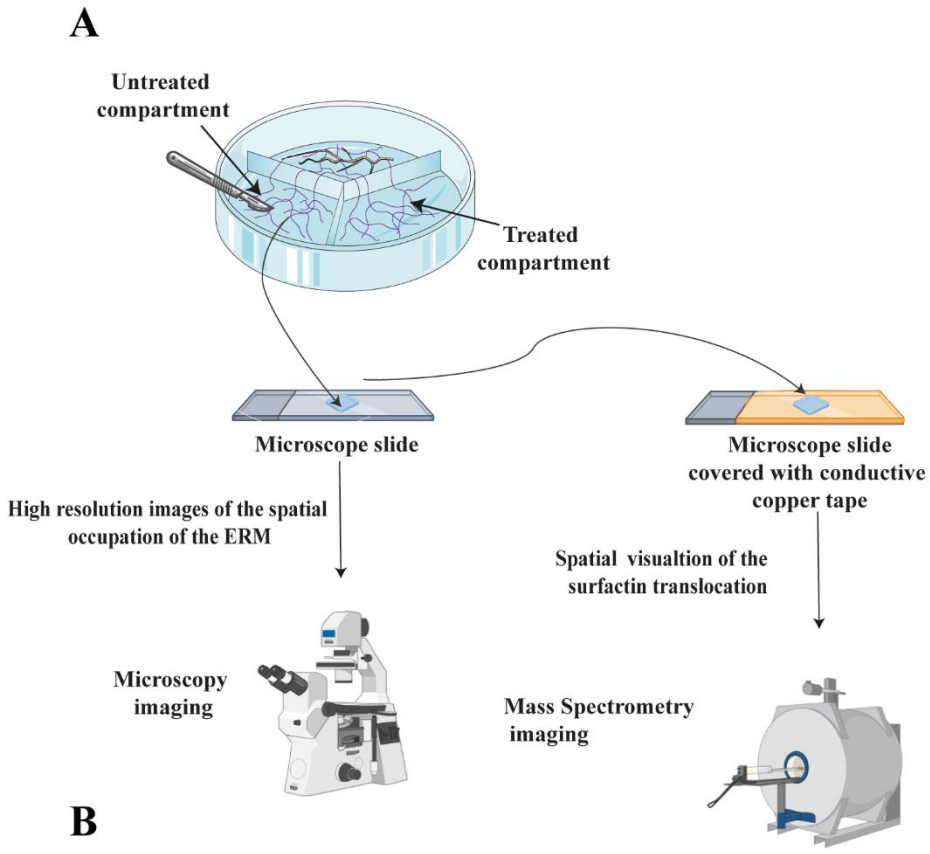
A
Untreated compartment
Treated compartment
Microscope slide
Microscope slide covered with conductive copper tape
High resolution images of the spatial occupation of the ERM
Spatial visualtion of the surfactin translocation
Microscopy imaging
Mass Spectrometry imaging
B
Microscopy imaging
Mass Spectrometry imaging
Extraradical mycelium (ERM) network
Intensity
Intensity
[1021.66+H+]
[1035.68+H+]

Figure 3-22: Spatial mapping of surfactin translocation through *R. irregularis*. A. Schematic representation of the workflow used for MSI (Mass Spectrometry Imaging) analysis. A portion of the ERM from the untreated compartment was transferred onto a microscope slide for composite bright-field imaging and onto a second slide covered with conductive copper tape for MSI acquisition. **B.** Left: Composite bright-field image showing the AM fungal hyphal network, taken prior to MSI. This image corresponds to an sample taken in the untreated compartment**.** Right: MSI visualizations of two specific surfactin ion species detected in the untreated compartment, 48 hours after application. These images confirm the presence and spatial distribution of surfactin along the fungal network, indicating long-distance translocation through the ERM.

3.7 Summary: The language with the plant, rewritten for microbial dialogue

RQ 2: What are the factors that drive this interkingdom interaction ?
Potentially the AM fungal LCOs and the bacterial BSMs Surfactin

In this chapter, we explore the molecular basis of the compatible interaction between *B. velezensis* and *R. irregularis*, highlighting how molecules known to be involved in communication with the plant are co-opted to mediate a microbial dialogue. This interkingdom crosstalk appears to be orchestrated by specific compounds: Myc-LCOs from *R. irregularis* and surfactins from *B. velezensis* (**Figure 3-23**).

We observed that *R. irregularis* attenuates the production of toxic compounds by *B. velezensis*, particularly fengycins. This repression seems independent of nutrient context and may potentially be mediated by fungal LCOs, which influence both bacterial metabolism and behaviour. Consequently, LCOs could promote *B. velezensis* colonization of the fungal network, as suggested in Chapter 2, indicating that these signals might foster physical association and compatibility. Despite fengycin attenuation, *B. velezensis* retains antifungal activity through the production of alternative metabolites such as bacilysin, particularly when cultivated on AM fungal exudates. Interestingly, these compounds are active against potential mycoparasites of AM fungi, supporting a model in which the fungus provides access to carbon-rich niches in the hyphosphere, while the bacterium helps protect *R. irregularis* from microbial competitors. This reciprocal benefit reflects a fine-tuned mutualism, in which antagonistic potential is conserved but redirected.

Importantly, surfactin emerges as a central component of this interaction. Beyond its role in promoting colonization, we show that surfactin enhances cytoplasmic streaming in the fungal hyphae, suggesting a enhanced vitality of the fungus in response to a bacterial cue. Moreover, using mass spectrometry imaging and biochemical assays, we demonstrated that surfactin can translocate across the ERM, pointing toward a long-distance signaling mechanism mediated by the fungal network.

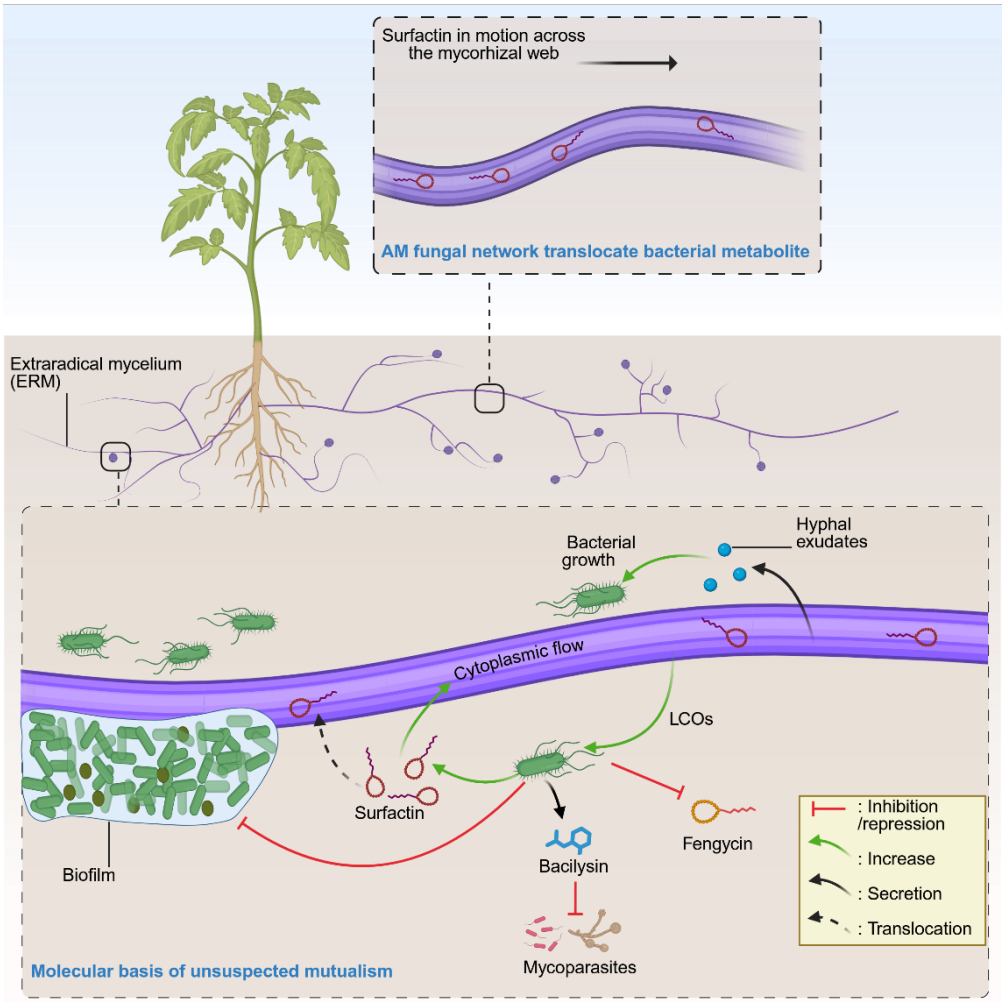

Figure 3-23: Schematic summary of the molecular crosstalk between *Bacillus velezensis* and *Rhizophagus irregularis* leading to a mutualistic interaction. This figure illustrate how *R. irregularis* and *B. velezensis* establish a sophisticated and dynamic chemical crosstalk. The AM fungus modulates bacterial behavior and secondary metabolism, fostering compatibility while maintaining a degree of protection. In turn, the bacterium adjusts its metabolome to support the interaction and safeguard its fungal partner. Figure was created with Biorender.com.

Chapter 4

Unity is strength

4.1 State of the art

The plant immune system orchestrates a delicate balance between defending against pathogens and accommodating beneficial microbes (Zhang & Kong, 2022; Zipfel & Oldroyd, 2017) (see also Chapter 3). Plants have evolved robust immune mechanisms to perceive and counteract a wide range of pathogenic organisms. This balance relies mainly on two major layers of innate immunity: Pattern-triggered immunity (PTI) or Microbe-Associated Molecular Pattern Triggered Immunity (MTI), which is activated by the detection of microbial-pathogen or damage-associated molecular patterns (MAMPs/PAMPs/DAMPs), and **effector-triggered immunity** (ETI), which is initiated by the recognition of pathogen effectors by intracellular resistance proteins (Bigeard et al., 2015; Cui et al., 2015; Jian et al., 2023; Peng et al., 2018; Yu et al., 2017). While these responses are highly effective against pathogens, they can be energetically costly and often result in growth penalties. Following pathogen recognition, these immune responses can also lead to the establishment of systemic acquired resistance (SAR), which provides broad and long-lasting protection to distal plant tissues (Fu & Dong, 2013; Ngou et al., 2022; Shah & Zeier, 2013).

Beneficial microbes such as *Bacillus* spp. and AM fungi induce distinct systemic response, induced systemic resistance (ISR) and mycorrhiza-induced resistance (MIR) respectively, that prime plants for future attacks by pathogens or herbivores but without major growth costs (**Figure 4-1**) (Fiorilli et al., 2024; Pieterse et al., 2014; Yu et al., 2019). Unlike SAR, these priming responses do not rely on the systemic accumulation of pathogenesis-related (PR) proteins but rather prepare the plant to react more rapidly and robustly upon subsequent challenge. Cellular and molecular studies have shown that during the early stages of colonization by AM fungi or PGPR, root cells activate a suite of defence responses, including characteristic Ca^{2+} signaling patterns, and ROS production. However, these responses remain weaker and more transient compared to those elicited by pathogenic microorganisms (Jian et al., 2023; Liu et al., 2024a; Yu et al., 2019). Both MIR and ISR responses rely primarily on the priming of plant defences, a form of immunological memory in which a mild initial stimulus enables faster and stronger activation of defences upon subsequent challenge (Buswell et al., 2018; Conrath et al., 2015; De Kesel et al., 2021; Mauch-Mani et al., 2017). This priming, which occurs not only in colonized roots but also in distal tissues, is considered an adaptive and energy-efficient strategy that minimizes metabolic costs while maximizing protection (Conrath et al., 2015; Mauch-Mani et al., 2017). The moderate transcriptomic changes associated with MIR and ISR, compared to the strong reprogramming observed during pathogenic attacks, support the idea that beneficial microbes fine-tune plant immunity to maintain growth–defence balance (Buswell et al., 2018; De Kesel et al., 2021; van Hulten et al., 2006).

Thus, upon subsequent challenge by pathogens or herbivores, plants primed by AM fungi or *Bacillus* spp. exhibit a faster and/or stronger activation of diverse defence traits. These include increased production of secondary metabolites, accumulation of defensive proteins, and the deposition of physical barriers such as callose. Transcriptomic and metabolomic analyses conducted across various plant species further confirm that both ISR and MIR primarily function through the primed activation of broad-spectrum defences, such as the accumulation of dormant signalling proteins, transcription factors and hormones, epigenetic alterations, and/or increased levels of receptors and coreceptors. This priming ultimately enhances the plant's resistance against a wide range of phytopathogens (Conrath et al., 2015; De Kesel et al., 2021; Pastor et al., 2014; Wilkinson et al., 2019).

Bacillus spp. have been widely studied for their ISR-inducing capabilities across numerous crops. Successful colonization and the production of bioactive compounds, particularly lipopeptides and, to a lesser extent, volatile organic compounds (VOCs), are key of this process (Crouzet et al., 2020; Dobránszki et al., 2025; Pršić & Ongena, 2020). Among these metabolites, surfactin is the most extensively studied plant immune elicitor produced by *Bacillus* spp. It has been shown to reduces disease severity in plants such as tomato and *Arabidopsis* by triggering ISR (Cawoy et al., 2014; Chowdhury et al., 2015; Crouzet et al., 2020; García-Gutiérrez et al., 2013; Le Mire et al., 2016). Other lipopeptides, including iturins and fengycins, have also been implicated in ISR induction, albeit to a lesser extent, in crops such as wheat, strawberry, and grapevine (Farzand et al., 2020; Mejri et al., 2018; Yamamoto et al., 2015). The effectiveness of these compounds is influenced by their structural characteristics, plant species and tissue type. Surfactin is more effective in dicots than monocots (Ongena et al., 2007; Rahman et al., 2015), while iturin is more effective when applied to leaves than to roots (Han et al., 2015; Yamamoto et al., 2015). The ISR-inducing activity of these lipopeptides depends on their interaction with plant plasma membranes and is influenced by factors such as fatty acid chain length and specific substitutions in the peptide ring (Jourdan et al., 2009; Kawagoe et al., 2015). Recent findings by Pršić et al. (2023) demonstrated that surfactin's ability to trigger ISR is associated with its incorporation into sphingolipid-enriched membrane microdomains, particularly those containing glucosylceramides. This indicate that the physical properties of the plasma membrane play a critical role in ISR activation and that this mechanism operates independently of classical immune receptor recognition (Schellenberger et al., 2019). In addition to lipopeptides, *Bacillus* can modulate plant immunity through cell wall-derived OGs. Boubsi et al. (2025) showed that *B. velezensis* generates specific short-chain OGs (mainly DP 4) from pectin via pectate lyase activity. These short OGs help the bacterium evading local immune responses at the root level while simultaneously triggering systemic resistance in infected leave. Unlike longer OGs produced by pathogens (DP 10–15), which activate strong immune responses, *Bacillus*-derived short OGs prime systemic immunity without compromising plant fitness. This indicates a dual strategy in which OGs suppress immediate immune responses at the infection site, facilitating root colonization, while

priming the plant for systemic defence, revealing a more intricate interaction between *Bacillus* and plant immunity.

Likewise, AM symbiosis not only improves nutrition but also increases plant tolerance to pathogens through multiple mechanisms. By occupying physical space and consuming resources in the rhizosphere, AM fungi reduce the availability of niches for pathogens. In addition, AM fungi can prime systemic immune defence, a mechanism referred to as MIR (**Figure 4-1**) (Fiorilli et al., 2018, 2024; Rivero et al., 2021; Sanmartín et al., 2020). Myc factors, such as short-chain COs and LCOs, produced by AM fungi, are proposed as modulators of the host immune response. Although the SYM signaling pathway is primarily required for the establishment of mutualism, these chitin-derived signals can also trigger mild and transient immune responses. LCOs and COs have been shown to induce both localized and systemic defences (Luo et al., 2024; Makechemu et al., 2024).

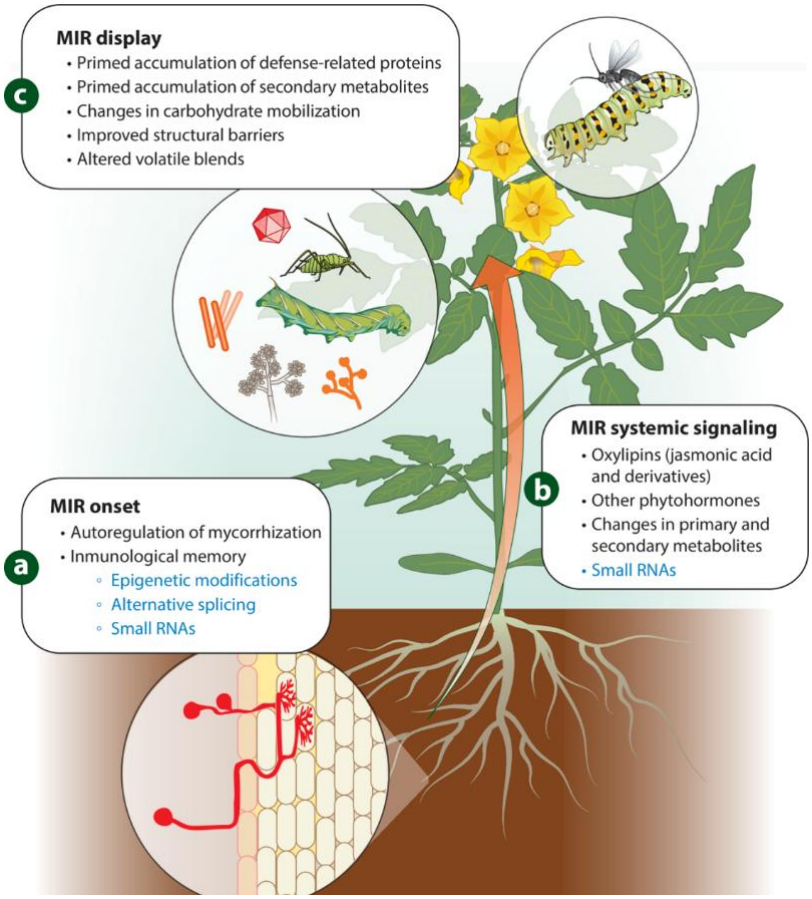

Figure 4-1: Plant immune response triggered by AM fungi, known as mycorrhiza-induced resistance (MIR). (a) Establishment of the AM symbiosis in the roots; (b) subsequent systemic signaling from roots to leaves; and (c) associated transcriptomic and metabolic reprogramming that enhances plant resistance to phytopathogens. Illustration from Fiorilli et al. (2024).

4.2 Gap of knowledge and Research Question outline

B. velezensis and AM fungi are both well-documented for their ability to enhance plant defences through ISR and MIR, respectively. Our previous results demonstrated that *B. velezensis* and *R. irregularis* can establish a mutualistic partnership built on molecular crosstalk and reciprocal functional benefits. However, it remains unknown whether this association also translates into enhanced protection of the host plant against pathogenic threats. From an agronomic perspective, such synergy could be highly valuable, yet there is currently no evidence on the added benefit of combining these two microbes specifically for plant protection. Co-inoculation of beneficial microbes has already shown promise in improving plant resistance against phytopathogens. *Bacillus* spp. in particular may act synergistically with other beneficial organisms, like *Trichoderma*, *Pseudomonas*, or *Streptomyces* strains, to strengthen biocontrol efficacy (Agnolucci et al., 2015; Borriss, 2020; Izquierdo-García et al., 2020; Le Mire et al., 2016; Molina-Santiago et al., 2019). This leads us to the following research question:

RQ3: Is it advantageous to combine an AM fungus and a bacterial biocontrol agent for promoting plant health?

The objective of this chapter was therefore to investigate the practical relevance of this microbial partnership under greenhouse conditions. Specifically, we tested whether the combined application of these two plant-beneficial organisms could enhance tomato resistance to *Botrytis cinerea*, compared to treatments with each microorganism applied separately. In parallel, we monitored plant growth parameters and microbial establishment, both individually and in combination, to determine whether co-inoculation leads to a synergistic enhancement of plant resistance. Building on our previous findings, we also aimed to explore whether AM fungi might contribute to plant protection by facilitating or amplifying the immune-activating effects of surfactin. To this end, we evaluated whether the application of purified surfactin to the extraradical mycelial network of *R. irregularis* could further enhance plant immunity against foliar pathogens.

4.3 *B. velezensis* and *R. irregularis* interaction provides enhanced ISR functionality

To evaluate this potential synergy, we conducted a greenhouse experiment in which we infected the leaves of two tomato (*Solanum lycopersicum*) cultivars, Ailsa Craig and MoneyMaker, with the necrotrophic fungal pathogen *B. cinerea*. Briefly, surface-sterilized seeds of both cultivars were sown in pots containing a sterile substrate. Each treatment included 16 replicate pots. For AM fungal inoculation, 5 g of *R. irregularis* inoculum containing colonized roots and spores (*R.i.*) were mixed into the substrate prior to sowing. For bacterial treatment, 10 mL of a *B. velezensis* suspension (*B.v.*) were applied to the substrate of 16 plants. A co-inoculated group received both the AM fungal inoculum and the bacterial suspension (*R.i.* + *B.v.*). A second bacterial application was performed 12 weeks after planting using the same inoculation procedure and concentration. This time point was defined as 0 days post-inoculation (dpi) with *B. velezensis*. Control plants (n = 16) received 5 g of sterilized AM fungal inoculum and were watered with Hoagland-P solution without bacterial addition. At week 13, the plants were infected with *B. cinerea*.

Disease severity was quantified by measuring the size of the necrotic lesions on infected leaves, while disease incidence was determined by counting the number of emerging or spreading lesions. These parameters allowed us to assess ISR rather than direct antagonism of *B. cinerea*, as both *R. irregularis* and *B. velezensis* were applied exclusively at the root level, and no bacterial colonization was detected in the aerial parts at the time of infection (no fluorescent colonies detected; detection threshold < 10^3 CFU/g fresh weight). This spatial separation ensures that any observed protection is systemic rather than due to direct antifungal activity.

Interestingly, the results revealed cultivar-specific responses. In Ailsa Craig, co-inoculation with *R. irregularis* and *B. velezensis* led to a substantial reduction in both disease severity (approximately 60%) and disease incidence (approximately 75%) compared to control plants. In contrast, single inoculations with either the AM fungus or the bacterium resulted in only moderate and significantly weaker protective effects (**Figure 4-2 A** and **Figure 4-2 B**).

In the MoneyMaker cultivar, no protection was observed in terms of disease incidence when plants were treated with either microbe alone or in combination (**Figure 4-2 C**). However, a significant reduction in disease severity was still recorded when both microorganisms were applied together, suggesting a limitation in pathogen spread despite no suppression of initial lesion emergence (**Figure 4-2 D**). These findings suggest that MoneyMaker is overall more susceptible to *B. cinerea* than Ailsa Craig, but that co-inoculation of both microbes can partially mitigate disease progression, although not its initial establishment.

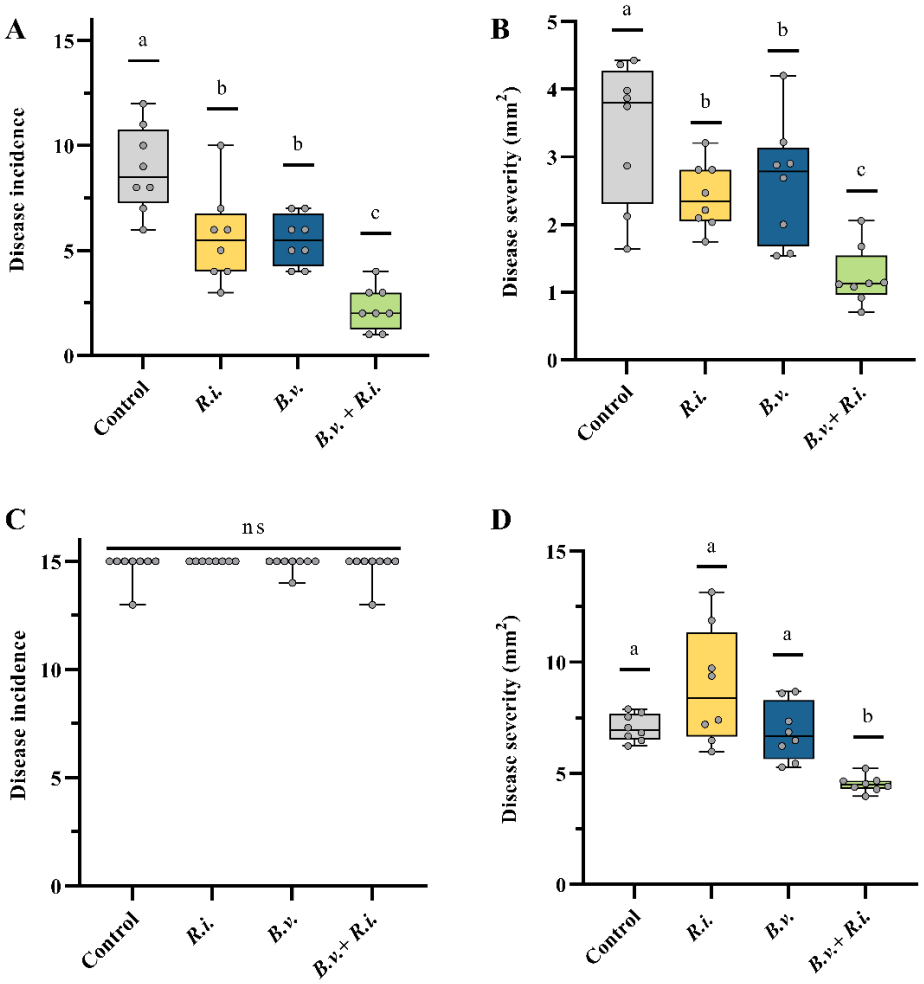

Figure 4-2:The interaction between *B. velezensis* and *R. irregularis* enhances plant protection against *Botrytis cinerea*. **A-C**, Disease incidence quantified as the number of emerging or spreading lesions on 15 leaves from 8 *Solanum lycopersicum* plants of the cultivars Ailsa Craig (**A**) and MoneyMaker (**C**), at 14 and 7 days post-infection with *B. cinerea*, respectively. Plants were treated with *R. irregularis* (*R.i.*, yellow), *B. velezensis* (*B.v.,* blue), the combination of both (*R.i.*+ *B.v.*, green) or with Hoagland solution as Control (gray). **B-D**, Size of emerging lesions (Disease severity) quantified by ImageJ Fiji, on leaves of Ailsa Craig (**B**) and MoneyMaker (**D**), at 14 and 7 dpi, respectively. Plants were treated with *R. irregularis* (*R.i.*), *B. velezensis* (*B.v.*), the combination of both (*R.i.*+ *B.v.*, green) or with Hoagland solution as Control. For all panels, the boxes encompass the 1st and 3rd quartiles, the whiskers extend to the minimum and maximum points, and the midline indicates the median. The individual points represent 8 biological replicates. n = 8; Letters a to c indicate statistically significant differences according to one-way analysis of variance (ANOVA) and Tukey's HSD test (α = 0.05). ns = not significant.

Moreover, the infection by *B. cinerea* did not significantly impact the microbial populations in the root compartment. Both *B. velezensis* and *R. irregularis* populations remained unchanged in infected versus non-infected plants, indicating that the microbes were not actively recruited or enriched in response to a potential "cry for help" from the host. This is likely due to their already well-established presence in the rhizosphere at the time of infection (at 7dpi of the *B. velezensis*).

Interestingly, when comparing the two tomato cultivars before *B. cinerea* inoculation (i.e., 7 dpi of *B. velezensis*), we observed significantly higher microbial populations in Ailsa Craig (**Figure 4-3 A** and **Figure 4-3 B**) compared to MoneyMaker (**Figure 4-3 C** and **Figure 4-3 D**), for both *B. velezensis* and *R. irregularis*. These findings suggest that cultivar-specific differences in root colonization efficiency may explain the variation in protection levels observed previously. Ailsa Craig, which supported stronger colonization by both microbes, also exhibited superior resistance to *B. cinerea* under co-inoculation, reinforcing the link between effective root colonization and enhanced systemic protection.

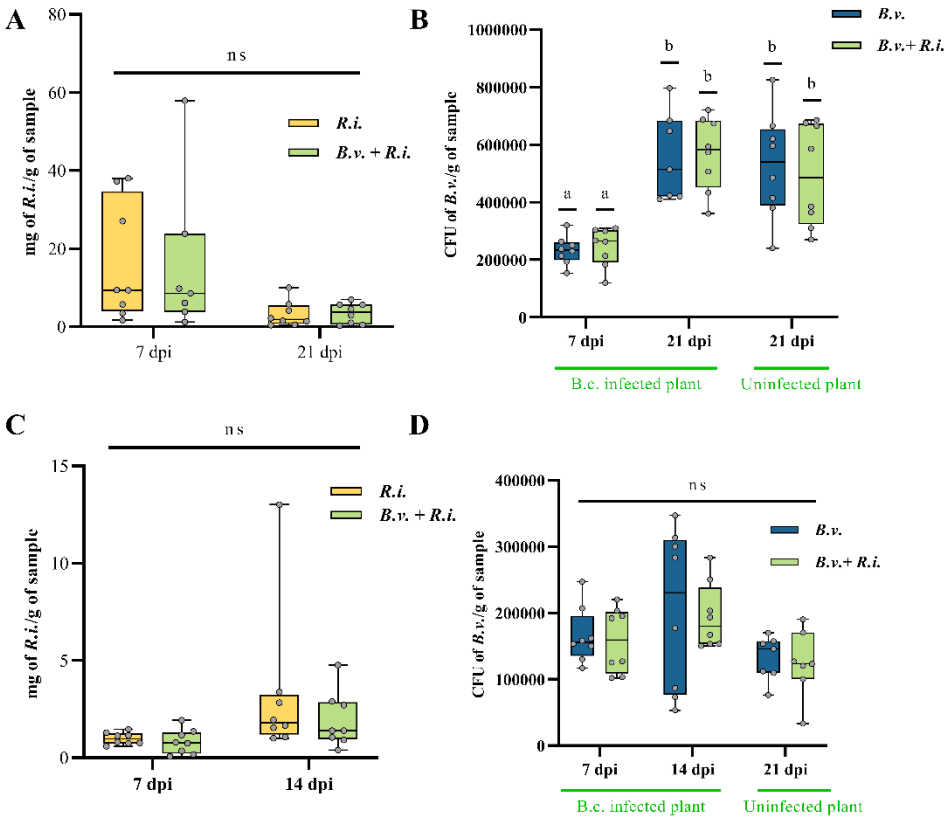

Figure 4-3: Co-inoculation with *B. velezensis* and *R. irregularis* does not alter their microbial population dynamics and is not influenced by pathogen infection. A-C, Fungal biomass of *R. irregularis* quantified by qPCR and expressed as mg of fungal material per gram of roots with attached rhizospheric substrate, at 7 and 21 days post-inoculation (dpi) with *B. velezensis* for the tomato cultivar Ailsa Craig (**A**), and at 7 and 14 dpi for MoneyMaker (**C**). Plants were either co-inoculated with *B. velezensis* (B.v. + R.i., green) or inoculated with *R. irregularis* alone (R.i., yellow). **B-D**, Bacterial population of GFP-tagged *B. velezensis* GA1 quantified by colony-forming unit (CFU) counts per gram of roots with attached rhizospheric substrate, at 7 and 21 dpi in Ailsa Craig (B), and at 7 and 14 dpi in MoneyMaker (D), either in the presence (B.v. + R.i., green) or absence (B.v., blue) of *R. irregularis*. For all the panels, the boxes encompass the 1st and 3rd quartiles, the whiskers extend to the minimum and maximum points, and the midline indicates the median. The individual points represent 8 biological replicates. n = 8; Student's t-test ($\alpha = 0.05$): ns = not significant.

On the other hand, co-inoculation with *B. velezensis* and *R. irregularis* did not lead to any significant increase in plant size or biomass compared to the control (**Figure 4-4**).

Actually, none of the treatments, whether single or combined, promoted plant growth. Notably, inoculation with *R. irregularis* alone led to a reduction in both plant size and fresh weight. However, this growth-limiting effect of the AM fungus was mitigated by the presence of *B. velezensis*. This suggests that while *R. irregularis* alone may exert a negative impact on tomato growth under our experimental conditions, the bacterium counteracts this effect without altering AM fungal colonization rate (**Figure 4-4**).

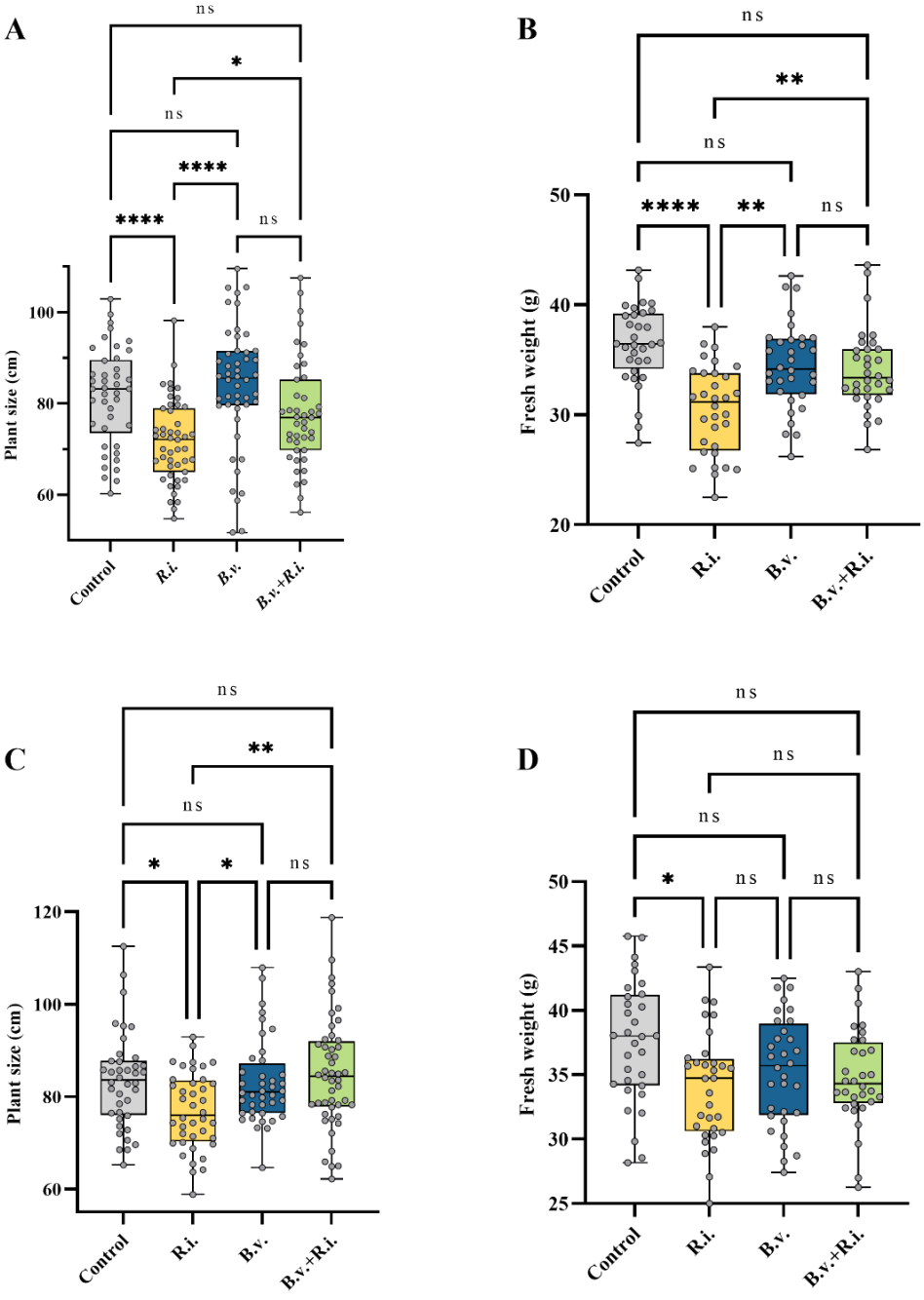
A
ns
*
ns
****
****
ns
Plant size (cm)
100
80
60
Control
R.i.
B.v.
B.v.+R.i.
B
ns
**
ns
****
**
ns
Fresh weight (g)
50
40
30
20
Control
R.i.
B.v.
B.v.+R.i.
C
ns
**
ns
*
*
ns
Plant size (cm)
120
100
80
60
Control
R.i.
B.v.
B.v.+R.i.
D
ns
ns
ns
*
ns
ns
Fresh weight (g)
50
45
40
35
30
25
Control
R.i.
B.v.
B.v.+R.i.

Figure 4-4: Influence of *R. irregularis* and *B. velezensis* on tomato plant growth. A-C, tomato plant size for the cultivars Ailsa Craig (**A**) and MoneyMaker (**C**), either co-inoculated with *B. velezensis* (B.v. + R.i., green), inoculated with *R. irregularis* alone (R.i., yellow), with *B. velezensis* alone (B.v., blue), or with Hoagland solution as control (gray).Measurement were taken at 7 days post-inoculation (dpi) with *B. velezensis*, prior to pathogen infection. **B-D**, **f**resh weight of tomato plants from the Ailsa Craig (B) and MoneyMaker (D) cultivars, measured at 14 dpi (Ailsa Craig) or 21 dpi (MoneyMaker) after infection with *B. cinerea* or not. Treatments included *R. irregularis* (R.i., yellow), *B. velezensis* (B.v., blue), the combination of both (B.v. + R.i., green), and Hoagland solution as control (gray). For all the panels, the boxes encompass the 1st and 3rd quartiles, the whiskers extend to the minimum and maximum points, and the midline indicates the median. The individual points represent 32 biological replicates. n = 32; Student's t-test ($\alpha = 0.05$): ns = not significant.

4.4 Pure surfactin provides protection in mycorrhized plants

Based on our previous findings highlighting the key role played by surfactin in the interaction with *R. irregularis* and its translocation through the ERM, we sought to determine whether the application of pure surfactin directly onto the ERM, in the absence of plant roots, could enhance plant protection.

To test this hypothesis under more ecologically relevant conditions, we adapted our bi-pot system (**Figure 4-5**). This design enabled us to evaluate the impact of the combined application of *R. irregularis* and surfactin on tomato disease resistance, while simultaneously assessing the capacity of surfactin to translocate through the ERM and contribute to systemic plant immunity.

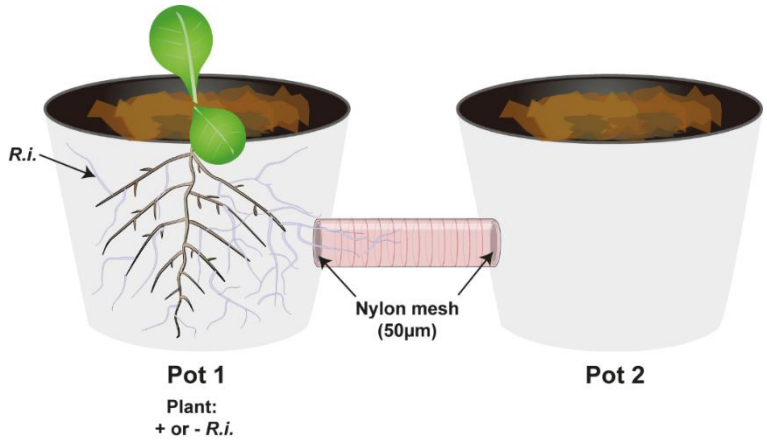

Figure 4-5: Experimental setup to evaluate whether surfactin and AM fungi, in the absence of roots, can enhance tomato plant immunity. This schematic illustrates the experimental design used to assess the potential systemic influence of surfactin via *Rhizophagus irregularis* on plant immunity. One plant of *Solanum lycopersicum* (Pot 1) was physically connected to a second pot (Pot 2) by a tube sealed at both ends with a 50 µm nylon mesh. This mesh barrier allowed fungal hyphae to pass through while preventing root intrusion. During transplantation, Pot 1 was inoculated (+R.i.) or not (-R.i.) with *R. irregularis*, while Pot 2 remained free of any direct microbial inoculation. In conditions where the AM fungus was present in Pot 1, this setup enabled the development of an ERM extending into Pot 2.

The **Figure 4-6** illustrates the experimental design and the various treatment modalities used to determine whether the combination of surfactin and *R. irregularis* provides superior protection compared to individual treatments or untreated controls. Using this setup, we observed that tomato plants colonized by *R. irregularis* and treated with surfactin (Pot 1 + R.i. + Srf; **Figure 4-6**) exhibited significantly enhanced resistance to *B. cinerea* (**Figure 4-7 A**) compared to untreated controls (Pot 1). Treatments with either *R. irregularis* alone (Pot 1 + R.i.) or surfactin alone (Pot 1 + Srf) also conferred protection, but to a lesser extent.

Moreover, this separated-pots system allowed us to test whether surfactin applied on ERM not in contact with roots (Pot 2) could still enhance disease resistance in the presence of a well-developed ERM (Pot 2 + R.i. + Srf; **Figure 4-6)**. We observed a significant reduction in disease symptoms when surfactin was applied in Pot 2 containing fungal hyphae (Pot 2 + R.i. + Srf; **Figure 4-7 A**), indicating that either the response elicited in the fungus by surfactin is particularly effective, or that translocation via the ERM is efficient to deliver the lipopeptide to the root zone, where it activates host immunity. Acetonitrile extraction of roots with attached rhizospheric soil provided additional evidence under more realistic conditions of the translocation of surfaction by the AM fungus. These analyses demonstrated that *R. irregularis* was

able to translocate surfactin from the treated pot (Pot 2) to the untreated pot (Pot 1), delivering the molecule either directly to the roots or at least to their immediate vicinity (**Figure 4-7 B**).

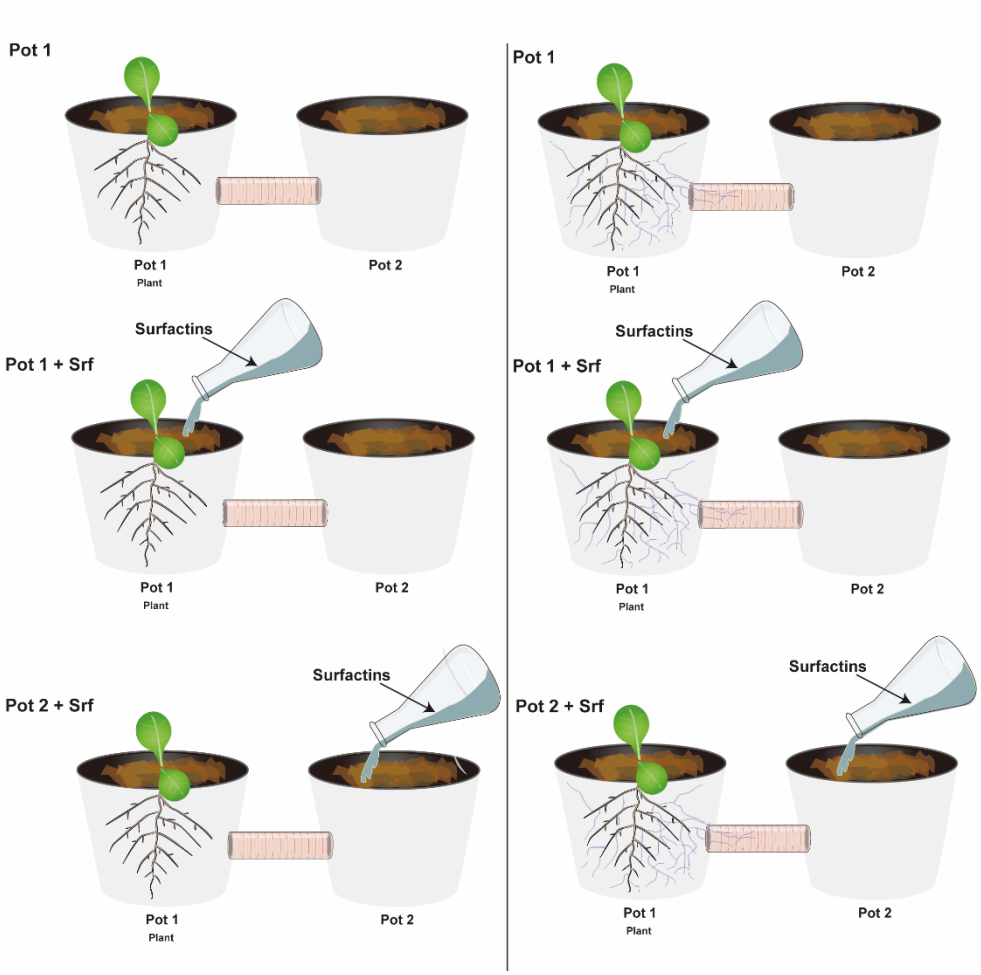

Figure 4-6: Experimental design and treatment modalities used to evaluate the contribution of *R. irregularis* and surfactin, alone or in combination, to the enhancement of plant resistance against *Botrytis cinerea*. The experiment was conducted using a bi-compartmental pot system composed of two physically separated pot (Pot 1 and Pot 2) connected by a tube sealed at both ends with a 50 µm nylon mesh. This mesh barrier allowed fungal hyphae to pass through while preventing root intrusion Tomato plants were grown in Pot 1, which was either inoculated with *R. irregularis* (+R.i.) or left uninoculated (-R.i.). Surfactin was applied either directly into Pot 1 (near the root system) or into Pot 2 (at a distance, accessible only through the extraradical mycelium of *R. irregularis*). The following conditions were tested: (i) untreated control (Pot 1), (ii) *R. irregularis* alone (Pot 1 + R.i.), (iii) surfactin alone (Pot 1 + Srf), (iv) *R. irregularis* + surfactin co-application in Pot 1 (Pot 1 + R.i. + Srf), (v) surfactin application in Pot 2 with *R. irregularis* present (Pot 2 + R.i. + Srf), and (vi) surfactin application in Pot 2 without *R. irregularis* (Pot 2 − R.i. + Srf). This setup allowed us to assess both the local and systemic effects of the treatments and to investigate the capacity of the AM fungal network to mediate the functional delivery of surfactin from Pot 2 to the tomato roots.

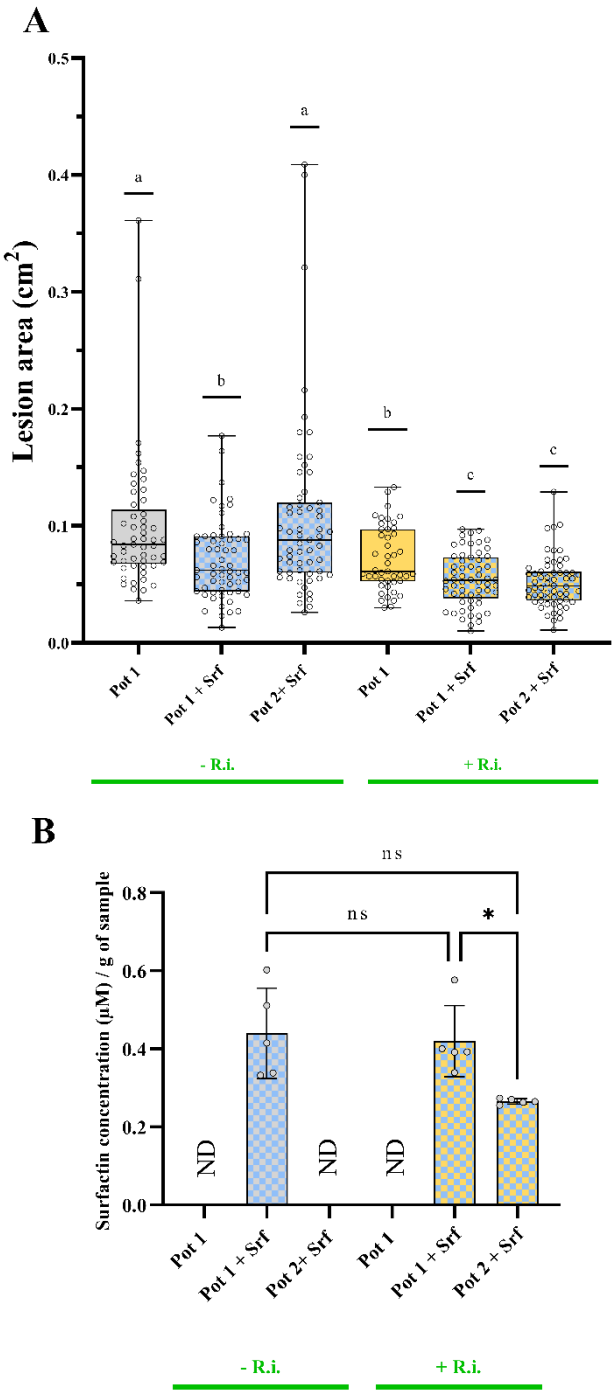
A
Lesion area (cm2)
0.5
0.4
0.3
0.2
0.1
0.0
a
b
a
b
c
c
Pot 1
Pot 1 + Srf
Pot 2+ Srf
Pot 1
Pot 1 + Srf
Pot 2 + Srf
- R.i.
+ R.i.
B
Surfactin concentration (µM) / g of sample
0.8
0.6
0.4
0.2
0.0
ns
ns
*
ND
ND
ND
Pot 1
Pot 1 + Srf
Pot 2+ Srf
Pot 1
Pot 1 + Srf
Pot 2 + Srf
- R.i.
+ R.i.

Figure 4-7: Enhancement of tomato resistance against *Botrytis cinerea* by *R. irregularis*, surfactin, and fungal-mediated translocation of surfactin via the ERM. A, Disease severity was assessed by measuring lesion size on tomato leaves (cv. Ailsa Craig) 14 days post-infection with *B. cinerea*, using ImageJ Fiji for quantification. Plants were grown in Pot 1 and either associated with *R. irregularis* (+R.i., yellow) or not (-R.i.). Surfactin (Srf, blue) was applied either directly in Pot 1 (near the roots) or in Pot 2 (distant compartment connected only by the ERM of *R. irregularis*). Treatment conditions included: Control (Hoagland solution, gray), *R. irregularis* alone (+R.i.), surfactin alone (+Srf), and combined *R. irregularis* + surfactin treatment (+R.i. + Srf, yellow and blue checkered). Additional conditions tested surfactin translocation by applying it in Pot 2 of plants previously colonized (or not) by *R. irregularis*. Data represent lesion size from 10 leaflets per plant across 6 biological replicates $45 \leq n \leq 60$; Letters a to c indicate statistically significant differences according to one-way analysis of variance (ANOVA) and Tukey's HSD test ($\alpha = 0.05$). **B**, Surfactin quantification in root compartments (Pot1) was performed using UPLC-qTOF/MS and expressed as µM surfactin per gram of roots with attached rhizospheric substrate. Surfactin quantification was performed across the different treatment modalities, specifically to compare its accumulation in root compartments when applied either in Pot 1 (directly at the root level) or in Pot 2 (distant compartment), under conditions with or without colonization by *R. irregularis*. Data represent mean values from 5 biological replicates ($n = 5$). Statistical analysis was performed using one-way ANOVA and Tukey's HSD test ($\alpha = 0.05$); "ns" indicates no significant differences., $*$, $p < 0.05$.

4.5 Summary: MIR and ISR in a harmonized concert

RQ3: Is it advantageous to combine an AM fungus and a bacterial biocontrol agent for promoting plant health? YES.

In this chapter (**Figure 4-8**), we demonstrate that the combined application of *B. velezensis* and *R. irregularis* provides enhanced protection of tomato plants against *B. cinerea* compared to treatments with each microorganism alone. This improved resistance appears to be associated primarily with activation of the plant immune system rather than with increased plant growth. Importantly, we observed that the colonization dynamics of each microorganism were not significantly altered by the presence of the other, further indicating stable coexistence within the host plant. However, inoculation with *R. irregularis* alone led to a slight reduction in plant growth, highlighting a fitness cost linked to mycorrhizal colonization. By contrast, co-inoculation with *B. velezensis* mitigated this effect while simultaneously strengthening disease resistance. Our results suggest that this enhanced plant protection likely arises from functional synergy, through additive or complementary immune-priming mechanisms.

Moreover, we found that the application of surfactin to mycorrhizal plants further boosted resistance compared to either treatment alone. Remarkably, applying surfactin directly to the extraradical mycelium of *R. irregularis* produced a comparable increase in plant resistance, which coincided with the detection of surfactin at the root level. This observation indicates functional translocation of the molecule through the AM fungal network. Together, these findings provide novel insights into the interplay between microbial signaling and systemic plant defence under greenhouse conditions. They support a model in which *R. irregularis* not only tolerates surfactin but may actively facilitate its spatial redistribution within the rhizosphere, thereby amplifying its immunomodulatory effects. This highlights the potential of fungal-mediated delivery of bacterial elicitors as a powerful mechanism in interkingdom cooperation, reinforcing the concept that microbial alliances can stabilize and enhance plant-beneficial traits beyond the capabilities of individual partners.

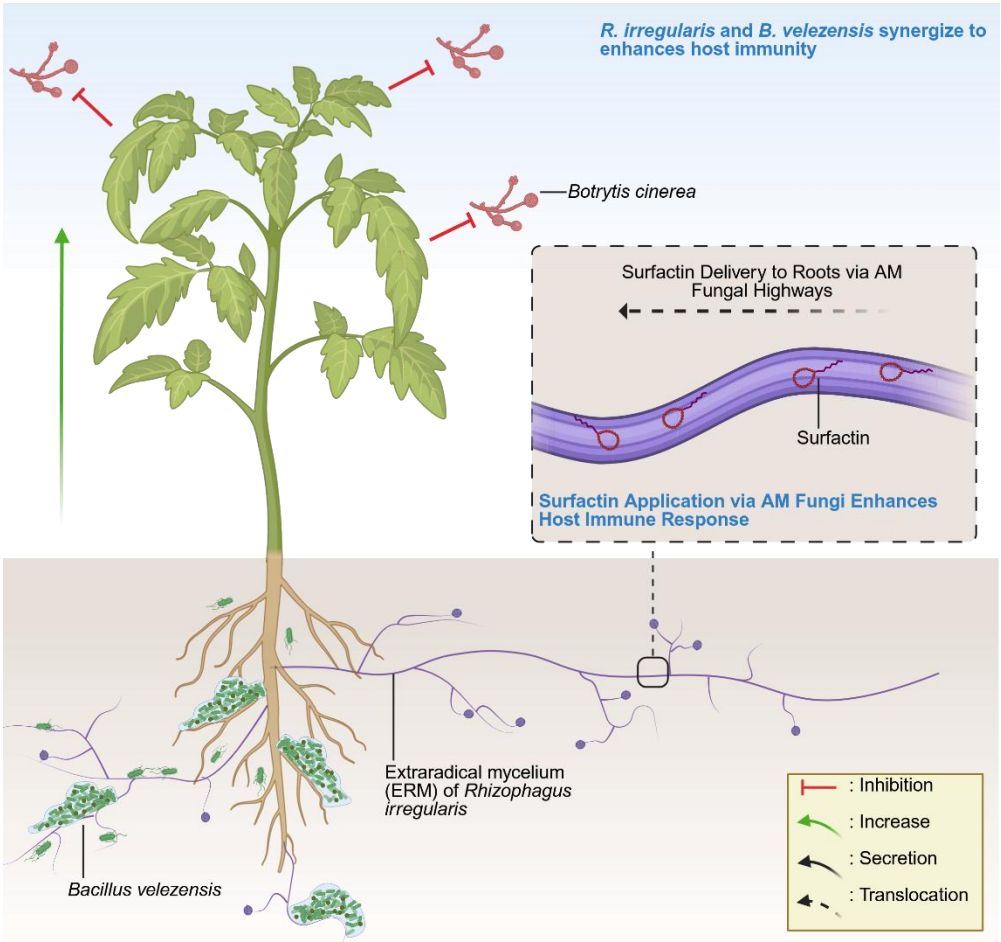

Figure 4-8: Schematic summary of the synergistic protection conferred by soilborne *B. velezensis* and *R. irregularis* against a foliar pathogen. This illustration depicts how root colonization by the beneficial microorganisms *Bacillus velezensis* and *Rhizophagus irregularis* enhances host resistance against the foliar fungal pathogen *Botrytis cinerea*. It also highlights that the application of surfactin on the ERM of *R. irregularis*, even at a distance from the root system, can further amplify plant immunity. Additionally, in a more realistic soil-based context, we confirmed the translocation of surfactin through the fungal network toward the plant roots. Figure was created with Biorender.com.

Chapter 5

Discussion: Let’s talk and live together

This work has been built around a set of RQs aimed at deciphering the interaction between *R. irregularis* and *B. velezensis*. The results obtained (**Figure 5-1**) not only shed light on previously unexplored aspects of this partnership but also open the door to new lines of inquiry. These new research questions emerge from our findings and now form the backbone of the discussion and perspectives developed in this thesis. For each, I discuss the conceptual framework emerging from these questions and outline potential approaches to address them, serving of perspectives. The following section aims to explore these new directions, critically examine the fundamental relevance of the current findings, and reflect on their broader implications for understanding interkingdom microbial cooperation and plant immunity.

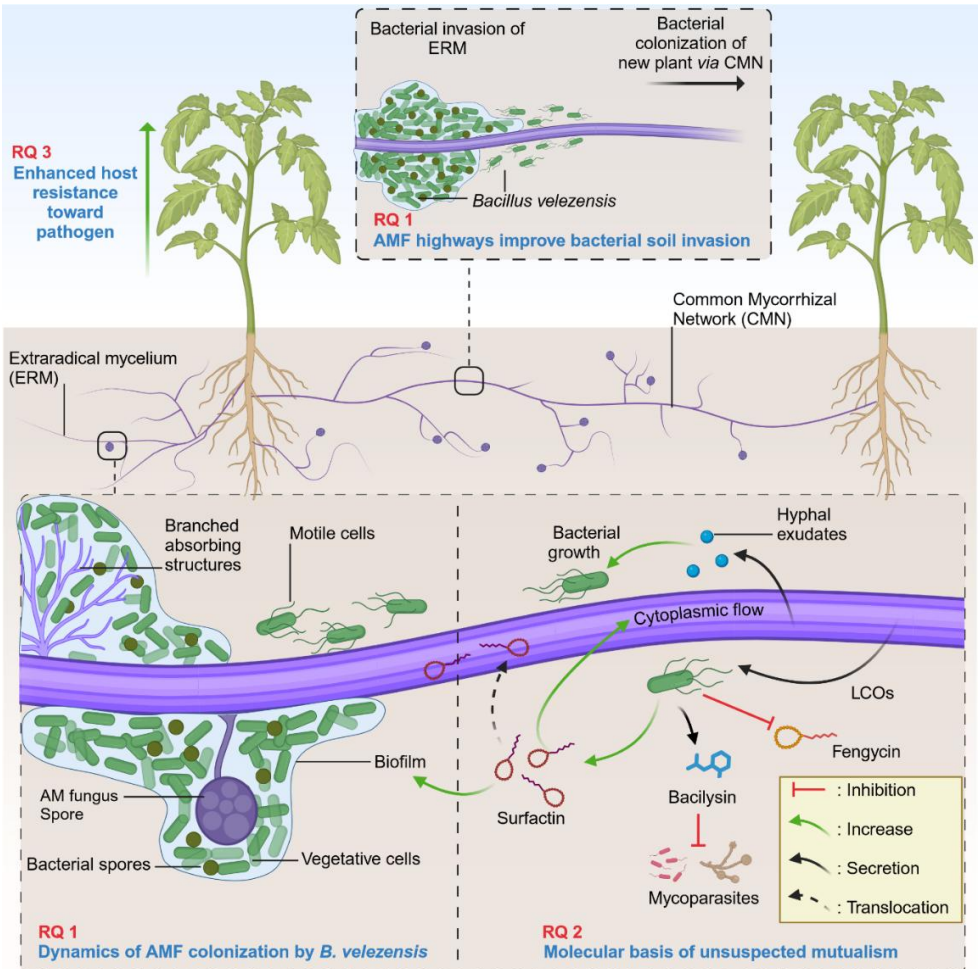

Figure 5-1: Schematic summary of the interaction between *B. velezensis* and *R. irregularis* draw on the basis of the Research Question. This illustration shown how *R. irregularis* and *B. velezensis* exemplified the mutualism between mututalist of plant enhancing synergistically the health of their plant host. Figure was created with Biorender.com.

5.1 Is the *Bacillus*-AM fungus interaction an anomaly or evidence of a broader phenomenon?

5.1.1 Highlights

- *B. velezensis* colonizes the entire mycelial network more efficiently than roots
- *Bacillus* uses fungal hyphae as highways for soil invasion and to colonize new plant
- *B. velezensis* and *R. irregularis* form a stable relationship without antagonism

5.1.2 The *Bacillus*-AM Fungal mutualism: A story going back in time?

The colonization of terrestrial ecosystems by early land plants approximately 450 million years ago is thought to have relied heavily on symbiotic associations with microorganisms, notably ancestral AM fungi. Fossil evidence and molecular phylogenies support the view that these associations co-evolved, with plants and AM fungi developing intricate nutritional dependencies. These evolutionary pressures likely contributed to the obligate biotrophic nature of modern AM fungi, shaped by adaptive gene loss. This foundational evolutionary event underscores the pivotal role of microbial symbioses in shaping terrestrial life (James et al., 2006; Luginbuehl et al., 2017; Martin et al., 2017; Redecker et al., 2000; Rich et al., 2021). Drawing from this evolutionary framework, the interaction between *B. velezensis* and AM fungi described in this work may represent a parallel case of co-evolution between microorganisms occupying a common ecological niche. *Bacillus* species, well known for their rhizosphere competence, have evolved sophisticated strategies to thrive in competitive environments, including the production of a wide array of BSMs and the ability to modulate colonization behaviour through chemical crosstalk with plant hosts. Thus, similar mechanisms may have been co-opted or re-adapted by some bacilli to engage in beneficial associations not only with plants but also with other key rhizospheric mutualists such as AM fungi.

In this context, our *in vitro* findings suggest that *B. velezensis* is not merely a passive occupant of the hyphosphere but has developed active and specific strategies to exploit this fungal niche. These include the capacity to utilize hyphal exudates as nutrient sources, to form robust biofilms on the extraradical mycelium, and to colonize AM fungal networks with remarkable efficiency, without impairing fungal development or viability. The ability of *B. velezensis* to colonize AM fungi was observed

consistently across multiple *Rhizophagus* species, suggesting broad compatibility rather than specialization toward a single fungal partner. To further explore the potential co-evolution and adaptability of this association, it is essential to extend the study beyond the *Rhizophagus* genus. For instance, evaluating colonization efficiency in phylogenetically distant AM fungal genera such as *Funneliformis*, *Glomus*, and notably *Gigaspora* (e.g., *G. margarita*) would be highly informative. Notably, AM fungal spores of diverse genera and species have been shown to harbour diverse communities of endobacteria (Lastovetsky et al., 2024). *G. margarita* is of particular interest because it produces large runner hyphae and hosts endobacteria (Salvioli et al., 2016; Venice et al., 2020), making it a particularly relevant model to assess whether *B. velezensis* can behave as an endosymbiont. This could be tested using GFP- or mCherry-tagged *Bacillus* strains to track intracellular colonization dynamics.

On the other side of the interaction, it appears that the ability to colonize AM fungal hyphae is not unique to *B. velezensis*, but may be more broadly distributed across the *Bacillus* genus (Nadeem et al., 2014; Nanjundappa et al., 2019; Romero-Munar et al., 2023; Savastano & Bais, 2024; Yadav et al., 2020). For instance, *B. filamentosus* strains have been observed colonizing the ERM of *R. irregularis*, forming biofilms and increasing phosphorus uptake. Moreover, co-inoculation with *B. filamentosus* has been shown to enhance AM fungal sporulation (Pandit et al., 2022). However, not all interactions between AM fungi and *Bacillus* spp. are beneficial. Certain *B. subtilis* strains have been reported to reduce arbuscule density in wheat and maize roots (Wilkes et al., 2020; Xiao et al., 2008). These divergent outcomes underscore the strong context-dependence of *Bacillus*–AM fungi interactions and highlight the importance of monitoring microbial dynamics in order to fully understand, and ultimately harness, their plant-beneficial potential. Thus, the overall picture remains fragmented, emphasizing the need to broaden the scope of investigation into the factors governing the ability of *Bacillus* spp. to associate with AM fungal hyphae. Comparative studies involving other root-associated species such as *B. subtilis*, *B. amyloliquefaciens*, *B. licheniformis*, and *B. pumilus* could determine whether the capacity for AM fungal colonization is a conserved or specialized trait. Furthermore, extending the analysis to more distantly related clades, such as the *B. cereus* and *B. flexus* groups, through broader phylogenetic approaches could reveal whether this ability is a conserved feature (**Figure 5-2**). These investigations would provide valuable insight into the evolutionary drivers and ecological determinants underlying bacterial adaptation to fungal hosts.

Additionally, it remains an open question whether *B. velezensis* colonization efficiency is influenced by the functional traits of AM fungi, particularly their capacity to confer benefits to host plants. Prior studies have shown that plants preferentially allocate more carbon to AM fungal partners that provide greater nutritional benefits (Kiers et al., 2011). In this context, *Bacillus* colonization could depend on the level of carbon allocated to the AM fungus by the host plant. Therefore, the colonization success of *B. velezensis* may be indirectly influenced by the trade balance between

plant and fungus, potentially favouring AM fungal strains that are better rewarded and metabolically more active (Hammerstein & Noë, 2016; Noë & Kiers, 2018; Selosse & Rousset, 2011). Conversely, our data suggest that *B. velezensis* can positively impact AM fungal fitness by enhancing cytoplasmic flow. However, the extent of these effects appears to vary between AM fungal species, indicating that *B. velezensis* may selectively promote certain partners, such as *R. irregularis*, and thus potentially influence AM fungal community composition. This hypothesis merits further investigation.

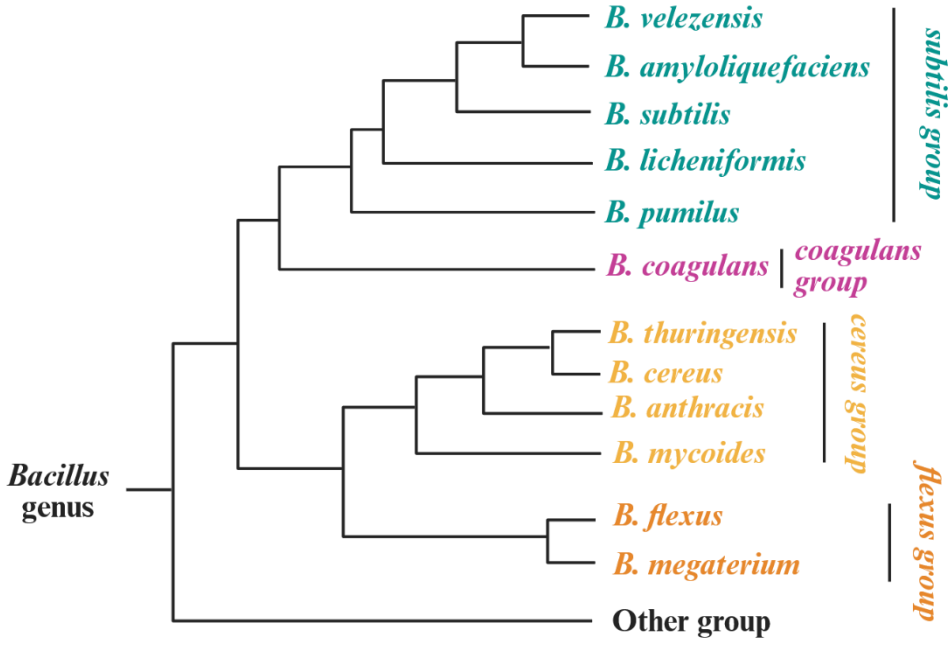

Figure 5-2: *Bacillus* diversity. Phylogenetic tree presenting the major groups within the *Bacillus* genus, along with representative species from each group. Adapted from Asif et al. (2023), Huang et al. (2012), Balleux et al. (2025) and Qin et al. (2013).

5.1.3 Do good trades make good neighbours?

Efficient colonization of the ERM confers significant ecological advantages to *B. velezensis*. By exploiting the dense and expansive hyphal networks of AM fungi as a fungal highway, *B. velezensis* can extend its presence into soil volumes that are otherwise inaccessible to plant roots, thereby enhancing its spatial persistence and niche invasion. Our spatio-temporal tracking experiments provide some of the first compelling evidence that AM fungal networks act as effective conduits for bacterial dispersal well beyond the rhizosphere. This supports and extends previous findings

such as Kohlmeier et al. (2005), who described a similar "fungal highway" phenomenon with *F. oxysporum*, *Rhexocercosporidium* spp., and associated bacteria (Abeysinghe et al., 2020). More recently, bacterial migration along AM hyphae was demonstrated for PSB *R. aquatilis* (Jiang et al., 2021), further validating the generality of this dispersal mechanism (Sharma et al., 2020b; Vieira et al., 2025). Our results additionally show that AM fungal networks serve also as effective vectors for bacterial spread between plant individuals, facilitating the colonization of new ecological niches. Future studies should investigate whether CMN-mediated dispersal of *B. velezensis* occurs across a broader range of plant species, belonging to different families, thereby reflecting more complex and realistic ecological scenarios. In natural systems, plants often host multiple AM fungal species simultaneously, and resource allocation is typically biased toward the most functionally efficient symbionts (e.g., those delivering higher phosphorus inputs) (Kiers et al., 2011). In such multispecies contexts, it would be particularly interesting to examine whether AM fungal diversity influences *B. velezensis* colonization dynamics, mobility, and biofilm development.

AM fungal hyphae provide more than just a “fungal highway”. They also release carbon-rich exudates that support bacterial growth and biofilm formation. Biofilm formation protects bacterial communities from abiotic stress and competitive infiltration, largely due to the barrier created by the hydrophobin matrix (Arnaouteli et al., 2021; Flemming et al., 2016; Molina-Santiago et al., 2019). Beyond self-protection, such biofilm structure may also serve as a protective shield for the AM fungal host. Our results show that the *B. velezensis* BSMs exerts inhibitory effects on microorganisms known to negatively affect AM fungi. Although we did not identify the full spectrum of BSMs involved, our analyses confirmed that *B. velezensis* produces several antimicrobial compounds within biofilms. These molecules likely serve a dual role, safeguarding *B. velezensis* itself and providing chemical defence for its AM fungal partner with low antimicrobial capabilities. To experimentally test the “protective shield” potential, an *in vitro* confrontation assay could be developed where AM hyphae colonized by *B. velezensis* are exposed to known AM fungal competitors. Applying MSI in this context would allow spatial resolution of antagonistic metabolite localization, directly visualizing the formation and extent of this chemical barrier. In parallel, the use of knockouts *B. velezensis* mutants, particularly encoding key secondary metabolites, could help identify the specific bacterial compounds involved in the protective effect. To validate these findings under more realistic conditions, greenhouse experiments could evaluate whether *B. velezensis* provides protective benefits when AM fungi are challenged by antagonistic fungi in soil.

This would reinforce the concept of “mutualism between mutualists,” in which the AM fungus supports bacterial growth and dispersal, while the bacterium, in turn, protects the fungal host from microbial antagonists. This mutualistic loop may be a key strategy contributing to the ecological success and stability of both partners in competitive soil environments.

5.1.4 *B. velezensis*: A root-associated or a mycorrhiza-associated bacterium?

Many *Bacillus* species including *B. velezensis* are described as root-associated bacteria. However, their abundance in the rhizosphere appears to be highly variable and influenced by factors such as plant species, soil type, and plant developmental stage, suggesting a certain degree of ecological versatility (Acharya et al., 2023; Akinola et al., 2021; Lopes & Schachtman, 2023). In contrast, other metagenomic studies report a higher relative abundance of *Bacillus* spp. and even *B. velezensis* in bulk soil than in the rhizosphere (Alenezi et al., 2021; Wang et al., 2024a; Xu et al., 2024). This may indicate that plant roots are not the primary ecological niche for *B. velezensis*, but rather a secondary, opportunistic habitat. A plausible explanation lies in its preferential colonization of AM fungal ERM. Our observations support this hypothesis, as *B. velezensis* consistently exhibits a stronger colonization along AM fungal hyphae than for root surfaces. Therefore, the presence of *Bacillus* in bulk soil may not reflect a preference for uncolonized environments but instead indicate its close association with fungal networks that bridge the rhizosphere and bulk soil.

The rhizosphere microbiome is typically dominated by Proteobacteria, particularly *Pseudomonas* spp., which are often considered fast growing and strong competitors. This pattern aligns with *in vitro* studies showing that *Pseudomonas* strains can outcompete *Bacillus* strains in co-culture on plant roots (Andrić et al., 2021; Elhady et al., 2025; Lyng et al., 2024; Lyng & Kovács, 2023). However, such reductionist systems do not capture the full complexity of the rhizosphere where *Bacillus* spp. are often found and should not be generalized to all *Pseudomonas* and *Bacillus* species interaction. Nonetheless, these observations raise an important question: do microbial competition and colonization dynamics differ between the root surface and the AM fungal hyphosphere? Within this distinct microhabitat, *B. velezensis* may gain a competitive advantage or establish stable coexistence, potentially even outcompeting *Pseudomonas* spp.. Such findings would support the hypothesis of niche partitioning and specialization, reinforcing the idea that *Bacillus* species are more intimately associated with the hyphosphere of AM fungi than with plant roots. As a first step, a reductionist approach could be employed to evaluate the colonization dynamics of *B. velezensis* on roots versus AM fungal hyphae, using a *Pseudomonas* strain known to outcompete *B. velezensis*. However, the AM fungal hyphosphere harbours a complex microbial community, raising important questions about how *B. velezensis* interacts with other inhabitants of this niche. Does it outcompete other beneficial or neutral microbes, or does it synergize within a stable microbial consortium? Likewise, under conditions of nutrient limitation, environmental stress, or competition with other microbial partners, the interaction may also shift toward neutrality or even antagonism. Elucidating the ecological stability and functional flexibility of this association will be essential for harnessing its full potential in sustainable agricultural systems.

The differential recruitment of bacterial communities by roots and AM fungi may also reflect a host-driven strategy to diversify microbial associations, thereby reducing the risk of dependency on a single microbial partner and enhancing functional redundancy and ecosystem resilience. By maintaining distinct microbial niches, plants and AM fungi may enhance their ability to respond to localized stress signals, such as the "cry for help," and improve overall resilience through ecological niche partitioning (Wen et al., 2023) .

5.1.5 Is the AM fungal hyphal network better adapted to *B. velezensis* colonization?

Several factors likely contribute to the preferential colonization of AM fungal hyphae by *B. velezensis* compared to plant roots. Time-lapse microscopy revealed marked behavioural differences in bacterial colonization depending on the host. Upon contact with AM fungal hyphae, *B. velezensis* retained active motility and progressively formed continuous, uniform biofilms along the hyphal surface. In contrast, on plant roots, the bacterium quickly transitioned to a sessile lifestyle, forming spatially restricted macrocolonies (Massalha et al., 2017; Stoll et al., 2021). This contrast may result from the hyphosphere providing a more favourable microenvironment that supports sustained bacterial metabolism and growth. Thus, AM fungal hyphae not only serve as a carbon-rich resources but may also shape bacterial behaviour and physiology. Fungal exudates likely act as selective cues that promote cooperative traits in *B. velezensis*, including sustained motility, EPS production, and reduced sporulation (Kovács, 2019; Martin et al., 2020). The extensive biofilm formation observed on AM hyphae compared to roots may also result from differences in host exudate composition. Carbon source availability is a known determinant of biofilm architecture. For example, sucrose stimulates surfactin production and hyperflagellation in *B. subtilis*; root-derived sucrose can induce levan-oligosaccharide synthesis, enhancing motility and colonization (Dobrange & Van den Ende, 2025; Dogsa et al., 2013, 2024; Tian et al., 2021). Moreover, sucrose contributes to the stability of floating biofilms through its incorporation into the EPS matrix (Dobrange & Van den Ende, 2025; Dogsa et al., 2013). Actually, root exudates of Solanaceae are composed primarily of organic acids (67%) and, to a lesser extent, sugars (33%), while *Rhizophagus irregularis* exudates show the opposite profile, being enriched in sugars (Luthfiana et al., 2021; Nihorimbere et al., 2012; Toljander et al., 2007; Zhang et al., 2022). Sugar-rich environments associated with AM fungi may therefore promote robust and homogeneous biofilm development, whereas organic acid-rich root exudates may constrain biofilm expansion and contribute to spatial heterogeneity (Dogsa et al., 2024; Even et al., 2017). Further influencing bacterial physiology, certain plant-derived polysaccharides, such as pectin, are known to modulate *Bacillus* behaviour by promoting biofilm and triggering sporulation (Beauregard et al., 2013; Boubsi et al., 2023). These molecules are absent from AM

fungi, potentially explaining the lower sporulation levels observed in hyphae-associated bacterial populations in our study. Colonization patterns may also be influenced by host surface complexity. Plant roots display strong axial differentiation, root tips, elongation zones, and maturation zones, each characterized by distinct exudate profiles (Kranawetter et al., 2021). This spatial heterogeneity may lead to localized colonization and patchy biofilm formation. In contrast, AM fungal hyphae offer a relatively homogeneous surface, enabling a more uniform and continuous bacterial proliferation. Moreover, the hydrophilic nature of the fungal cell wall promotes the formation of a thin, continuous water film surrounding the hyphae, which may enhance bacterial movement and dispersal along hyphae (Allen, 2007; Kohlmeier et al., 2005a; Vieira et al., 2025; Vila et al., 2016).

To determine whether these differences reflect host-specific bacterial responses, comparative transcriptomics (e.g., RNA-seq) between *B. velezensis* populations colonizing AM hyphae versus plant roots would be informative. Such comparison could reveal whether the hyphosphere promotes gene expression programs associated with growth and motility, while the rhizosphere favours stress adaptation and sporulation. To further explore how exudate influence bacterial phenotypes, *in vitro* biofilm assays could be conducted using media supplemented either with AM fungal or plant root exudates or using synthetic media mimicking exudate compositions. Monitoring bacterial population dynamics, biofilm formation and sporulation over time would offer a comparative framework linking *in vitro* observations to *in planta* colonization patterns.

5.1.6 Do AM fungi respond to *Bacillus velezensis* as plants do?

While the molecular strategies used by pathogens to suppress plant defences are well characterized, the mechanisms by which mutualists, such as *Bacillus* spp., evade or modulate host immunity remain less understood. Still, *Bacillus* sp. can attenuate the expression of defence-related genes, facilitating root colonization (Lakshmanan et al., 2013). A well-described strategy involves modification of MAMPs, such as flagellin (Liu et al., 2024a; Pieterse et al., 2014). *B. velezensis* produces a variant of the flg22 epitope that elicits a significantly attenuated oxidative burst compared to flg22 from pathogenic bacteria. This dampened host response limits ROS production, facilitating colonization. Interestingly, the moderate ROS levels triggered by *B. velezensis* flg22 also stimulate bacterial auxin synthesis, which in turn enhances stress tolerance and promotes biofilm formation (Tzipilevich et al., 2021). Directly or indirectly, transient ROS bursts may thus be perceived by the bacterium as environmental stress, possibly initiating physiological transitions such as biofilm formation and sporulation (Boubsi et al., 2025). Compatibility of *B. velezensis* with AM fungi may involve a distinct scenario, possibly characterized by a reduced or absence of production of immune-related response. Although, Fester & Hause (2005) reported ROS production in *Glomus intraradices* following mechanical injury,

suggesting that AM fungi possess the capacity to perceive and respond to environmental perturbations. Whether *B. velezensis* triggers ROS production in AM fungi thus remains unknown. Determining the presence or absence of such immune-like responses would provide valuable insights into the molecular basis of compatibility and host specificity. It would be informative to quantify classical stress markers in the fungus during bacterial interaction. These could include measuring ROS levels using fluorescent probes like DCFH-DA, assessing glutathione content, and evaluating the activity of antioxidant enzymes (Bui & Franken, 2018; Fester & Hause, 2005). Additionally, monitoring calcium fluxes within fungal hyphae using dyes such as Fluo-4 AM could help reveal whether conserved eukaryotic signaling pathways are activated in response to *B. velezensis* (Nair et al., 2011; Yang et al., 2024b). So, elucidating whether AM fungi possess immune-like detection systems, and how these are modulated by beneficial bacteria and *B. velezensis* in particular could help explain the observed differences in colonization patterns between plant and fungal hosts.

5.1.7 Could *B. velezensis* act as a Mycorrhiza Helper Bacterium (MHB)?

Some bacteria, known as **mycorrhiza helper bacteria** (MHB), have been identified for their ability to promote AM fungal symbiosis through two main mechanisms: (1) enhancing the function of an already established AM fungal symbiosis, such as improving mineral nutrient uptake from the soil, and (2) stimulating the initial establishment of fungal symbionts on host plants (Nasslahsen et al., 2022; Sangwan & Prasanna, 2022; Sharma et al., 2020b). Some *Bacillus* species, including *B. thuringiensis*, *B. amyloliquefaciens* (Xie et al., 2018), and *B. subtilis* (Flores et al., 2007; Gebreslassie et al., 2024), have been shown to increase AM fungal spore density, root colonization rate, or overall AM fungal activity. We can wonder if *B. velezensis* may also act as MHB but, in our greenhouse experiment, co-inoculation with *B. velezensis* did not significantly increase *R. irregularis* colonization of tomato roots. However, the experiment was not specifically designed to evaluate this effect and several factors may explain this observation. The late timing of sampling likely captured a mature symbiotic stage, potentially missing early microbial interactions that facilitate colonization. Moreover, AM fungal colonization was assessed by qPCR targeting fungal DNA. While informative, this method may not reflect structural or functional parameters such as arbuscule formation, vesicle presence, or fungal viability. Future studies focusing on the early stages of AM fungal colonization, and integrating microscopy with quantitative parameters such as spore formation and arbuscule abundance, could provide valuable insights into whether and how *B. velezensis* functions as a MHB (Kiddee et al., 2024).

Interestingly, our results show that *R. irregularis* alone negatively affected plant growth, whereas co-application with *B. velezensis* mitigated this effect. One possible explanation is that the bacterium could dampen the plant immune response, thereby

creating a more permissive environment for fungal colonization. This immune attenuation might explain why plants in the co-inoculated treatment displayed better growth despite fungal colonization, making it plausible that *B. velezensis* promotes AM fungal colonization by modulating the host immune system. Recently, Boubsi et al. (2025) demonstrated that *B. velezensis* evades plant immunity by producing OGs with short DP (mainly DP 4) through the partial degradation of root cell wall pectin, by pectate lyase that are conserved within the *B. subtilis* group (Boubsi et al., 2023). Likewise, AM fungi, which also have a limited set of root cell wall–degrading enzymes, might similarly release short OGs during root penetration, suggesting a convergent strategy to evade immune detection. Comparative profiling of OGs released by *B. velezensis* and *R. irregularis* could reveal whether such "immune-silent" fragments are produced by both partners, supporting the hypothesis that *B. velezensis* contributes to AM colonization through immune modulation. Although the precise manner by which *B. velezensis* modulates plant immunity is still poorly understood, surfactin produced by *B. velezensis*, may also contribute to immune modulation or even symbiotic signalling. It would therefore be relevant to explore whether short OGs and/or surfactin produced by *B. velezensis* can activate genes of the SYM pathway and/or suppress plant immunity to facilitate AM fungal establishment. RNA-seq analysis on roots treated with culture filtrates or mutant strains deficient in surfactin production or in pectate lyase involved in the production of short OGs could clarify the ability of *Bacillus* to modulate plant immunity in favor of AM fungal colonization. To investigate whether *B. velezensis* modulates plant immune responses in a way that could facilitate fungal colonization, monitoring early immune signalling events such as ROS production and calcium influx would be informative. For instance, pre-treating roots with *Bacillus* culture filtrate or purified compounds such as OGs and surfactin, followed by exposure to AM fungal exudates, could help determine whether prior bacterial contact influences the amplitude or dynamics of plant immune signalling.

Further, exploring this effect in typically mycorrhizal incompatible plants could help disentangle immune suppression from symbiotic signalling. Mycorrhizal incompatibility in plants like *Arabidopsis thaliana* is often attributed to the absence of key symbiotic genes but also to the activation of a strong adverse immune response (Fernández et al., 2019). However, Cosme et al. (2021) showed that *R. irregularis* could minimally colonize Arabidopsis roots when infection occurs through a common mycorrhizal network established by an adapted host plant, though arbuscules and vesicles were absent. This suggests that immune suppression alone may allow partial colonization even in non-hosts plant. In this line, we could evaluate AM fungal colonization of a mycorrhiza-incompatible plant via a CMN formed by *R. irregularis* when the extraradical mycelium is colonized by *B. velezensis*.

Beyond immune modulation, *B. velezensis* might promote AM fungal colonization through other mechanisms. Some bacteria associated with AM fungal spores, like *Paenibacillus validus*, can stimulate spore germination and fungal growth

(Hildebrandt et al., 2006). Interestingly, Kameoka et al. (2019) identified (S)-12-methyltetradecanoic acid in *Paenibacillus* cultures, which stimulated secondary spore formation in *R. irregularis*, allowing the culture of AM fungi without a plant host. Since AM fungi metabolize absorbed fatty acids via desaturases expressed in intraradical hyphae, testing whether *B. velezensis* culture filtrate promotes *R. irregularis* spore germination *in vitro* and identifying active compounds through fractionation or mutant analysis could reveal additional MHB mechanisms.

Further studies will be essential to reveal the full extent of the potential of *B. velezensis* as MHB. More broadly, while the number of bacteria identified as MHBs is increasing, the molecular and ecological mechanisms by which bacteria improve AM fungal colonization remain poorly understood. Exploring the interaction between AM fungi and *B. velezensis* on these aspects could help identify the factors that define MHBs and ultimately guide the discovery of new bacterial strains with MHB traits.

5.1.8 Do AM fungi facilitate *B. velezensis* rhizosphere invasion?

Our results show that bacterial abundance in the rhizospheric soil attached to roots of mycorrhizal plants was higher than in non-mycorrhizal plants. Due to the experimental setup, it was difficult to distinguish whether this increase reflected strictly higher root colonization, or included bacteria associated with the ERM. Still, it shows that *B. velezensis* benefits from the presence of *R. irregularis* and suggests that AM fungal colonization may also promote *B. velezensis* root establishment. This enhanced colonization could be explained by several factors. AM fungi are known to attenuate the plant immune response locally, which could create a more permissive environment for bacterial colonization, or they may alter root exudation patterns to favour the establishment of specific bacterial partners such as *B. velezensis*. Additionally, AM fungal colonization is associated with localized ROS bursts within the root. While these oxidative conditions may deter less tolerant microbes, *B. velezensis* shows notable oxidative stress resistance, potentially giving it a competitive advantage in colonizing AM-colonized roots (Tzipilevich et al., 2021). Furthermore, AM fungi influence root architecture by promoting lateral root formation and branching, which are known to be preferential colonization sites for *B. velezensis* (Massalha et al., 2017; Stoll et al., 2021). The modulation of root structure and physiology by AM fungi might therefore indirectly enhance bacterial establishment.

However, it remains challenging to disentangle whether improved *B. velezensis* colonization arises from the physical presence of *R. irregularis*, from the ROS it induces, or from broader physiological changes in the plant. Testing whether exudates from *R. irregularis* alone or synthetic Myc factors such as CO4 and LCOs can induce ROS production and enhance *B. velezensis* colonization could help clarify this mechanism.

In summary, the colonization of one microbial partner can promote the establishment of the other at the root level, suggesting a cooperative strategy that enhances co-existence.

5.2 What are the underlying mechanisms driving interkingdom microbial networks?

5.2.1 Highlights

- Compatibility is associated with reduced fengycin production
- The lipopeptide surfactin plays a central role in the chemical ecology of the interaction
- *R. irregularis* translocate the bacterial metabolite surfactin throughout its entire network
- Myc-Lipochitooligosaccharides modulate the metabolome and behaviour of *B. velezensis*

5.2.2 Does surfactin act as a signal molecule or as a surfactant?

Based on our findings *B. velezensis* and *R. irregularis* may have evolved a molecular dialogue enabling mutual recognition and compatibility. Drawing inspiration from how these microbes are recognized by plants, we hypothesize that similar signaling principles could govern this fungal–microbe interactions. Notably, we observed that *B. velezensis* induces physiological changes in the fungus that enhances cytoplasmic streaming within the hyphal network. This phenomenon could play a role in reinforcing compatibility and facilitating resource allocation. However, the precise nature of this response remains unclear. It could reflect enhanced nutrient availability, improved transfer efficiency, or alternatively a stress-induced physiological adjustment.

The cLP surfactin appears to act as a central modulator of the fungal response. From a mechanistic viewpoint, surfactin could act through interactions with the fungal plasma membrane (PM) by analogy with what is observed for interactions with plant cells in the context of immunity stimulation (Deleu et al., 2013; Henry et al., 2011; Hoff et al., 2021; Ongena et al., 2007; Pršić et al., 2023). AM fungi are lipid auxotrophs and rely on the host plant for lipid supply. However, they are capable of modifying or remodelling these host-derived lipids for their own metabolic integration (Luginbuehl et al., 2017; Rich et al., 2017, 2021; Wewer et al., 2014). Consequently, the PM composition of AM fungi could resemble that of plant cells, potentially leading to a similar mode of interaction between surfactin and both fungal and plant membranes.

Indeed, based on studies focused on the arbuscule interface and/or global lipidomics, AM fungi are particularly rich in phosphatidylcholine with fatty acid chains such as palmitic (16:0) and linoleic (18:2) acids, and their major sphingolipids include glucosylceramide (GluCer) and glycosyl inositol phosphoryl ceramides (GIPCs) (See **Table 5-1**). These lipid species are also the most abundant in plant PM and these similarities support the hypothesis that comparable membrane-based sensing mechanisms might underly surfactin-AM fungal interaction (**Table 5-1**). However, it is important to note that a detailed and specific characterization of the PM in ERM is still lacking and needed. To explore surfactin-AM fungal PM molecular interaction, fluorescent probes sensitive to lipid order (e.g., 4-ANEPPDHQ) could be used to visualize PM reorganization after surfactin exposure by confocal microscopy (Santos et al., 2018; Suchodolski & Krasowska, 2019; Zhao et al., 2015). However, investigating surfactin–membrane interactions *in vivo* may be technically challenging. Complementary biophysical approaches using biomimetic membranes, constructed from synthetic lipid mixtures matching AM fungal PM composition, or liposomes prepared from AM fungal lipid extracts could offer a more tractable system to dissect surfactin–membrane interactions (Deleu et al., 2014; Gilliard et al., 2024; Henry et al., 2011; Pršić et al., 2023).

Table 5-1: Comparison of plasma membrane composition in plants, fungi, and AM fungi. This table summarizes the main components of the plasma membrane (PM) in plants, fungi, and AM fungi. The three major classes of molecules that structure the PM are phospholipids, sphingolipids, and sterols. Due to the high variability of phospholipid composition among fungal species and the influence of growth conditions, this table focuses on the sphingolipid and sterol content, which are more conserved and taxonomically informative.

Species	Sphingolipids	Sterols	References
Plant	Glucosylceramide (GluCer) and Glycosyl inositol phosphoryl ceramides (GIPCs)	Free sterol: Sitosterol (24-ethyl cholesterol) Campesterol Stigmaterol Conjugated sterol: Streyl ester Steryl glycoside Acyl steryl glycoside	Ferrer et al., 2017; Lynch & Dunn, 2004 Michaelson et al., 2016 Rogowska & Szakiel, 2020 X. M. Zhu et al., 2023
Fungi	mannosyl inositol phosphorylceramides (MIPC) and Glucosylceramide (GluCer)	ergosterol	Santos et al., 2020 Usmani et al., 2023 X. M. Zhu et al., 2023

AM fungi	Glucosylceramide (GluCer) and Glycosyl inositol phosphoryl ceramides (GIPCs)	24-ethyl cholesterol	Kameoka & Gutjahr, 2022 Weete et al., 2010 Wewer et al., 2014

Importantly, the biological significance of this increased cytoplasmic flow remains unknown but it could reflect enhanced carbon transfer from the plant to the fungus and, potentially, to the bacterium. To address this, future work could directly quantify resource dynamics by measuring triacylglycerol accumulation (Jiang et al., 2021) in the extraradical mycelium upon surfactin treatment, using a bi-compartmented system. This would clarify whether increased flow corresponds to higher carbon mobilization and whether this metabolic shift benefits the bacterium, ultimately facilitating colonization. Global transcriptomic analyses (RNA-seq) could reveal whether exposure to surfactin, regulates fungal genes, especially those related to sugar transport, ion channels, ATPases, and stress responses. Untargeted metabolomics could complement transcriptomics by identifying fungal metabolites whose production is influenced by surfactin and potentially revealing new molecules involved in AM fungal signaling. UPLC-MS/MS should be coupled with strong data processing via MZmine (https://mzmine.io/) and GNPS (https://gnps.ucsd.edu/) for molecular networking and identification of structurally related but novel compounds (Rigolet et al., 2024). It would be particularly interesting to assess whether this cLP influences carbon allocation by the host plant. For example, monitoring the expression of *SWEET* genes in roots could reveal whether surfactin enhances plant sugar export toward the fungus. Such findings would support the idea of a coordinated tripartite regulatory mechanism involving the plant, the fungus and the bacterium (Duan et al., 2024; Luginbuehl et al., 2017).

Integrating data from these various experimental approaches will further feature surfactin as keystone molecule in the establishment of cross-kingdom microbial mutualism. To better understand this phenomenon, it would be informative to assess whether surfactin-induced acceleration of cytoplasmic flow is required for bacterial colonization, whether the effect is conserved across other AM fungal species, and whether structurally related cLPs, such as pumilacidin or lichenysin, produce similar responses (**Figure 5-3**). Since surfactin is produced by nearly members of the *B. subtilis* group, widespread in soil environments, and since cLPs are also produced by other rhizobacteria such as *Pseudomonas* spp. (Balleux et al., 2025; Raaijmakers et al., 2010), cLP-mediated interkingdom signalling may represent a broader, conserved mode of communication in the rhizosphere.

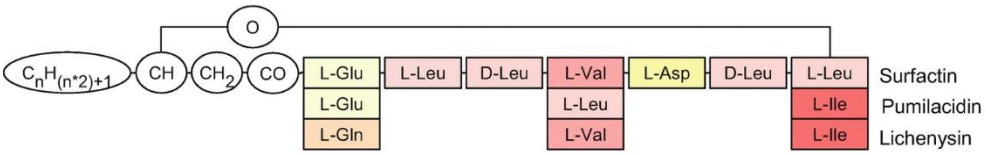

Figure 5-3:Chemical structures of the main variants within the surfactin family. The first three molecules are typical surfactins produced by *B. subtilis*, *B. velezensis*, and related species, pumilacidin, produced by *B. pumilus*, and lichenysin, produced by *B. licheniformis*. Structures credit to Théatre et al. (2022).

5.2.3 Do AM fungi transport bacterial metabolite(s)?

We observed that surfactin is translocated along the hyphal network of *R. irregularis*, strongly suggesting that the AM fungus is capable of actively transporting this bacterial metabolite. This observation implies that surfactin is internalized and redistributed within the ERM. However, further experimental evidence is needed to confirm this hypothesis. A first approach to trace the localization and transport of surfactin within fungal hyphae would involve fluorescence labelling of the molecule. Yet, this strategy presents significant challenges due to the chemical structure of surfactin. The molecule contains a lactone ring formed via an ester bond, which is chemically labile and sensitive to basic conditions (Lundberg et al., 2023; Shao et al., 2015). Moreover, surfactin lacks free amine groups, complicating conjugation with conventional NHS ester-based fluorophores (Munusamy et al., 2020). Additionally, conjugation with fluorophores may alter surfactin conformation and compromise its biological activity. Therefore, before biological assays, it would be critical to verify the structural integrity of labelled surfactin and validate its functional activity, for example through cytoplasmic flow assays in AM hyphae.

Moreover, it would be relevant to elucidate the mechanism by which the fungus could internalize surfactin.. Given the concentrations detected in the hyphosphere, surfactin may first insert into the PM and then be internalized via **endocytosis**, intracellular micelle formation, inclusion into lipid globules, or transporter-mediated uptake. Advanced imaging techniques such as **electron tomography** could visualize the formation of inward vesicles or membrane deformations in response to surfactin exposure. Complementary biophysical analyses would also be valuable to characterize surfactin impact on membrane fluidity, curvature, and integrity. Moreover, biomimetic PM models composed of defined lipid mixtures could be employed to assess surfactin–lipid interactions and membrane insertion dynamics and on potential effects on membrane behaviour in general. The role of specific fungal organelles in surfactin transport remains largely speculative due to technical challenges in manipulating and imaging living AM fungal hyphae. The dynamic nature of fungal organelles, combined with limited direct observations, makes it

difficult to assign definitive functions. Nevertheless, the high levels of intracellular trafficking observed in both extraradical and intraradical hyphae suggest that active transport mechanisms could contribute to surfactin redistribution, potentially involving pathways connected to arbuscules (**Figure 5-4**).

Global transcriptomic profiling (RNA-seq) would contribute to decipher the fungal response to surfactin. By comparing the transcriptomes of *R. irregularis* exposed to *B. velezensis*, purified surfactin, or a cLP-deficient mutant, it would be possible to determine whether surfactin alone can trigger transcriptional changes. Particular attention should be paid to genes involved in membrane trafficking and endocytosis, such as those encoding clathrin or proteins involved in clathrin-mediated endocytosis, as their induction would strongly support specific internalization mechanisms (He et al., 2023; Holland & Roth, 2023; Russo et al., 2019). It is also important to consider that surfactin may not be the only bacterial metabolite transported by the fungus. Other metabolites produced by *B. velezensis* could also be internalized and redistributed through the ERM, potentially contributing to fungal modulation. Untargeted metabolomics analyses of ERM samples treated with bacterial supernatant could reveal additional bacterial metabolites transported by the fungus.

In conclusion, our data provide the first evidence that an AM fungus can take up and transport a bacterial metabolite. Further investigation into the diversity of metabolites transported, their uptake mechanisms, and their ecological or physiological consequences will significantly advance our understanding of interkingdom interactions and mutualistic communication in the rhizosphere.

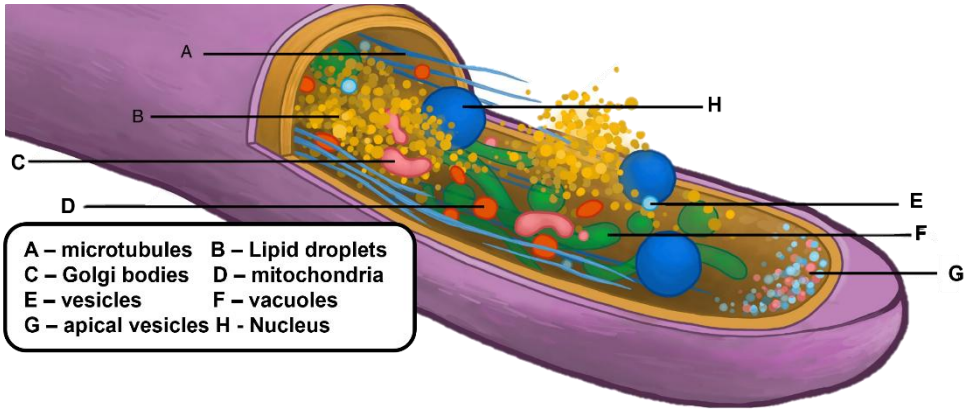

Figure 5-4: Organelles within the cytoplasm of AM fungi. Overview of the potential intracellular compartments and structures that could participate in the transport of surfactin within the fungal cytoplasm. Several cellular components may play a role in this process:

- Cytoskeleton: Cytoskeleton could participate in the intracellular movement of surfactin, by mediating vesicle trafficking and endocytosis, potentially involving actin filaments or clathrin-coated vesicles.
- Microtubules: Bundled microtubules have been observed in both the large trunk hyphae and the fine branches of arbuscules, suggesting they may serve as conduits for transporting molecules such as surfactin from hyphal tips to arbuscules.
- Tubular vacuoles: ERM of AM fungi is traversed by extensive tubular vacuoles, forming longitudinal arrays and bundles from tip to base. These structures are associated with cytoplasmic streaming and are hypothesized to play a role in long-distance intracellular transport.
- Vesicles, lipids droplets and free vacuoles: In addition to active transport along cytoskeletal elements, surfactin may also associate with intracellular membranes, potentially diffusing freely via vesicular transport or within vacuoles.

Adapted from Cargill et al. (2025).

5.2.4 Are AM fungi naturally resistant to *Bacillus* antifungal activity?

Throughout this study, a central question emerged: why does *B. velezensis*, a bacterium with potent antifungal properties, inhibit phytopathogens while remaining compatible with the AM fungus *R. irregularis* ? *B. velezensis* dwelling in the hyphosphere efficiently produces iturin-type lipopeptides known for their strong antifungal properties against a wide range of phytopathogens (Arrebola et al., 2010; Calvo et al., 2019; Jiang et al., 2018; Ongena & Jacques, 2008) but which appears not toxic to *R. irregularis* at the concentrations tested. Thus, unlike *R. irregularis* at

20μM, several phytopathogenic fungi are highly sensitive to iturin at similar or lower concentrations, with reported minimum inhibitory concentrations (MICs) ≤ 20 μM against *B. cinerea* (16.9 μM), *Monilinia fructicola* (8.5 μM), *Penicillium digitatum* (16.9 μM), *A. niger* (2.5 μM), *F. oxysporum* (5 μM), *Alternaria brunsii* (2.5 μM), and *F. graminarium* (5 μM) (Calvo et al., 2019; Gong et al., 2015; Pathak & Keharia, 2014; Wang et al., 2024b). The antifungal activity of cLPs is closely linked to the lipid composition and structural organization of the fungal plasma membrane. Their mode of action typically involves insertion into membranes, leading to pore formation or bilayer disruption. Notably, their efficacy is critically modulated by the presence of membrane sterols, particularly ergosterol, which plays a central role in maintaining membrane integrity and fluidity in many phytopathogenic fungi (Bakker et al., 2024; Balleza et al., 2019; Botcazon et al., 2022; Fiedler & Heerklotz, 2015; Gilliard et al., 2024; Nasir & Besson, 2012; Sur et al., 2018; Wise et al., 2014). Consequently, fungal susceptibility to *Bacillus*-derived cLPs often correlates with ergosterol content and phospholipid composition (Balleza et al., 2019; Fiedler & Heerklotz, 2015; Gilliard et al., 2024; Leconte et al., 2024; Mantil et al., 2019; Yang et al., 2024a; Zakharova et al., 2019). Interestingly, AM fungi are seemingly less susceptible to iturin toxicity, potentially because of their specific membrane lipid composition (**Table 5-1**). Compared to phytopathogenic fungi for which the major sterol is ergosterol, AM fungal PM seems to instead contain 24-ethyl cholesterol as main sterols (**Figure 5-5**) (Kameoka & Gutjahr, 2022; Weete et al., 2010; Wewer et al., 2014). This distinct lipid makeup may reduce membrane permeabilization by cLPs such as iturin, rendering AM fungi less susceptible to their disruptive effects. This could be investigated by comparing iturin affinity and leakage effect on artificial membrane systems mimicking PMs of AM fungi or pathogens like *Fusarium* and *Botrytis* (Balleza et al., 2019; Botcazon et al., 2024; Gilliard et al., 2024; Mantil et al., 2019).

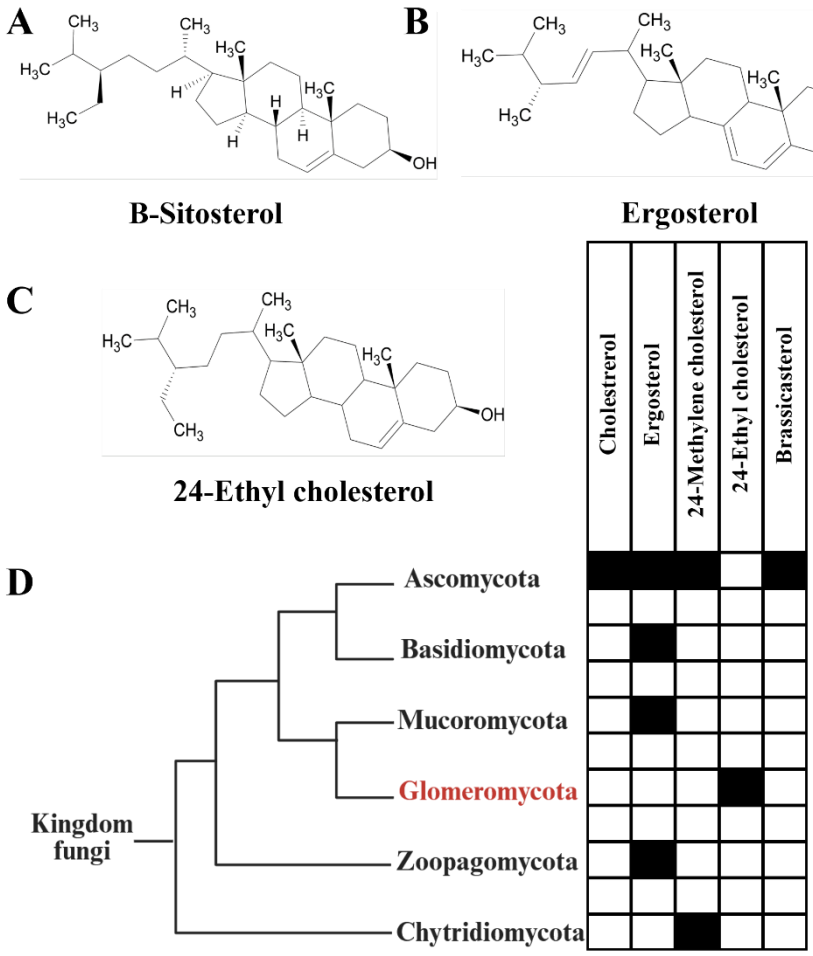

Figure 5-5: Structures of major sterols and their phylogenetic distribution in fungi. Main sterols in **A)** plants **B)** fungal phytopathogens and **C)** AM fungi such as *R. irregularis*. **D**. Fungal phylogenetic tree showing the major fungal taxa and their associated dominant sterols highlighting the unique sterol composition of Glomeromycota (i.e., arbuscular mycorrhizal fungi) compared to other major divisions of the fungal kingdom. Adapted from Weete et al. (2010) and Naranjo-Ortiz et al. (2019).

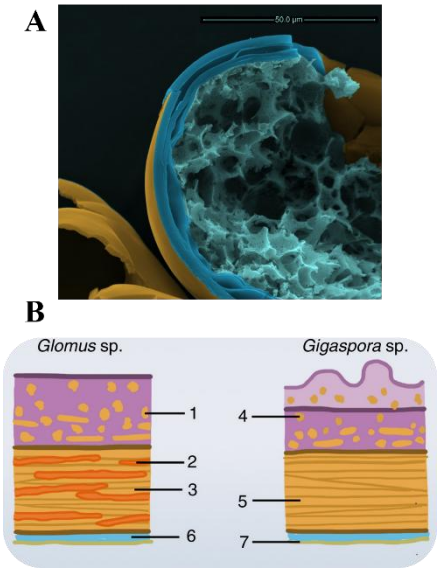

Figure 5-6: The cell walls of AM fungi. A. Image of a spore, showing the multi-layered cell wall. **B.** Proposed differences in 1.Monomeric chitin, 2. β-(1,3)-glucans, 3. Chitin polymer, 4. Monomeric chitin, 5.Chitin polymer, 6. Extracytoplasmic space, 7. Plasma membrane. Image and figure taken from Cargill et al. (2025)

Beyond membranes, cell wall composition may further contribute to resistance. While *B. velezensis* is known to produce chitinases and β-glucanases, the absence of antifungal effects against *R. irregularis* could reflect repression of these enzymes by AM fungal cues or structural resistance of AM fungal cell walls (**Figure 5-6**). Notably, AM fungi possess distinct cell wall features, such as highly branched β-1,6-glucans (Kelly et al., 2023), which have been associated with immune evasion in plant–fungal interactions (Chandrasekar et al., 2022; Wawra et al., 2016). These features may also help AM fungi avoid recognition by *B. velezensis* as fungal competitor.

Moreover, chitin in the ERM cell walls undergoes structural modification, likely becoming embedded in non-chitinous components (Cargill et al., 2025). This may protect AM fungi from chitinases and help explain the non-antagonistic interaction observed. In fungal systems such as zygomycetes, ascomycetes, and basidomycetes, substantial deacetylation of chitin to **chitosan** occurs, rendering the polymer more resistant to chitinase (Gow et al., 2017; Pinto et al., 2025). This modification not only increases resistance to microbial enzymes but also helps fungi evade recognition by plant chitin receptors (Geoghegan et al., 2017; Gow et al., 2017; Kongala & Kondreddy, 2023; Pinto et al., 2025). AM fungi have similarly been shown to modulate the expression of chitin deacetylase enzymes (Chen et al., 2018; Lanfranco et al., 2018; Salvioli et al., 2016). Therefore, it would be intriguing to investigate whether genes associated with cell wall remodeling are transcriptionally activated in *R. irregularis* during co-cultivation with *B. velezensis* or upon exposure to surfactin, as this could hint at an adaptive fungal response aimed at modulating membrane or wall properties to favor mutualistic compatibility and resist potential membrane perturbation.

Differences in cell wall architecture between members of Glomeraceae and Gigasporaceae have also been reported, including variations in the number of wall layers, outer wall composition, and β-(1,3)-glucan content. For example, β-(1,3)-glucan is detectable in *R. irregularis* but undetectable in *Gigaspora* species (**Figure 5-6 B**) (Cargill et al., 2025). These observations highlight the importance of

investigating *B. velezensis* colonization dynamics across different AM fungal genera, as cell wall composition could influence compatibility.

5.2.5 Does *B. velezensis* recognize AM fungi as "friends"?

In addition to potential structural resistance that AM fungi may possess against certain antifungal activities of *B. velezensis*, our results reveal pronounced metabolic shifts in the bacterium when exposed to AM fungal exudates, even in the absence of physical contact. This indicates that diffusible fungal signals alone can modulate *Bacillus* secondary metabolism. To explore the factors underlying the differential *Bacillus* response to AM fungi versus pathogenic fungi, we drew parallels with the evasion of plant immunity by AM fungi and the role of symbiotic signalling in plant–AM fungal interactions. In plants, recognition of AM fungi involves Myc-factors such as LCOs and short-chain COs, which promote symbiosis while suppressing defence responses. It is tempting to speculate that similar mechanisms might also influence *Bacillus*–AM fungal compatibility, although this remains to be experimentally demonstrated.

Supporting this hypothesis, we found that pure LCOs markedly reduced fengycin production in *B. velezensis*, mirroring the effect of crude *R. irregularis* exudates. Although LCOs have not yet been formally identified in AM fungal exudates under our conditions, the data suggest that Myc-factor like signals may contribute to bacterial perception of AM fungi and modulate secondary metabolism in a way that favours a compatible interaction.

Notably, LCOs and COs are not unique to AM fungal symbiosis but seem to be widely produced throughout the fungal kingdom. (Rush et al., 2020). Therefore, *B. velezensis* discrimination between beneficial and pathogenic fungi might depend on the structural specificity, ratios, or concentrations of these molecules, as observed in plant perception of Myc-factors (Tan et al., 2025). This possibility warrants further investigation through the identification and structural characterization of the full spectrum of Myc-factor compounds in AM fungal exudates. It also remains conceivable that *B. velezensis* itself could influence Myc-factor biosynthesis in *R. irregularis*, as suggested by previous studies where bacterial fatty acids triggered hyphal branching and potentially induced LCO production (Hildebrandt et al., 2006; Kameoka et al., 2019). Testing whether *R. irregularis* exposed to *Bacillus* culture filtrates exhibits increased Myc-factor production would thus provide valuable insights.

While our study focused on LCOs, it remains uncertain whether the observed effects are attributable solely to these molecules or to other co-secreted fungal metabolites. Short-chain COs (e.g., CO4) and additional diffusible compounds may also participate in bacterial recognition of AM fungi. Beyond Myc-factors, other signals such as

effector proteins or plant-derived compounds (e.g., methyl salicylate) transported via the extraradical mycelium are known to mediate interkingdom communication (Babikova et al., 2013; Duhamel et al., 2013; Kobayashi, 2015; Park et al., 2007) and could likewise contribute to *Bacillus* metabolic reprogramming. Untargeted metabolomic profiling of fungal exudates during bacterial co-cultivation could help reveal such signaling molecules. If Myc-factor compounds are indeed involved, they may also mask fungal MAMPs, as observed in AM fungal–plant interactions, thereby preventing *Bacillus* from triggering a strong antifungal response. Co-incubation of *Bacillus* with mixtures of Myc-factors and fungal MAMPs could test whether these symbiotic signals attenuate typical fungal pathogen-associated cues. Collectively, these approaches could clarify whether AM fungi mitigate *Bacillus* antifungal activity through Myc-factor–mediated mechanisms, though at this stage, this remains a working hypothesis that requires direct validation.

Understanding the mechanisms through which *B. velezensis* differentiates between fungal patterns from AM fungi versus phytopathogens would provide valuable insights into microbial compatibility. Mapping the "molecular identity" of AM fungi, including traits like LCO production, membrane composition, and exudate chemistry, could help explain how *B. velezensis* selectively modulates its antifungal activity. Our findings highlight AM fungi as an underexplored source of unique bioactive compounds capable of shaping bacterial metabolism and position these symbionts as a distinct category of soil organisms influencing the chemical ecology of *Bacillus* (Anckaert et al., 2021; Andrić et al., 2020; Balleux et al., 2025). Deciphering how *B. velezensis* senses and responds differently to beneficial versus pathogenic fungi offers new perspectives on the molecular dialogues that govern rhizosphere assembly and microbial compatibility.

5.3 Could AM fungi be central players to coordinate plant health?

5.3.1 Highlights

- The microbial partnership enhances tomato systemic resistance against *B. cinerea*
- Application of surfactin on the ERM of *R. irregularis*, even far from the root system, amplifies plant immunity

5.3.2 Does combining *Bacillus* and AM fungi overcome inconsistency ?

Single inoculations with *B. velezensis* or AM fungi often yield variable outcomes in plant protection, due to differences in colonization efficiency and plant immune activation, which can depend on plant genotype and the challenging pathogen (Anckaert et al., 2021; Garrido et al., 2010; Hu et al., 2022; Kaminsky et al., 2019; Kang et al., 2018; Mauch-Mani et al., 2017; Mayjonade et al., 2024; Qiu et al., 2019; Rabbee et al., 2019; Rouphael et al., 2015; Salloum et al., 2016; Salvioli di Fossalunga & Bonfante, 2023; Sun & Shahrajabian, 2023). In our study, co-inoculation with *B. velezensis* and *R. irregularis* consistently improved resistance to *B. cinerea* in two tomato cultivars. Moreover, our results indicate that improved protection is not attributable to greater microbial abundance or enhanced plant growth. This suggests a functional complementarity in which the AM fungus may facilitate bacterial establishment or enhance its efficacy, while *Bacillus* may provide additional protection in cases where AM fungi alone confer limited defence.

Such synergy could arise from the complementary activation of distinct but convergent immune pathways, ISR by *Bacillus* and MIR by *Rhizophagus*, resulting in a more robust plant immune response. This synergy could be further investigated through transcriptomic analysis to identify the immune pathways and genes activated during pathogen challenge. The interaction between the two microorganisms may also enhance elicitor production by both partners. The bacterium could enhance the MIR functionality of the AM fungus. In our experiments, treatment of surfactin to soil colonized by the ERM of *R. irregularis* (without direct root contact) significantly increased host resistance to *B. cinerea*. This suggests that surfactin may thus act as trigger boosting the immunogenic potential of the AM fungus. Untargeted metabolomic profiling (e.g., UPLC-qTOF-MS/MS) of AM fungal extracts could lead to the discovery of candidate elicitor compounds induced by the bacterium. More globally, it would pave the way to uncover novel AM fungal-derived immune elicitors whose synthesis is stimulated by microbial interactions and shed light on a potential

molecular basis for the synergistic enhancement of ISR- based biocontrol activity. Conversely, *R. irregularis* may also enhance the elicitor potential of *B. velezensis*. The AM fungus can induce root architectural changes (Hürter et al., 2018; Su, 2023) that might improve *Bacillus*-mediated immune activation, either by fostering biofilm subpopulations with higher cLP production or by increasing plant sensitivity to bacterial immune elicitor, particularly surfactin. Based on our unpublished observations, it is possible that only certain root cell types are responsive to surfactin-induced immune activation. It would therefore be highly relevant to test whether AM fungi expand the regions where surfactin can be perceived efficiently as an immune trigger. Spatial transcriptomics and single-cell RNA-seq could pinpoint responsive root cell types and reveal whether AM symbiosis broadens the zones competent for surfactin elicitation (Jovic et al., 2022; Serrano et al., 2024).

Taken together, these perspectives emphasize the need for integrated approaches, combining chemical analyses, molecular profiling, and spatially resolved methods, to unravel the cross-kingdom signaling underlying ISR–MIR synergy. Understanding these mechanisms will allow the rational design of microbial consortia with predictable, robust biocontrol potential, supporting the transition to more sustainable crop protection strategies. Co-inoculating *B. velezensis* and AM fungi represents a promising avenue for next-generation bioinoculants, and fully decoding the nature and dynamics of their interaction will be crucial for engineering stable, high-performance microbial partnerships. However, future research should investigate whether this synergistic effect extends to other crops and pathogens, including both fungal and bacterial species, under greenhouse and field conditions. It would also be valuable to test whether co-inoculation improves biocontrol of soilborne root pathogens. To fully unlock the potential of *Bacillus*–AM fungal consortia, expanding this approach to other *Bacillus* strains and AM fungal species could clarify whether the observed synergy is genus-specific, strain-specific, or functionally redundant. While our data highlight a central role for surfactin in this tripartite interaction, other *Bacillus* metabolites could also contribute. To dissect these contributions, future experiments should compare ISR induction in the presence and absence of *R. irregularis* using wild-type *B. velezensis*, a surfactin-deficient mutant, and purified surfactin. Testing other beneficial bacteria such as *Pseudomonas* spp., which produce different cLPs with strong elicitor activity, could reveal whether similar or even stronger defence enhancement can be achieved in combination with AM fungi.

5.3.3 Is AM fungal symbiosis the secret weapon for *Bacillus* to unleash plant defences through ISR ?

The AM symbiosis is primarily characterized by the establishment of a specialized interface that enables nutrient exchange essential for both fungal development and plant growth. This exchange takes place within arbuscules, highly branched fungal structures formed inside root cortical cells. Although AM fungal hyphae penetrate the

root cortex, they do not disrupt the plant plasma membrane. Instead, the plant generates a new membrane structure, the periarbuscular membrane (PAM), which tightly envelops the arbuscule, creating a periarbuscular space (PAS) where molecular exchange occurs. The PAM, derived from the plant plasma membrane through extensive remodelling, plays a central role in bidirectional signaling and nutrient transfer. While the physical organization of this symbiotic interface is well described, the molecular mechanisms governing plant–fungus communication remain poorly understood. A promising hypothesis is that **extracellular vesicles** (EVs) could contribute to this interkingdom dialogue (Holland & Roth, 2023; Qiao & Roth, 2025). EVs are membrane-enclosed nanoparticles that carry diverse cargoes such as proteins, lipids, RNAs, and metabolites. In plant–pathogen interactions, they are well documented for their roles in defence and signaling (Colombo et al., 2014; Wang et al., 2023b; Xiong et al., 2024; Zhang et al., 2024b). In such contexts, plant-derived EVs have been shown to deliver small RNAs and defensive proteins to fungal pathogens, suppressing virulence genes and inhibiting fungal growth (Cai et al., 2018; Huang et al., 2025). Conversely, pathogens like *B. cinerea* release EVs containing small RNAs that can target and dampen plant immunity (He et al., 2021). These findings highlight EVs as key actors in cross-kingdom molecular warfare (Ratsoma et al., 2025; Wang et al., 2023b; Zhang et al., 2024b).

Likewise, Silvestri et al. (2024) propose that the symbiosis between plants and AM fungi involves a bidirectional transfer of functional small RNAs between the two partners. These sRNAs are thought to modulate gene expression in both organisms, thereby facilitating the establishment and regulation of the symbiotic relationship through EV-mediated delivery (**Figure 5-7**) (Ledford et al., 2024; Xie & Fan, 2025). In AM symbiosis, electron tomography studies (Ivanov et al., 2019; Roth et al., 2019) have revealed EV-like particles within the PAS, suggesting their potential involvement in nutrient and/or signal exchange. Intriguingly, two EV subpopulations were observed: one clearly originating from the plant PAM, and another of unknown origin, without obvious association to either plant or fungal membranes. This points to a heterogeneous EV population at the interface, though their exact cargoes and roles remain elusive.

Our data show that surfactin applied to the ERM but at distance from the roots triggers ISR and that the lipopeptide can be translocated across hyphae. Therefore, we hypothesizes that the AM fungus could act as a carrier to deliver surfactin at the symbiotic zone where molecular exchanges occur with root cells. There, surfactin could be transported within EVs across the PAS to the PAM and be perceived at the root cell PM to activate immune responses. In support to such mechanism, fungal EVs have been proposed to carry secondary metabolites (Ahmad et al., 2024; Maximo et al., 2023). Alternatively, passive diffusion or accumulation through the fungal network could also enable surfactin to reach the PAM in a EV-independent process.

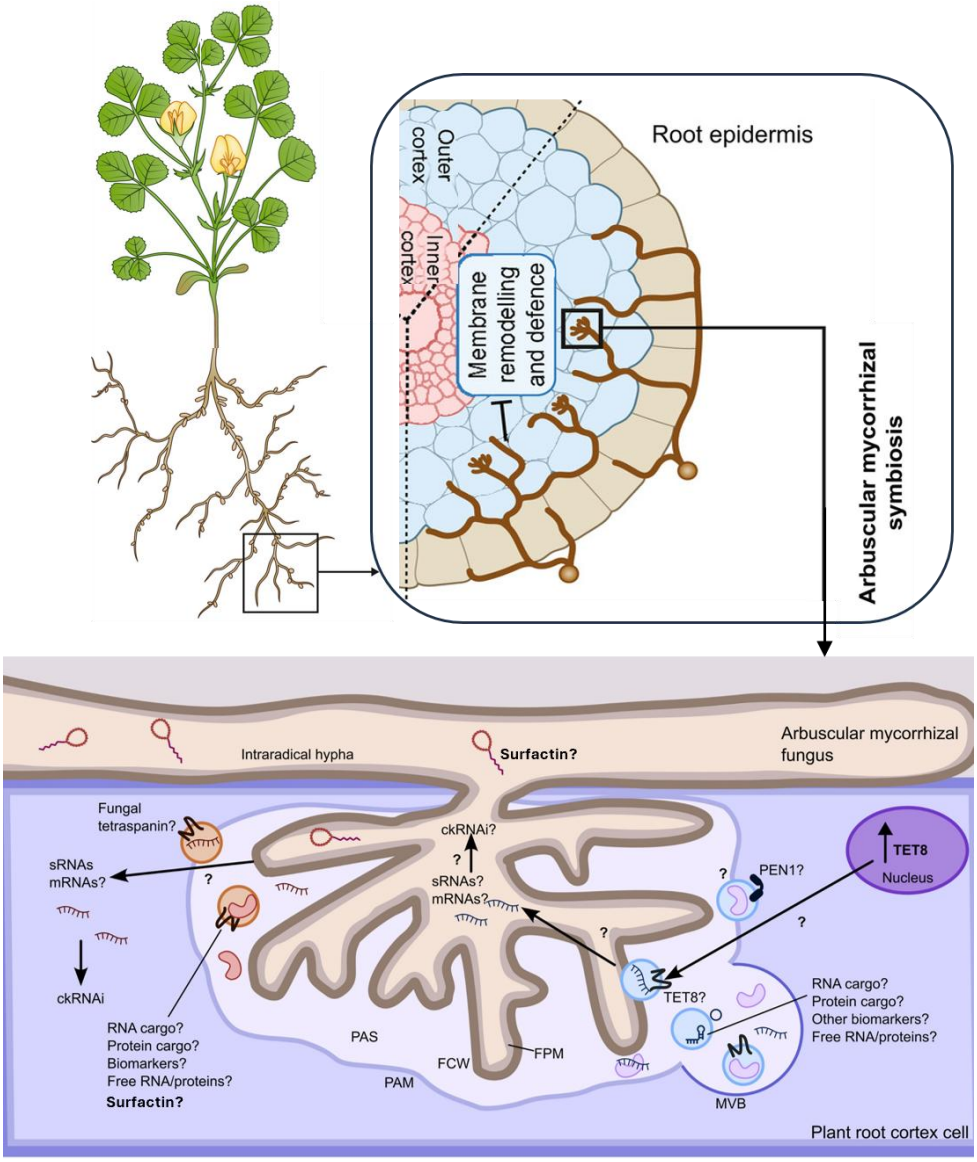

Figure 5-7: Hypothetical roles of extracellular vesicles (EVs) in the peri-arbuscular space during AM symbiosis. Schematic representation summarizing current knowledge and hypotheses regarding the involvement of EVs in molecular exchanges between the AM fungus and its host plant. The illustration depicts proposed functions for both fungal-derived (orange) and plant-derived (blue) EVs in mediating communication across the peri-arbuscular membrane (PAM). In plants, tetraspanins have emerged as key EV biomarkers associated with RNA transport during plant–microbe interactions. For instance, *At*TET8 has been identified in *A. thaliana* EVs that mediate small RNA (sRNA) delivery to *Botrytis cinerea*, leading to cross-kingdom RNA interference (ckRNAi) and silencing of fungal virulence genes. AtTET8 is localized in intraluminal vesicles within multivesicular bodies (MVBs), validating its role as a canonical plant exosome marker. A TET8 homologue has also been detected in *Phaseolus vulgaris* and proposed to participate in root nodule formation and AM symbiosis. Although TET8 expression is upregulated in response to AM colonization, its presence in plant-derived EVs during AM symbiosis remains to be demonstrated (indicated by question marks in the figure). Similarly, plant MVBs have been observed near the PAM and EV-like structures detected in the peri-arbuscular space (PAS), but direct evidence linking them to specific biomarkers, cargoes, or ckRNAi mechanisms targeting the fungus is still lacking. Conversely, fungal sRNAs capable of triggering ckRNAi in the host plant have been described in AM symbiosis, yet their potential delivery through fungal EVs remains hypothetical (orange). Further research is required to elucidate whether both partners use EV-mediated transport as a bidirectional communication mechanism to regulate and stabilize the AM symbiotic interface.

Abbreviations: **PAM** – peri-arbuscular membrane; **PAS** – peri-arbuscular space; **FCW** – fungal cell wall, **FPM** – fungal plasma membrane. Adapted from Qiao and Roth (2025), Qiao et al. (2023), and the review by Holland and Roth (2023).

Confirming the involvement of EVs in this context is challenging due to the difficulties of their isolation, quantification, imaging, and functional characterization at the microscale of the PAM–PAS interface. However, EVs could be isolated from mycorrhizal roots using ultracentrifugation and analysed for their content in surfactin. Confirming that surfactin reaches the PAM–PAS interface would substantially advance our understanding of bacterial–fungal–plant communication and the role of the AM symbiosis in immune priming. At the plant cell level, changes in early immune-related events, such as Ca^{2+} influx and/or ROS burst, can be monitored and compared upon surfactin application in mycorrhizal and non-mycorrhizal roots (either directly or via the ERM) (Giovannetti et al., 2024b; a). If similar Ca^{2+} signatures arise from surfactin application directly on roots and via the ERM, this would support the hypothesis that surfactin is transferred through the AM symbiosis and perceived at the PAM. Furthermore, comparing responses between mycorrhizal and non-mycorrhizal roots could reveal whether the AM fungus modulates plant sensitivity to bacterial signals.

Chapter 6

Conclusion, is this thesis a Myth or a Reality?

What is the real meaning, the true significance, of this work?

Yet beyond the scientific novelty of our findings, I kept asking myself: does this matter for the world besides research labs? Can it truly have an impact on agriculture and the way we produce food, or will it remain shared by a small community of experts and confined to academic circles?

These questions led me to reflect on the parallel between our scientific practices and the evolution of human health management. For decades, humans relied heavily on curative approaches, overusing antibiotics without considering preventive strategies (Grießhammer et al., 2025; Kumar et al., 2025b; Weersma et al., 2020) . Today, we recognize that maintaining a healthy microbiota, for example through probiotics, plays a crucial role in strengthening natural defences (Guarner & Malagelada, 2003; Kamada et al., 2013; Piewngam et al., 2018). Shouldn't agriculture follow the same shift in thinking, moving from curative to preventive approaches by promoting microbial symbioses before disease occurs? After all, just as gut health requires both beneficial microbes and a balanced diet, plant health depends not only on microbial inputs but also on the cultivation practices that shape the rhizosphere (Ilyaskina et al., 2025).

And yet, the current reality of agricultural practice does not reflect this vision. While certain biofertilizers and biocontrol agents are already available on the market, their use remains marginal, often hindered by regulatory obstacles, inconsistent efficiency, or limited interest from farmers. I was particularly struck during discussions with farmers involved in regional projects (MicroSoilSytem, Walloon project) by how little interest there was in using microorganisms as biocontrol agents, except in specific cases like nitrogen-fixing bacteria. The broader adoption of beneficial microbes faces multiple barriers: strong reliance on mineral fertilization, lack of knowledge, inconsistent product performance, and, most importantly, agricultural practices that often degrade the ecological structures needed for these organisms to function.

For instance, intensive tillage disrupts the CMNs essential for nutrient cycling and microbial recruitment. Recent work suggests that reducing soil disturbance could improve both soil health and microbial diversity (van Rijssel et al., 2025). But transitioning to such systems requires profound cultural and economic shifts, making microbial-based strategies inseparable from the broader question of how we design and manage agricultural ecosystems.

These reflections connect directly to the "One Health" vision promoted by the World Health Organization, which recognizes that the health of plants, animals, humans, and the environment are all interdependent. The simplification of ecosystems, the over-domestication of plants, and their increasing reliance on external inputs have likely made modern crops more vulnerable. Domestication may have

rendered many plants “lazy”, reducing their capacity or need to engage in symbioses like mycorrhizal associations (Bennett & Groten, 2022; Ilyaskina et al., 2025; Ramirez-Villacis et al., 2025). Why invest in partnerships if all essential nutrients are artificially provided? Yet in doing so, we may have weakened the resilience of cropping systems to future stresses, including those induced by climate change.

Moving forward, I believe the future of sustainable agriculture will depend not only on adding beneficial microbes but also on rebuilding ecological balances within the rhizosphere. Microbial inoculants should not be sold as universal solutions but integrated into tailored strategies based on local soils, crop species, and farming practices (Zhou et al., 2023). More than offering a product, it would be far more valuable to provide a service, an approach that combines ecological diagnostics, adapted microbial consortia, and long-term support for farmers (Berruto & Demirer, 2024; Lutz et al., 2023; Ramirez-Villacis et al., 2025). Such approaches already exist for certain crops like trees or vineyards and proposed by some companies like Mycophyto in France (https://www.mycophyto.fr/) but need to be extended to larger-scale agriculture.

Finally, I want to emphasize that introducing microbial diversity into cropping systems is not just about productivity; it’s about resilience. Higher microbial diversity translates into better stability of the agroecosystem, reduced dependence on fertilizers, and greater capacity to face environmental fluctuations (Ilyaskina et al., 2025; Ramirez-Villacis et al., 2025; Xun et al., 2021). The tools and concepts explored in this thesis, from bacterial-fungal interactions (Chapter 2) to Plant immune implement (Chapter 5) could contribute to these emerging strategies.

Thus, this work may not provide a single “solution,” but it offers a step toward rethinking how we interact with the invisible microbial world that supports plant life. Research alone is not enough, change will come through integrating fundamental knowledge into agricultural practices, fostering dialogue between science and society, and breaking the inertia of conventional systems.

So, is this thesis a myth or a reality? Perhaps both. Research produces ideas, but their transformation into reality depends on choices: of farmers, of policymakers, of politic legislation, of all of us as consumers. Searching for knowledge is good. But changing practices is better.

Chapter 7

Materials and Methods

7.1 Materials

Table 7-1: Key resources table

REAGENT or RESOURCE	SOURCE	IDENTIFIER
Chemicals, peptides, and recombinant proteins		
MOPS	SIGMA-ALDRICH	Cat#M1254
Phytagel™	SIGMA-ALDRICH	Cat#P8169
Agarose	NIPPON Genetics Europe	Cat#AG02
Propidium Iodide	ThermoFisher Scientific	Cat# P1304MP
DNAzol™ Reagent	ThermoFisher Scientific	Cat#10503027
Nitro Blue Tetrazolium (NBT)	SIGMA-ALDRICH	Cat#N6639
Chloramphenicol	AppliChem	Cat#A1806
Phleomycin	InvivoGen	Cat#ant-ph-1
Surfactin	Prof. Ongena Marc, Microbial Processes and Interactions Laboratory, Uliège, Belgium	N/A
Fengycin	Prof. Ongena Marc, Microbial Processes and Interactions Laboratory, Uliège, Belgium	N/A

Iturin	Prof. Ongena Marc, Microbial Processes and Interactions Laboratory, Uliège, Belgium	N/A
Tris-HCl	Sigma	Cat#T3253
Tween20	Sigma	Cat#P9416
Critical commercial assays		
NucleoSpin RNA Kit	Macherey Nagel	Cat#740955.250
Luna® Universal One-Step RT-qPCR Kit	New England Biolabs	Cat#E3005L
QuantiFluor dsDNA system	Promega	Cat#E2670
GenEluteTM Soil DNA Isolation kit	SIGMA-ALDRICH	Cat#DNB100
Deposited data		

Experimental models: Organisms/strains		
Bacterial strains (see Table 7-2)		
Solanum lycopersicum cv Ailsa Criag and cv MoneyMakers	EnGraineToi	NA
Botrytis cinerea MUCL 43839	BCCM/MUCL	Cat# MUCL43839
Solanum tuberosum L. var. Bintje	Station de Haute Belgique	NA
Trichoderma harzianum Rifai MUCL 29707	BCCM/MUCL	Cat# MUCL29707
Rhizophagus irregularis (Błaszk,Wubet, Renker, and Buscot) C. Walker and A. Schüßler as ("irregulare") MUCL 41833	BCCM/MUCL - GINCO	Cat#MUCL41833
Rhizophagus clarus (T.H. Nicolson & N.C. Schenck) C. Walker & A. Schüßler MUCL 46238	BCCM/MUCL - GINCO	Cat# MUCL46238
Rhizophagus intraradices (N.C. Schenck & G.S. Sm.) C. Walker & Schuessler MUCL 49410	BCCM/MUCL – GINCO	Cat#MUCL 49410
Rhizophagus aggregatus (N.C. Schenck & G.S. Sm.) C. Walker MUCL 49408	BCCM/MUCL – GINCO	Cat# MUCL 49408
Oligonucleotides		
Primers (see Table 7-3)		

Software and Algorithms		
Fiji	(Schindelin et al., 2012)	
MassHunter v10.0	Agilent	https://www.agilent.com/en/product/software-informatics/mass-spectrometry-software
NIS-Element AR software	Nikon	https://www.microscope.healthcare.nikon.com/products/software/nis-elements/nis-elements-advanced-research
GraphPad Prism 9	GraphPad Software	https://www.graphpad.com/features
TrackMate	(Tinevez et al., 2017)	
Other		
SPARK multiplate reader	Tecan	https://lifesciences.tecan.com/multimode-plate-reader
NanoDrop 2000	ThermoFisher Scientific	Cat#ND-2000

StepOne™ Real-Time PCR system	ThermoFisher Scientific	Scientific Cat#4376357
UHPLC Agilent 1290 Infinity II	Agilent	https://www.agilent.com/en/product/liquid-chromatography/hplc-systems/analytical-hplc-systems/1290-infinity-ii-lc-system
Acquity UPLC BEH C18 column (2.1 x 50mm x 1.7µm)	Waters	Cat#186002350
6530 Q-TOF mass spectrometer	Agilent	Cat#G6530AA
Nikon Ti2-E inverted microscope	Nikon	https://www.microscope.healthcare.nikon.com/products/inverted-microscopes/eclipse-ti2-series
Petri dishes- 90mm, 3 compartments, vents	VWR	Cat#KART363
Petri dishes- 90mm, 2 compartments, vents	Greiner bio-one	Cat#635161

7.1.1 Biological materials

Rhizophagus irregularis (Błaszk,Wubet, Renker, and Buscot) C. Walker and A. Schüßler as ("irregulare") MUCL 41833, *Rhizophagus clarus* (T.H. Nicolson & N.C. Schenck) C. Walker & A. Schüßler MUCL 46238, *Rhizophagus aggregatus* (N.C. Schenck & G.S. Sm.) C. Walker MUCL 49408 *and Rhizophagus intraradices* (N.C. Schenck & G.S. Sm.) C. Walker & Schuessler MUCL 49410 were obtained from the Glomeromycota *in vitro* collection (GINCO). AM fungi were proliferated *in vitro* on Ri T-DNA transformed roots of carrot (*Daucus carota* L.) clone DC2 in bi-compartmented Petri plates (90 × 15 mm) containing the Modified Strullu-Romand (MSR) medium.100 The Petri plates were incubated in the dark at 27 °C until sufficient spores were produced.

Bacillus velezensis GA1 and its mutants are listed in Table 7-2. The construction of knockout mutant strains of *B. velezensis* GA1 involved gene replacement through homologous recombination as previously described by Hoff et al. (2021). The procedure involved PCR amplification of the 1 kb upstream region of the target gene, the antibiotic marker (chloramphenicol, kanamycin and/or phleomycin cassette), and the 1kb downstream region of the target gene, using appropriate primers. The primers used for this study have been previously described by Andrić et al. (2023) and listed in Table 7-3.To introduce the recombinant cassette into GA1, a slightly modified protocol developed by Jarmer et al.101 was employed by inducing natural competence through nitrogen depletion. Initially, a colony of *B. velezensis* was inoculated on lysogeny broth (LB) medium (10 g l^{-1} NaCl, 5 g l^{-1} yeast extract, and 10 g l^{-1} tryptone) and incubated at 37°C under shaking for 6 h. The cells were then washed and resuspended in MMG medium. Subsequently, the recombinant cassette (1 µg) was added to the GA1 cell suspension, adjusted to an OD_{600} of 0.01. The incubation was carried out at 37°C under shaking for 24 h. Colonies that had integrated the cassette through a double crossing over event were selected on LB plates supplemented with chloramphenicol (5 µg ml^{-1}), phleomycin (4 µg ml^{-1}) or kanamycin (5 µg ml^{-1}). The successful gene deletions were confirmed by PCR analysis using specific upstream and downstream primers (UpF and DwR) and by UPLC-MS to check the absence of production of the corresponding bioactive secondary metabolites. Mutants of *B. velezensis* were grown on LB medium supplemented with adapted antibiotics.

Table 7-2: Bacterial strains used in this study

	Relevant genotype, description (Genome bank number when sequenced)	Reference or sources
Bacillus velezensis		
GA1	Wild type (CP046386)	(Toure et al., 2004)
GA1 Δ*amyE*::cat+P_{veg} - *gfpmut3* (called GA1 GFP)	GA1 disrupted of *amyE* gene; Cm^R and harbouring a constitutive transcriptional fusion (P_{veg}-*gfpmut3*)	(Hoff et al., 2021)
GA1 Δ*srfaA* ::cat-Δ*fenA* ::phleo	GA1 deleted of *srfaA* and *fenA* genes; unable to produce surfactin and fengycin family	This study
GA1 Δ*srfaA* ::cat-Δ*ituA* ::phleo	GA1 deleted of *srfaA* and *ituA* genes; unable to produce surfactin and iturin family	This study
GA1 Δ*fenA* ::cat-Δ*ituA* ::phleo	GA1 deleted of *fenA* and *ituA* genes; unable to produce fengycin and iturin family	This study

GA1 Δ*fenA* ::cat-Δ*ituA* ::phleo-Δ*srfaA* ::kana	GA1 deleted of *fenA*, *ituA* and *srfaA* genes; unable to produce surfactin, fengycin and iturin family	This study
GA1 Δ*sfp* ::cat	GA1 deleted of *sfp* gene; unable to produce lipopeptides and polyketides	(Andrić et al., 2023)
GA1 Δ*bacA* ::cat Δ*sfp* ::;phleo	GA1 deleted of *bacA* and *sfp* genes; unable to produce bacilysin, lipopeptides and polyketides	This study
GA1 Δ*srfaA* ::cat	GA1 deleted of *srfaA* gene; unable to produce surfactin family	(Hoff et al., 2021)
GA1 Δ*bacA* ::cat	GA1 deleted of bacA gene; unable to produce bacilysin	(Andrić et al., 2023)

Trichoderma harzianum Rifai MUCL 29707 was obtained from the Mycothèque de l'Université catholique de Louvain (BCCM/MUCL). The strain was reactivated and periodically cultured on PDA. *Collimonas fungivorans* LMG 21973 was grown on TSA medium (Sigma-Aldrich, India) and obtain from the collection BCCM/LMG.

Solanum tuberosum L. var. Bintje was provided by the "Station de Haute Belgique" (Libramont, Belgium) as *in vitro* plants. The plants were micropropagated every 4 weeks in culture microboxes, sealed with breathing filters in the lid (ref: 0118/120 + OD118, SacO2, Belgium). They were grown on sterilized (121°C for 15 min) Murashige and Skoog (MS) medium (Duchefa, Netherlands) supplemented with 10 g l^{-1} sucrose and solidified with 4.2 g l^{-1} phytagel (Sigma-Aldrich, St. Louis, USA). The microboxes were placed in a growth chamber (Snijders Scientific B.V., Netherlands), under a temperature of 20/18°C (day/night), a relative humidity (RH) of 75%, a photoperiod of 16 h day-1 and a photosynthetic photon flux (PPF) of 50 µmol s^{-1} m^{-2}.

Table 7-3: Primers used in this study

Targeted gene	Primer name	Primer Sequence (5'→3')
B. velezensis GA1		
srfaA	UpsrfaAF	TCAGCAAAACTGCGTGGTAG
	UpsrfaAR	CCAATTTTCGAATTCTTTTACCGCGATAAAAAGTTATTTCCATATGTGTGC
	DwsrfAF	CAGCTCCAGATCCTCTACGCCGGACACGCTTTATATCGTGCCGAA
	DwsrfAR	AAGAAATGATCATAAATACC

fenA	UpFenAF	AGCAAAAACCGGGTCACTA
	UpFenAR	CCAATTTTCGAATTCTTTTACCGCGTTCGTCTGACATGACAAGCA
	DwFenAF	CAGCTCCAGATCCTCTACGCCGGACAAAGGACTTTAATTTCATAAAAAGGTG
	DwFenAR	CCTTTTTGAGAAGAGAAGAAAAAG
ituA	UpItuAF	ATGCAGGAAATAGGGGTGA
	UpItuAR	CCAATTTTCGAATTCTTTTACCGCGGGTATACATAGGTCCCCTCCTG
	DwItuAF	CAGCTCCAGATCCTCTACGCCGGACCAATTGAACTTTTAGGGAAAAGCA
	DwItuAR	GCGACTAACGTATCGGGTTG
bacA	UpbacAF	GATGGGTCTGATCGTGTCAA
	UpbacAR	CCAATTTTCGAATTCTTTTACCGCGCATGAGCACCAACCAATCTG
	DwbacAF	CAGCTCCAGATCCTCTACGCCGGACAACTGAACAAGATTTGCAGG
	DwbacAR	GAATCGGGGCGACAATTT
TasA	UptasAFw	CGCCATATGACACAGGGACA
	Up-tasARv	CAGGAAACAGCTATGACCAATCGGAACATGCCTTACC
	DwtasAFw	GTAAAACGACGGCCAGTAACTAATCCGAAAGTCGGAC
	DwtasARv	TCGCCAGATGGAAAAAGGAC
sfp	sfpUpFw	TCGTCACCCATGAAATCAAA
	sfpUpRv	CCAATTTTCGAATTCTTTTACCGCGCATGTCCAGATCCTCCGTCT
	sfpDwFw	CAGCTCCAGATCCTCTACGCCGGACGACGGGATTGAGATGAAAA

	sfpDwRv	CATTGAGACGTACCCGCTTT
epsA-O	epsA-OUpFw	CGGGCAAATAGAGCCGTACG
	epsA-OUpRv	CAGGAAACAGCTATGACATTCTCATTCATGTAATTAC
	epsA-ODwFw	GTAAAACGACGGCCAGTCTTTGAATGAGCGGAAGGTT
	epsA-ODwRv	AGCTGGATGTCAGGAAACGA
Antibiotic marker		
Chloramphenicol marker	CatF	CGCGGTAAAAGAATTCGAAAA
	CatR	GTCCGGCGTAGAGGATCTG
Phleomycin marker	PhleoF	GTCATAGCTGTTTCCTGCCAAAAGGGGGTTTCATTTT
	PhleoR	ACTGGCCGTCGTTTTACTCCAATAAATGCGACACCAA
Kanamycin marker	nptIIF	GAGGATCGTTTCGCATGATT
	nptIIR	CGCTCAGAAGAACTCGTCAA
RT-qPCR for *R. irregularis* MUCL41833		
mtLSU	mtLSUFw	AAGTCCTCTAGGTCGTAGCA
	mtLSURv	ACAGGTATTTATCAAATCCTTCCC

Solanum lycopersicum cv Ailsa Criag and cv MoneyMakers seeds were obtained from EnGraineToi (Sussargues, France). Seeds were sterilized by immersion in 70% (v/v) ethanol for 1 min and 10% (v/v) sodium hypochlorite (NaOCl, 12%) for 4 min, then thoroughly rinsed in sterile water before their use in experiments.

The protective effect of tomato due to induced systemic resistance was performed using *Botrytis cinerea* MUCL 43839 as pathogen agent. The strain was obtained from BCCM/MUCL.

7.2 Methods

7.2.2 Set up of experimental *in-vitro* system

During the implementation of the bi-compartmental setup, several optimizations and observations were made to allow for a robust analysis of the interaction between *Bacillus velezensis* and *Rhizophagus irregularis.*

In the root compartment (RC), Phytagel supplemented with sucrose was used to ensure optimal root development and efficient mycorrhization. In contrast, the hyphal compartment (HC) was filled with high-purity agarose devoid of any added carbon source. This was a crucial adjustment, as we observed residual bacterial growth on Phytagel- and agar-based media (data not shown). The use of sugar-free agarose ensured that any bacterial proliferation in the HC was solely due to the consumption of hyphal exudates, and not from the medium itself. When necessary, to maintain the physical separation between roots and hyphae, roots that occasionally crossed the plastic barrier into the HC were carefully redirected into the RC. This allowed us to investigate the *Bacillus–Rhizophagus* interaction without direct root influence.

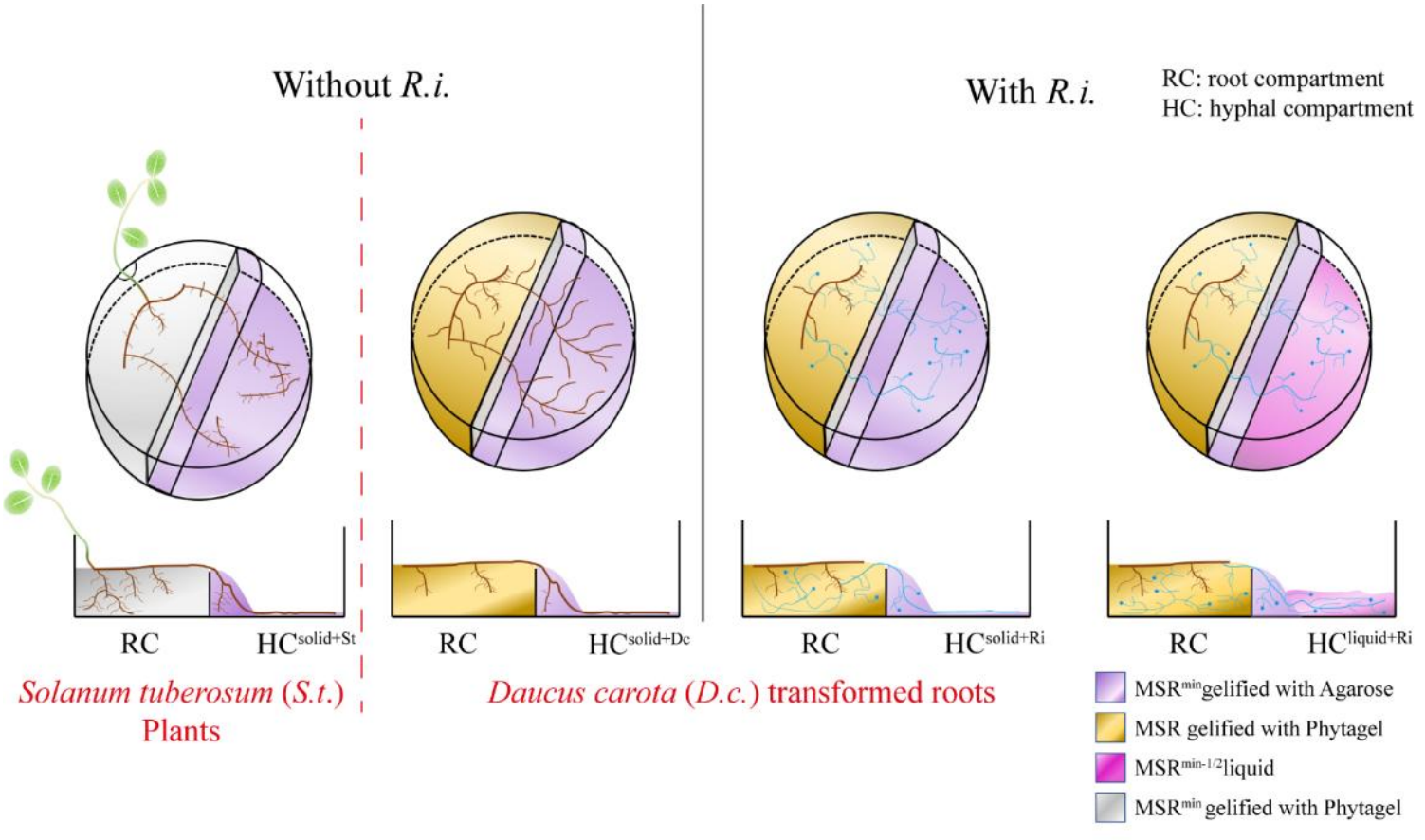
Without *R.i.*
With *R.i.*
RC: root compartment
HC: hyphal compartment
RC
HC^solid+St
RC
HC^solid+Dc
RC
HC^solid+Ri
RC
HC^liquid+Ri
Solanum tuberosum (*S.t.*) Plants
Daucus carota (*D.c.*) transformed roots
MSR^min gelified with Agarose
MSR gelified with Phytagel
MSR^min-1/2 liquid
MSR^min gelified with Phytagel

Figure 7-1: Schematic representation of experimental set-up. Schematic view of systems consisted of bi-compartement Petri plates with a root compartment (RC) containing roots of *S. tuberosum* plants or roots of *D. carota clone* DC2 associated or not to *R. irregularis* and a hyphal compartment (HC) containing only roots of *S. tuberosum* ($HC^{solid+St}$) or of *D. carota* ($HC^{solid+DC}$) or hyphae of *R. irregularis* ($HC^{solid+Ri}$ and $HC^{liquid+Ri}$). In the HC, roots or ERM were allowed to proliferate on solid ($HC^{solid+St}$, $HC^{solid+Dc}$ and $HC^{solid+Ri}$) or in liquid ($HC^{liquid+Ri}$) minimal media without any added carbon source. Brown, transformed roots of D. carota or roots of S. tuberosum; Blue, ERM of *R. irregularis*.

Bi-compartmented Petri plates (90 × 15 mm) were used to grow transformed carrot roots with the AM fungi as detailed in Cranenbrouck et al. (2005) and St-Arnaud et al., (1996). In one compartment (the root compartment – RC), the root and AM fungus were associated on 25 ml MSR medium (Cranenbrouck et al., 2005). The MSR medium was solidified with 4.2 g l^{-1} Phytagel, while in the other compartment (the hyphal compartment - HC), only the extraradical mycelium of the fungus was allowed to grow. The fungus extended in the HC via a slope (from top to bottom of the plastic barrier separating the RC from the HC) made of 5 ml MSR medium, without sucrose and vitamins (MSR^{min}), gelified with 10 g l^{-1} agarose. Ten ml of the same solid medium were poured in the HC (HC^{solid}). Agarose with high-purity ,without added sugar, was used to prevent residual bacterial growth, which we observed on Phytagel and agar-solidified media. After circa 3 months of growth, the extraradical mycelium (ERM) network of *R. irregularis*, *R. clarus*, *R. aggregatus* and *R intraradices* extended profusely in the HC (thereafter $HC^{solid+Ri}$) (**Figure 7-1**). A control treatment consisting of non-mycorrhizal excised transformed carrot roots was included and roots were allowed to cross the partition wall separating RC from HC to grow for circa 3 months in the HC (thereafter $HC^{solid+Dc}$) (**Figure 7-1**). The system was further developed with the HC containing liquid MSR medium, with the exception of the slope (Toljander et al., 2007). Briefly, in the HC, 15 ml of liquid MSR^{min} medium diluted twice ($MS^{min-½}$) was added (HC^{liquid}). After 3 months, a profuse ERM has developed in the HC ($HC^{liquid+Ri}$) (Figure 7-1). Bi-compartmented Petri plates were incubated in the dark at 27 °C.

Similarly, to the above, bi-compartmented Petri plates were used to grown *Solanum tuberosum* var Bintje plantlets. Twenty days old in vitro *S. tuberosum* plantlets were transferred in the Petri plates with their shoot protruding outside the plate via a small opening in the lid, plastered with sterile silicon grease to avoid contaminations, and the roots developing in the RC on 20 ml MSR^{min} medium. The roots crossed the partition wall and developed in the HC on the MSR^{min} medium gelified with 10 g l^{-1} of agarose ($HC^{solid+St}$) (**Figure 7-1**). Fresh medium was added weekly to keep medium at the top of the partition wall in the RC. The plants were kept for ~3 months

in a growth chamber (Snijders Scientific B.V., Netherlands), under a temperature of 20/18°C (day/night), a RH of 75%, a photoperiod of 16 h day^{-1} under a PPF of 50 µmol s^{-1} m^{-2}.

In complement to the bi-compartmented Petri plates, a tri-compartmented *in vitro* culture setup was developed only for *R. irregularis* MUCL 41833. In this system, the roots were paired with the AM fungus in one compartment (referred to as the root compartment - RC). From this RC, the ERM extended into two adjacent compartments (referred to as the hyphal compartments - HC). The compartment containing the root culture was supplied with MSR, whereas the two hyphal compartments contained MSR without sucrose and vitamin (MSR^{min}) and were solidified with agarose (HC^{solid}). In these HCs, only the ERM of the fungus was allowed to grow ($HC^{solid+Ri}$), while the roots were confined to the RC (**Figure 3-19 A**). When necessary, roots that crossed the plastic barrier into the HC were either redirected back into RC to prevent them from growing into the hyphal compartment.

7.2.3 Root and hyphae colonization by *B. velezensis in vitro*

After 4 weeks of growth, the ERM in the $HC^{solid+Ri}$ or transformed roots in the $HC^{Solid+Dc}$ treatments were inoculated with *B. velezensis* GFP-tagged and colonization of hyphae or roots was monitored by microscopy. To do so, the bacterial cells were precultured overnight in liquid root exudates mimicking exudates of Solanaceae (RE) (Nihorimbere et al., 2012) medium under shaking (180 rpm). The cells were then washed twice with physiological water (NaCl 0.9%, w/v) and bacterial concentration was adjusted to 7.5×10^8 CFU ml^{-1}. A single *R. irregularis* hyphae or root of *D. carota* was inoculated with one drop of 1 µl of bacterial suspension. The colonization of GA1 GFP-tagged was monitored at regular intervals. Microscopic composite pictures were obtained by epifluorescence microscopy to determine the speed of bacterial colonization along hyphae or roots of *D. carota*. The speed of colonization was quantified by measuring the distance travelled by *B. velezensis* from the inoculation drop divided by the day post inoculation (dpi). The quantification was performed from the biological material of minimum 7 plates (biological replicates) at 3, 7 and 14 dpi.

Microscopy imaging was performed using a Nikon Ti2-E inverted microscope (Nikon, Japan) equipped with ×20/0.45 NA S Plan Fluor objective lenses (Nikon, Switzerland) and a Nikon DS-Qi2 monochrome microscope camera. Images and videos taken in the bright field channel were acquired using a Ti2 Illuminator-DIA and an exposure time of 20 ms. *B. velezensis* GFP-tagged was visualized by conventional epifluorescence microscopy. A lumencor sola illuminator (Lumencor, USA) was used as source of excitation with an exposure time of 500 ms and the GFP-B HC Bright-Line Basic Filter was used.

7.2.4 Velocity of cytoplasmic flow

The velocity of cytoplasmic flow inside hyphae of *R. irregularis*, colonized or not by *B. velezensis,* was measured at 3, 7 and 14 dpi of the bacterium or for the control, by capturing videos in the bright field channel as described in section "Root and hyphae colonization by *B. velezensis in vitro*". The inoculation of hyphae by *B. velezensis* or GA1 mutants was also performed as previously described in section "Root and hyphae colonization by *B. velezensis in vitro*". The control treatment involved treating non-colonized hyphae with 1 µl of physiological water. The velocity of cytoplasmic flow colonized by *B. velezensis* mutants was evaluated only at 7 dpi. The cytoplasmic flow velocity of *R. irregularis* was also quantified in the presence of pure surfactin. Hyphae of *R. irregularis* were inoculated with 1 µl of pure surfactin solubilized by sonication in PBS at 2 µM, 20 µM or 50 µM concentration. A control treatment with only 1 µl PBS was included.

To investigate the impact of surfactin on the distal regions of the *R. irregularis* ERM network away from direct contact with the lipopeptide, a second experiment was conducted using a three-compartment Petri plate system. One of the two hyphal compartments was treated (the Treated compartment), either with a pure surfactin solution at 2 µM ($HC^{solid+Ri+srf}$) or PBS ($HC^{solid+Ri+PBS}$). The second hyphal compartment remained untreated but was labelled according to its proximity to the treated compartment, either with surfactin ($HC^{solid+Ri-srf}$) or with PBS ($HC^{solid+Ri-PBS}$). These three compartments were separated by plastic barriers, preventing direct physical connections between them. However, the fungal ERM network itself remained continuous and interconnected through the root compartment. The velocity of cytoplasmic flow in *R. irregularis* was quantified in each one of the HC.

For all experiments, measurements were conducted on a minimum of 4 plates (biological replicates) in which minimum 4 video were taken (technical replicate) following the treatment. We processed the data by Manual tracking plug-in inside the Tracking tool in the Plug-in menu in Fiji (Hammer et al., 2024; Schindelin et al., 2012; Tinevez et al., 2017). Thus, using the Manual tracking minimum 8 particles were tracked in each video. For each graph regarding the velocity, each point represents the average of four measurements in each direction, which can be considered technical replicates. Velocity was calculated for each tracked object during minimum 10 frames with the video taken with a speed of 10 fps during 10 seconds (100 frames/video), depending on how long the object could be followed. At four mycelial locations, clear evidence of bi-directional transport was detected. Consequently, we measured the velocity of cellular contents similar to particle image velocimetry (PIV) analysis, as illustrated in **Video 4** and **5**. The isolation and tracking of cellular contents were performed from DIC images.

7.2.5 Succinate dehydrogenase (SDH) activity in hyphae

Histochemical staining was performed to quantify the **succinate dehydrogenase** (SDH) activity according to the adapted procedures of Schaffer & Peterson (1993). The SDH activity of *R. irregularis* hyphae was assessed 7 and 14 dpi with *B. velezensis* ($HC^{Solid+Ri}$) and compared to hyphae non-inoculated with the bacterium (1 µl of physiological water - 0.9 % (w/v)) and to hyphae killed with formaldehyde (2 % (v/v)) (Calonne et al., 2014). The inoculation of hyphae by *B. velezensis* was performed as previously described in section "Root and hyphae colonization by *B. velezensis in vitro"*. The AM fungal hyphae developing on the surface of the MSRmin medium in the $HC^{Solid+Ri}$ treatment were harvested with a needle. Briefly, hyphae were immersed in a solution containing 0.2 M Tris-HCl pH 7.4, 1 M sodium succinate hexa-hydrate, 1 mg ml^{-1} nitro blue tetrazolium (NBT) and 5 mM $MgCl_2$. The SDH, present in viable fungal hyphae, reacts with NBT and is reduced to a dark blue-violet formazan compound. The hyphae were washed with 1 ml of physiological water (0.9 % (w/v)). A second staining, was performed with fuchsin acid (0.1% (v/v)) to obtain better contrast. The samples were then cleaned in a solution of lactoglycerol. Pictures of the stained hyphae were taken in the brightfield channel by stereomicroscopy. A Nikon SMZ1270 stereomicroscope (Nikon, Japan) equipped with a Nikon DS-Qi2 monochrome microscope camera and a DS-F 2.5 F-mount Adapter 2.5× was used. The stereomicroscope was used with an ED Plan 2×/WF objective (Nikon, Switzerland) and an OCC illuminator allowing the image capture in the brightfield channel at an exposure time of 40 ms. The images were processed using Fiji (Schindelin et al., 2012) by measuring, by threshold settings, the total surface of the hyphae and the surface corresponding to potential SDH activity. The SDH activity was calculated by the following formula:

$$\text{relative dark area (\%)} = \frac{\text{dark area}}{\text{total area}} \times 100$$

The quantification was performed from the biological material of minimum 3 plates (biological replicates) where minimum 1 hyphae has been harvested by plate (technical replicate).

7.2.6 Impacts of BSMs on AM fungal hyphae

The impact of lipopeptides of *B. velezensis* (i.e. surfactin, iturin and fengycin) was tested on hyphae integrity. The potential permeabilization of the AM fungus membrane was quantified using fluorescent intercalating propidium iodide (PI) that is not internalized by healthy cells. Four hyphae per Petri plate developing at the surface of the $HC^{Solid+Ri}$ medium were exposed to one drop of 1 µl of 2 µM, 20 µM or 50 µM of iturin, surfactin or fengycin and incubated at room temperature for 30 min. Ten

µl of PI solution at 50 µg ml^{-1} was then applied on each hyphae for 15 min at room temperature in the dark. The stained hyphae were visualized by fluorescence microscopy (Nikon Ti2-E) with appropriate filters (TexasRed HC BrightLine Basic Filter). A PBS solution (Control) and a positive control in which hyphae were treated with 1% Triton X-100 with 2% formaldehyde (Killed) were considered. PI fluorescence was quantified using NIS-Element AR software (Nikon, Japan). The membrane permeabilization was assessed by threshold settings to obtain the region of interest (ROI) within the images taken in the bright field channel corresponding to hyphae area. Within this ROI, the mean of red intensity (MeanRed), equivalent at the arithmetic mean of pixel intensities, was quantified in the images taken in the red channel. The experiment was performed in 3 biological replicates (3 Petri plates) per treatment.

7.2.7 Bacterial CFU counting *in vitro*

The colonization density of *B. velezensis* GA1 GFP-tagged on *D. carota* transformed roots ($HC^{solid+Dc}$), *R. irregularis* hyphae ($HC^{solid+Ri}$) and *S. tuberosum* roots ($HC^{solid+St}$) was quantified. Bacterial inoculation was performed as previously described in the section "Root and hyphae colonization by *B. velezensis in vitro* ". The colonization density of roots and hyphae as well as spores produced by the bacteria were evaluated at 3, 7 and 14 dpi of *B. velezensis* for AM fungal hyphae and roots of *D. carota*, while for *S. tuberosum* roots, it was performed at 14 dpi. Colonization was evaluated on 2 cm of roots or AM fungal hyphae proximal of the inoculation drop area. Bacterial cells were detached from roots and hyphae by vortexing them for 5 min in a solution of physiological water supplemented with 0.1% (vol/vol) Tween 80 and 6 glass beads. To evaluate the number of bacterial spores, half of each solution was incubated at 80°C during 25 min to kill all vegetative cells. The colonies were counted by performing serial dilutions plated onto LB medium solidified with 14 g l^{-1} of agar. Plates were incubated for 12 h at 30°C. The quantification was performed from the biological material of minimum 4 replicates (i.e. plates) divided into 3 sample for each treatment. The results were expressed following the available area provided by each host depending of the sampling length (2cm) and of the average diameter of each host (**Figure 7-4**). This approach allows to evaluate bacterial colonization for the same length of sample and according to the colonizable surface area for each host.

Likewise, the colonization density of *B. velezensis* GA1 GFP-tagged on *R. clarus, R. aggregatus* and *R. intraradices* was evaluated also at 7 dpi. The colonization of the different mutants (ΔituA-ΔfenA, ΔsrfaA, ΔsrfaA-fenA, ΔsrfaA-ΔituA, ΔsrfaA-ΔituA-ΔfenA and Δsfp) were evaluated only on *R. irregularis* MUCL 41833.

7.2.8 *B. velezensis* biofilm formation along AM fungal hyphae of *R. irregularis*

To evaluated the formation of biofilm by *B.velezensis* on AM fungal hyphae of *R. irregularis*, we assessed the colonization density of *B. velezensis* GA1-GFP tagged and the knockout mutants Δ*epsA-O* and Δ*tasA*, as previously described. The growth of these mutants was tested to confirm that the mutations did not impact growth. To further validate this, we monitored the continuous growth kinetics of *B. velezensis* WT and knockout mutants in RE medium using 96-well microplates. First, a pre-culture of *B. velezensis* and of mutants were prepared at 30°C in liquid RE medium under shaking (180 rpm) overnight. The pre-cultures were washed twice with physiological water (0.9% w/v NaCl). The bacterial suspensions were then adjusted to an OD_{600} of 0.05 in the 96-well microplate, with a final volume of 200 µl per well. The growth kinetics of B. velezensis WT and mutants (OD_{600}) were monitored every hour for 36 h using a Tecan Spark automatic plate reader (Tecan Group Ltd, Männedorf, Switzerland) under continuous shaking at 30°C (**Figure 7-5**). By this ways, we verified that the two mutants are not impaired in growth as they form similar final biomass and growth kinetics compared to the wild type upon cultivation in liquid medium.

7.2.9 *B. velezensis* metabolite production along AM fungal hyphae

Metabolites produced by *B. velezensis* GA1 GFP-tagged developing in contact with hyphae were extracted and analysed by LC-MS. As previously described in the section "Root and hyphae colonization by *B. velezensis in vitro* ", *B. velezensis* was inoculated on the surface of hyphae in the HC ($HC^{Solid+Ri}$). After 9 days, a plug of agarose gel (0.5 cm × 2.5 cm) containing *R. irregularis* hyphae and the bacterium was sampled. BSMs were extracted via the application of 400 µl of acetonitrile (ACN) (75 %, vol/vol) during 30 min. Then, the extract was filtered with hydrophilic PTFE syringe filters ROCC S.A. (0.22 µm pore size) before UPLC-qTOF MS analysis.

Briefly, the extracts were analysed using a Agilent 1290 Infinity II apparatus coupled with a diode array detector and mass detector (Jet Stream ESI-Q-TOF 6530) with the parameters: capillary voltage: 3.5 kV; nebulizer pressure: 35 psi; drying gas: 8 l min-1; drying gas temperature: 300°C; flow rate of sheath gas: 11 l min-1 sheath gas temperature: 350 °C; fragmentor voltage: 175 V; skimmer voltage: 65 V; octopole RF: 750 V. Accurate mass spectra were recorded in positive mode in the range of m/z =100–1700. Metabolites (injection volume, 10 µl) were separated on C18 Acquity UPLC BEH column (2.1 × 50 mm × 1.7 µm; Waters, milford, MA, USA) and elution was performed as follows: acetonitrile and distilled water as solvents (both supplemented with 0.1% (vol/vol) formic acid), a flow rate of 0.6 ml min^{-1} and gradient over 20 min (programme: initial 10% (vol/vol) acetonitrile during 1 min before increase to 100% (vol/vol) over 20 min, held at 100% (vol/vol) for 3.5 min. The identified BSMs were quantified by their peak area values using MassHunter

v10.0 workstation. The cLPs were quantified based on their retention times and accurate masses compared with pure molecule standards.

The relative proportion of the detected cLPs was then calculated by following formula:

$$\text{Relative lipopeptide proportion (\%)} = \frac{\text{Lipopeptide area (One family)}}{\text{Lipopeptides total area (All families)}} \times 100$$

7.2.10 *B. velezensis* metabolite production on *R. irregularis* exudates

The metabolite production of *B. velezensis* grown on *R. irregularis* exudates was analysed by LC-MS. To observe the effect of *R. irregularis* exudates on the BSMs production of GA1, the ERM of *R. irregularis* was cultivated on MSR $^{\text{min-1/2}}$ liquid medium ($HC^{Liquid+Ri}$). After 4 weeks of *R. irregularis* growth, the liquid medium was collected and hyphal exudates of 5 different plates were grouped. At least 15 hyphal exudate solutions from 15 individual plates were grouped in 3 distinct solutions. The exudates harvested were freeze-dried (Freeze-dryer Alpha 3-4 LSCbasic brand Christ), resuspended and concentrated 5 times with a solution containing MOPS buffer (10.5 g l^{-1}) and $(NH_4)_2SO_4$ (1 g l^{-1}). The exudates concentrated 5 times were sterilized with CA syringe filters ROCC S.A. (0.22 µm pore size).

Then, the continuous growth kinetics of *B. velezensis* in AM fungal exudates was followed in 96 wells microplates. First, a pre-culture of *B. velezensis* was done at 30°C in liquid RE medium (Nihorimbere et al., 2012) under shaking (180 rpm) overnight. The preculture was washed twice with physiological water (Na Cl 0.9 % w/v). The bacterial suspension was adjusted to obtain an OD_{600} of 0.05 into the 96 wells microplate in a final volume of 200 µl per well. The growth of *B. velezensis* was measured in 5 times concentrated exudates of *R. irregularis*. The growth kinetics of *B. velezensis* (OD_{600}) was followed every hour during 36 h on a Tecan Spark automatic plate reader (Tecan Group Ltd, Männedorf, Switzerland) under continuous shaking at 30°C. To study the effect of hyphal exudates on the GA1 metabolome, 3 wells of each condition were grouped, filtered (0.22 µm) and then analysed by LC-MS as previously described in the section "*B. velezensis* metabolite production along AM fungal hyphae". At least 3 distinct concentrated hyphal solutions (biological replicates) were inoculated with minimum 2 distinct *B. velezensis* precultures.

7.2.11 *B. velezensis* metabolite production on carbohydrate compounds present in *R. irregularis* exudates

The influence of carbohydrate compounds in the hyphal exudates of the AM fungus, often reported in the literature, was evaluated on BSMs production of GA1 WT. The

carbon sources of AM fungus exudates individually and collectively (10 mM of fructose, glucose, inositol, citric acid, 5 mM trehalose and 15 mM succinic acid) were solubilized in M9 minimal salts medium (KH_2PO_4 3 g l^{-1}; NaCl 0.5 g l^{-1}; Na_2HPO_4 6.78 g l^{-1}; NH_4Cl 1 g l^{-1}) supplemented with 2 mM $MgSO_4$, 0.1 mM $CaCl_2$, 10 µM $FeSO_4$ and buffered at pH 6.8 with MOPS (10.5 g l^{-1}) forming the so-called Arbuscular Mycorrhizal Fungi Exudate Mimicking Medium (AMF-EMM) when the carbon sources are put together. The metabolite production of GA1 was followed as previously described in the section "*B. velezensis* metabolite production along AM fungal hyphae". The experiment was performed in 3 biological replicates (3 precultures of *B. velezensis*) with minimum 4 technical replicates for each biological replicate.

7.2.12 *B. velezensis* metabolite production and development in presence of Myc-Lipochitooligosacharides (LCOs)

Pure Myc-LCOs (see Figure 3-16) were provided by Dr. Sébastien Fort (CNRS Senior Scientist, CERMAV Laboratory). The various LCOs were solubilized in ultrapure water and mixed in equimolar proportions to obtain a final concentration of 1×10^{-8} M. This stock solution was used to assess the influence of Myc-LCOs on *B. velezensis* metabolite production, growth, and biofilm formation.

To evaluate the effects of Myc-LCOs on *B. velezensis* growth and metabolome, a pre-culture was first prepared by incubating the bacterium overnight at 30 °C in RE medium under shaking (180 rpm). The culture was then washed twice with sterile physiological water (0.9% NaCl, w/v). Cells were inoculated to OD_{600} = 0.05 into AMF-EMM medium, either untreated (control) or supplemented with 1% (v/v) of the LCO mix or *R. irregularis* exudates (1% v/v). OD_{600} was measured hourly, and culture supernatants were collected, filtered (0.22 µm), and analysed by LC-MS to quantify lipopeptide production, following the procedure described in the section "*B. velezensis* metabolite production along AM fungal hyphae." A minimum of three biological replicates were performed, each using a distinct *B. velezensis* pre-culture.

To assess the impact of Myc-LCOs on biofilm formation, a standard crystal violet assay was performed. B. velezensis was inoculated into 96-well microplates containing 200 µL of AMF-EMM, supplemented or not with 0.1% (v/v) of the LCO mix. Plates were incubated for 24 h at 30 °C without shaking. After incubation, planktonic cells were removed and wells were gently washed with PBS. The attached biofilm was stained with 0.1% (v/v) crystal violet for 10 minutes, washed three times with PBS, and the stain was solubilized with 30% (v/v) acetic acid. Absorbance was measured at 595 nm to quantify total biofilm biomass.

7.2.13 *B. velezensis* antimicrobial activity assays on hyphal exudates

Antimicrobial activity of GA1 wild type (WT) or GA1 mutant cell-free supernatants (CFS) produced on hyphal exudates of *R. irregularis* was assessed against *Trichoderma harzianum* Rifai MUCL 29707 and *Collimonas fungivorans* LMG 21973. To do so, GA1 WT and its mutants (Supplementary Table 1) were cultivated on exudates of *R. irregularis* as describe in section "*B. velezensis* metabolite production on R. irregularis exudates". The CFS of these cultures were obtained by centrifugation of the bacterial culture at 10000 rpm and sterilization with a PTFE syringe filters ROCC S.A. (0.22 µm pore size).

To observe the effects of GA1 WT or GA1 mutant CFS on the growth of *T. harzianum,* fungal spores were harvested from 10 days old PDA cultures and suspended at a concentration of 2×105 CFU mL-1 with physiological water supplemented with 0.1% (vol/vol) Tween 80. Ten µl of fungal spores were then resuspended into a 96 wells microplates with final volume of 200 µl / wells adjusted with PDB medium supplemented with 20% (vol/vol) of GA1 WT or GA1 mutant CFS. The control was complemented with physiological water supplemented with 0.1% (vol/vol) Tween 80. The growth kinetics of *T. harzianum* (OD_{600}) was followed every hour during 36 h with a Tecan Spark automatic plate reader (Tecan Group Ltd, Männedorf, Switzerland) under continuous shaking at 26°C. Three independent assays, each involving minimum 4 technical replicates, were performed.

To evaluate the impact of CFS on the growth of *C. fungivorans*, a bacterial suspension of this bacterium was prepared by centrifuging the overnight preculture, washing the cells twice, and resuspending them in physiological water. The bacterial suspension was adjusted to obtain an OD_{600} of 0.05 into the 96 wells microplate, with a final volume of 200 µl / well-adjusted with TSA medium (Sigma-Aldrich, India) supplemented with 20% (vol/vol) of GA1 WT or GA1 mutant CFS. The control was complemented with physiological water. The growth kinetics of *C. fungivorans* (OD_{600}) was followed every hour during 24 h on a Tecan Spark automatic plate reader (Tecan Group Ltd, Männedorf, Switzerland) with continuous shaking at 26°C. Three independent assays each involving 6 technical replicates were performed.

7.2.14 Translocation of surfactin via the AM fungal network

The transport of surfactin across the fungal network was assessed using the tri-compartment Petri plate system, as described in section "Velocity of Cytoplasmic Flow". To investigate the effectiveness of AM fungal hyphae in transporting surfactin, 10 ml of a 20 µM surfactin solution we applied to one of the hyphal compartments, covering the entire compartment (referred to as $HC^{solid+Ri+srf}$). To determine whether surfactin was translocated through the ERM, a control experiment was conducted in which the *R. irregularis* ERM network was cut before the surfactin application along the entire length of the compartment and on 0.5 cm of width, creating an air gap in the non-inoculated compartment. Subsequently, we collected the medium from the treated

and the non-treated hyphal compartments. After extraction, the surfactin contents in each hyphal compartment were determined by LC-QTOF MS analysis of the surfactin contents of each hyphal compartment, following the procedures outlined in section "*B. velezensis* Metabolite Production Along AM Fungal Hyphae". This experiment was carried out in 3 biological replicates, with 3 plates for each condition.

7.2.15 Visualization of surfactin translocation by *R. irregularis* using MSI

To assess the long-distance transport of surfactin by the AM fungus, we employed the tri-compartment Petri plate system described previously (see section "Velocity of Cytoplasmic Flow"). A portion of the untreated hyphal compartment ($HC^{solid+Ri\text{-}srf}$), located distal from the surfactin application zone, was excised for mass spectrometry imaging (MSI) analysis. Prior to MSI, the ERM was imaged using large-field brightfield microscopy, as detailed in the section "Root and Hyphae Colonization by *B. velezensis in vitro*." The selected hyphal network was gently cut from the agar and transferred to microscope slides (VWR, USA). After the sample was transferred on another slide pre-coated with double-sided conductive copper tape (3M). Slides were then dried for 2 hours at 40°C. A matrix of α-Cyano-4-hydroxycinnamic acid (CHCA) was prepared at 5 mg/mL in 80:20 acetonitrile/water with 0.1% formic acid and applied using a SunChrom matrix sprayer. The spraying protocol consisted of four cycles with incremental flow rates: 10 µL/min (1st layer), 20 µL/min (2nd), 30 µL/min (3rd), 40 µL/min (4th), and 60 µL/min for the final three layers. Track speed and spacing were set to 800 mm/min and 2 mm, respectively. MSI data were acquired using a Solarix XR 9.4T FT-ICR mass spectrometer (Bruker Daltonics, Bremen, Germany) with a pixel size of 200 µm. External calibration was performed with red phosphorus in acetone, achieving a mass accuracy better than 0.2 ppm in the 150–1600 m/z range. Spectra acquisition was carried out using FlexImaging v5 software (Bruker), with each spectrum obtained from 20 laser shots (200 Hz repetition rate, 14% power, small beam focus). Resulting data were processed and visualized using SCiLS Lab 2016b to generate mass distribution maps of surfactin ions across the fungal network.

7.2.16 Experimental design of greenhouse trial for *B. velezensis* common mycorrhizal network colonization

Two 500 ml pots, referred as Pot 1 and Pot 2, were connected by a 4.5 cm diameter pipe made of HDPE (High-density polyethylene) (Figure 2-17 A). Both ends of the tube were sealed with a nylon mesh of 50 µm porosity to prevent the passage of plant roots from one pot to the other. Each pot contained a sterile mixture of sand/vermiculite/loam (45%:45%:10%, v/v/v). One 20 day-old *S. tuberosum* plantlet grown *in vitro* was planted in each pot. Prior to the planting, 8 plants in pot 1 were inoculated with 10 g of *R. irregularis* inoculum (+ R.i.). The inoculum was obtained

by associating isolated spores from an *in vitro* culture of the AM fungus with maize plants (*Zea mays* L. cultivar ES Ballade) grown in sterilized lava stone (DCM, Belgium) for 4 months. The total root colonization by *R. irregularis* MUCL41833 reached 88%. The roots and the rhizospheric substrate attached to these plants were homogenized and used as *R. irregularis* inoculum (Garcés-Ruiz et al., 2017; Gbongue et al., 2019). Additionally, 8 other plants of pots 1 were inoculated with 10 g of autoclaved (121°C for 15 min) *R. irregularis* inoculum (- R.i.). The plants were grown in greenhouse at 25 °C with a RH of 75% and a 16/8 h (day/night) photoperiod under a PPF of 120 mmol s^{-1} m^{-2}. The plants were watered once a week with distilled water and fertilized once a week with Hoagland nutrient solution impoverished in phosphorus (Hoagland-P) 103. After 3 months of growth, each plant in pot 1 was inoculated with 50 ml of a bacterial suspension of *B. velezensis* GA1 GFP-tagged. This suspension was prepared by centrifuging an overnight culture (RE medium, 26°C), washing the cells twice, and resuspending them in Hoagland-P to a cellular density of 5×10^8 CFU ml^{-1}. The 16 uninoculated plants in pots 2 were treated with 50 ml of Hoagland-P solution without any microorganisms. The colonization of *R. irregularis* and *B. velezensis* on the roots of plants in pots 1 and in pots 2 were quantified 20 days after the inoculation of *B. velezensis* as described in section "Microbial root colonization under greenhouse trials".

7.2.17 Effect of *B. velezensis* colonization on AM fungal population under greenhouse trial

The potential influence of the bacterial colonization on the *R. irregularis* population was evaluated under greenhouse conditions. Briefly, 16 pots were inoculated with 5 g of *R. irregularis* inoculum as previously described in section "Experimental design of greenhouse trial for *B. velezensis* common mycorrhizal network colonization". At the same time, a sterilized seed of tomato cv Money Makers was sown in each pot. The plants were grown in greenhouse at 25 °C with a RH of 75% and 16/8 h (day/night) photoperiod under a PPF of 120 mmol s^{-1} m^{-2}. The plants were watered once a week with distilled water and fertilized once a week with Hoagland-P. After 5 months, to observe the effect of *B. velezensis* on *R. irregularis* population, 8 pots containing plants were watered with 50 ml of a bacterial solution of GA1 GFP-tagged as previously described (B.v.+ R.i.). The remaining pots were watered with 50 ml of Hoagland-P solution without *B. velezensis* (R.i.). The colonization of *R. irregularis* and *B. velezensis* on the roots of plants for each condition was quantified before the bacterial inoculation and 7 days after the inoculation of *B. velezensis* as described in section "Microbial root colonization under greenhouse trials"

7.2.18 ISR induction in tomato plants under greenhouse condition

Sterilized Ailsa Craig and MoneyMakers seeds were transferred to 1 l pots containing a sterile substrate of sand/vermiculite/loam (45%:45%:10%,v/v/v). For

each treatment, 16 pots were used. Each one of the 16 pots was supplemented with 5 g of *R. irregularis* inoculum containing AM fungal-colonized roots and spores (R.i.) prepared as previously described in section "Experimental design of greenhouse trial for *B. velezensis* common mycorrhizal network colonization". The inoculation of tomato plants with *R. irregularis* was done by mixing the substrate with the AM fungal inoculum prior to sowing.

Likewise, 16 plants were watered with 10 ml of a bacterial solution (B.v.) as described in section "Experimental design of greenhouse trial for *B. velezensis* common mycorrhizal network colonization". Additionally, 16 pots were co-inoculated with both the bacteria and the AM fungus (R.i. +B.v.) as described for the treatment with one microorganism. A second bacterial application was performed after 12 weeks of plant growth by inoculating the plants with 10 ml of a bacterial solution at the same concentration. A control group composed of 16 non-inoculated plants and supplemented with the same amount (5 g) of AM fungal sterilized (121°C for 15 min) inoculum substrate was treated with Hoagland-P solution without the bacterial solution. The plants were grown in the greenhouse at 20 °C with a RH of 75% and 16/8 h (day/night) photoperiod under a PPF of 120 mmol s^{-1} m^{-2} for 3 months. They were watered once a week with non-sterilized distilled water and were also fertilized once a week with Hoagland-P. The pots were arranged in a fully randomized design.

At week 13, the plants were infected with *B. cinerea* MUCL 43839. Prior to infection, the size of the plants was measured to assess the impact of the combined treatment on plant growth compared to the control plants (n = 16/treatment). *B. cinerea* was routinely cultured on potato dextrose agar at 26°C from a spore suspension stored at -80°C. *B. cinerea* spores were collected from 15 days-old cultures in physiological water containing 0.01% Tween 20. The spore suspension was then filtered (Whatman, Grade1), quantified and adjusted to a concentration of 5×10^6 spores ml^{-1}. Infection was performed by applying 10 µl droplets of the spore suspension onto 5 leaflets of the third, fifth and sixth leaves of each plant (15 infected leaflets/plant). The disease severity of *B. cinerea* on tomato leaves was assessed 14 dpi for Ailsa craig plants and 7 dpi for MoneyMaker plants by measuring the lesion area using ImageJ (n = 8/treatment). The colonization of *R. irregularis* and *B. velezensis* in the combined treatment (B.v. + R.i.) was quantified at 14 and 21 dpi after the second GA1 treatment (n = 8/times) as described below.

Using the experimental system described in section "Experimental design of greenhouse trial for *B. velezensis* common mycorrhizal network colonization", we evaluated the plant protection potential of surfactin when applied to the ERM of *R. irregularis*.

Tomato seeds (*S. lycopersicum* cv. Ailsa Craig) were surface-sterilized and were transferred to Pot 1 of a two-Pot system. Half of the plants were inoculated with *R. irregularis* as described in section "Experimental design of greenhouse trial for *B. velezensis* common mycorrhizal network colonization". The other half served as a non-mycorrhized control and received 5 g of sterilized AM fungal inoculum (autoclaved at 121 °C for 15 min). No plant was placed in Pot 2, which was separated by a mesh allowing only fungal hyphae, but not roots, to cross between the compartments. Plants were cultivated in a greenhouse under controlled conditions: 20 °C, 75% RH, a 16/8 h light/dark photoperiod, and a PPF of 120 µmol s^{-1} m^{-2}. They were watered weekly with non-sterile distilled water and fertilized once a week with Hoagland solution lacking phosphate (Hoagland-P). Pots were arranged in a fully randomized design and grown for 4 months to allow for ERM development between compartments.

After 4 months, surfactin (Kaneka, Japan) was applied at a 20 µM (20 mL) either directly into Pot 1 (on the roots, referred to as Pot 1 + Srf) or into Pot 2 (accessible only via the AM fungal ERM, referred to as Pot 2 + Srf). This was done in the presence or absence of *R. irregularis* in Pot 1. Control treatments received the same volume of Hoagland-P solution applied to either Pot 1 or Pot 2 (see Figure 4-6). Seven days after surfactin application, plants in Pot 1 were infected with *Botrytis cinerea* as previously described. Disease severity was assessed 14 days post-infection by measuring necrotic lesion size on tomato leaves using ImageJ (FIJI).

7.2.19 Microbial root colonization under greenhouse trials

To determine *B. velezensis* (B.v.)colonization, bacterial cells were detached from samples of 1 g of roots including attached rhizospheric substrate samples by vortexing for 5 min in a solution of physiological water supplemented with 0.1% (vol/vol) Tween 80 and 6 glass beads. The colonies were counted by performing serial dilutions plated onto LB medium supplemented with chloramphenicol 5 µg l^{-1}. Plates were incubated for 12 h at 30 °C, and the results were expressed as the number of CFU of B.v. g^{-1} of sample.

To determine the mycorrhizal status of the plants, roots with attached rhizospheric substrate were sampled to quantify the presence of *R. irregularis* by qPCR. Frozen roots were crushed in liquid nitrogen, and DNA was extracted from a 500 mg crushed root sample using GenEluteTM Soil DNA Isolation kit (Sigma-Aldrich, Canada) with slight modifications. Prior to extraction, a lysis step was performed using DNAzol™ Reagent under shaking and homogenization with FastPrep-24™ (MP Biomedical's, Germany). The concentration and purity of the extracted DNA were assessed with the UV-vis spectrophotometer NanoDrop 2000 (Thermo scientific). qPCR was performed in an ABI StepOne™ qPCR apparatus (Applied Biosystems) using the kit Luna® Universal qPCR Master Mix Kit (New England Biolabs, Ipswich, MA, United States).

PCRs were conducted in a total volume of 20 µl containing 10 µl of Luna Universal qPCR Mix, 0.5 µl of each primer (10 µM) and 5 µl of DNA. The qPCR protocol consisted of an initial denaturation step at 95°C (1 min), followed by 40 cycles of denaturation (95°C, 15 s) and extension (60°C, 30 s). Melting curves were also generated from 65 to 95°C with an increase rate of 0.5°C/ 5 s to evaluate the specificity of the amplified products. The strain-specific primer pair for R. irregularis MUCL41833 targeting the mtLSU region was used: forward 5'-AAGTCCTCTAGGTCGTAGCA-3' and reverse 5'-ACAGGTATTTATCAAATCCTTCCC-3'. The resulting concentrations were expressed as mg of R.i. g-1 of sample. The quantification of *R. irregularis* was performed based on the standard calibration curves (**Figure 7-6**). To prepare standards for the qPCR experiment, DNA extracted from *R. irregularis* spores and mycelium grown *in vitro* were used. Spores/mycelium of 3 months old cultures were extracted from HC following solubilization of the phytagel with citrate-buffer. Five mg of spores/mycelium were quantified and lysed with DNAzoleTM. A serial 4-fold dilutions of the lysed extraction with DNAzole (5×10^{-1}–10^{-4} mg µl−1) was performed prior to the DNA extraction, following the same procedure described above for roots.

7.2.20 Statistical analyses

Data were processed using GraphPad Prism 9.2.0 software to perform statistical analysis. The impact of factors (experiments, treatments, biological materials and dpi) on variability were considered in the statistical general analyses to analyse repeated measure experiments. Differences were considered statistically significant at $p < 0.05$.

Chapter 8

References

Abdallah, D. Ben, Krier, F., Jacques, P., Tounsi, S., & Frikha-Gargouri, O. (2020). *Agrobacterium tumefaciens* C58 presence affects *Bacillus velezensis* 32a ecological fitness in the tomato rhizosphere. *Environmental Science and Pollution Research*, *27*(22), 28429–28437. https://doi.org/10.1007/s11356-020-09124-1

Abeysinghe, G., Kuchira, M., Kudo, G., Masuo, S., Ninomiya, A., Takahashi, K., Utada, A. S., Hagiwara, D., Nomura, N., Takaya, N., Obana, N., & Takeshita, N. (2020). Fungal mycelia and bacterial thiamine establish a mutualistic growth mechanism. *Life Science Alliance*, *3*(12), e202000878. https://doi.org/10.26508/lsa.202000878

Acharya, S. M., Yee, M. O., Diamond, S., Andeer, P. F., Baig, N. F., Aladesanmi, O. T., Northen, T. R., Banfield, J. F., & Chakraborty, R. (2023). Fine scale sampling reveals early differentiation of rhizosphere microbiome from bulk soil in young *Brachypodium* plant roots. *ISME Communications*, *3*(1). https://doi.org/10.1038/s43705-023-00265-1

Agnolucci, M., Battini, F., Cristani, C., & Giovannetti, M. (2015). Diverse bacterial communities are recruited on spores of different arbuscular mycorrhizal fungal isolates. *Biology and Fertility of Soils*, *51*(3), 379–389. https://doi.org/10.1007/s00374-014-0989-5

Ahmad, M., Liu, Y., Huang, S., Huo, Y., Yi, G., Liu, C., Jamil, W., Yang, X., Zhang, W., Li, Y., Xiang, D., Huoqing, H., Liu, S., Wang, W., & Li, C. (2024). Isolation, Characterization, and Proteomic Analysis of Crude and Purified Extracellular Vesicles Extracted from *Fusarium oxysporum f. sp. cubense*. *Plants*, *13*(24), 3534. https://doi.org/10.3390/plants13243534

Akinola, S., Ayangbenro, A., & Babalola, O. (2021). Metagenomic Insight into the Community Structure of Maize-Rhizosphere Bacteria as Predicted by Different Environmental Factors and Their Functioning within Plant Proximity. *Microorganisms*, *9*(7), 1419. https://doi.org/10.3390/microorganisms9071419

Akiyama, K., Ogasawara, S., Ito, S., & Hayashi, H. (2010). Structural Requirements of Strigolactones for Hyphal Branching in AM Fungi. *Plant and Cell Physiology*, *51*(7), 1104–1117. https://doi.org/10.1093/pcp/pcq058

Al-Ali, A., Deravel, J., Krier, F., Béchet, M., Ongena, M., & Jacques, P. (2018). Biofilm formation is determinant in tomato rhizosphere colonization by *Bacillus velezensis* FZB42. *Environmental Science and Pollution Research*, *25*(30), 29910–29920. https://doi.org/10.1007/s11356-017-0469-1

Alamri, S. A. (2015). Enhancing the efficiency of the bioagent *Bacillus subtilis* JF419701 against soil-borne phytopathogens by increasing the productivity of fungal cell wall degrading enzymes. *Archives Of Phytopathology And Plant Protection*, *48*(2), 159–170. https://doi.org/10.1080/03235408.2014.884671

Alaux, P.-L., Naveau, F., Declerck, S., & Cranenbrouck, S. (2020). Common Mycorrhizal Network Induced JA/ET Genes Expression in Healthy Potato Plants Connected to Potato Plants Infected by *Phytophthora infestans*. *Frontiers in Plant Science*, *11*. https://doi.org/10.3389/fpls.2020.00602

Alenezi, F. N., Slama, H. Ben, Bouket, A. C., Cherif-Silini, H., Silini, A., Luptakova, L., Nowakowska, J. A., Oszako, T., & Belbahri, L. (2021). *Bacillus velezensis*: A Treasure House of Bioactive Compounds of Medicinal, Biocontrol and Environmental Importance. *Forests*, *12*(12), 1714. https://doi.org/10.3390/f12121714

Allard-Massicotte, R., Tessier, L., Lécuyer, F., Lakshmanan, V., Lucier, J.-F., Garneau, D., Caudwell, L., Vlamakis, H., Bais, H. P., & Beauregard, P. B. (2016). *Bacillus subtilis* Early Colonization of *Arabidopsis thaliana* Roots Involves Multiple Chemotaxis Receptors. *MBio*, *7*(6). https://doi.org/10.1128/mBio.01664-16

Allen, M. F. (2007). Mycorrhizal Fungi: Highways for Water and Nutrients in Arid Soils. *Vadose Zone Journal*, *6*(2), 291–297. https://doi.org/10.2136/vzj2006.0068

Almoneafy, A. A., Kakar, K. U., Nawaz, Z., Li, B., Saand, M. A., Chun-lan, Y., & Xie, G.-L. (2014). Tomato plant growth promotion and antibacterial related-mechanisms of four rhizobacterial *Bacillus* strains against *Ralstonia solanacearum*. *Symbiosis*, *63*(2), 59–70. https://doi.org/10.1007/s13199-014-0288-9

Anckaert, A., Arguelles Arias, A., Hoff, G., Calonne-Salmon, M., Declerck, S., Agro-Bio Tech, G., Arias, A. A., Hoff, G., Calonne-Salmon, M., Declerck, S., & Ongena, M. (2021). The use of *Bacillus* spp. as bacterial biocontrol agents to control plant diseases. In R. W. Köhl J (Ed.), *Microbial bioprotectants for plant disease management* (Issue November, pp. 247–300). Burleigh Dodds Science Publishing. https://doi.org/10.19103/AS.2021.0093.10

Andrić, S., Meyer, T., & Ongena, M. (2020). *Bacillus* Responses to Plant-Associated Fungal and Bacterial Communities. *Frontiers in Microbiology*, *11*, 550488. https://doi.org/10.3389/fmicb.2020.01350

Andrić, S., Meyer, T., Rigolet, A., Prigent-Combaret, C., Höfte, M., Balleux, G., Steels, S., Hoff, G., De Mot, R., McCann, A., De Pauw, E., Argüelles Arias, A., & Ongena, M. (2021). Lipopeptide Interplay Mediates Molecular Interactions between Soil *Bacilli* and *Pseudomonads*. *Microbiology Spectrum*, *9*(3). https://doi.org/10.1128/spectrum.02038-21

Andrić, S., Rigolet, A., Argüelles Arias, A., Steels, S., Hoff, G., Balleux, G., Ongena, L., Höfte, M., Meyer, T., & Ongena, M. (2023). Plant-associated *Bacillus* mobilizes its secondary metabolites upon perception of the siderophore pyochelin produced by a *Pseudomonas* competitor. *The ISME Journal*, *17*(2), 263–275. https://doi.org/10.1038/s41396-022-01337-1

Antonioli Júnior, R., Poloni, J. de F., Pinto, É. S. M., & Dorn, M. (2022). Interdisciplinary Overview of Lipopeptide and Protein-Containing Biosurfactants. *Genes*, *14*(1), 76. https://doi.org/10.3390/genes14010076

Aparicio Chacón, M. V., Van Dingenen, J., & Goormachtig, S. (2023). Characterization of Arbuscular Mycorrhizal Effector Proteins. *International Journal of Molecular Sciences*, *24*(11), 9125.

https://doi.org/10.3390/ijms24119125

Arnaouteli, S., Bamford, N. C., Stanley-Wall, N. R., & Kovács, Á. T. (2021). *Bacillus subtilis* biofilm formation and social interactions. *Nature Reviews Microbiology*, *19*(9), 600–614. https://doi.org/10.1038/s41579-021-00540-9

Arrebola, E., Jacobs, R., & Korsten, L. (2010). Iturin A is the principal inhibitor in the biocontrol activity of *Bacillus amyloliquefaciens* PPCB004 against postharvest fungal pathogens. *Journal of Applied Microbiology*, *108*(2), 386–395. https://doi.org/10.1111/j.1365-2672.2009.04438.x

Arthikala, M.-K., Montiel, J., Nava, N., Santana, O., Sánchez-López, R., Cárdenas, L., & Quinto, C. (2013). PvRbohB negatively regulates *Rhizophagus irregularis* colonization in *Phaseolus vulgaris*. *Plant and Cell Physiology*, *54*(8), 1391–1402. https://doi.org/10.1093/pcp/pct089

Asif, M., Li-Qun, Z., Zeng, Q., Atiq, M., Ahmad, K., Tariq, A., Al-Ansari, N., Blom, J., Fenske, L., Alodaini, H. A., & Hatamleh, A. A. (2023). Comprehensive genomic analysis of *Bacillus paralicheniformis* strain BP9, pan-genomic and genetic basis of biocontrol mechanism. *Computational and Structural Biotechnology Journal*, *21*, 4647–4662. https://doi.org/10.1016/j.csbj.2023.09.043

Augé, R. M., Toler, H. D., & Saxton, A. M. (2015). Arbuscular mycorrhizal symbiosis alters stomatal conductance of host plants more under drought than under amply watered conditions: a meta-analysis. *Mycorrhiza*, *25*(1), 13–24. https://doi.org/10.1007/s00572-014-0585-4

Averill, C., Bhatnagar, J. M., Dietze, M. C., Pearse, W. D., & Kivlin, S. N. (2019). Global imprint of mycorrhizal fungi on whole-plant nutrient economics. *Proceedings of the National Academy of Sciences*, *116*(46), 23163–23168. https://doi.org/10.1073/pnas.1906655116

Aynalem, B., Muleta, D., Jida, M., Shemekite, F., & Aseffa, F. (2022). Biocontrol competence of *Beauveria bassiana*, *Metarhizium anisopliae* and *Bacillus thuringiensis* against tomato leaf miner, *Tuta absoluta* Meyrick 1917 under greenhouse and field conditions. *Heliyon*, *8*(6), e09694. https://doi.org/10.1016/j.heliyon.2022.e09694

Babel, H., Naranjo-Meneses, P., Trauth, S., Schulmeister, S., Malengo, G., Sourjik, V., & Bischofs, I. B. (2020). Ratiometric population sensing by a pump-probe signaling system in *Bacillus subtilis*. *Nature Communications*, *11*(1), 1176. https://doi.org/10.1038/s41467-020-14840-w

Babikova, Z., Gilbert, L., Bruce, T. J. A., Birkett, M., Caulfield, J. C., Woodcock, C., Pickett, J. A., & Johnson, D. (2013). Underground signals carried through common mycelial networks warn neighbouring plants of aphid attack. *Ecology Letters*, *16*(7), 835–843. https://doi.org/10.1111/ele.12115

Bacete, L., Mélida, H., Miedes, E., & Molina, A. (2018). Plant cell wall-mediated immunity: cell wall changes trigger disease resistance responses. *The Plant Journal*, *93*(4), 614–636. https://doi.org/10.1111/tpj.13807

Bago, B., Azcon-Aguilar, C., Goulet, A., & Piché, Y. (1998). Branched absorbing

structures (BAS): a feature of the extraradical mycelium of symbiotic arbuscular mycorrhizal fungi. *New Phytologist*, *139*(2), 375–388. https://doi.org/10.1046/j.1469-8137.1998.00199.x

Bago, B., Zipfel, W., Williams, R. M., Jun, J., Arreola, R., Lammers, P. J., Pfeffer, P. E., & Shachar-Hill, Y. (2002). Translocation and Utilization of Fungal Storage Lipid in the Arbuscular Mycorrhizal Symbiosis. *Plant Physiology*, *128*(1), 108–124. https://doi.org/10.1104/pp.010466

Bakker, C., Graham, H. R., Popescu, I., Li, M., McMullin, D. R., & Avis, T. J. (2024). Fungal membrane determinants affecting sensitivity to antifungal cyclic lipopeptides from *Bacillus* spp. *Fungal Biology*, *128*(7), 2080–2088. https://doi.org/10.1016/j.funbio.2024.08.006

Baldrich, P., & Meyers, B. C. (2019). Bacteria send messages to colonize plant roots. *Science*, *365*(6456), 868–869. https://doi.org/10.1126/science.aay7101

Balestrini, R., & Bonfante, P. (2014). Cell wall remodeling in mycorrhizal symbiosis: a way towards biotrophism. *Frontiers in Plant Science*, *5*(JUN), 1–10. https://doi.org/10.3389/fpls.2014.00237

Balleux, G., Höfte, M., Arguelles-Arias, A., Deleu, M., & Ongena, M. (2025). *Bacillus* lipopeptides as key players in rhizosphere chemical ecology. *Trends in Microbiology*, *33*(1), 80–95. https://doi.org/10.1016/j.tim.2024.08.001

Balleza, D., Alessandrini, A., & Beltrán García, M. J. (2019). Role of Lipid Composition, Physicochemical Interactions, and Membrane Mechanics in the Molecular Actions of Microbial Cyclic Lipopeptides. *The Journal of Membrane Biology*, *252*(2–3), 131–157. https://doi.org/10.1007/s00232-019-00067-4

Banasiak, J., Jamruszka, T., Murray, J. D., & Jasiński, M. (2021). A roadmap of plant membrane transporters in arbuscular mycorrhizal and legume–rhizobium symbioses. *Plant Physiology*, *187*(4), 2071–2091. https://doi.org/10.1093/plphys/kiab280

Banerjee, S., & van der Heijden, M. G. A. (2023). Soil microbiomes and one health. *Nature Reviews Microbiology*, *21*(1), 6–20. https://doi.org/10.1038/s41579-022-00779-w

Barbier, E. B., & Hochard, J. P. (2018). Land degradation and poverty. *Nature Sustainability*, *1*(11), 623–631. https://doi.org/10.1038/s41893-018-0155-4

Bareia, T., Pollak, S., & Eldar, A. (2017). Self-sensing in *Bacillus subtilis* quorum-sensing systems. *Nature Microbiology*, *3*(1), 83–89. https://doi.org/10.1038/s41564-017-0044-z

Barto, E. K., Weidenhamer, J. D., Cipollini, D., & Rillig, M. C. (2012). Fungal superhighways: do common mycorrhizal networks enhance below ground communication? *Trends in Plant Science*, *17*(11), 633–637. https://doi.org/10.1016/j.tplants.2012.06.007

Basiru, S., Ait Si Mhand, K., & Hijri, M. (2023). Disentangling arbuscular mycorrhizal fungi and bacteria at the soil-root interface. *Mycorrhiza 2023 33:3*, *33*(3), 119–137. https://doi.org/10.1007/S00572-023-01107-7

Beauregard, P. B., Chai, Y., Vlamakis, H., Losick, R., & Kolter, R. (2013). *Bacillus*

subtilis biofilm induction by plant polysaccharides. *Proceedings of the National Academy of Sciences*, *110*(17), E1621–E1630. https://doi.org/10.1073/pnas.1218984110

Beketov, M. A., Kefford, B. J., Schäfer, R. B., & Liess, M. (2013). Pesticides reduce regional biodiversity of stream invertebrates. *Proceedings of the National Academy of Sciences*, *110*(27), 11039–11043. https://doi.org/10.1073/pnas.1305618110

Bennett, A. E., & Groten, K. (2022). The Costs and Benefits of Plant–Arbuscular Mycorrhizal Fungal Interactions. *Annual Review of Plant Biology*, *73*(1), 649–672. https://doi.org/10.1146/annurev-arplant-102820-124504

Benoit, I., van den Esker, M. H., Patyshakuliyeva, A., Mattern, D. J., Blei, F., Zhou, M., Dijksterhuis, J., Brakhage, A. A., Kuipers, O. P., de Vries, R. P., & Kovács, Á. T. (2015). *Bacillus subtilis* attachment to *Aspergillus niger* hyphae results in mutually altered metabolism. *Environmental Microbiology*, *17*(6), 2099–2113. https://doi.org/10.1111/1462-2920.12564

Berruto, C. A., & Demirer, G. S. (2024). Engineering agricultural soil microbiomes and predicting plant phenotypes. *Trends in Microbiology*, *32*(9), 858–873. https://doi.org/10.1016/j.tim.2024.02.003

Besserer, A., Bécard, G., Jauneau, A., Roux, C., & Séjalon-Delmas, N. (2008). GR24, a Synthetic Analog of Strigolactones, Stimulates the Mitosis and Growth of the Arbuscular Mycorrhizal Fungus *Gigaspora rosea* by Boosting Its Energy Metabolism. *Plant Physiology*, *148*(1), 402–413. https://doi.org/10.1104/pp.108.121400

Besserer, A., Puech-Pagès, V., Kiefer, P., Gomez-Roldan, V., Jauneau, A., Roy, S., Portais, J.-C., Roux, C., Bécard, G., & Séjalon-Delmas, N. (2006). Strigolactones Stimulate Arbuscular Mycorrhizal Fungi by Activating Mitochondria. *PLoS Biology*, *4*(7), e226. https://doi.org/10.1371/journal.pbio.0040226

Betz, R., Heidt, S., Figueira-Galán, D., Hartmann, M., Langner, T., & Requena, N. (2024). Alternative splicing regulation in plants by SP7-like effectors from symbiotic arbuscular mycorrhizal fungi. *Nature Communications*, *15*(1), 7107. https://doi.org/10.1038/s41467-024-51512-5

Bigeard, J., Colcombet, J., & Hirt, H. (2015). Signaling Mechanisms in Pattern-Triggered Immunity (PTI). *Molecular Plant*, *8*(4), 521–539. https://doi.org/10.1016/j.molp.2014.12.022

Binci, F., Offer, E., Crosino, A., Sciascia, I., Kleine-Vehn, J., Genre, A., Giovannetti, M., & Navazio, L. (2024). Spatially and temporally distinct Ca2+ changes in *Lotus japonicus* roots orient fungal-triggered signalling pathways towards symbiosis or immunity. *Journal of Experimental Botany*, *75*(2), 605–619. https://doi.org/10.1093/jxb/erad360

Bischofs, I. B., Hug, J. A., Liu, A. W., Wolf, D. M., & Arkin, A. P. (2009). Complexity in bacterial cell–cell communication: Quorum signal integration and subpopulation signaling in the *Bacillus subtilis* phosphorelay. *Proceedings of*

the National Academy of Sciences, *106*(16), 6459–6464. https://doi.org/10.1073/pnas.0810878106

Blake, C., Christensen, M. N., & Kovács, Á. T. (2021). Molecular Aspects of Plant Growth Promotion and Protection by *Bacillus subtilis*. *Molecular Plant-Microbe Interactions®*, *34*(1), 15–25. https://doi.org/10.1094/MPMI-08-20-0225-CR

Bleich, R., Watrous, J. D., Dorrestein, P. C., Bowers, A. A., & Shank, E. A. (2015). Thiopeptide antibiotics stimulate biofilm formation in *Bacillus subtilis*. *Proceedings of the National Academy of Sciences*, *112*(10), 3086–3091. https://doi.org/10.1073/pnas.1414272112

Bonhomme, M., Bensmihen, S., André, O., Amblard, E., Garcia, M., Maillet, F., Puech-Pagès, V., Gough, C., Fort, S., Cottaz, S., Bécard, G., & Jacquet, C. (2021). Distinct genetic basis for root responses to lipo-chitooligosaccharide signal molecules from different microbial origins. *Journal of Experimental Botany*, *72*(10), 3821–3834. https://doi.org/10.1093/jxb/erab096

Borrelli, P., Panagos, P., Alewell, C., Ballabio, C., de Oliveira Fagundes, H., Haregeweyn, N., Lugato, E., Maerker, M., Poesen, J., Vanmaercke, M., & Robinson, D. A. (2022). Policy implications of multiple concurrent soil erosion processes in European farmland. *Nature Sustainability*, *6*(1), 103–112. https://doi.org/10.1038/s41893-022-00988-4

Borriss, R. (2020). Phytostimulation and Biocontrol by the Plant-Associated *Bacillus amyloliquefaciens* FZB42: An Update. In M. Kumar, V. Kumar, & R. Prasad (Eds.), *Phyto-Microbiome in Stress Regulation. Environmental and Microbial Biotechnology* (pp. 1–20). Springer, Singapore. https://doi.org/10.1007/978-981-15-2576-6_1

Botcazon, C., Bergia, T., Lecouturier, D., Dupuis, C., Rochex, A., Acket, S., Nicot, P., Leclère, V., Sarazin, C., & Rippa, S. (2022). Rhamnolipids and fengycins, very promising amphiphilic antifungal compounds from bacteria secretomes, act on *Sclerotiniaceae* fungi through different mechanisms. *Frontiers in Microbiology*, *13*, 977633. https://doi.org/10.3389/fmicb.2022.977633

Botcazon, C., Ramos-Martín, F., Rodríguez-Moraga, N., Bergia, T., Acket, S., Sarazin, C., & Rippa, S. (2024). Rhamnolipids and fengycins interact differently with biomimetic lipid membrane models of *Botrytis cinerea* and *Sclerotinia sclerotiorum*: Lipidomics profiles and biophysical studies. *Biophysical Chemistry*, *314*, 107305. https://doi.org/10.1016/j.bpc.2024.107305

Boubsi, F., Anckaert, A., Argüelles-Arias, A., & Ongena, M. (2025). Pectin-derived oligogalacturonides shape mutualistic interactions between *Bacillus*and its host plant. *The ISME Journal*. https://doi.org/10.1093/ismejo/wraf232

Boubsi, F., Hoff, G., Arguelles Arias, A., Steels, S., Andrić, S., Anckaert, A., Roulard, R., Rigolet, A., van Wuytswinkel, O., & Ongena, M. (2023). Pectic homogalacturonan sensed by *Bacillus* acts as host associated cue to promote establishment and persistence in the rhizosphere. *IScience*, *26*(10), 107925. https://doi.org/10.1016/j.isci.2023.107925

Bravo, A., York, T., Pumplin, N., Mueller, L. A., & Harrison, M. J. (2016). Genes

conserved for arbuscular mycorrhizal symbiosis identified through phylogenomics. *Nature Plants*, *2*(2), 15208. https://doi.org/10.1038/nplants.2015.208

Brundrett, M. C., & Tedersoo, L. (2018). Evolutionary history of mycorrhizal symbioses and global host plant diversity. *New Phytologist*, *220*(4), 1108–1115. https://doi.org/10.1111/nph.14976

Brunet, M., Amin, S. A., Bodachivskyi, I., Kuzhiumparambil, U., Seymour, J. R., & Raina, J.-B. (2025). An atlas of metabolites driving chemotaxis in prokaryotes. *Nature Communications*, *16*(1), 1242. https://doi.org/10.1038/s41467-025-56410-y

Buendia, L., Girardin, A., Wang, T., Cottret, L., & Lefebvre, B. (2018). LysM receptor-like kinase and lysM receptor-like protein families: An update on phylogeny and functional characterization. *Frontiers in Plant Science*, *871*, 409605. https://doi.org/10.3389/FPLS.2018.01531/XML

Buendia, L., Maillet, F., O'Connor, D., van de-Kerkhove, Q., Danoun, S., Gough, C., Lefebvre, B., & Bensmihen, S. (2019). Lipo-chitooligosaccharides promote lateral root formation and modify auxin homeostasis in <i>Brachypodium distachyon. *New Phytologist*, *221*(4), 2190–2202. https://doi.org/10.1111/nph.15551

Bui, V. C., & Franken, P. (2018). Acclimatization of *Rhizophagus irregularis* Enhances Zn Tolerance of the Fungus and the Mycorrhizal Plant Partner. *Frontiers in Microbiology*, *9*, 424175. https://doi.org/10.3389/fmicb.2018.03156

Buswell, W., Schwarzenbacher, R. E., Luna, E., Sellwood, M., Chen, B., Flors, V., Pétriacq, P., & Ton, J. (2018). Chemical priming of immunity without costs to plant growth. *New Phytologist*, *218*(3), 1205–1216. https://doi.org/10.1111/nph.15062

Buysens, C., Alaux, P.-L., César, V., Huret, S., Declerck, S., & Cranenbrouck, S. (2017). Tracing native and inoculated *Rhizophagus irregularis* in three potato cultivars (Charlotte, Nicola and Bintje) grown under field conditions. *Applied Soil Ecology*, *115*, 1–9. https://doi.org/10.1016/j.apsoil.2017.03.007

Calonne, M., Fontaine, J., Tisserant, B., Dupré de Boulois, H., Grandmougin-Ferjani, A., Declerck, S., & Lounès-Hadj Sahraoui, A. (2014). Polyaromatic hydrocarbons impair phosphorus transport by the arbuscular mycorrhizal fungus *Rhizophagus irregularis*. *Chemosphere*, *104*, 97–104. https://doi.org/10.1016/j.chemosphere.2013.10.070

Calvo, H., Mendiara, I., Arias, E., Blanco, D., & Venturini, M. E. (2019). The role of iturin A from *B. amyloliquefaciens* BUZ-14 in the inhibition of the most common postharvest fruit rots. *Food Microbiology*, *82*, 62–69. https://doi.org/10.1016/j.fm.2019.01.010

Cameron, D. D., Neal, A. L., van Wees, S. C. M., & Ton, J. (2013). Mycorrhiza-induced resistance: more than the sum of its parts? *Trends in Plant Science*, *18*(10), 539–545. https://doi.org/10.1016/j.tplants.2013.06.004

Cao, X., Zhao, Y., Xia, R.-X., Wu, Q.-S., Hashem, A., & Abd_Allah, E. F. (2024). Interactions between Root Hair Development and Arbuscular Mycorrhizal Fungal Colonization in Trifoliate Orange Seedlings in Response to P Levels. *Agriculture*, *14*(5), 763. https://doi.org/10.3390/agriculture14050763

Cao, Y., Pi, H., Chandrangsu, P., Li, Y., Wang, Y., Zhou, H., Xiong, H., Helmann, J. D., & Cai, Y. (2018). Antagonism of Two Plant-Growth Promoting *Bacillus velezensis* Isolates Against *Ralstonia solanacearum* and *Fusarium oxysporum*. *Scientific Reports*, *8*(1), 4360. https://doi.org/10.1038/s41598-018-22782-z

Cargill, R. I. M., Shimizu, T. S., Kiers, E. T., & Kokkoris, V. (2025). Cellular anatomy of arbuscular mycorrhizal fungi. *Current Biology*, *35*(11), R545–R562. https://doi.org/10.1016/j.cub.2025.03.053

Caulier, S., Gillis, A., Colau, G., Licciardi, F., Liépin, M., Desoignies, N., Modrie, P., Legrève, A., Mahillon, J., & Bragard, C. (2018). Versatile Antagonistic Activities of Soil-Borne *Bacillus* spp. and *Pseudomonas* spp. against *Phytophthora infestans* and Other Potato Pathogens. *Frontiers in Microbiology*, *9*(FEB). https://doi.org/10.3389/fmicb.2018.00143

Caulier, S., Nannan, C., Gillis, A., Licciardi, F., Bragard, C., & Mahillon, J. (2019). Overview of the Antimicrobial Compounds Produced by Members of the *Bacillus subtilis* Group. *Frontiers in Microbiology*, *10*(FEB), 435128. https://doi.org/10.3389/fmicb.2019.00302

Cawoy, H., Debois, D., Franzil, L., De Pauw, E., Thonart, P., & Ongena, M. (2015). Lipopeptides as main ingredients for inhibition of fungal phytopathogens by *Bacillus subtilis/amyloliquefaciens*. *Microbial Biotechnology*, *8*(2), 281–295. https://doi.org/10.1111/1751-7915.12238

Cawoy, H., Mariutto, M., Henry, G., Fisher, C., Vasilyeva, N., Thonart, P., Dommes, J., & Ongena, M. (2014). Plant Defense Stimulation by Natural Isolates of *Bacillus* Depends on Efficient Surfactin Production. *Molecular Plant-Microbe Interactions®*, *27*(2), 87–100. https://doi.org/10.1094/MPMI-09-13-0262-R

Chandrasekar, B., Wanke, A., Wawra, S., Saake, P., Mahdi, L., Charura, N., Neidert, M., Poschmann, G., Malisic, M., Thiele, M., Stühler, K., Dama, M., Pauly, M., & Zuccaro, A. (2022). Fungi hijack a ubiquitous plant apoplastic endoglucanase to release a ROS scavenging β-glucan decasaccharide to subvert immune responses. *The Plant Cell*, *34*(7), 2765–2784. https://doi.org/10.1093/plcell/koac114

Chaparro, J. M., Badri, D. V., & Vivanco, J. M. (2014). Rhizosphere microbiome assemblage is affected by plant development. *The ISME Journal*, *8*(4), 790–803. https://doi.org/10.1038/ismej.2013.196

Charron-Lamoureux, V., & Beauregard, P. B. (2019). *Arabidopsis thaliana* Seedlings Influence *Bacillus subtilis* Spore Formation. *Molecular Plant-Microbe Interactions®*, *32*(9), 1188–1195. https://doi.org/10.1094/MPMI-10-18-0278-R

Chen, E. C. H., Morin, E., Beaudet, D., Noel, J., Yildirir, G., Ndikumana, S., Charron, P., St-Onge, C., Giorgi, J., Krüger, M., Marton, T., Ropars, J., Grigoriev, I. V., Hainaut, M., Henrissat, B., Roux, C., Martin, F., & Corradi, N. (2018). High

intraspecific genome diversity in the model arbuscular mycorrhizal symbiont *Rhizophagus irregularis*. *New Phytologist*, *220*(4), 1161–1171. https://doi.org/10.1111/nph.14989

Chen, X.-H., Koumoutsi, A., Scholz, R., & Borriss, R. (2009a). More than Anticipated – Production of Antibiotics and Other Secondary Metabolites by *Bacillus amyloliquefaciens* FZB42. *Microbial Physiology*, *16*(1–2), 14–24. https://doi.org/10.1159/000142891

Chen, X. H., Scholz, R., Borriss, M., Junge, H., Mögel, G., Kunz, S., & Borriss, R. (2009b). Difficidin and bacilysin produced by plant-associated *Bacillus amyloliquefaciens* are efficient in controlling fire blight disease. *Journal of Biotechnology*, *140*(1–2), 38–44. https://doi.org/10.1016/j.jbiotec.2008.10.015

Chen, X. H., Vater, J., Piel, J., Franke, P., Scholz, R., Schneider, K., Koumoutsi, A., Hitzeroth, G., Grammel, N., Strittmatter, A. W., Gottschalk, G., Süssmuth, R. D., & Borriss, R. (2006). Structural and functional characterization of three polyketide synthase gene clusters in Bacillus amyloliquefaciens FZB 42. *Journal of Bacteriology*, *188*(11), 4024–4036. https://doi.org/10.1128/JB.00052-06

Chialva, M., Fangel, J. U., Novero, M., Zouari, I., Salvioli di Fossalunga, A., Willats, W. G. T., Bonfante, P., & Balestrini, R. (2019). Understanding Changes in Tomato Cell Walls in Roots and Fruits: The Contribution of Arbuscular Mycorrhizal Colonization. *International Journal of Molecular Sciences*, *20*(2), 415. https://doi.org/10.3390/ijms20020415

Chialva, M., Lanfranco, L., & Bonfante, P. (2022). The plant microbiota: composition, functions, and engineering. *Current Opinion in Biotechnology*, *73*, 135–142. https://doi.org/10.1016/j.copbio.2021.07.003

Chiu, C. H., Roszak, P., Orvošová, M., & Paszkowski, U. (2022). Arbuscular mycorrhizal fungi induce lateral root development in angiosperms via a conserved set of MAMP receptors. *Current Biology*, *32*(20), 4428-4437.e3. https://doi.org/10.1016/j.cub.2022.08.069

Choi, J., Summers, W., & Paszkowski, U. (2018). Mechanisms Underlying Establishment of Arbuscular Mycorrhizal Symbioses. *Annual Review of Phytopathology*, *56*(1), 135–160. https://doi.org/10.1146/annurev-phyto-080516-035521

Chowdhury, S. P., Dietel, K., Rändler, M., Schmid, M., Junge, H., Borriss, R., Hartmann, A., & Grosch, R. (2013). Effects of *Bacillus amyloliquefaciens* FZB42 on Lettuce Growth and Health under Pathogen Pressure and Its Impact on the Rhizosphere Bacterial Community. *PLoS ONE*, *8*(7), e68818. https://doi.org/10.1371/journal.pone.0068818

Chowdhury, S. P., Uhl, J., Grosch, R., Alquéres, S., Pittroff, S., Dietel, K., Schmitt-Kopplin, P., Borriss, R., & Hartmann, A. (2015). Cyclic Lipopeptides of *Bacillus amyloliquefaciens* subsp. plantarum Colonizing the Lettuce Rhizosphere Enhance Plant Defense Responses Toward the Bottom Rot Pathogen Rhizoctonia solani. *Molecular Plant-Microbe Interactions®*, *28*(9), 984–995.

https://doi.org/10.1094/MPMI-03-15-0066-R

Collinge, D. B., Jensen, D. F., Rabiey, M., Sarrocco, S., Shaw, M. W., & Shaw, R. H. (2022). Biological control of plant diseases – What has been achieved and what is the direction? *Plant Pathology*, *71*(5), 1024–1047. https://doi.org/10.1111/ppa.13555

Colombo, M., Raposo, G., & Théry, C. (2014). Biogenesis, Secretion, and Intercellular Interactions of Exosomes and Other Extracellular Vesicles. *Annual Review of Cell and Developmental Biology*, *30*(1), 255–289. https://doi.org/10.1146/annurev-cellbio-101512-122326

Compant, S., Cassan, F., Kostić, T., Johnson, L., Brader, G., Trognitz, F., & Sessitsch, A. (2025). Harnessing the plant microbiome for sustainable crop production. *Nature Reviews Microbiology*, *23*(1), 9–23. https://doi.org/10.1038/s41579-024-01079-1

Compant, S., Samad, A., Faist, H., & Sessitsch, A. (2019). A review on the plant microbiome: Ecology, functions, and emerging trends in microbial application. *Journal of Advanced Research*, *19*, 29–37. https://doi.org/10.1016/j.jare.2019.03.004

Conrath, U., Beckers, G. J. M., Langenbach, C. J. G., & Jaskiewicz, M. R. (2015). Priming for Enhanced Defense. *Annual Review of Phytopathology*, *53*(1), 97–119. https://doi.org/10.1146/annurev-phyto-080614-120132

Cosme, M., Fernández, I., Declerck, S., van der Heijden, M. G. A., & Pieterse, C. M. J. (2021). A coumarin exudation pathway mitigates arbuscular mycorrhizal incompatibility in *Arabidopsis thaliana*. *Plant Molecular Biology*, *106*(4–5), 319–334. https://doi.org/10.1007/s11103-021-01143-x

Cranenbrouck, S., Voets, L., Bivort, C., Renard, L., Strullu, D.-G., & Declerck, S. (2005). Methodologies for *in Vitro* Cultivation of Arbuscular Mycorrhizal Fungi with Root Organs. In S. Declerck, J. A. Fortin, & D.-G. Strullu (Eds.), *In Vitro Culture of Mycorrhizas. Soil Biology, vol 4.* (pp. 341–375). Springer, Berlin, Heidelberg. https://doi.org/10.1007/3-540-27331-X_18

Crouzet, J., Arguelles-Arias, A., Dhondt-Cordelier, S., Cordelier, S., Pršić, J., Hoff, G., Mazeyrat-Gourbeyre, F., Baillieul, F., Clément, C., Ongena, M., & Dorey, S. (2020). Biosurfactants in Plant Protection Against Diseases: Rhamnolipids and Lipopeptides Case Study. *Frontiers in Bioengineering and Biotechnology*, *8*. https://doi.org/10.3389/fbioe.2020.01014

Cui, H., Tsuda, K., & Parker, J. E. (2015). Effector-Triggered Immunity: From Pathogen Perception to Robust Defense. *Annual Review of Plant Biology*, *66*(1), 487–511. https://doi.org/10.1146/annurev-arplant-050213-040012

D'Hondt, K., Kostic, T., McDowell, R., Eudes, F., Singh, B. K., Sarkar, S., Markakis, M., Schelkle, B., Maguin, E., & Sessitsch, A. (2021). Microbiome innovations for a sustainable future. *Nature Microbiology*, *6*(2), 138–142. https://doi.org/10.1038/s41564-020-00857-w

De Jaeger, N., Declerck, S., & De La Providencia, I. E. (2010). Mycoparasitism of arbuscular mycorrhizal fungi: a pathway for the entry of saprotrophic fungi into

roots. *FEMS Microbiology Ecology*, *73*(2), 312–322. https://doi.org/10.1111/J.1574-6941.2010.00903.X

De Kesel, J., Conrath, U., Flors, V., Luna, E., Mageroy, M. H., Mauch-Mani, B., Pastor, V., Pozo, M. J., Pieterse, C. M. J., Ton, J., & Kyndt, T. (2021). The Induced Resistance Lexicon: Do's and Don'ts. *Trends in Plant Science*, *26*(7), 685–691. https://doi.org/10.1016/j.tplants.2021.01.001

DeFalco, T. A., & Zipfel, C. (2021). Molecular mechanisms of early plant pattern-triggered immune signaling. *Molecular Cell*, *81*(17), 3449–3467. https://doi.org/10.1016/j.molcel.2021.07.029

DeFilippi, S., Groulx, E., Megalla, M., Mohamed, R., & Avis, T. J. (2018). Fungal Competitors Affect Production of Antimicrobial Lipopeptides in *Bacillus subtilis* Strain B9–5. *Journal of Chemical Ecology*, *44*(4), 374–383. https://doi.org/10.1007/s10886-018-0938-0

Delaux, P.-M., & Gutjahr, C. (2024). Evolution of small molecule-mediated regulation of arbuscular mycorrhiza symbiosis. *Philosophical Transactions of the Royal Society B: Biological Sciences*, *379*(1914). https://doi.org/10.1098/rstb.2023.0369

Deleu, M., Crowet, J.-M., Nasir, M. N., & Lins, L. (2014). Complementary biophysical tools to investigate lipid specificity in the interaction between bioactive molecules and the plasma membrane: A review. *Biochimica et Biophysica Acta (BBA) - Biomembranes*, *1838*(12), 3171–3190. https://doi.org/10.1016/j.bbamem.2014.08.023

Deleu, M., Lorent, J., Lins, L., Brasseur, R., Braun, N., El Kirat, K., Nylander, T., Dufrêne, Y. F., & Mingeot-Leclercq, M. P. (2013). Effects of surfactin on membrane models displaying lipid phase separation. *Biochimica et Biophysica Acta (BBA) - Biomembranes*, *1828*(2), 801–815. https://doi.org/10.1016/j.bbamem.2012.11.007

Deleu, M., Paquot, M., & Nylander, T. (2005). Fengycin interaction with lipid monolayers at the air–aqueous interface—implications for the effect of fengycin on biological membranes. *Journal of Colloid and Interface Science*, *283*(2), 358–365. https://doi.org/10.1016/j.jcis.2004.09.036

Deleu, M., Paquot, M., & Nylander, T. (2008). Effect of Fengycin, a Lipopeptide Produced by *Bacillus subtilis*, on Model Biomembranes. *Biophysical Journal*, *94*(7), 2667–2679. https://doi.org/10.1529/biophysj.107.114090

Desaki, Y., Miyata, K., Suzuki, M., Shibuya, N., & Kaku, H. (2018). Plant immunity and symbiosis signaling mediated by LysM receptors. *Innate Immunity*, *24*(2), 92–100. https://doi.org/10.1177/1753425917738885

Ding, Y., Lesterps, Z., Gasciolli, V., Fuchs, A. L., Gaston, M., Medioni, L., de-Regibus, A., Remblière, C., Vicédo, C., Bensmihen, S., Bono, J. J., Cullimore, J., Reyt, G., Dalmais, M., Saffray, C., Mazeau, S., Bendahmane, A., Sibout, R., Vandenbussche, M., … Lefebvre, B. (2025). Several groups of LysM-RLKs are involved in symbiotic signal perception and arbuscular mycorrhiza establishment. *Nature Communications 2025 16:1*, *16*(1), 1–14.

https://doi.org/10.1038/s41467-025-60717-1

Ding, Y., Wang, T., Gasciolli, V., Reyt, G., Remblière, C., Marcel, F., François, T., Bendahmane, A., He, G., Bono, J. J., & Lefebvre, B. (2024). The LysM Receptor-Like Kinase SlLYK10 Controls Lipochitooligosaccharide Signaling in Inner Cell Layers of Tomato Roots. *Plant And Cell Physiology*, *65*(7), 1149–1159. https://doi.org/10.1093/pcp/pcae035

Dobrange, E., & Van den Ende, W. (2025). Bacterial cell differentiation during plant root colonization: the putative role of fructans. *Physiologia Plantarum*, *177*(1), e70095. https://doi.org/10.1111/ppl.70095

Dobránszki, J., Agius, D. R., Berger, M. M. J., Moschou, P. N., Gallusci, P., & Martinelli, F. (2025). Plant memory and communication of encounters. *Trends in Plant Science*, *30*(2), 199–212. https://doi.org/10.1016/j.tplants.2024.09.012

Dogsa, I., Bellich, B., Blaznik, M., Lagatolla, C., Ravenscroft, N., Rizzo, R., Stopar, D., & Cescutti, P. (2024). *Bacillus subtilis* EpsA-O: A novel exopolysaccharide structure acting as an efficient adhesive in biofilms. *Npj Biofilms and Microbiomes*, *10*(1), 98. https://doi.org/10.1038/s41522-024-00555-z

Dogsa, I., Brloznik, M., Stopar, D., & Mandic-Mulec, I. (2013). Exopolymer Diversity and the Role of Levan in *Bacillus subtilis* Biofilms. *PLoS ONE*, *8*(4), e62044. https://doi.org/10.1371/journal.pone.0062044

Duan, S., Feng, G., Limpens, E., Bonfante, P., Xie, X., & Zhang, L. (2024). Cross-kingdom nutrient exchange in the plant–arbuscular mycorrhizal fungus–bacterium continuum. *Nature Reviews Microbiology*, *22*(12), 773–790. https://doi.org/10.1038/s41579-024-01073-7

Duan, S., Jin, Z., Zhang, L., & Declerck, S. (2025). Mechanisms of cooperation in the plants-arbuscular mycorrhizal fungi-bacteria continuum. *The ISME Journal*, *19*(1), 23. https://doi.org/10.1093/ismejo/wraf023

Duban, M., Cociancich, S., & Leclère, V. (2022). Nonribosomal Peptide Synthesis Definitely Working Out of the Rules. *Microorganisms*, *10*(3), 577. https://doi.org/10.3390/microorganisms10030577

Duhamel, M., Pel, R., Ooms, A., Bücking, H., Jansa, J., Ellers, J., van Straalen, N. M., Wouda, T., Vandenkoornhuyse, P., & Kiers, E. T. (2013). Do fungivores trigger the transfer of protective metabolites from host plants to arbuscular mycorrhizal hyphae? *Ecology*, *94*(9), 2019–2029. https://doi.org/10.1890/12-1943.1

Dunlap, C. A. (2019). Taxonomy of registered Bacillus spp. strains used as plant pathogen antagonists. *Biological Control*, *134*, 82–86. https://doi.org/10.1016/J.BIOCONTROL.2019.04.011

Durant, E., Hoysted, G. A., Howard, N., Sait, S. M., Childs, D. Z., Johnson, D., & Field, K. J. (2023). Herbivore-driven disruption of arbuscular mycorrhizal carbon-for-nutrient exchange is ameliorated by neighboring plants. *Current Biology*, *33*(12), 2566-2573.e4. https://doi.org/10.1016/j.cub.2023.05.033

Elhady, A., Alghanmi, L., Sheikh, A. H., Saad, M. M., & Hirt, H. (2025). Coexistence ecology of pathogen-inhibiting microbes in the phytobiome. *Trends in Plant Science*. https://doi.org/10.1016/j.tplants.2025.05.001

Emmett, B. D., Lévesque-Tremblay, V., & Harrison, M. J. (2021). Conserved and reproducible bacterial communities associate with extraradical hyphae of arbuscular mycorrhizal fungi. *The ISME Journal*, *15*(8), 2276–2288. https://doi.org/10.1038/s41396-021-00920-2

Even, C., Marlière, C., Ghigo, J. M., Allain, J. M., Marcellan, A., & Raspaud, E. (2017). Recent advances in studying single bacteria and biofilm mechanics. *Advances in Colloid and Interface Science*, *247*, 573–588. https://doi.org/10.1016/J.CIS.2017.07.026

Faghihinia, M., Jansa, J., Halverson, L. J., Staddon, P. L., Larry, ·, Halverson, J., & Staddon, P. L. (2022). Hyphosphere microbiome of arbuscular mycorrhizal fungi: a realm of unknowns. *Biology and Fertility of Soils 2022 59:1*, *1*. https://doi.org/10.1007/s00374-022-01683-4

Fan, B., Wang, C., Song, X., Ding, X., Wu, L., Wu, H., Gao, X., & Borriss, R. (2018). *Bacillus velezensis* FZB42 in 2018: The Gram-Positive Model Strain for Plant Growth Promotion and Biocontrol. *Frontiers in Microbiology*, *9*(OCT), 408393. https://doi.org/10.3389/fmicb.2018.02491

Farzand, A., Moosa, A., Zubair, M., Khan, A. R., Ayaz, M., Massawe, V. C., & Gao, X. (2020). Transcriptional Profiling of Diffusible Lipopeptides and Fungal Virulence Genes During *Bacillus amyloliquefaciens* EZ1509-Mediated Suppression of *Sclerotinia sclerotiorum*. *Phytopathology®*, *110*(2), 317–326. https://doi.org/10.1094/PHYTO-05-19-0156-R

Feng, F., Sun, J., Radhakrishnan, G. V., Lee, T., Bozsóki, Z., Fort, S., Gavrin, A., Gysel, K., Thygesen, M. B., Andersen, K. R., Radutoiu, S., Stougaard, J., & Oldroyd, G. E. D. (2019). A combination of chitooligosaccharide and lipochitooligosaccharide recognition promotes arbuscular mycorrhizal associations in *Medicago truncatula*. *Nature Communications*, *10*(1), 5047. https://doi.org/10.1038/s41467-019-12999-5

Feng, H., Fu, R., Hou, X., Lv, Y., Zhang, N., Liu, Y., Xu, Z., Miao, Y., Krell, T., Shen, Q., & Zhang, R. (2021). Chemotaxis of Beneficial Rhizobacteria to Root Exudates: The First Step towards Root–Microbe Rhizosphere Interactions. *International Journal of Molecular Sciences*, *22*(13), 6655. https://doi.org/10.3390/ijms22136655

Feng, H., Zhang, N., Du, W., Zhang, H., Liu, Y., Fu, R., Shao, J., Zhang, G., Shen, Q., & Zhang, R. (2018). Identification of Chemotaxis Compounds in Root Exudates and Their Sensing Chemoreceptors in Plant-Growth-Promoting Rhizobacteria *Bacillus amyloliquefaciens* SQR9. *Molecular Plant-Microbe Interactions®*, *31*(10), 995–1005. https://doi.org/10.1094/MPMI-01-18-0003-R

Fernández, I., Cosme, M., Stringlis, I. A., Yu, K., de Jonge, R., van Wees, S. M., Pozo, M. J., Pieterse, C. M. J., & van der Heijden, M. G. A. (2019). Molecular dialogue between arbuscular mycorrhizal fungi and the nonhost plant *Arabidopsis thaliana* switches from initial detection to antagonism. *New Phytologist*, *223*(2), 867–881. https://doi.org/10.1111/nph.15798

Ferrer, A., Altabella, T., Arró, M., & Boronat, A. (2017). Emerging roles for

conjugated sterols in plants. *Progress in Lipid Research*, *67*, 27–37. https://doi.org/10.1016/j.plipres.2017.06.002

Ferro, R., Rennig, M., Hernández-Rollán, C., Daley, D. O., & Nørholm, M. H. H. (2018). A synbio approach for selection of highly expressed gene variants in Gram-positive bacteria. *Microbial Cell Factories*, *17*(1), 37. https://doi.org/10.1186/s12934-018-0886-y

Fester, T., & Hause, G. (2005). Accumulation of reactive oxygen species in arbuscular mycorrhizal roots. *Mycorrhiza*, *15*(5), 373–379. https://doi.org/10.1007/s00572-005-0363-4

Fiedler, S., & Heerklotz, H. (2015). Vesicle Leakage Reflects the Target Selectivity of Antimicrobial Lipopeptides from *Bacillus subtilis*. *Biophysical Journal*, *109*(10), 2079–2089. https://doi.org/10.1016/j.bpj.2015.09.021

Fifani, B., Steels, S., Helmus, C., Delacuvellerie, A., Deracinois, B., Phalip, V., Delvigne, F., & Jacques, P. (2022). Coculture of *Trichoderma harzianum* and *Bacillus velezensis* Based on Metabolic Cross-Feeding Modulates Lipopeptide Production. *Microorganisms*, *10*(5), 1059. https://doi.org/10.3390/microorganisms10051059

Fiorilli, V., Martínez-Medina, A., Pozo, M. J., & Lanfranco, L. (2024). Plant Immunity Modulation in Arbuscular Mycorrhizal Symbiosis and Its Impact on Pathogens and Pests. *Annual Review of Phytopathology*, *62*(1), 127–156. https://doi.org/10.1146/annurev-phyto-121423-042014

Fiorilli, V., Vannini, C., Ortolani, F., Garcia-Seco, D., Chiapello, M., Novero, M., Domingo, G., Terzi, V., Morcia, C., Bagnaresi, P., Moulin, L., Bracale, M., & Bonfante, P. (2018). Omics approaches revealed how arbuscular mycorrhizal symbiosis enhances yield and resistance to leaf pathogen in wheat. *Scientific Reports*, *8*(1), 9625. https://doi.org/10.1038/s41598-018-27622-8

Flemming, H.-C., van Hullebusch, E. D., Neu, T. R., Nielsen, P. H., Seviour, T., Stoodley, P., Wingender, J., & Wuertz, S. (2023). The biofilm matrix: multitasking in a shared space. *Nature Reviews Microbiology*, *21*(2), 70–86. https://doi.org/10.1038/s41579-022-00791-0

Flemming, H.-C., Wingender, J., Szewzyk, U., Steinberg, P., Rice, S. A., & Kjelleberg, S. (2016). Biofilms: an emergent form of bacterial life. *Nature Reviews Microbiology*, *14*(9), 563–575. https://doi.org/10.1038/nrmicro.2016.94

Flores, A. C., Luna, A. A. E., & Portugal, V. O. (2007). Yield and Quality Enhancement of Marigold Flowers by Inoculation with *Bacillus subtilis* and *Glomus fasciculatum*. *Journal of Sustainable Agriculture*, *31*(1), 21–31. https://doi.org/10.1300/J064v31n01_04

French, E., Kaplan, I., Iyer-Pascuzzi, A., Nakatsu, C. H., & Enders, L. (2021). Emerging strategies for precision microbiome management in diverse agroecosystems. *Nature Plants*, *7*(3), 256–267. https://doi.org/10.1038/s41477-020-00830-9

Fu, Z. Q., & Dong, X. (2013). Systemic Acquired Resistance: Turning Local Infection

into Global Defense. *Annual Review of Plant Biology*, *64*(1), 839–863. https://doi.org/10.1146/annurev-arplant-042811-105606

Fukuda, H., Mamiya, R., Akamatsu, A., & Takeda, N. (2024). Two *LysM* receptor-like kinases regulate arbuscular mycorrhiza through distinct signaling pathways in *Lotus japonicus*. *New Phytologist*, *243*(2), 519–525. https://doi.org/10.1111/nph.19863

Fukushima, T. (2003). Transcriptional, Functional and Cytochemical Analyses of the veg Gene in *Bacillus subtilis*. *Journal of Biochemistry*, *133*(4), 475–483. https://doi.org/10.1093/jb/mvg062

Gallegos-Monterrosa, R., & Kovács, Á. T. (2023). Phenotypic plasticity: The role of a phosphatase family Rap in the genetic regulation of Bacilli. *Molecular Microbiology*, *120*(1), 20–31. https://doi.org/10.1111/mmi.15060

Garcés-Ruiz, M., Calonne-Salmon, M., Plouznikoff, K., Misson, C., Navarrete-Mier, M., Cranenbrouck, S., & Declerck, S. (2017). Dynamics of Short-Term Phosphorus Uptake by Intact Mycorrhizal and Non-mycorrhizal Maize Plants Grown in a Circulatory Semi-Hydroponic Cultivation System. *Frontiers in Plant Science*, *8*. https://doi.org/10.3389/fpls.2017.01471

García-Gutiérrez, L., Zeriouh, H., Romero, D., Cubero, J., de Vicente, A., & Pérez-García, A. (2013). The antagonistic strain *Bacillus subtilis* UMAF 6639 also confers protection to melon plants against cucurbit powdery mildew by activation of jasmonate- and salicylic acid-dependent defence responses. *Microbial Biotechnology*, *6*(3), 264–274. https://doi.org/10.1111/1751-7915.12028

Garrido, E., Bennett, A. E., Fornoni, J., & Strauss, S. Y. (2010). Variation in arbuscular mycorrhizal fungi colonization modifies the expression of tolerance to above-ground defoliation. *Journal of Ecology*, *98*(1), 43–49. https://doi.org/10.1111/j.1365-2745.2009.01586.x

Gbongue, L.-R., Lalaymia, I., Zeze, A., Delvaux, B., & Declerck, S. (2019). Increased Silicon Acquisition in Bananas Colonized by *Rhizophagus irregularis* MUCL 41833 Reduces the Incidence of *Pseudocercospora fijiensis*. *Frontiers in Plant Science*, *9*. https://doi.org/10.3389/fpls.2018.01977

Gebreslassie, S., Jida, M., Puente, M. L., Covacevich, F., & Belay, Z. (2024). Inoculation of Native Arbuscular Mycorrhizae and *Bacillus subtilis* Can Improve Growth in Vegetable Crops. *International Journal of Microbiology*, *2024*(1). https://doi.org/10.1155/2024/9226715

Genre, A., Chabaud, M., Balzergue, C., Puech-Pagès, V., Novero, M., Rey, T., Fournier, J., Rochange, S., Bécard, G., Bonfante, P., & Barker, D. G. (2013). Short-chain chitin oligomers from arbuscular mycorrhizal fungi trigger nuclear Ca^{2+} spiking in *Medicago truncatula* roots and their production is enhanced by strigolactone. *New Phytologist*, *198*(1), 190–202. https://doi.org/10.1111/nph.12146

Genre, A., Lanfranco, L., Perotto, S., & Bonfante, P. (2020). Unique and common traits in mycorrhizal symbioses. *Nature Reviews Microbiology*, *18*(11), 649–

660. https://doi.org/10.1038/s41579-020-0402-3

Genre, A., & Russo, G. (2016). Does a Common Pathway Transduce Symbiotic Signals in Plant–Microbe Interactions? *Frontiers in Plant Science*, *7*(FEB2016), 96. https://doi.org/10.3389/fpls.2016.00096

Geoghegan, I., Steinberg, G., & Gurr, S. (2017). The Role of the Fungal Cell Wall in the Infection of Plants. *Trends in Microbiology*, *25*(12), 957–967. https://doi.org/10.1016/j.tim.2017.05.015

Ghelardi, E., Salvetti, S., Ceragioli, M., Gueye, S. A., Celandroni, F., & Senesi, S. (2012). Contribution of Surfactin and SwrA to Flagellin Expression, Swimming, and Surface Motility in *Bacillus subtilis*. *Applied and Environmental Microbiology*, *78*(18), 6540–6544. https://doi.org/10.1128/AEM.01341-12

Gilliard, G., Demortier, T., Boubsi, F., Jijakli, M. H., Ongena, M., De Clerck, C., & Deleu, M. (2024). Deciphering the distinct biocontrol activities of lipopeptides fengycin and surfactin through their differential impact on lipid membranes. *Colloids and Surfaces B: Biointerfaces*, *239*, 113933. https://doi.org/10.1016/j.colsurfb.2024.113933

Giovannetti, M., Binci, F., Navazio, L., & Genre, A. (2024a). Fungal signals and calcium-mediated transduction pathways along the plant defence–symbiosis continuum. *New Phytologist*, *242*(4), 1404–1407. https://doi.org/10.1111/nph.19759

Giovannetti, M., Binci, F., Navazio, L., & Genre, A. (2024b). Nonbinary fungal signals and calcium-mediated transduction in plant immunity and symbiosis. *New Phytologist*, *241*(4), 1393–1400. https://doi.org/10.1111/nph.19433

Giovannetti, M., & Genre, A. (2024). Walking on a tightrope: cell wall-associated kinases act as sensors and regulators of immunity and symbiosis. *New Phytologist*, *242*(5), 1851–1853. https://doi.org/10.1111/nph.19634

Girardin, A., Wang, T., Ding, Y., Keller, J., Buendia, L., Gaston, M., Ribeyre, C., Gasciolli, V., Auriac, M.-C., Vernié, T., Bendahmane, A., Ried, M. K., Parniske, M., Morel, P., Vandenbussche, M., Schorderet, M., Reinhardt, D., Delaux, P.-M., Bono, J.-J., & Lefebvre, B. (2019). LCO Receptors Involved in Arbuscular Mycorrhiza Are Functional for Rhizobia Perception in Legumes. *Current Biology*, *29*(24), 4249-4259.e5. https://doi.org/10.1016/j.cub.2019.11.038

Gong, A.-D., Li, H.-P., Yuan, Q.-S., Song, X.-S., Yao, W., He, W.-J., Zhang, J.-B., & Liao, Y.-C. (2015). Antagonistic Mechanism of Iturin A and Plipastatin A from *Bacillus amyloliquefaciens* S76-3 from Wheat Spikes against *Fusarium graminearum*. *PLOS ONE*, *10*(2), e0116871. https://doi.org/10.1371/journal.pone.0116871

Gow, N. A. R., Latge, J.-P., & Munro, C. A. (2017). The Fungal Cell Wall: Structure, Biosynthesis, and Function. *Microbiology Spectrum*, *5*(3). https://doi.org/10.1128/microbiolspec.FUNK-0035-2016

Grau, R. R., de Oña, P., Kunert, M., Leñini, C., Gallegos-Monterrosa, R., Mhatre, E., Vileta, D., Donato, V., Hölscher, T., Boland, W., Kuipers, O. P., & Kovács, Á. T. (2015). A Duo of Potassium-Responsive Histidine Kinases Govern the

Multicellular Destiny of *Bacillus subtilis*. *MBio*, *6*(4), 1–16. https://doi.org/10.1128/mBio.00581-15

Grießhammer, A., de la Cuesta-Zuluaga, J., Müller, P., Gekeler, C., Homolak, J., Chang, H., Schmitt, K., Planker, C., Schmidtchen, V., Gallage, S., Bohn, E., Nguyen, T. H., Hetzer, J., Heikenwälder, M., Huang, K. C., Zahir, T., & Maier, L. (2025). Non-antibiotics disrupt colonization resistance against enteropathogens. *Nature*, 1–9. https://doi.org/10.1038/s41586-025-09217-2

Grubbs, K. J., Bleich, R. M., Santa Maria, K. C., Allen, S. E., Farag, S., Shank, E. A., & Bowers, A. A. (2017). Large-Scale Bioinformatics Analysis of Bacillus Genomes Uncovers Conserved Roles of Natural Products in Bacterial Physiology. *MSystems*, *2*(6), e00040-17. https://doi.org/10.1128/mSystems.00040-17

Guarner, F., & Malagelada, J.-R. (2003). Gut flora in health and disease. *The Lancet*, *361*(9356), 512–519. https://doi.org/10.1016/S0140-6736(03)12489-0

Gutjahr, C., Banba, M., Croset, V., An, K., Miyao, A., An, G., Hirochika, H., Imaizumi-Anraku, H., & Paszkowski, U. (2008). Arbuscular Mycorrhiza–Specific Signaling in Rice Transcends the Common Symbiosis Signaling Pathway. *The Plant Cell*, *20*(11), 2989–3005. https://doi.org/10.1105/tpc.108.062414

Hammer, E. C., Arellano-Caicedo, C., Mafla-Endara, P. M., Kiers, E. T., Shimizu, T., Ohlsson, P., & Aleklett, K. (2024). Hyphal exploration strategies and habitat modification of an arbuscular mycorrhizal fungus in microengineered soil chips. *Fungal Ecology*, *67*, 101302. https://doi.org/10.1016/j.funeco.2023.101302

Hammerstein, P., & Noë, R. (2016). Biological trade and markets. *Philosophical Transactions of the Royal Society B: Biological Sciences*, *371*(1687), 20150101. https://doi.org/10.1098/rstb.2015.0101

Han, Q., Wu, F., Wang, X., Qi, H., Shi, L., Ren, A., Liu, Q., Zhao, M., & Tang, C. (2015). The bacterial lipopeptide iturins induce *Verticillium dahliae* cell death by affecting fungal signalling pathways and mediate plant defence responses involved in pathogen-associated molecular pattern-triggered immunity. *Environmental Microbiology*, *17*(4), 1166–1188. https://doi.org/10.1111/1462-2920.12538

Hanif, A., Zhang, F., Li, P., Li, C., Xu, Y., Zubair, M., Zhang, M., Jia, D., Zhao, X., Liang, J., Majid, T., Yan, J., Farzand, A., Wu, H., Gu, Q., & Gao, X. (2019). Fengycin Produced by *Bacillus amyloliquefaciens* FZB42 Inhibits *Fusarium graminearum* Growth and Mycotoxins Biosynthesis. *Toxins*, *11*(5), 295. https://doi.org/10.3390/toxins11050295

Haq, I. U., Calixto, R. O. da R., Yang, P., dos Santos, G. M. P., Barreto-Bergter, E., & van Elsas, J. D. (2016). Chemotaxis and adherence to fungal surfaces are key components of the behavioral response of *Burkholderia terrae* BS001 to two selected soil fungi. *FEMS Microbiology Ecology*, *92*(11), fiw164. https://doi.org/10.1093/femsec/fiw164

Harwood, C. R., Mouillon, J.-M., Pohl, S., & Arnau, J. (2018). Secondary metabolite

production and the safety of industrially important members of the *Bacillus subtilis* group. *FEMS Microbiology Reviews*, *42*(6), 721–738. https://doi.org/10.1093/femsre/fuy028

He, B., Cai, Q., Qiao, L., Huang, C.-Y., Wang, S., Miao, W., Ha, T., Wang, Y., & Jin, H. (2021). RNA-binding proteins contribute to small RNA loading in plant extracellular vesicles. *Nature Plants*, *7*(3), 342–352. https://doi.org/10.1038/s41477-021-00863-8

He, B., Wang, H., Liu, G., Chen, A., Calvo, A., Cai, Q., & Jin, H. (2023). Fungal small RNAs ride in extracellular vesicles to enter plant cells through clathrin-mediated endocytosis. *Nature Communications*, *14*(1), 4383. https://doi.org/10.1038/s41467-023-40093-4

He, J., Zhang, C., Dai, H., Liu, H., Zhang, X., Yang, J., Chen, X., Zhu, Y., Wang, D., Qi, X., Li, W., Wang, Z., An, G., Yu, N., He, Z., Wang, Y.-F., Xiao, Y., Zhang, P., & Wang, E. (2019). A LysM Receptor Heteromer Mediates Perception of Arbuscular Mycorrhizal Symbiotic Signal in Rice. *Molecular Plant*, *12*(12), 1561–1576. https://doi.org/10.1016/j.molp.2019.10.015

He, X.-H., Critchley, C., & Bledsoe, C. (2003). Nitrogen Transfer Within and Between Plants Through Common Mycorrhizal Networks (CMNs). *Critical Reviews in Plant Sciences*, *22*(6), 531–567. https://doi.org/10.1080/713608315

Henry, G., Deleu, M., Jourdan, E., Thonart, P., & Ongena, M. (2011). The bacterial lipopeptide surfactin targets the lipid fraction of the plant plasma membrane to trigger immune-related defence responses. *Cellular Microbiology*, *13*(11), 1824–1837. https://doi.org/10.1111/j.1462-5822.2011.01664.x

Herold, L., Ordon, J., Hua, C., Kohorn, B. D., Nürnberger, T., DeFalco, T. A., & Zipfel, C. (2024). Arabidopsis WALL-ASSOCIATED KINASES are not required for oligogalacturonide-induced signaling and immunity. *The Plant Cell*, *37*(1). https://doi.org/10.1093/plcell/koae317

Hijri, M., & Sanders, I. R. (2005). Low gene copy number shows that arbuscular mycorrhizal fungi inherit genetically different nuclei. *Nature*, *433*(7022), 160–163. https://doi.org/10.1038/nature03069

Hildebrandt, U., Ouziad, F., Marner, F.-J., & Bothe, H. (2006). The bacterium *Paenibacillus validus* stimulates growth of the arbuscular mycorrhizal fungus *Glomus intraradices* up to the formation of fertile spores. *FEMS Microbiology Letters*, *254*(2), 258–267. https://doi.org/10.1111/j.1574-6968.2005.00027.x

Hiller, E., Off, M., Hermann, A., Vahidinasab, M., Benatto Perino, E. H., Lilge, L., & Hausmann, R. (2024). The influence of growth rate-controlling feeding strategy on the surfactin production in *Bacillus subtilis* bioreactor processes. *Microbial Cell Factories*, *23*(1), 260. https://doi.org/10.1186/s12934-024-02531-w

Hoefler, B. C., Gorzelnik, K. V., Yang, J. Y., Hendricks, N., Dorrestein, P. C., & Straight, P. D. (2012). Enzymatic resistance to the lipopeptide surfactin as identified through imaging mass spectrometry of bacterial competition. *Proceedings of the National Academy of Sciences*, *109*(32), 13082–13087. https://doi.org/10.1073/pnas.1205586109

Hoff, G., Arguelles Arias, A., Boubsi, F., Pršić, J., Meyer, T., Ibrahim, H. M. M., Steels, S., Luzuriaga, P., Legras, A., Franzil, L., Lequart-Pillon, M., Rayon, C., Osorio, V., de Pauw, E., Lara, Y., Deboever, E., de Coninck, B., Jacques, P., Deleu, M., … Ongena, M. (2021). Surfactin Stimulated by Pectin Molecular Patterns and Root Exudates Acts as a Key Driver of the *Bacillus* -Plant Mutualistic Interaction. *MBio*, *12*(6). https://doi.org/10.1128/mBio.01774-21

Holland, S., & Roth, R. (2023). Extracellular Vesicles in the Arbuscular Mycorrhizal Symbiosis: Current Understanding and Future Perspectives. *Molecular Plant-Microbe Interactions®*, *36*(4), 235–244. https://doi.org/10.1094/MPMI-09-22-0189-FI

Hu, Y., You, J., Wang, Y., Long, Y., Wang, S., Pan, F., & Yu, Z. (2022). Biocontrol efficacy of *Bacillus velezensis* strain YS-AT-DS1 against the root-knot nematode *Meloidogyne incognita* in tomato plants. *Frontiers in Microbiology*, *13*, 1035748. https://doi.org/10.3389/fmicb.2022.1035748

Hürter, A.-L., Fort, S., Cottaz, S., Hedrich, R., Geiger, D., & Roelfsema, M. R. G. (2018). Mycorrhizal lipochitinoligosaccharides (LCOs) depolarize root hairs of *Medicago truncatula*. *PLOS ONE*, *13*(5), e0198126. https://doi.org/10.1371/journal.pone.0198126

Ilyaskina, D., Altveş, S., Dong, L., Bouwmeester, H., & El Aidy, S. (2025). Adaptive and metabolic convergence in rhizosphere and gut microbiomes. *Microbiome*, *13*(1), 173. https://doi.org/10.1186/s40168-025-02179-7

Izquierdo-García, L. F., González-Almario, A., Cotes, A. M., & Moreno-Velandia, C. A. (2020). *Trichoderma virens* Gl006 and *Bacillus velezensis* Bs006: a compatible interaction controlling *Fusarium* wilt of cape gooseberry. *Scientific Reports*, *10*(1), 6857. https://doi.org/10.1038/s41598-020-63689-y

Jakobsen, I., & Rosendahl, L. (1990). Carbon flow into soil and external hyphae from roots of mycorrhizal cucumber plants. *New Phytologist*, *115*(1), 77–83. https://doi.org/10.1111/j.1469-8137.1990.tb00924.x

James, T. Y., Kauff, F., Schoch, C. L., Matheny, P. B., Hofstetter, V., Cox, C. J., Celio, G., Gueidan, C., Fraker, E., Miadlikowska, J., Lumbsch, H. T., Rauhut, A., Reeb, V., Arnold, A. E., Amtoft, A., Stajich, J. E., Hosaka, K., Sung, G.-H., Johnson, D., … Vilgalys, R. (2006). Reconstructing the early evolution of Fungi using a six-gene phylogeny. *Nature*, *443*(7113), 818–822. https://doi.org/10.1038/nature05110

Jany, J., & Pawlowska, T. E. (2010). Multinucleate Spores Contribute to Evolutionary Longevity of Asexual Glomeromycota. *The American Naturalist*, *175*(4), 424–435. https://doi.org/10.1086/650725

Jautzus, T., van Gestel, J., & Kovács, Á. T. (2022). Complex extracellular biology drives surface competition during colony expansion in *Bacillus subtilis*. *The ISME Journal*, *16*(10), 2320–2328. https://doi.org/10.1038/s41396-022-01279-8

Jeffries, P., Gianinazzi, S., Perotto, S., Turnau, K., & Barea, J.-M. (2003). The contribution of arbuscular mycorrhizal fungi in sustainable maintenance of plant

health and soil fertility. *Biology and Fertility of Soils*, *37*(1), 1–16. https://doi.org/10.1007/s00374-002-0546-5

Jian, Y., Gong, D., Wang, Z., Liu, L., He, J., Han, X., & Tsuda, K. (2023). How plants manage pathogen infection. *EMBO Reports*, *25*(1), 31–44. https://doi.org/10.1038/s44319-023-00023-3

Jiang, C.-H., Liao, M.-J., Wang, H.-K., Zheng, M.-Z., Xu, J.-J., & Guo, J.-H. (2018). *Bacillus velezensis*, a potential and efficient biocontrol agent in control of pepper gray mold caused by *Botrytis cinerea*. *Biological Control*, *126*, 147–157. https://doi.org/10.1016/j.biocontrol.2018.07.017

Jiang, F., Zhang, L., Zhou, J., George, T. S., & Feng, G. (2021). Arbuscular mycorrhizal fungi enhance mineralisation of organic phosphorus by carrying bacteria along their extraradical hyphae. *New Phytologist*, *230*(1), 304–315. https://doi.org/10.1111/nph.17081

Jin, Y., Chen, Z., Yang, J., Mysore, K. S., Wen, J., Huang, J., Yu, N., & Wang, E. (2018). IPD3 and IPD3L function redundantly in rhizobial and mycorrhizal symbioses. *Frontiers in Plant Science*, *9*, 337886. https://doi.org/10.3389/FPLS.2018.00267/BIBTEX

Jin, Y., Zhu, H., Luo, S., Yang, W., Zhang, L., Li, S., Jin, Q., Cao, Q., Sun, S., & Xiao, M. (2019). Role of Maize Root Exudates in Promotion of Colonization of *Bacillus velezensis* Strain S3-1 in Rhizosphere Soil and Root Tissue. *Current Microbiology*, *76*(7), 855–862. https://doi.org/10.1007/s00284-019-01699-4

Jin, Z., Duan, S., Declerck, S., & Zhang, L. (2025). Bacterial community in the hyphosphere of an arbuscular mycorrhizal fungus differs from that in the surrounding environment and is influenced by hyphal disruption. *Mycorrhiza*, *35*(1), 10. https://doi.org/10.1007/s00572-025-01186-8

Jin, Z., Jiang, F., Wang, L., Declerck, S., Feng, G., & Zhang, L. (2024). Arbuscular mycorrhizal fungi and *Streptomyces*: brothers in arms to shape the structure and function of the hyphosphere microbiome in the early stage of interaction. *Microbiome*, *12*(1), 83. https://doi.org/10.1186/s40168-024-01811-2

Johnson, D., & Gilbert, L. (2015). Interplant signalling through hyphal networks. *New Phytologist*, *205*(4), 1448–1453. https://doi.org/10.1111/nph.13115

Jourdan, E., Henry, G., Duby, F., Dommes, J., Barthélemy, J. P., Thonart, P., & Ongena, M. (2009). Insights into the defense-related events occurring in plant cells following perception of surfactin-type lipopeptide from *Bacillus subtilis*. *Molecular Plant-Microbe Interactions : MPMI*, *22*(4), 456–468. https://doi.org/10.1094/MPMI-22-4-0456

Jovic, D., Liang, X., Zeng, H., Lin, L., Xu, F., & Luo, Y. (2022). Single-cell RNA sequencing technologies and applications: A brief overview. *Clinical and Translational Medicine*, *12*(3), e694. https://doi.org/10.1002/ctm2.694

Jung, S. C., Martinez-Medina, A., Lopez-Raez, J. A., & Pozo, M. J. (2012). Mycorrhiza-Induced Resistance and Priming of Plant Defenses. *Journal of Chemical Ecology*, *38*(6), 651–664. https://doi.org/10.1007/s10886-012-0134-6

Kafri, M., Metzl-Raz, E., Jona, G., & Barkai, N. (2016). The Cost of Protein

Production. *Cell Reports*, *14*(1), 22–31. https://doi.org/10.1016/j.celrep.2015.12.015

Kakar, K. U., Ren, X. -l., Nawaz, Z., Cui, Z. -Q., Li, B., Xie, G. -L., Hassan, M. A., Ali, E., & Sun, G. -C. (2016). A consortium of rhizobacterial strains and biochemical growth elicitors improve cold and drought stress tolerance in rice (*Oryza sativa* L.). *Plant Biology*, *18*(3), 471–483. https://doi.org/10.1111/plb.12427

Kalamara, M., Spacapan, M., Mandic-Mulec, I., & Stanley-Wall, N. R. (2018). Social behaviours by *Bacillus subtilis* : quorum sensing, kin discrimination and beyond. *Molecular Microbiology*, *110*(6), 863–878. https://doi.org/10.1111/mmi.14127

Kamada, N., Chen, G. Y., Inohara, N., & Núñez, G. (2013). Control of pathogens and pathobionts by the gut microbiota. *Nature Immunology 2013 14:7*, *14*(7), 685–690. https://doi.org/10.1038/ni.2608

Kameoka, H., & Gutjahr, C. (2022). Functions of Lipids in Development and Reproduction of Arbuscular Mycorrhizal Fungi. *Plant and Cell Physiology*, *63*(10), 1356–1365. https://doi.org/10.1093/pcp/pcac113

Kameoka, H., Tsutsui, I., Saito, K., Kikuchi, Y., Handa, Y., Ezawa, T., Hayashi, H., Kawaguchi, M., & Akiyama, K. (2019). Stimulation of asymbiotic sporulation in arbuscular mycorrhizal fungi by fatty acids. *Nature Microbiology*, *4*(10), 1654–1660. https://doi.org/10.1038/s41564-019-0485-7

Kaminsky, L. M., Trexler, R. V., Malik, R. J., Hockett, K. L., & Bell, T. H. (2019). The Inherent Conflicts in Developing Soil Microbial Inoculants. *Trends in Biotechnology*, *37*(2), 140–151. https://doi.org/10.1016/j.tibtech.2018.11.011

Kang, X., Zhang, W., Cai, X., Zhu, T., Xue, Y., & Liu, C. (2018). *Bacillus velezensis* CC09: A Potential 'Vaccine' for Controlling Wheat Diseases. *Molecular Plant-Microbe Interactions®*, *31*(6), 623–632. https://doi.org/10.1094/MPMI-09-17-0227-R

Karygianni, L., Ren, Z., Koo, H., & Thurnheer, T. (2020). Biofilm Matrixome: Extracellular Components in Structured Microbial Communities. *Trends in Microbiology*, *28*(8), 668–681. https://doi.org/10.1016/j.tim.2020.03.016

Kaspar, F., Neubauer, P., & Gimpel, M. (2019). Bioactive Secondary Metabolites from *Bacillus subtilis* : A Comprehensive Review. *Journal of Natural Products*, *82*(7), 2038–2053. https://doi.org/10.1021/acs.jnatprod.9b00110

Kawagoe, Y., Shiraishi, S., Kondo, H., Yamamoto, S., Aoki, Y., & Suzuki, S. (2015). Cyclic lipopeptide iturin A structure-dependently induces defense response in *Arabidopsis* plants by activating SA and JA signaling pathways. *Biochemical and Biophysical Research Communications*, *460*(4), 1015–1020. https://doi.org/10.1016/j.bbrc.2015.03.143

Kee, Y. J., Ogawa, S., Ichihashi, Y., Shirasu, K., & Yoshida, S. (2023). Strigolactones in Rhizosphere Communication: Multiple Molecules With Diverse Functions. *Plant And Cell Physiology*, *64*(9), 955–966. https://doi.org/10.1093/pcp/pcad055

Kelly, S., Hansen, S. B., Rübsam, H., Saake, P., Pedersen, E. B., Gysel, K., Madland,

E., Wu, S., Wawra, S., Reid, D., Sullivan, J. T., Blahovska, Z., Vinther, M., Muszynski, A., Azadi, P., Thygesen, M. B., Aachmann, F. L., Ronson, C. W., Zuccaro, A., … Stougaard, J. (2023). A glycan receptor kinase facilitates intracellular accommodation of arbuscular mycorrhiza and symbiotic rhizobia in the legume *Lotus japonicus*. *PLOS Biology*, *21*(5), e3002127. https://doi.org/10.1371/journal.pbio.3002127

Khezri, M., Jouzani, G. S., & Ahmadzadeh, M. (2016). *Fusarium culmorum* affects expression of biofilm formation key genes in *Bacillus subtilis*. *Brazilian Journal of Microbiology*, *47*(1), 47–54. https://doi.org/10.1016/j.bjm.2015.11.019

Khokhani, D., Carrera Carriel, C., Vayla, S., Irving, T. B., Stonoha-Arther, C., Keller, N. P., & Ané, J.-M. (2021). Deciphering the Chitin Code in Plant Symbiosis, Defense, and Microbial Networks. *Annual Review of Microbiology*, *75*(1), 583–607. https://doi.org/10.1146/annurev-micro-051921-114809

Kiddee, S., Wongdee, J., Piromyou, P., Songwattana, P., Greetatorn, T., Boonkerd, N., Teaumroong, N., Saito, K., & Tittabutr, P. (2024). Unveiling the tripartite synergistic interaction of plant-arbuscular mycorrhizal fungus symbiosis by endophytic *Bacillus velezensis* S141 in *Lotus japonicus*. *Symbiosis*, *92*(3), 355–367. https://doi.org/10.1007/s13199-024-00975-7

Kiers, E. T., Duhamel, M., Beesetty, Y., Mensah, J. A., Franken, O., Verbruggen, E., Fellbaum, C. R., Kowalchuk, G. A., Hart, M. M., Bago, A., Palmer, T. M., West, S. A., Vandenkoornhuyse, P., Jansa, J., & Bücking, H. (2011). Reciprocal Rewards Stabilize Cooperation in the Mycorrhizal Symbiosis. *Science*, *333*(6044), 880–882. https://doi.org/10.1126/science.1208473

Kierul, K., Voigt, B., Albrecht, D., Chen, X.-H., Carvalhais, L. C., & Borriss, R. (2015). Influence of root exudates on the extracellular proteome of the plant growth-promoting bacterium *Bacillus amyloliquefaciens* FZB42. *Microbiology*, *161*(1), 131–147. https://doi.org/10.1099/mic.0.083576-0

Kiesewalter, H. T., Lozano-Andrade, C. N., Wibowo, M., Strube, M. L., Maróti, G., Snyder, D., Jørgensen, T. S., Larsen, T. O., Cooper, V. S., Weber, T., & Kovács, Á. T. (2021). Genomic and Chemical Diversity of *Bacillus subtilis* Secondary Metabolites against Plant Pathogenic Fungi. *MSystems*, *6*(1). https://doi.org/10.1128/mSystems.00770-20

Kistner, C., & Parniske, M. (2002). Evolution of signal transduction in intracellular symbiosis. *Trends in Plant Science*, *7*(11), 511–518. https://doi.org/10.1016/S1360-1385(02)02356-7

Kjeldgaard, B., Listian, S. A., Ramaswamhi, V., Richter, A., Kiesewalter, H. T., & Kovács, Á. T. (2019). Fungal hyphae colonization by *Bacillus subtilis* relies on biofilm matrix components. *Biofilm*, *1*, 100007. https://doi.org/10.1016/j.bioflm.2019.100007

Kloppholz, S., Kuhn, H., & Requena, N. (2011). A Secreted Fungal Effector of *Glomus intraradices* Promotes Symbiotic Biotrophy. *Current Biology*, *21*(14), 1204–1209. https://doi.org/10.1016/j.cub.2011.06.044

Knights, H. E., Jorrin, B., Haskett, T. L., & Poole, P. S. (2021). Deciphering bacterial

mechanisms of root colonization. *Environmental Microbiology Reports*, *13*(4), 428–444. https://doi.org/10.1111/1758-2229.12934

Kobayashi, K. (2015). Plant methyl salicylate induces defense responses in the rhizobacterium *Bacillus subtilis*. *Environmental Microbiology*, *17*(4), 1365–1376. https://doi.org/10.1111/1462-2920.12613

Kodama, K., Rich, M. K., Yoda, A., Shimazaki, S., Xie, X., Akiyama, K., Mizuno, Y., Komatsu, A., Luo, Y., Suzuki, H., Kameoka, H., Libourel, C., Keller, J., Sakakibara, K., Nishiyama, T., Nakagawa, T., Mashiguchi, K., Uchida, K., Yoneyama, K., … Kyozuka, J. (2022). An ancestral function of strigolactones as symbiotic rhizosphere signals. *Nature Communications*, *13*(1), 3974. https://doi.org/10.1038/s41467-022-31708-3

Köhl, J., Kolnaar, R., & Ravensberg, W. J. (2019). Mode of Action of Microbial Biological Control Agents Against Plant Diseases: Relevance Beyond Efficacy. *Frontiers in Plant Science*, *10*(845), 1–19. https://doi.org/10.3389/fpls.2019.00845

Kohlmeier, S., Smits, T. H. M., Ford, R. M., Keel, C., Harms, H., & Wick, L. Y. (2005a). Taking the fungal highway: mobilization of pollutant-degrading bacteria by fungi. *Environmental Science & Technology*, *39*(12), 4640–4646. https://doi.org/10.1021/ES047979Z

Kohlmeier, S., Smits, T. H. M., Ford, R. M., Keel, C., Harms, H., & Wick, L. Y. (2005b). Taking the Fungal Highway: Mobilization of Pollutant-Degrading Bacteria by Fungi. *Environmental Science & Technology*, *39*(12), 4640–4646. https://doi.org/10.1021/es047979z

Kongala, S. I., & Kondreddy, A. (2023). A review on plant and pathogen derived carbohydrates, oligosaccharides and their role in plant's immunity. *Carbohydrate Polymer Technologies and Applications*, *6*, 100330. https://doi.org/10.1016/j.carpta.2023.100330

Köster, P., DeFalco, T. A., & Zipfel, C. (2022). Ca 2+ signals in plant immunity. *The EMBO Journal*, *41*(12). https://doi.org/10.15252/embj.2022110741

Kovács, Á. T. (2019). *Bacillus subtilis*. *Trends in Microbiology*, *27*(8), 724–725. https://doi.org/10.1016/j.tim.2019.03.008

Kranawetter, C., Zeng, S., Joshi, T., & Sumner, L. W. (2021). A *Medicago truncatula* Metabolite Atlas Enables the Visualization of Differential Accumulation of Metabolites in Root Tissues. *Metabolites*, *11*(4), 238. https://doi.org/10.3390/metabo11040238

Kumar, A., Gao, J.-P., & Murray, J. D. (2025a). How plants discriminate mutualistic symbiosis from immunity. *Molecular Plant*, *18*(10), 1616–1618. https://doi.org/10.1016/j.molp.2025.08.005

Kumar, A., Sun, R., Habib, B., Deng, T., Bencivenga-Barry, N. A., Palm, N. W., Ivanov, I. I., Tamblyn, R., & Goodman, A. L. (2025b). Identification of medication–microbiome interactions that affect gut infection. *Nature*, 1–10. https://doi.org/10.1038/s41586-025-09273-8

Laforge, N., Calabre, M., Jules, M., & Planson, A.-G. (2025). Multiplex Genome

Editing and Regulation in *Bacillus subtilis* with CRISPR-MAD7. *ACS Synthetic Biology*, *14*(8), 3142–3153. https://doi.org/10.1021/acssynbio.5c00274

Lakshmanan, V., Castaneda, R., Rudrappa, T., & Bais, H. P. (2013). Root transcriptome analysis of *Arabidopsis thaliana* exposed to beneficial *Bacillus subtilis* FB17 rhizobacteria revealed genes for bacterial recruitment and plant defense independent of malate efflux. *Planta*, *238*(4), 657–668. https://doi.org/10.1007/s00425-013-1920-2

Lam, A. H. C., Cooke, A., Wright, H., Lawson, D. M., & Charpentier, M. (2024). Evolution of endosymbiosis-mediated nuclear calcium signaling in land plants. *Current Biology*, *34*(10), 2212-2220.e7. https://doi.org/10.1016/j.cub.2024.03.063

Lambou, K., Tharreau, D., Kohler, A., Sirven, C., Marguerettaz, M., Barbisan, C., Sexton, A. C., Kellner, E. M., Martin, F., Howlett, B. J., Orbach, M. J., & Lebrun, M.-H. (2008). Fungi have three tetraspanin families with distinct functions. *BMC Genomics*, *9*(1), 63. https://doi.org/10.1186/1471-2164-9-63

Lanfranco, L., Bonfante, P., & Genre, A. (2016). The Mutualistic Interaction between Plants and Arbuscular Mycorrhizal Fungi. *Microbiology Spectrum*, *4*(6). https://doi.org/10.1128/microbiolspec.FUNK-0012-2016

Lanfranco, L., Fiorilli, V., Venice, F., & Bonfante, P. (2018). Strigolactones cross the kingdoms: plants, fungi, and bacteria in the arbuscular mycorrhizal symbiosis. *Journal of Experimental Botany*, *69*(9), 2175–2188. https://doi.org/10.1093/jxb/erx432

Lastovetsky, O. A., Caruso, T., Brennan, F. P., Wall, D., Pylni, S., & Doyle, E. (2024). Spores of arbuscular mycorrhizal fungi host surprisingly diverse communities of endobacteria. *New Phytologist*, *242*(4), 1785–1797. https://doi.org/10.1111/nph.19605

Le Mire, G., Nguyen, M. L., Fassotte, B., Du Jardin, P., Verheggen, F., Delaplace, P., & Jijakli, M. H. (2016). Review: implementing plant biostimulants and biocontrol strategies in the agroecological management of cultivated ecosystems. *BASE*, 299–313. https://doi.org/10.25518/1780-4507.12717

Leach, J. E., Triplett, L. R., Argueso, C. T., & Trivedi, P. (2017). Communication in the Phytobiome. *Cell*, *169*(4), 587–596. https://doi.org/10.1016/j.cell.2017.04.025

Leake, J., Johnson, D., Donnelly, D., Muckle, G., Boddy, L., & Read, D. (2004). Networks of power and influence: the role of mycorrhizal mycelium in controlling plant communities and agroecosystem functioning. *Canadian Journal of Botany*, *82*(8), 1016–1045. https://doi.org/10.1139/b04-060

Leconte, A., Jacquin, J., Duban, M., Deweer, C., Trapet, P., Laruelle, F., Farce, A., Compère, P., Sahmer, K., Fiévet, V., Hoste, A., Siah, A., Lounès-Hadj Sahraoui, A., Jacques, P., Coutte, F., Deleu, M., & Muchembled, J. (2024). Deciphering the mechanisms involved in reduced sensitivity to azoles and fengycin lipopeptide in Venturia inaequalis. *Microbiological Research*, *286*, 127816. https://doi.org/10.1016/j.micres.2024.127816

Ledford, W. C., Silvestri, A., Fiorilli, V., Roth, R., Rubio-Somoza, I., & Lanfranco, L. (2024). A journey into the world of small RNAs in the arbuscular mycorrhizal symbiosis. *New Phytologist*, *242*(4), 1534–1544. https://doi.org/10.1111/nph.19394

Lee, E.-H., Eo, J.-K., Ka, K.-H., & Eom, A.-H. (2013). Diversity of Arbuscular Mycorrhizal Fungi and Their Roles in Ecosystems. *Mycobiology*, *41*(3), 121–125. https://doi.org/10.5941/MYCO.2013.41.3.121

Leontidou, K., Genitsaris, S., Papadopoulou, A., Kamou, N., Bosmali, I., Matsi, T., Madesis, P., Vokou, D., Karamanoli, K., & Mellidou, I. (2020). Plant growth promoting rhizobacteria isolated from halophytes and drought-tolerant plants: genomic characterisation and exploration of phyto-beneficial traits. *Scientific Reports*, *10*(1), 14857. https://doi.org/10.1038/s41598-020-71652-0

Li, T., Shi, X., Wang, J., Zhou, Y., Wang, T., Xu, Y., Xu, Z., Raza, W., Liu, D., & Shen, Q. (2025). Turning antagonists into allies: Bacterial-fungal interactions enhance the efficacy of controlling *Fusarium* wilt disease. *Science Advances*, *11*(7), 5089. https://doi.org/10.1126/sciadv.ads5089

Li, T., Tang, J., Karuppiah, V., Li, Y., Xu, N., & Chen, J. (2020). Co-culture of *Trichoderma atroviride* SG3403 and *Bacillus subtilis* 22 improves the production of antifungal secondary metabolites. *Biological Control*, *140*, 104122. https://doi.org/10.1016/j.biocontrol.2019.104122

Li, X. R., Sun, J., Albinsky, D., Zarrabian, D., Hull, R., Lee, T., Jarratt-Barnham, E., Chiu, C. H., Jacobsen, A., Soumpourou, E., Albanese, A., Kohlen, W., Luginbuehl, L. H., Guillotin, B., Lawrensen, T., Lin, H., Murray, J., Wallington, E., Harwood, W., … Oldroyd, G. E. D. (2022). Nutrient regulation of lipochitooligosaccharide recognition in plants via NSP1 and NSP2. *Nature Communications 2022 13:1*, *13*(1), 1–15. https://doi.org/10.1038/s41467-022-33908-3

Li, X., Zhao, R., Li, D., Wang, G., Bei, S., Ju, X., An, R., Li, L., Kuyper, T. W., Christie, P., Bender, F. S., Veen, C., van der Heijden, M. G. A., van der Putten, W. H., Zhang, F., Butterbach-Bahl, K., & Zhang, J. (2023). Mycorrhiza-mediated recruitment of complete denitrifying *Pseudomonas* reduces N2O emissions from soil. *Microbiome*, *11*(1), 45. https://doi.org/10.1186/s40168-023-01466-5

Liang, X., Ishfaq, S., Liu, Y., Jijakli, M. H., Zhou, X., Yang, X., & Guo, W. (2024). Identification and genomic insights into a strain of *Bacillus velezensis* with phytopathogen-inhibiting and plant growth-promoting properties. *Microbiological Research*, *285*, 127745. https://doi.org/10.1016/j.micres.2024.127745

Liu, H., Li, T., Li, Y., Wang, X., & Chen, J. (2022). Effects of *Trichoderma atroviride* SG3403 and *Bacillus subtilis* 22 on the Biocontrol of Wheat Head Blight. *Journal of Fungi*, *8*(12), 1250. https://doi.org/10.3390/jof8121250

Liu, Q., Cheng, L., Nian, H., Jin, J., & Lian, T. (2023). Linking plant functional genes to rhizosphere microbes: a review. *Plant Biotechnology Journal*, *21*(5), 902–

917. https://doi.org/10.1111/pbi.13950

Liu, Y., Feng, H., Chen, L., Zhang, H., Dong, X., Xiong, Q., & Zhang, R. (2020a). Root-Secreted Spermine Binds to *Bacillus amyloliquefaciens* SQR9 Histidine Kinase KinD and Modulates Biofilm Formation. *Molecular Plant-Microbe Interactions®*, *33*(3), 423–432. https://doi.org/10.1094/MPMI-07-19-0201-R

Liu, Y., Feng, H., Fu, R., Zhang, N., Du, W., Shen, Q., & Zhang, R. (2020b). Induced root-secreted d-galactose functions as a chemoattractant and enhances the biofilm formation of *Bacillus velezensis* SQR9 in an McpA-dependent manner. *Applied Microbiology and Biotechnology*, *104*(2), 785–797. https://doi.org/10.1007/s00253-019-10265-8

Liu, Y., Kyle, S., & Straight, P. D. (2018). Antibiotic Stimulation of a *Bacillus subtilis* Migratory Response. *MSphere*, *3*(1). https://doi.org/10.1128/mSphere.00586-17

Liu, Y., Xu, Z., Chen, L., Xun, W., Shu, X., Chen, Y., Sun, X., Wang, Z., Ren, Y., Shen, Q., & Zhang, R. (2024a). Root colonization by beneficial rhizobacteria. *FEMS Microbiology Reviews*, *48*(1), 1–20. https://doi.org/10.1093/femsre/fuad066

Liu, Y., Zhang, H., Wang, J., Gao, W., Sun, X., Xiong, Q., Shu, X., Miao, Y., Shen, Q., Xun, W., & Zhang, R. (2024b). Nonpathogenic *Pseudomonas syringae* derivatives and its metabolites trigger the plant "cry for help" response to assemble disease suppressing and growth promoting rhizomicrobiome. *Nature Communications*, *15*(1), 1907. https://doi.org/10.1038/s41467-024-46254-3

Liu, Y., Zhang, N., Qiu, M., Feng, H., Vivanco, J. M., Shen, Q., & Zhang, R. (2014). Enhanced rhizosphere colonization of beneficial *Bacillus amyloliquefaciens* SQR9 by pathogen infection. *FEMS Microbiology Letters*, *353*(1), 49–56. https://doi.org/10.1111/1574-6968.12406

Loján, P., Demortier, M., Velivelli, S. L. S., Pfeiffer, S., Suárez, J. P., de Vos, P., Prestwich, B. D., Sessitsch, A., & Declerck, S. (2017). Impact of plant growth-promoting rhizobacteria on root colonization potential and life cycle of *Rhizophagus irregularis* following co-entrapment into alginate beads. *Journal of Applied Microbiology*, *122*(2), 429–440. https://doi.org/10.1111/jam.13355

Lopes, L. D., & Schachtman, D. P. (2023). Rhizosphere and bulk soil bacterial community succession is influenced more by changes in soil properties than in rhizosphere metabolites across a maize growing season. *Applied Soil Ecology*, *189*, 104960. https://doi.org/10.1016/j.apsoil.2023.104960

Lopez-Gomollon, S., & Baulcombe, D. C. (2022). Roles of RNA silencing in viral and non-viral plant immunity and in the crosstalk between disease resistance systems. *Nature Reviews Molecular Cell Biology*, *23*(10), 645–662. https://doi.org/10.1038/s41580-022-00496-5

Lu, H., Qian, S., Muhammad, U., Jiang, X., Han, J., & Lu, Z. (2016). Effect of fructose on promoting fengycin biosynthesis in *Bacillus amyloliquefaciens* fmb-60. *Journal of Applied Microbiology*, *121*(6), 1653–1664. https://doi.org/10.1111/jam.13291

Luginbuehl, L. H., Menard, G. N., Kurup, S., Van Erp, H., Radhakrishnan, G. V.,

Breakspear, A., Oldroyd, G. E. D., & Eastmond, P. J. (2017). Fatty acids in arbuscular mycorrhizal fungi are synthesized by the host plant. *Science*, *356*(6343), 1175–1178. https://doi.org/10.1126/science.aan0081

Luginbuehl, L. H., & Oldroyd, G. E. D. (2017). Understanding the Arbuscule at the Heart of Endomycorrhizal Symbioses in Plants. *Current Biology*, *27*(17), R952–R963. https://doi.org/10.1016/j.cub.2017.06.042

Luna-Bulbarela, A., Romero-Gutiérrez, M. T., Tinoco-Valencia, R., Ortiz, E., Martínez-Romero, M. E., Galindo, E., & Serrano-Carreón, L. (2024). Response of *Bacillus velezensis* 83 to interaction with *Colletotrichum gloeosporioides* resembles a Greek phalanx-style formation: A stress resistant phenotype with antibiosis capacity. *Microbiological Research*, *280*, 127592. https://doi.org/10.1016/j.micres.2023.127592

Luna-Bulbarela, A., Tinoco-Valencia, R., Corzo, G., Kazuma, K., Konno, K., Galindo, E., & Serrano-Carreón, L. (2018). Effects of bacillomycin D homologues produced by *Bacillus amyloliquefaciens* 83 on growth and viability of *Colletotrichum gloeosporioides* at different physiological stages. *Biological Control*, *127*, 145–154. https://doi.org/10.1016/j.biocontrol.2018.08.004

Lundberg, D., Stjerndahl, M., & Holmberg, K. (2023). Ester-based surfactants: Are they stable enough? *Journal of Surfactants and Detergents*, *26*(3), 229–236. https://doi.org/10.1002/jsde.12628

Luo, C., Zhou, H., Zou, J., Wang, X., Zhang, R., Xiang, Y., & Chen, Z. (2015). Bacillomycin L and surfactin contribute synergistically to the phenotypic features of *Bacillus subtilis* 916 and the biocontrol of rice sheath blight induced by *Rhizoctonia solani*. *Applied Microbiology and Biotechnology*, *99*(4), 1897–1910. https://doi.org/10.1007/s00253-014-6195-4

Luo, X., Jiang, J., Zhou, J., Chen, J., Cheng, B., & Li, X. (2024). MyC Factor Analogue CO5 Promotes the Growth of *Lotus japonicus* and Enhances Stress Resistance by Activating the Expression of Relevant Genes. *Journal of Fungi*, *10*(7), 458. https://doi.org/10.3390/jof10070458

Luthfiana, N., Inamura, N., Tantriani, Sato, T., Saito, K., Oikawa, A., Chen, W., & Tawaraya, K. (2021). Metabolite profiling of the hyphal exudates of *Rhizophagus clarus* and *Rhizophagus irregularis* under phosphorus deficiency. *Mycorrhiza*, *31*(3), 403–412. https://doi.org/10.1007/s00572-020-01016-z

Lutz, S., Bodenhausen, N., Hess, J., Valzano-Held, A., Waelchli, J., Deslandes-Hérold, G., Schlaeppi, K., & van der Heijden, M. G. A. (2023). Soil microbiome indicators can predict crop growth response to large-scale inoculation with arbuscular mycorrhizal fungi. *Nature Microbiology*, *8*(12), 2277–2289. https://doi.org/10.1038/s41564-023-01520-w

Lynch, D. V., & Dunn, T. M. (2004). An introduction to plant sphingolipids and a review of recent advances in understanding their metabolism and function. *New Phytologist*, *161*(3), 677–702. https://doi.org/10.1111/j.1469-8137.2004.00992.x

Lyng, M., & Kovács, Á. T. (2023). Frenemies of the soil: *Bacillus* and *Pseudomonas*

interspecies interactions. *Trends in Microbiology*, *31*(8), 845–857. https://doi.org/10.1016/j.tim.2023.02.003

Lyng, M., Þórisdóttir, B., Sveinsdóttir, S. H., Hansen, M. L., Jelsbak, L., Maróti, G., & Kovács, Á. T. (2024). Taxonomy of *Pseudomonas* spp. determines interactions with *Bacillus subtilis*. *MSystems*, *9*(10). https://doi.org/10.1128/msystems.00212-24

Maan, H., Itkin, M., Malitsky, S., Friedman, J., & Kolodkin-Gal, I. (2022). Resolving the conflict between antibiotic production and rapid growth by recognition of peptidoglycan of susceptible competitors. *Nature Communications*, *13*(1), 431. https://doi.org/10.1038/s41467-021-27904-2

MacLean, A. M., Bravo, A., & Harrison, M. J. (2017). Plant Signaling and Metabolic Pathways Enabling Arbuscular Mycorrhizal Symbiosis. *The Plant Cell*, *29*(10), 2319–2335. https://doi.org/10.1105/tpc.17.00555

Maillet, F., Poinsot, V., André, O., Puech-Pagès, V., Haouy, A., Gueunier, M., Cromer, L., Giraudet, D., Formey, D., Niebel, A., Martinez, E. A., Driguez, H., Bécard, G., & Dénarié, J. (2011). Fungal lipochitooligosaccharide symbiotic signals in arbuscular mycorrhiza. *Nature*, *469*(7328), 58–63. https://doi.org/10.1038/nature09622

Makechemu, M., Goto, Y., Zbinden, H., Widrig, V., Keller, B., & Zipfel, C. (2024). Chitin soil amendment triggers systemic plant disease resistance through enhanced pattern-triggered immunity. *BioRxiv*, 2024.12.08.627391. https://doi.org/10.1101/2024.12.08.627391

Mantil, E., Buznytska, I., Daly, G., Ianoul, A., & Avis, T. J. (2019). Role of Lipid Composition in the Interaction and Activity of the Antimicrobial Compound Fengycin with Complex Membrane Models. *The Journal of Membrane Biology*, *252*(6), 627–638. https://doi.org/10.1007/s00232-019-00100-6

Marrone, P. G. (2024). Status of the biopesticide market and prospects for new bioherbicides. *Pest Management Science*, *80*(1), 81–86. https://doi.org/10.1002/ps.7403

Martin, F. M., Uroz, S., & Barker, D. G. (2017). Ancestral alliances: Plant mutualistic symbioses with fungi and bacteria. *Science*, *356*(6340). https://doi.org/10.1126/science.aad4501

Martin, M., Dragoš, A., Otto, S. B., Schäfer, D., Brix, S., Maróti, G., & Kovács, Á. T. (2020). Cheaters shape the evolution of phenotypic heterogeneity in *Bacillus subtilis* biofilms. *The ISME Journal*, *14*(9), 2302–2312. https://doi.org/10.1038/s41396-020-0685-4

Massalha, H., Korenblum, E., Malitsky, S., Shapiro, O. H., & Aharoni, A. (2017). Live imaging of root–bacteria interactions in a microfluidics setup. *Proceedings of the National Academy of Sciences*, *114*(17), 4549–4554. https://doi.org/10.1073/pnas.1618584114

Mattei, B., Lira, R. B., Perez, K. R., & Riske, K. A. (2017). Membrane permeabilization induced by Triton X-100: The role of membrane phase state and edge tension. *Chemistry and Physics of Lipids*, *202*, 28–37.

https://doi.org/10.1016/j.chemphyslip.2016.11.009

Mauch-Mani, B., Baccelli, I., Luna, E., & Flors, V. (2017). Defense Priming: An Adaptive Part of Induced Resistance. *Annual Review of Plant Biology*, *68*(1), 485–512. https://doi.org/10.1146/annurev-arplant-042916-041132

Maximo, M. F., Fill, T. P., & Rodrigues, M. L. (2023). A Close Look into the Composition and Functions of Fungal Extracellular Vesicles Produced by Phytopathogens. *Molecular Plant-Microbe Interactions®*, *36*(4), 228–234. https://doi.org/10.1094/MPMI-09-22-0184-FI

Mayjonade, B., Zamar, R., Carrere, S., & Roux, F. (2024). The relative effects of abiotic and biotic factors in explaining the structure of soil bacterial communities at diverse taxonomic levels. *BioRxiv*, 2024.10.29.620845. https://doi.org/10.1101/2024.10.29.620845

Mazheika, I., Voronko, O., Kolomiets, O., & Kamzolkina, O. (2024). Instantaneous change in hyphal diameter in basidiomycete fungi. In *bioRxiv* (p. 2024.02.12.579893). Cold Spring Harbor Laboratory. https://doi.org/10.1101/2024.02.12.579893

Medeot, D. B., Bertorello-Cuenca, M., Liaudat, J. P., Alvarez, F., Flores-Cáceres, M. L., & Jofré, E. (2017). Improvement of biomass and cyclic lipopeptides production in *Bacillus amyloliquefaciens* MEP218 by modifying carbon and nitrogen sources and ratios of the culture media. *Biological Control*, *115*, 119–128. https://doi.org/10.1016/j.biocontrol.2017.10.002

Mejri, S., Siah, A., Coutte, F., Magnin-Robert, M., Randoux, B., Tisserant, B., Krier, F., Jacques, P., Reignault, P., & Halama, P. (2018). Biocontrol of the wheat pathogen *Zymoseptoria tritici* using cyclic lipopeptides from *Bacillus subtilis*. *Environmental Science and Pollution Research*, *25*(30), 29822–29833. https://doi.org/10.1007/s11356-017-9241-9

Mendes, R., Kruijt, M., de Bruijn, I., Dekkers, E., van der Voort, M., Schneider, J. H. M., Piceno, Y. M., DeSantis, T. Z., Andersen, G. L., Bakker, P. A. H. M., & Raaijmakers, J. M. (2011). Deciphering the Rhizosphere Microbiome for Disease-Suppressive Bacteria. *Science*, *332*(6033), 1097–1100. https://doi.org/10.1126/science.1203980

Michaelson, L. V., Napier, J. A., Molino, D., & Faure, J.-D. (2016). Plant sphingolipids: Their importance in cellular organization and adaption. *Biochimica et Biophysica Acta (BBA) - Molecular and Cell Biology of Lipids*, *1861*(9), 1329–1335. https://doi.org/10.1016/j.bbalip.2016.04.003

Mihalache, G., Balaes, T., Gostin, I., Stefan, M., Coutte, F., & Krier, F. (2018). Lipopeptides produced by *Bacillus subtilis* as new biocontrol products against fusariosis in ornamental plants. *Environmental Science and Pollution Research*, *25*(30), 29784–29793. https://doi.org/10.1007/s11356-017-9162-7

Miljaković, D., Marinković, J., & Balešević-Tubić, S. (2020). The Significance of *Bacillus* spp. in Disease Suppression and Growth Promotion of Field and Vegetable Crops. *Microorganisms*, *8*(7), 1037. https://doi.org/10.3390/microorganisms8071037

Ming, L. J., & Epperson, J. D. (2002). Metal binding and structure-activity relationship of the metalloantibiotic peptide bacitracin. *Journal of Inorganic Biochemistry*, *91*(1), 46–58. https://doi.org/10.1016/S0162-0134(02)00464-6

Mitter, B., Brader, G., Pfaffenbichler, N., & Sessitsch, A. (2019). Next generation microbiome applications for crop production — limitations and the need of knowledge-based solutions. *Current Opinion in Microbiology*, *49*, 59–65. https://doi.org/10.1016/j.mib.2019.10.006

Miyata, K., Hasegawa, S., Nakajima, E., Nishizawa, Y., Kamiya, K., Yokogawa, H., Shirasaka, S., Maruyama, S., Shibuya, N., & Kaku, H. (2022). OsCERK2/OsRLK10, a homolog of OsCERK1, has a potential role for chitin-triggered immunity and arbuscular mycorrhizal symbiosis in rice. *Plant Biotechnology*, *39*(2), 21.1222a. https://doi.org/10.5511/plantbiotechnology.21.1222a

Miyata, K., Hosotani, M., Akamatsu, A., Takeda, N., Jiang, W., Sugiyama, T., Takaoka, R., Matsumoto, K., Abe, S., Shibuya, N., & Kaku, H. (2023). OsSYMRK Plays an Essential Role in AM Symbiosis in Rice (Oryza sativa). *Plant and Cell Physiology*, *64*(4), 378–391. https://doi.org/10.1093/PCP/PCAD006

Miyata, K., Kozaki, T., Kouzai, Y., Ozawa, K., Ishii, K., Asamizu, E., Okabe, Y., Umehara, Y., Miyamoto, A., Kobae, Y., Akiyama, K., Kaku, H., Nishizawa, Y., Shibuya, N., & Nakagawa, T. (2014). The Bifunctional Plant Receptor, OsCERK1, Regulates Both Chitin-Triggered Immunity and Arbuscular Mycorrhizal Symbiosis in Rice. *Plant and Cell Physiology*, *55*(11), 1864–1872. https://doi.org/10.1093/pcp/pcu129

Miyauchi, S., Kiss, E., Kuo, A., Drula, E., Kohler, A., Sánchez-García, M., Morin, E., Andreopoulos, B., Barry, K. W., Bonito, G., Buée, M., Carver, A., Chen, C., Cichocki, N., Clum, A., Culley, D., Crous, P. W., Fauchery, L., Girlanda, M., … Martin, F. M. (2020). Large-scale genome sequencing of mycorrhizal fungi provides insights into the early evolution of symbiotic traits. *Nature Communications*, *11*(1), 5125. https://doi.org/10.1038/s41467-020-18795-w

Mohd Din, A. R. J., Mohamad Azam, Z., Othman, N. Z., & Yong, J. W. H. (2025). *Trichoderma*-bacterial network: A balance inter-kingdom interaction for agricultural relevance. *The Microbe*, *7*, 100360. https://doi.org/10.1016/j.microb.2025.100360

Molina-Santiago, C., Pearson, J. R., Navarro, Y., Berlanga-Clavero, M. V., Caraballo-Rodriguez, A. M., Petras, D., García-Martín, M. L., Lamon, G., Haberstein, B., Cazorla, F. M., de Vicente, A., Loquet, A., Dorrestein, P. C., & Romero, D. (2019). The extracellular matrix protects *Bacillus subtilis* colonies from *Pseudomonas* invasion and modulates plant co-colonization. *Nature Communications*, *10*(1), 1919. https://doi.org/10.1038/s41467-019-09944-x

Molina, A., Jordá, L., Torres, M. Á., Martín-Dacal, M., Berlanga, D. J., Fernández-Calvo, P., Gómez-Rubio, E., & Martín-Santamaría, S. (2024). Plant cell wall-mediated disease resistance: Current understanding and future perspectives.

Molecular Plant, *17*(5), 699–724. https://doi.org/10.1016/j.molp.2024.04.003

Molinatto, G., Puopolo, G., Sonego, P., Moretto, M., Engelen, K., Viti, C., Ongena, M., & Pertot, I. (2016). Complete genome sequence of *Bacillus amyloliquefaciens* subsp. *plantarum* S499, a rhizobacterium that triggers plant defences and inhibits fungal phytopathogens. *Journal of Biotechnology*, *238*, 56–59. https://doi.org/10.1016/j.jbiotec.2016.09.013

Montoliu-Nerin, M., Sánchez-García, M., Bergin, C., Kutschera, V. E., Johannesson, H., Bever, J. D., & Rosling, A. (2021). In-depth Phylogenomic Analysis of Arbuscular Mycorrhizal Fungi Based on a Comprehensive Set of de novo Genome Assemblies. *Frontiers in Fungal Biology*, *2*, 716385. https://doi.org/10.3389/ffunb.2021.716385

Mortier, J., Cambré, A., Schack, S., Christie, G., & Aertsen, A. (2023). Impact of Protein Aggregates on Sporulation and Germination of *Bacillus subtilis*. *Microorganisms*, *11*(9), 2365. https://doi.org/10.3390/microorganisms11092365

Mukherjee, A., & Ané, J.-M. (2011). Germinating Spore Exudates from Arbuscular Mycorrhizal Fungi: Molecular and Developmental Responses in Plants and Their Regulation by Ethylene. *Molecular Plant-Microbe Interactions®*, *24*(2), 260–270. https://doi.org/10.1094/MPMI-06-10-0146

Munusamy, S., Conde, R., Bertrand, B., & Munoz-Garay, C. (2020). Biophysical approaches for exploring lipopeptide-lipid interactions. *Biochimie*, *170*, 173–202. https://doi.org/10.1016/j.biochi.2020.01.009

Nacoon, S., Jogloy, S., Riddech, N., Mongkolthanaruk, W., Kuyper, T. W., & Boonlue, S. (2020). Interaction between Phosphate Solubilizing Bacteria and Arbuscular Mycorrhizal Fungi on Growth Promotion and Tuber Inulin Content of *Helianthus tuberosus* L. *Scientific Reports*, *10*(1), 1–10. https://doi.org/10.1038/s41598-020-61846-x

Nadeem, S. M., Ahmad, M., Zahir, Z. A., Javaid, A., & Ashraf, M. (2014). The role of mycorrhizae and plant growth promoting rhizobacteria (PGPR) in improving crop productivity under stressful environments. *Biotechnology Advances*, *32*(2), 429–448. https://doi.org/10.1016/j.biotechadv.2013.12.005

Nagahashi, G., & Douds, D. D. (2011). The effects of hydroxy fatty acids on the hyphal branching of germinated spores of AM fungi. *Fungal Biology*, *115*(4–5), 351–358. https://doi.org/10.1016/j.funbio.2011.01.006

Nair, R., Raina, S., Keshavarz, T., & Kerrigan, M. J. P. (2011). Application of fluorescent indicators to analyse intracellular calcium and morphology in filamentous fungi. *Fungal Biology*, *115*(4–5), 326–334. https://doi.org/10.1016/j.funbio.2010.12.012

Nanjundappa, A., Bagyaraj, D. J., Saxena, A. K., Kumar, M., & Chakdar, H. (2019). Interaction between arbuscular mycorrhizal fungi and *Bacillus* spp. in soil enhancing growth of crop plants. *Fungal Biology and Biotechnology*, *6*(1), 23. https://doi.org/10.1186/s40694-019-0086-5

Nannan, C., Vu, H. Q., Gillis, A., Caulier, S., Nguyen, T. T. T., & Mahillon, J. (2021).

Bacilysin within the *Bacillus subtilis* group: gene prevalence versus antagonistic activity against Gram-negative foodborne pathogens. *Journal of Biotechnology*, *327*, 28–35. https://doi.org/10.1016/j.jbiotec.2020.12.017

Nasir, M. N., & Besson, F. (2012). Interactions of the antifungal mycosubtilin with ergosterol-containing interfacial monolayers. *Biochimica et Biophysica Acta (BBA) - Biomembranes*, *1818*(5), 1302–1308. https://doi.org/10.1016/j.bbamem.2012.01.020

Nasir, M. N., Thawani, A., Kouzayha, A., & Besson, F. (2010). Interactions of the natural antimicrobial mycosubtilin with phospholipid membrane models. *Colloids and Surfaces B: Biointerfaces*, *78*(1), 17–23. https://doi.org/10.1016/j.colsurfb.2010.01.034

Nasslahsen, B., Prin, Y., Ferhout, H., Smouni, A., & Duponnois, R. (2022). Mycorrhizae helper bacteria for managing the mycorrhizal soil infectivity. *Frontiers in Soil Science*, *2*, 979246. https://doi.org/10.3389/fsoil.2022.979246

Nayfach, S., Roux, S., Seshadri, R., Udwary, D., Varghese, N., Schulz, F., Wu, D., Paez-Espino, D., Chen, I.-M., Huntemann, M., Palaniappan, K., Ladau, J., Mukherjee, S., Reddy, T. B. K., Nielsen, T., Kirton, E., Faria, J. P., Edirisinghe, J. N., Henry, C. S., … Eloe-Fadrosh, E. A. (2021). A genomic catalog of Earth's microbiomes. *Nature Biotechnology*, *39*(4), 499–509. https://doi.org/10.1038/s41587-020-0718-6

Naz, M., Afzal, M. R., Raza, M. A., Tariq, M., Yan, M., Dai, Z., Qi, S., & Du, D. (2025). The significant effects of Strigolactones on plant growth and microbe interactions: a review. *Plant Growth Regulation*, *105*(4), 937–957. https://doi.org/10.1007/s10725-025-01325-3

Ngou, B. P. M., Jones, J. D. G., & Ding, P. (2022). Plant immune networks. *Trends in Plant Science*, *27*(3), 255–273. https://doi.org/10.1016/j.tplants.2021.08.012

Nicholson, W. L., Munakata, N., Horneck, G., Melosh, H. J., & Setlow, P. (2000). Resistance of *Bacillus* Endospores to Extreme Terrestrial and Extraterrestrial Environments. *Microbiology and Molecular Biology Reviews*, *64*(3), 548–572. https://doi.org/10.1128/MMBR.64.3.548-572.2000

Nicolopoulou-Stamati, P., Maipas, S., Kotampasi, C., Stamatis, P., & Hens, L. (2016). Chemical Pesticides and Human Health: The Urgent Need for a New Concept in Agriculture. *Frontiers in Public Health*, *4*, 178764. https://doi.org/10.3389/fpubh.2016.00148

Nihorimbere, V., Cawoy, H., Seyer, A., Brunelle, A., Thonart, P., & Ongena, M. (2012). Impact of rhizosphere factors on cyclic lipopeptide signature from the plant beneficial strain *Bacillus amyloliquefaciens*S499. *FEMS Microbiology Ecology*, *79*(1), 176–191. https://doi.org/10.1111/j.1574-6941.2011.01208.x

Noë, R., & Kiers, E. T. (2018). Mycorrhizal Markets, Firms, and Co-ops. *Trends in Ecology & Evolution*, *33*(10), 777–789. https://doi.org/10.1016/j.tree.2018.07.007

Nomura, T., Seto, Y., & Kyozuka, J. (2024). Unveiling the complexity of strigolactones: exploring structural diversity, biosynthesis pathways, and

signaling mechanisms. *Journal of Experimental Botany*, *75*(4), 1134–1147. https://doi.org/10.1093/jxb/erad412

Oakleaf, J., Kennedy, C., Wolff, N. H., Terasaki Hart, D. E., Ellis, P., Theobald, D. M., Fariss, B., Burkart, K., & Kiesecker, J. (2024). Mapping global land conversion pressure to support conservation planning. *Scientific Data*, *11*(1), 830. https://doi.org/10.1038/s41597-024-03639-9

Ochi, K. (2017). Insights into microbial cryptic gene activation and strain improvement: principle, application and technical aspects. *The Journal of Antibiotics*, *70*(1), 25–40. https://doi.org/10.1038/ja.2016.82

Ogran, A., Yardeni, E. H., Keren-Paz, A., Bucher, T., Jain, R., Gilhar, O., & Kolodkin-Gal, I. (2019). The Plant Host Induces Antibiotic Production To Select the Most-Beneficial Colonizers. *Applied and Environmental Microbiology*, *85*(13), e00512-19. https://doi.org/10.1128/AEM.00512-19

Oldroyd, G. E. D. (2013). Speak, friend, and enter: signalling systems that promote beneficial symbiotic associations in plants. *Nature Reviews Microbiology*, *11*(4), 252–263. https://doi.org/10.1038/nrmicro2990

Olsson, L., Barbosa, H., Bhadwal, S., Cowie, A., Delusca, K., Flores-Renteria, D., Hermans, K., Jobbagy, E., Kurz, W., Li, D., Sonwa, D. J., & Stringer, L. (2019). *Land Degradation: IPCC Special Report on Climate Change, Desertification, Land 5 Degradation, Sustainable Land Management, Food Security, and 6 Greenhouse gas fluxes in Terrestrial Ecosystems* (Intergovernmental Panel on Climate Change (IPCC) (ed.)). IPCC Special Report. https://portal.research.lu.se/en/publications/land-degradation-ipcc-special-report-on-climate-change-desertific

Ongena, M., & Jacques, P. (2008). *Bacillus* lipopeptides: versatile weapons for plant disease biocontrol. *Trends in Microbiology*, *16*(3), 115–125. https://doi.org/10.1016/j.tim.2007.12.009

Ongena, M., Jourdan, E., Adam, A., Paquot, M., Brans, A., Joris, B., Arpigny, J., & Thonart, P. (2007). Surfactin and fengycin lipopeptides of *Bacillus subtilis* as elicitors of induced systemic resistance in plants. *Environmental Microbiology*, *9*(4), 1084–1090. https://doi.org/10.1111/j.1462-2920.2006.01202.x

Orgiazzi, A., Panagos, P., Fernández-Ugalde, O., Wojda, P., Labouyrie, M., Ballabio, C., Franco, A., Pistocchi, A., Montanarella, L., & Jones, A. (2022). LUCAS Soil Biodiversity and LUCAS Soil Pesticides, new tools for research and policy development. *European Journal of Soil Science*, *73*(5), e13299. https://doi.org/10.1111/ejss.13299

Oslizlo, A., Stefanic, P., Dogsa, I., & Mandic-Mulec, I. (2014). Private link between signal and response in *Bacillus subtilis* quorum sensing. *Proceedings of the National Academy of Sciences*, *111*(4), 1586–1591. https://doi.org/10.1073/pnas.1316283111

Overkamp, W., Beilharz, K., Detert Oude Weme, R., Solopova, A., Karsens, H., Kovács, Á. T., Kok, J., Kuipers, O. P., & Veening, J.-W. (2013). Benchmarking Various Green Fluorescent Protein Variants in *Bacillus subtilis*, *Streptococcus*

pneumoniae, and *Lactococcus lactis* for Live Cell Imaging. *Applied and Environmental Microbiology*, *79*(20), 6481–6490. https://doi.org/10.1128/AEM.02033-13

Owen, D., Williams, A. P., Griffith, G. W., & Withers, P. J. A. (2015). Use of commercial bio-inoculants to increase agricultural production through improved phosphrous acquisition. *Applied Soil Ecology*, *86*, 41–54. https://doi.org/10.1016/j.apsoil.2014.09.012

Oyarte Galvez, L., Bisot, C., Bourrianne, P., Cargill, R., Klein, M., van Son, M., van Krugten, J., Caldas, V., Clerc, T., Lin, K.-K., Kahane, F., van Staalduine, S., Stewart, J. D., Terry, V., Turcu, B., van Otterdijk, S., Babu, A., Kamp, M., Seynen, M., … Shimizu, T. S. (2025). A travelling-wave strategy for plant–fungal trade. *Nature*, *639*(8053), 172–180. https://doi.org/10.1038/s41586-025-08614-x

Panagos, P., Borrelli, P., Jones, A., & Robinson, D. A. (2024a). A 1 billion euro mission: A Soil Deal for Europe. *European Journal of Soil Science*, *75*(1), e13466. https://doi.org/10.1111/ejss.13466

Panagos, P., Broothaerts, N., Ballabio, C., Orgiazzi, A., De Rosa, D., Borrelli, P., Liakos, L., Vieira, D., Van Eynde, E., Arias Navarro, C., Breure, T., Fendrich, A., Köninger, J., Labouyrie, M., Matthews, F., Muntwyler, A., Jimenez, J. M., Wojda, P., Yunta, F., … Jones, A. (2024b). How the EU Soil Observatory is providing solid science for healthy soils. *European Journal of Soil Science*, *75*(3), e13507. https://doi.org/10.1111/ejss.13507

Pandin, C., Darsonval, M., Mayeur, C., Le Coq, D., Aymerich, S., & Briandet, R. (2019). Biofilm Formation and Synthesis of Antimicrobial Compounds by the Biocontrol Agent *Bacillus velezensis* QST713 in an *Agaricus bisporus* Compost Micromodel. *Applied and Environmental Microbiology*, *85*(12). https://doi.org/10.1128/AEM.00327-19

Pandin, C., Le Coq, D., Canette, A., Aymerich, S., & Briandet, R. (2017). Should the biofilm mode of life be taken into consideration for microbial biocontrol agents? *Microbial Biotechnology*, *10*(4), 719–734. https://doi.org/10.1111/1751-7915.12693

Pandin, C., Le Coq, D., Deschamps, J., Védie, R., Rousseau, T., Aymerich, S., & Briandet, R. (2018). Complete genome sequence of *Bacillus velezensis* QST713: A biocontrol agent that protects *Agaricus bisporus* crops against the green mould disease. *Journal of Biotechnology*, *278*, 10–19. https://doi.org/10.1016/j.jbiotec.2018.04.014

Pandit, A., Johny, L., Srivastava, S., Adholeya, A., Cahill, D., Brau, L., & Kochar, M. (2022). Recreating in vitro tripartite mycorrhizal associations through functional bacterial biofilms. *Applied Microbiology and Biotechnology*, *106*(11), 4237–4250. https://doi.org/10.1007/s00253-022-11996-x

Park, S.-W., Kaimoyo, E., Kumar, D., Mosher, S., & Klessig, D. F. (2007). Methyl Salicylate Is a Critical Mobile Signal for Plant Systemic Acquired Resistance. *Science*, *318*(5847), 113–116. https://doi.org/10.1126/science.1147113

Parniske, M. (2008). Arbuscular mycorrhiza: the mother of plant root endosymbioses. *Nature Reviews Microbiology*, *6*(10), 763–775. https://doi.org/10.1038/nrmicro1987

Pastor, V., Balmer, A., Gamir, J., Flors, V., & Mauch-Mani, B. (2014). Preparing to fight back: generation and storage of priming compounds. *Frontiers in Plant Science*, *5*(JUN), 94827. https://doi.org/10.3389/fpls.2014.00295

Pathak, K. V., & Keharia, H. (2014). Identification of surfactins and iturins produced by potent fungal antagonist, *Bacillus subtilis* K1 isolated from aerial roots of banyan (*Ficus benghalensis*) tree using mass spectrometry. *3 Biotech*, *4*(3), 283–295. https://doi.org/10.1007/s13205-013-0151-3

Peng, Y., van Wersch, R., & Zhang, Y. (2018). Convergent and Divergent Signaling in PAMP-Triggered Immunity and Effector-Triggered Immunity. *Molecular Plant-Microbe Interactions®*, *31*(4), 403–409. https://doi.org/10.1094/MPMI-06-17-0145-CR

Pérez-Lorente, A. I., Molina-Santiago, C., Vela-Corcía, D., Stincone, P., Hierrezuelo, J., Grifé, M., Pakkir Shah, A. K., de Vicente, A., Petras, D., & Romero, D. (2025). The offensive role of the *Bacillus* extracellular matrix in driving metabolite-mediated dialogue and adaptive strategies with pathogenic fungi. *BioRxiv*, 2025.02.06.636830. https://doi.org/10.1101/2025.02.06.636830

Philippot, L., Raaijmakers, J. M., Lemanceau, P., & van der Putten, W. H. (2013). Going back to the roots: the microbial ecology of the rhizosphere. *Nature Reviews Microbiology*, *11*(11), 789–799. https://doi.org/10.1038/nrmicro3109

Pieterse, C. M. J., Zamioudis, C., Berendsen, R. L., Weller, D. M., Van Wees, S. C. M., & Bakker, P. A. H. M. (2014). Induced Systemic Resistance by Beneficial Microbes. *Annual Review of Phytopathology*, *52*(1), 347–375. https://doi.org/10.1146/annurev-phyto-082712-102340

Piewngam, P., Zheng, Y., Nguyen, T. H., Dickey, S. W., Joo, H.-S., Villaruz, A. E., Glose, K. A., Fisher, E. L., Hunt, R. L., Li, B., Chiou, J., Pharkjaksu, S., Khongthong, S., Cheung, G. Y. C., Kiratisin, P., & Otto, M. (2018). Pathogen elimination by probiotic *Bacillus* via signalling interference. *Nature*, *562*(7728), 532–537. https://doi.org/10.1038/s41586-018-0616-y

Pimprikar, P., Carbonnel, S., Paries, M., Katzer, K., Klingl, V., Bohmer, M. J., Karl, L., Floss, D. S., Harrison, M. J., Parniske, M., & Gutjahr, C. (2016). A CCaMK-CYCLOPS-DELLA Complex Activates Transcription of RAM1 to Regulate Arbuscule Branching. *Current Biology*, *26*(8), 987–998. https://doi.org/10.1016/j.cub.2016.01.069

Pinto, L., Soler-López, L., Serrano, A., & Sánchez-Rodríguez, C. (2025). Between Host and Invaders: The Subcellular Cell Wall Dynamics at the Plant–Pathogen Interface. *Annual Review of Plant Biology*, *76*(1), 255–284. https://doi.org/10.1146/annurev-arplant-061824-115733

Prăvălie, R. (2021). Exploring the multiple land degradation pathways across the planet. *Earth-Science Reviews*, *220*, 103689. https://doi.org/10.1016/j.earscirev.2021.103689

Prăvălie, R., Borrelli, P., Panagos, P., Ballabio, C., Lugato, E., Chappell, A., Miguez-Macho, G., Maggi, F., Peng, J., Niculiță, M., Roșca, B., Patriche, C., Dumitrașcu, M., Bandoc, G., Nita, I.-A., & Birsan, M.-V. (2024). A unifying modelling of multiple land degradation pathways in Europe. *Nature Communications*, *15*(1), 3862. https://doi.org/10.1038/s41467-024-48252-x

Prăvălie, R., Patriche, C., Borrelli, P., Panagos, P., Roșca, B., Dumitraşcu, M., Nita, I.-A., Săvulescu, I., Birsan, M.-V., & Bandoc, G. (2021). Arable lands under the pressure of multiple land degradation processes. A global perspective. *Environmental Research*, *194*, 110697. https://doi.org/10.1016/j.envres.2020.110697

Pršić, J., Gilliard, G., Ibrahim, H., Argüelles-Arias, A., Rondelli, V., Crowet, J.-M., Genva, M., Luzuriaga-Loaiza, W. P., Deboever, E., Nasir, M. N., Lins, L., Mathelie-Guinlet, M., Boubsi, F., Eschrig, S., Ranf, S., Dorey, S., Coninck, B. De, Nürnberger, T., Mongrand, S., … Ongena, M. (2023). Mechanosensing and Sphingolipid-Docking Mediate Lipopeptide-Induced Immunity in *Arabidopsis*. *BioRxiv*, 2023.07.04.547613. https://doi.org/10.1101/2023.07.04.547613

Pršić, J., & Ongena, M. (2020). Elicitors of Plant Immunity Triggered by Beneficial Bacteria. *Frontiers in Plant Science*, *11*, 594530. https://doi.org/10.3389/fpls.2020.594530

Purin, S., & Rillig, M. C. (2008). Parasitism of arbuscular mycorrhizal fungi: reviewing the evidence. *FEMS Microbiology Letters*, *279*(1), 8–14. https://doi.org/10.1111/j.1574-6968.2007.01007.x

Put, H., Gerstmans, H., Vande Capelle, H., Fauvart, M., Michiels, J., & Masschelein, J. (2024). *Bacillus subtilis* as a host for natural product discovery and engineering of biosynthetic gene clusters. *Natural Product Reports*, *41*(7), 1113–1151. https://doi.org/10.1039/D3NP00065F

Qiao, S. A., & Roth, R. (2025). Messenger and message: Uncovering the roles, rhythm and regulation of extracellular vesicles in plant biotic interactions. *Current Opinion in Plant Biology*, *83*, 102672. https://doi.org/10.1016/j.pbi.2024.102672

Qiu, M., Xu, Z., Li, X., Li, Q., Zhang, N., Shen, Q., & Zhang, R. (2014). Comparative Proteomics Analysis of *Bacillus amyloliquefaciens* SQR9 Revealed the Key Proteins Involved in in Situ Root Colonization. *Journal of Proteome Research*, *13*(12), 5581–5591. https://doi.org/10.1021/pr500565m

Qiu, Z., Egidi, E., Liu, H., Kaur, S., & Singh, B. K. (2019). New frontiers in agriculture productivity: Optimised microbial inoculants and in situ microbiome engineering. *Biotechnology Advances*, *37*(6), 107371. https://doi.org/10.1016/j.biotechadv.2019.03.010

Raaijmakers, J. M., De Bruijn, I., Nybroe, O., & Ongena, M. (2010). Natural functions of lipopeptides from *Bacillus* and *Pseudomonas* : more than surfactants and antibiotics. *FEMS Microbiology Reviews*, *34*(6), 1037–1062. https://doi.org/10.1111/j.1574-6976.2010.00221.x

Rabbee, M. F., Ali, M. S., Choi, J., Hwang, B. S., Jeong, S. C., & Baek, K. (2019).

Bacillus velezensis: A Valuable Member of Bioactive Molecules within Plant Microbiomes. *Molecules*, *24*(6), 1046. https://doi.org/10.3390/molecules24061046

Rabbee, M. F., Hwang, B.-S., & Baek, K.-H. (2023). *Bacillus velezensis*: A Beneficial Biocontrol Agent or Facultative Phytopathogen for Sustainable Agriculture. *Agronomy*, *13*(3), 840. https://doi.org/10.3390/agronomy13030840

Rahman, A., Uddin, W., & Wenner, N. G. (2015). Induced systemic resistance responses in perennial ryegrass against *Magnaporthe oryzae* elicited by semi-purified surfactin lipopeptides and live cells of *Bacillus amyloliquefaciens*. *Molecular Plant Pathology*, *16*(6), 546–558. https://doi.org/10.1111/mpp.12209

Rajavel, M., Mitra, A., & Gopal, B. (2009). Role of Bacillus subtilis BacB in the synthesis of bacilysin. *The Journal of Biological Chemistry*, *284*(46), 31882–31892. https://doi.org/10.1074/JBC.M109.014522

Ramirez-Villacis, D. X., Leon-Reyes, A., Pieterse, C. M. J., & Raaijmakers, J. M. (2025). Born to rewild: Reconnecting beneficial plant-microbiome alliances for resilient future crops. *Cell Host & Microbe*, *33*(8), 1241–1255. https://doi.org/10.1016/j.chom.2025.06.017

Rasmussen, S. R., Füchtbauer, W., Novero, M., Volpe, V., Malkov, N., Genre, A., Bonfante, P., Stougaard, J., & Radutoiu, S. (2016). Intraradical colonization by arbuscular mycorrhizal fungi triggers induction of a lipochitooligosaccharide receptor. *Scientific Reports*, *6*(1), 29733. https://doi.org/10.1038/srep29733

Ratsoma, M. F., Santana, Q. C., Wingfield, B. D., Steenkamp, E. T., & Motaung, T. E. (2025). Understanding cargo sorting and interactive effects of membrane vesicles in fungal phytopathogens: Current knowledge and research gaps. *Fungal Biology Reviews*, *51*, 100411. https://doi.org/10.1016/j.fbr.2025.100411

Raymaekers, K., Ponet, L., Holtappels, D., Berckmans, B., & Cammue, B. P. A. (2020). Screening for novel biocontrol agents applicable in plant disease management – A review. *Biological Control*, *144*(104240), 104240. https://doi.org/10.1016/j.biocontrol.2020.104240

Redecker, D., Kodner, R., & Graham, L. E. (2000). Glomalean Fungi from the Ordovician. *Science*, *289*(5486), 1920–1921. https://doi.org/10.1126/science.289.5486.1920

Ren, B., Wang, X., Duan, J., & Ma, J. (2019). Rhizobial tRNA-derived small RNAs are signal molecules regulating plant nodulation. *Science*, *365*(6456), 919–922. https://doi.org/10.1126/science.aav8907

Ribeiro, I. D. A., Volpiano, C. G., Vargas, L. K., Granada, C. E., Lisboa, B. B., & Passaglia, L. M. P. (2020). Use of Mineral Weathering Bacteria to Enhance Nutrient Availability in Crops: A Review. *Frontiers in Plant Science*, *11*, 590774. https://doi.org/10.3389/fpls.2020.590774

Rich, M. K., Nouri, E., Courty, P.-E., & Reinhardt, D. (2017). Diet of Arbuscular Mycorrhizal Fungi: Bread and Butter? *Trends in Plant Science*, *22*(8), 652–660. https://doi.org/10.1016/j.tplants.2017.05.008

Rich, M. K., Vigneron, N., Libourel, C., Keller, J., Xue, L., Hajheidari, M.,

Radhakrishnan, G. V., Le Ru, A., Diop, S. I., Potente, G., Conti, E., Duijsings, D., Batut, A., Le Faouder, P., Kodama, K., Kyozuka, J., Sallet, E., Bécard, G., Rodriguez-Franco, M., … Delaux, P.-M. (2021). Lipid exchanges drove the evolution of mutualism during plant terrestrialization. *Science*, *372*(6544), 864–868. https://doi.org/10.1126/science.abg0929

Richter, A., Blei, F., Hu, G., Schwitalla, J. W., Lozano-Andrade, C. N., Xie, J., Jarmusch, S. A., Wibowo, M., Kjeldgaard, B., Surabhi, S., Xu, X., Jautzus, T., Phippen, C. B. W., Tyc, O., Arentshorst, M., Wang, Y., Garbeva, P., Larsen, T. O., Ram, A. F. J., … Kovács, Á. T. (2024). Enhanced surface colonisation and competition during bacterial adaptation to a fungus. *Nature Communications 2024 15:1*, *15*(1), 1–13. https://doi.org/10.1038/s41467-024-48812-1

Rigolet, A., Argüelles Arias, A., Anckaert, A., Quinton, L., Rigali, S., Tellatin, D., Burguet, P., & Ongena, M. (2024). Lipopeptides as rhizosphere public goods for microbial cooperation. *Microbiology Spectrum*, *12*(1). https://doi.org/10.1128/spectrum.03106-23

Rivero, J., Lidoy, J., Llopis-Giménez, Á., Herrero, S., Flors, V., & Pozo, M. J. (2021). Mycorrhizal symbiosis primes the accumulation of antiherbivore compounds and enhances herbivore mortality in tomato. *Journal of Experimental Botany*, *72*(13), 5038–5050. https://doi.org/10.1093/jxb/erab171

Rogowska, A., & Szakiel, A. (2020). The role of sterols in plant response to abiotic stress. *Phytochemistry Reviews*, *19*(6), 1525–1538. https://doi.org/10.1007/s11101-020-09708-2

Romero-Munar, A., Aroca, R., Zamarreño, A. M., García-Mina, J. M., Perez-Hernández, N., & Ruiz-Lozano, J. M. (2023). Dual Inoculation with *Rhizophagus irregularis* and *Bacillus megaterium* Improves Maize Tolerance to Combined Drought and High Temperature Stress by Enhancing Root Hydraulics, Photosynthesis and Hormonal Responses. *International Journal of Molecular Sciences*, *24*(6), 5193. https://doi.org/10.3390/ijms24065193

Romero, D. (2013). Bacterial determinants of the social behavior of *Bacillus subtilis*. *Research in Microbiology*, *164*(7), 788–798. https://doi.org/10.1016/j.resmic.2013.06.004

Roper, M., Lee, C., Hickey, P. C., & Gladfelter, A. S. (2015). Life as a moving fluid: fate of cytoplasmic macromolecules in dynamic fungal syncytia. *Current Opinion in Microbiology*, *26*, 116–122. https://doi.org/10.1016/j.mib.2015.07.001

Roth, R., & Paszkowski, U. (2017). Plant carbon nourishment of arbuscular mycorrhizal fungi. *Current Opinion in Plant Biology*, *39*, 50–56. https://doi.org/10.1016/j.pbi.2017.05.008

Rouphael, Y., Franken, P., Schneider, C., Schwarz, D., Giovannetti, M., Agnolucci, M., Pascale, S. De, Bonini, P., & Colla, G. (2015). Arbuscular mycorrhizal fungi act as biostimulants in horticultural crops. *Scientia Horticulturae*, *196*, 91–108. https://doi.org/10.1016/j.scienta.2015.09.002

Rozmoš, M., Bukovská, P., Hršelová, H., Kotianová, M., Dudáš, M., Gančarčíková,

K., & Jansa, J. (2022). Organic nitrogen utilisation by an arbuscular mycorrhizal fungus is mediated by specific soil bacteria and a protist. *The ISME Journal*, *16*(3), 676–685. https://doi.org/10.1038/s41396-021-01112-8

Rudrappa, T., Czymmek, K. J., Paré, P. W., & Bais, H. P. (2008). Root-Secreted Malic Acid Recruits Beneficial Soil Bacteria. *Plant Physiology*, *148*(3), 1547–1556. https://doi.org/10.1104/pp.108.127613

Rui, Y., & Dinneny, J. R. (2020). A wall with integrity: surveillance and maintenance of the plant cell wall under stress. *New Phytologist*, *225*(4), 1428–1439. https://doi.org/10.1111/nph.16166

Rush, T. A., Puech-Pagès, V., Bascaules, A., Jargeat, P., Maillet, F., Haouy, A., Maës, A. Q., Carriel, C. C., Khokhani, D., Keller-Pearson, M., Tannous, J., Cope, K. R., Garcia, K., Maeda, J., Johnson, C., Kleven, B., Choudhury, Q. J., Labbé, J., Swift, C., … Ané, J.-M. (2020). Lipo-chitooligosaccharides as regulatory signals of fungal growth and development. *Nature Communications*, *11*(1), 3897. https://doi.org/10.1038/s41467-020-17615-5

Rush, T. A., Tannous, J., Lane, M. J., Gopalakrishnan Meena, M., Carrell, A. A., Golan, J. J., Drott, M. T., Cottaz, S., Fort, S., Ané, J.-M., Keller, N. P., Pelletier, D. A., Jacobson, D. A., Kainer, D., Abraham, P. E., Giannone, R. J., & Labbé, J. L. (2022). Lipo-Chitooligosaccharides Induce Specialized Fungal Metabolite Profiles That Modulate Bacterial Growth. *MSystems*, *7*(6), e01052-22. https://doi.org/10.1128/msystems.01052-22

Russo, G., Carotenuto, G., Fiorilli, V., Volpe, V., Chiapello, M., Van Damme, D., & Genre, A. (2019). Ectopic activation of cortical cell division during the accommodation of arbuscular mycorrhizal fungi. *New Phytologist*, *221*(2), 1036–1048. https://doi.org/10.1111/nph.15398

Salloum, M. S., Guzzo, M. C., Velazquez, M. S., Sagadin, M. B., & Luna, C. M. (2016). Variability in colonization of arbuscular mycorrhizal fungi and its effect on mycorrhizal dependency of improved and unimproved soybean cultivars. *Canadian Journal of Microbiology*, *62*(12), 1034–1040. https://doi.org/10.1139/cjm-2016-0383

Salvioli, A., Ghignone, S., Novero, M., Navazio, L., Venice, F., Bagnaresi, P., & Bonfante, P. (2016). Symbiosis with an endobacterium increases the fitness of a mycorrhizal fungus, raising its bioenergetic potential. *The ISME Journal*, *10*(1), 130–144. https://doi.org/10.1038/ismej.2015.91

Salvioli di Fossalunga, A., & Bonfante, P. (2023). Arbuscular mycorrhizal fungi as biofertilisers. *Current Biology*, *33*(11), R462–R463. https://doi.org/10.1016/j.cub.2023.01.056

Sangwan, S., & Prasanna, R. (2022). Mycorrhizae Helper Bacteria: Unlocking Their Potential as Bioenhancers of Plant–Arbuscular Mycorrhizal Fungal Associations. *Microbial Ecology*, *84*(1), 1–10. https://doi.org/10.1007/s00248-021-01831-7

Sanmartín, N., Sánchez-Bel, P., Pastor, V., Pastor-Fernández, J., Mateu, D., Pozo, M. J., Cerezo, M., & Flors, V. (2020). Root-to-shoot signalling in mycorrhizal

tomato plants upon *Botrytis cinerea* infection. *Plant Science*, *298*, 110595. https://doi.org/10.1016/j.plantsci.2020.110595

Santos, F. C., Lobo, G. M., Fernandes, A. S., Videira, A., & de Almeida, R. F. M. (2018). Changes in the Biophysical Properties of the Cell Membrane Are Involved in the Response of *Neurospora crassa* to Staurosporine. *Frontiers in Physiology*, *9*(OCT), 410343. https://doi.org/10.3389/fphys.2018.01375

Santos, F. C., Marquês, J. T., Bento-Oliveira, A., & de Almeida, R. F. M. (2020). Sphingolipid-enriched domains in fungi. *FEBS Letters*, *594*(22), 3698–3718. https://doi.org/10.1002/1873-3468.13986

Sasse, J., Martinoia, E., & Northen, T. (2018). Feed Your Friends: Do Plant Exudates Shape the Root Microbiome? *Trends in Plant Science*, *23*(1), 25–41. https://doi.org/10.1016/j.tplants.2017.09.003

Savastano, N., & Bais, H. (2024). Synergism or Antagonism: Do Arbuscular Mycorrhizal Fungi and Plant Growth-Promoting Rhizobacteria Work Together to Benefit Plants? *International Journal of Plant Biology*, *15*(4), 944–958. https://doi.org/10.3390/ijpb15040067

Schaffer, G. F., & Peterson, R. L. (1993). Modifications to clearing methods used in combination with vital staining of roots colonized with vesicular-arbuscular mycorrhizal fungi. *Mycorrhiza*, *4*(1), 29–35. https://doi.org/10.1007/BF00203248

Schellenberger, R., Touchard, M., Clément, C., Baillieul, F., Cordelier, S., Crouzet, J., & Dorey, S. (2019). Apoplastic invasion patterns triggering plant immunity: plasma membrane sensing at the frontline. *Molecular Plant Pathology*, *20*(11), 1602–1616. https://doi.org/10.1111/mpp.12857

Scheublin, T. R., Sanders, I. R., Keel, C., & van der Meer, J. R. (2010). Characterisation of microbial communities colonising the hyphal surfaces of arbuscular mycorrhizal fungi. *The ISME Journal*, *4*(6), 752–763. https://doi.org/10.1038/ismej.2010.5

Schindelin, J., Arganda-Carreras, I., Frise, E., Kaynig, V., Longair, M., Pietzsch, T., Preibisch, S., Rueden, C., Saalfeld, S., Schmid, B., Tinevez, J.-Y., White, D. J., Hartenstein, V., Eliceiri, K., Tomancak, P., & Cardona, A. (2012). Fiji: an open-source platform for biological-image analysis. *Nature Methods*, *9*(7), 676–682. https://doi.org/10.1038/nmeth.2019

Sędzielewska Toro, K., & Brachmann, A. (2016). The effector candidate repertoire of the arbuscular mycorrhizal fungus *Rhizophagus clarus*. *BMC Genomics*, *17*(1), 101. https://doi.org/10.1186/s12864-016-2422-y

Selosse, M.-A., & Rousset, F. (2011). The Plant-Fungal Marketplace. *Science*, *333*(6044), 828–829. https://doi.org/10.1126/science.1210722

Serrano, K., Bezrutczyk, M., Goudeau, D., Dao, T., O'Malley, R., Malmstrom, R. R., Visel, A., Scheller, H. V., & Cole, B. (2024). Spatial co-transcriptomics reveals discrete stages of the arbuscular mycorrhizal symbiosis. *Nature Plants*, *10*(4), 673–688. https://doi.org/10.1038/s41477-024-01666-3

Sexton, D. J., & Schuster, M. (2017). Nutrient limitation determines the fitness of

cheaters in bacterial siderophore cooperation. *Nature Communications*, *8*(1), 230. https://doi.org/10.1038/s41467-017-00222-2

Shah, J., & Zeier, J. (2013). Long-distance communication and signal amplification in systemic acquired resistance. *Frontiers in Plant Science*, *4*(FEB), 43095. https://doi.org/10.3389/fpls.2013.00030

Shao, C., Liu, L., Gang, H., Yang, S., & Mu, B. (2015). Structural Diversity of the Microbial Surfactin Derivatives from Selective Esterification Approach. *International Journal of Molecular Sciences*, *16*(1), 1855–1872. https://doi.org/10.3390/ijms16011855

Sharma, M., Saleh, D., Charron, J.-B., & Jabaji, S. (2020a). A Crosstalk Between *Brachypodium* Root Exudates, Organic Acids, and *Bacillus velezensis* B26, a Growth Promoting Bacterium. *Frontiers in Microbiology*, *11*, 575578. https://doi.org/10.3389/fmicb.2020.575578

Sharma, S., Compant, S., Ballhausen, M.-B., Ruppel, S., & Franken, P. (2020b). The interaction between *Rhizoglomus irregulare* and hyphae attached phosphate solubilizing bacteria increases plant biomass of *Solanum lycopersicum*. *Microbiological Research*, *240*, 126556. https://doi.org/10.1016/j.micres.2020.126556

Shi, J., Wang, X., & Wang, E. (2023). Mycorrhizal Symbiosis in Plant Growth and Stress Adaptation: From Genes to Ecosystems. *Annual Review of Plant Biology*, *74*(1), 569–607. https://doi.org/10.1146/annurev-arplant-061722-090342

Silvestri, A., Ledford, W. C., Fiorilli, V., Votta, C., Scerna, A., Tucconi, J., Mocchetti, A., Grasso, G., Balestrini, R., Jin, H., Rubio-Somoza, I., & Lanfranco, L. (2024). A fungal sRNA silences a host plant transcription factor to promote arbuscular mycorrhizal symbiosis. *New Phytologist*. https://doi.org/10.1111/NPH.20273

Simard, S. W., Beiler, K. J., Bingham, M. A., Deslippe, J. R., Philip, L. J., & Teste, F. P. (2012). Mycorrhizal networks: Mechanisms, ecology and modelling. *Fungal Biology Reviews*, *26*(1), 39–60. https://doi.org/10.1016/j.fbr.2012.01.001

Singh, D., Lee, S. H., & Lee, C. H. (2022). Non-obligate pairwise metabolite cross-feeding suggests ammensalic interactions between *Bacillus amyloliquefaciens* and *Aspergillus oryzae*. *Communications Biology*, *5*(1), 232. https://doi.org/10.1038/s42003-022-03181-7

Smith, S. E., Smith, F. A., & Jakobsen, I. (2003). Mycorrhizal Fungi Can Dominate Phosphate Supply to Plants Irrespective of Growth Responses. *Plant Physiology*, *133*(1), 16–20. https://doi.org/10.1104/pp.103.024380

Sourjik, V., & Wingreen, N. S. (2012). Responding to chemical gradients: bacterial chemotaxis. *Current Opinion in Cell Biology*, *24*(2), 262–268. https://doi.org/10.1016/j.ceb.2011.11.008

Spooren, J., van Bentum, S., Thomashow, L. S., Pieterse, C. M. J., Weller, D. M., & Berendsen, R. L. (2024). Plant-Driven Assembly of Disease-Suppressive Soil Microbiomes. *Annual Review of Phytopathology*, *62*(1), 1–30. https://doi.org/10.1146/annurev-phyto-021622-100127

St-Arnaud, M., Hamel, C., Vimard, B., Caron, M., & Fortin, J. A. (1996). Enhanced hyphal growth and spore production of the arbuscular mycorrhizal fungus *Glomus intraradices* in an in vitro system in the absence of host roots. *Mycological Research*, *100*(3), 328–332. https://doi.org/10.1016/S0953-7562(96)80164-X

Steinke, K., Mohite, O. S., Weber, T., & Kovács, Á. T. (2021). Phylogenetic Distribution of Secondary Metabolites in the *Bacillus subtilis* Species Complex. *MSystems*, *6*(2). https://doi.org/10.1128/msystems.00057-21

Stewart, N., Thomas, R., Schauer, M., Favretto, N., Quillérou, E., Etter, H., Anderson, S., Sutton, P., Kubiszewski, I., Costanza, R., Kubiszewski, I., Costanza, R., Anderson, S., Mikulcak, F., & Sutton, P. (2015). *The Economics of Land Degradation. The value of land: Prosperous lands and positive rewards through sustainable land management* (N. Stewart (ed.)). ELD Initiative. www.eld-initiative.org.

Stoll, A., Salvatierra-Martínez, R., González, M., & Araya, M. (2021). The Role of Surfactin Production by *Bacillus velezensis* on Colonization, Biofilm Formation on Tomato Root and Leaf Surfaces and Subsequent Protection (ISR) against *Botrytis cinerea*. *Microorganisms*, *9*(11), 2251. https://doi.org/10.3390/microorganisms9112251

Stracke, S., Kistner, C., Yoshida, S., Mulder, L., Sato, S., Kaneko, T., Tabata, S., Sandal, N., Stougaard, J., Szczyglowski, K., & Parniske, M. (2002). A plant receptor-like kinase required for both bacterial and fungal symbiosis. *Nature 2002 417:6892*, *417*(6892), 959–962. https://doi.org/10.1038/nature00841

Strullu-Derrien, C., Selosse, M., Kenrick, P., & Martin, F. M. (2018). The origin and evolution of mycorrhizal symbioses: from palaeomycology to phylogenomics. *New Phytologist*, *220*(4), 1012–1030. https://doi.org/10.1111/nph.15076

Su, C. (2023). Pectin modifications at the symbiotic interface. *New Phytologist*, *238*(1), 25–32. https://doi.org/10.1111/nph.18705

Suchodolski, J., & Krasowska, A. (2019). Plasma Membrane Potential of *Candida albicans* Measured by Di-4-ANEPPS Fluorescence Depends on Growth Phase and Regulatory Factors. *Microorganisms*, *7*(4), 110. https://doi.org/10.3390/microorganisms7040110

Sugiura, Y., Akiyama, R., Tanaka, S., Yano, K., Kameoka, H., Marui, S., Saito, M., Kawaguchi, M., Akiyama, K., & Saito, K. (2020). Myristate can be used as a carbon and energy source for the asymbiotic growth of arbuscular mycorrhizal fungi. *Proceedings of the National Academy of Sciences*, *117*(41), 25779–25788. https://doi.org/10.1073/pnas.2006948117

Sun, J., Miller, J. B., Granqvist, E., Wiley-Kalil, A., Gobbato, E., Maillet, F., Cottaz, S., Samain, E., Venkateshwaran, M., Fort, S., Morris, R. J., Ané, J.-M., Dénarié, J., & Oldroyd, G. E. D. (2015). Activation of Symbiosis Signaling by Arbuscular Mycorrhizal Fungi in Legumes and Rice. *The Plant Cell*, *27*(3), 823–838. https://doi.org/10.1105/tpc.114.131326

Sun, W., & Shahrajabian, M. H. (2023). The Application of Arbuscular Mycorrhizal

Fungi as Microbial Biostimulant, Sustainable Approaches in Modern Agriculture. *Plants*, *12*(17), 3101. https://doi.org/10.3390/plants12173101

Sur, S., Romo, T. D., & Grossfield, A. (2018). Selectivity and Mechanism of Fengycin, an Antimicrobial Lipopeptide, from Molecular Dynamics. *The Journal of Physical Chemistry B*, *122*(8), 2219–2226. https://doi.org/10.1021/acs.jpcb.7b11889

Tan, I. S., & Ramamurthi, K. S. (2014). Spore formation in *Bacillus subtilis*. *Environmental Microbiology Reports*, *6*(3), 212–225. https://doi.org/10.1111/1758-2229.12130

Tan, X., Wang, D., Zhang, X., Zheng, S., Jia, X., Liu, H., Liu, Z., Yang, H., Dai, H., Chen, X., Qian, Z., Wang, R., Ma, M., Zhang, P., Yu, N., & Wang, E. (2025). A pair of LysM receptors mediates symbiosis and immunity discrimination in *Marchantia*. *Cell*, *188*(5), 1330-1348.e27. https://doi.org/10.1016/j.cell.2024.12.024

Tanaka, K., Amaki, Y., Ishihara, A., & Nakajima, H. (2015a). Synergistic Effects of [Ile 7]Surfactin Homologues with Bacillomycin D in Suppression of Gray Mold Disease by *Bacillus amyloliquefaciens* Biocontrol Strain SD-32. *Journal of Agricultural and Food Chemistry*, *63*(22), 5344–5353. https://doi.org/10.1021/acs.jafc.5b01198

Tanaka, K., Cho, S.-H., Lee, H., Pham, A. Q., Batek, J. M., Cui, S., Qiu, J., Khan, S. M., Joshi, T., Zhang, Z. J., Xu, D., & Stacey, G. (2015b). Effect of lipo-chitooligosaccharide on early growth of C 4 grass seedlings. *Journal of Experimental Botany*, *66*(19), 5727–5738. https://doi.org/10.1093/jxb/erv260

Tanaka, S., Hashimoto, K., Kobayashi, Y., Yano, K., Maeda, T., Kameoka, H., Ezawa, T., Saito, K., Akiyama, K., & Kawaguchi, M. (2022). Asymbiotic mass production of the arbuscular mycorrhizal fungus *Rhizophagus clarus*. *Communications Biology*, *5*(1), 43. https://doi.org/10.1038/s42003-021-02967-5

Tang, F. H. M., Lenzen, M., McBratney, A., & Maggi, F. (2021). Risk of pesticide pollution at the global scale. *Nature Geoscience*, *14*(4), 206–210. https://doi.org/10.1038/s41561-021-00712-5

Tang, N., San Clemente, H., Roy, S., Bécard, G., Zhao, B., & Roux, C. (2016). A Survey of the Gene Repertoire of *Gigaspora rosea* Unravels Conserved Features among Glomeromycota for Obligate Biotrophy. *Frontiers in Microbiology*, *7*(MAR), 172534. https://doi.org/10.3389/fmicb.2016.00233

Tedersoo, L., Magurno, F., Alkahtani, S., & Mikryukov, V. (2024). Phylogenetic classification of arbuscular mycorrhizal fungi: new species and higher-ranking taxa in Glomeromycota and Mucoromycota (class Endogonomycetes). *MycoKeys*, *107*, 273–325. https://doi.org/10.3897/mycokeys.107.125549

Teulet, A., Quan, C., Evangelisti, E., Wanke, A., Yang, W., & Schornack, S. (2023). A pathogen effector FOLD diversified in symbiotic fungi. *New Phytologist*, *239*(3), 1127–1139. https://doi.org/10.1111/nph.18996

Teyssier, E., Grat, S., Landry, D., Ouradou, M., Rich, M. K., Fort, S., Keller, J.,

Lefebvre, B., Delaux, P.-M., & Mbengue, M. (2025). A plant Lysin Motif Receptor-Like Kinase plays an ancestral function in mycorrhiza. *Proceedings of the National Academy of Sciences*, *122*(24), e2426063122. https://doi.org/10.1073/pnas.2426063122

Théatre, A., Hoste, A. C. R., Rigolet, A., Benneceur, I., Bechet, M., Ongena, M., Deleu, M., & Jacques, P. (2021). *Bacillus* sp.: A Remarkable Source of Bioactive Lipopeptides. In R. Hausmann & M. Henkel (Eds.), *Biosurfactants for the Biobased Economy. Advances in Biochemical Engineering/Biotechnology* (Vol. 181, pp. 123–179). Springer. https://doi.org/10.1007/10_2021_182

Thérien, M., Kiesewalter, H. T., Auria, E., Charron-Lamoureux, V., Wibowo, M., Maróti, G., Kovács, Á. T., & Beauregard, P. B. (2020). Surfactin production is not essential for pellicle and root-associated biofilm development of *Bacillus subtilis*. *Biofilm*, *2*, 100021. https://doi.org/10.1016/j.bioflm.2020.100021

Thieron, H., Singh, M., & Panstruga, R. (2021). One microRNA-like small RNA – two silencing pathways? *New Phytologist*, *232*(2), 464–467. https://doi.org/10.1111/nph.17652

Tian, T., Sun, B., Shi, H., Gao, T., He, Y., Li, Y., Liu, Y., Li, X., Zhang, L., Li, S., Wang, Q., & Chai, Y. (2021). Sucrose triggers a novel signaling cascade promoting *Bacillus subtilis* rhizosphere colonization. *The ISME Journal*, *15*(9), 2723–2737. https://doi.org/10.1038/S41396-021-00966-2

Tilman, D., Fargione, J., Wolff, B., D'Antonio, C., Dobson, A., Howarth, R., Schindler, D., Schlesinger, W. H., Simberloff, D., & Swackhamer, D. (2001). Forecasting Agriculturally Driven Global Environmental Change. *Science*, *292*(5515), 281–284. https://doi.org/10.1126/science.1057544

Tinevez, J. Y., Perry, N., Schindelin, J., Hoopes, G. M., Reynolds, G. D., Laplantine, E., Bednarek, S. Y., Shorte, S. L., & Eliceiri, K. W. (2017). TrackMate: An open and extensible platform for single-particle tracking. *Methods*, *115*, 80–90. https://doi.org/10.1016/J.YMETH.2016.09.016

Tojo, S., Tanaka, Y., & Ochi, K. (2015). Activation of Antibiotic Production in *Bacillus* spp. by Cumulative Drug Resistance Mutations. *Antimicrobial Agents and Chemotherapy*, *59*(12), 7799–7804. https://doi.org/10.1128/AAC.01932-15

Toljander, J. F., Lindahl, B. D., Paul, L. R., Elfstrand, M., & Finlay, R. D. (2007). Influence of arbuscular mycorrhizal mycelial exudates on soil bacterial growth and community structure. *FEMS Microbiology Ecology*, *61*(2), 295–304. https://doi.org/10.1111/j.1574-6941.2007.00337.x

Tominaga, T., Ueno, K., Saito, H., Egusa, M., Yamaguchi, K., Shigenobu, S., & Kaminaka, H. (2023). Monoterpene glucosides in *Eustoma grandiflorum* roots promote hyphal branching in arbuscular mycorrhizal fungi. *Plant Physiology*, *193*(4), 2677–2690. https://doi.org/10.1093/plphys/kiad482

Toure, Y., Ongena, M., Jacques, P., Guiro, A., & Thonart, P. (2004). Role of lipopeptides produced by *Bacillus subtilis* GA1 in the reduction of grey mould disease caused by *Botrytis cinerea* on apple. *Journal of Applied Microbiology*, *96*(5), 1151–1160. https://doi.org/10.1111/j.1365-2672.2004.02252.x

Traxler, M. F., & Kolter, R. (2015). Natural products in soil microbe interactions and evolution. *Natural Product Reports*, *32*(7), 956–970. https://doi.org/10.1039/C5NP00013K

Trivedi, P., Leach, J. E., Tringe, S. G., Sa, T., & Singh, B. K. (2020). Plant–microbiome interactions: from community assembly to plant health. *Nature Reviews Microbiology*, *18*(11), 607–621. https://doi.org/10.1038/s41579-020-0412-1

Tsuzuki, S., Handa, Y., Takeda, N., & Kawaguchi, M. (2016). Strigolactone-Induced Putative Secreted Protein 1 Is Required for the Establishment of Symbiosis by the Arbuscular Mycorrhizal Fungus *Rhizophagus irregularis*. *Molecular Plant-Microbe Interactions®*, *29*(4), 277–286. https://doi.org/10.1094/MPMI-10-15-0234-R

Tzipilevich, E., Russ, D., Dangl, J. L., & Benfey, P. N. (2021). Plant immune system activation is necessary for efficient root colonization by auxin-secreting beneficial bacteria. *Cell Host & Microbe*, *29*(10), 1507-1520.e4. https://doi.org/10.1016/j.chom.2021.09.005

Usmani, S. A., Kumar, M., Arya, K., Ali, B., Bhardwaj, N., Gaur, N. A., Prasad, R., & Singh, A. (2023). Beyond membrane components: uncovering the intriguing world of fungal sphingolipid synthesis and regulation. *Research in Microbiology*, *174*(7), 104087. https://doi.org/10.1016/j.resmic.2023.104087

Vaghela, B., Vashi, R., Rajput, K., & Joshi, R. (2022). Plant chitinases and their role in plant defense: A comprehensive review. *Enzyme and Microbial Technology*, *159*, 110055. https://doi.org/10.1016/j.enzmictec.2022.110055

van Boerdonk, S., Saake, P., Wanke, A., Neumann, U., & Zuccaro, A. (2024). β-Glucan-binding proteins are key modulators of immunity and symbiosis in mutualistic plant–microbe interactions. *Current Opinion in Plant Biology*, *81*, 102610. https://doi.org/10.1016/j.pbi.2024.102610

van der Heijden, M. G. A., Martin, F. M., Selosse, M., & Sanders, I. R. (2015). Mycorrhizal ecology and evolution: the past, the present, and the future. *New Phytologist*, *205*(4), 1406–1423. https://doi.org/10.1111/nph.13288

van Hulten, M., Pelser, M., van Loon, L. C., Pieterse, C. M. J., & Ton, J. (2006). Costs and benefits of priming for defense in *Arabidopsis*. *Proceedings of the National Academy of Sciences*, *103*(14), 5602–5607. https://doi.org/10.1073/pnas.0510213103

Van Overbeek, L., & Van Elsas, J. D. (2008). Effects of plant genotype and growth stage on the structure of bacterial communities associated with potato (*Solanum tuberosum* L.). *FEMS Microbiology Ecology*, *64*(2), 283–296. https://doi.org/10.1111/j.1574-6941.2008.00469.x

van Rijssel, S. Q., Koorneef, G. J., Veen, G. F. (Ciska), Pulleman, M. M., de Goede, R. G. M., Comans, R. N. J., van der Putten, W. H., & Mason-Jones, K. (2025). Conventional and organic farms with more intensive management have lower soil functionality. *Science*, *388*(6745), 410–415. https://doi.org/10.1126/science.adr0211

Vasistha, P., Singh, P. P., Srivastava, D., Johny, L., & Shukla, S. (2025). Effector proteins of *Funneliformis mosseae* BR221: unravelling plant-fungal interactions through reference-based transcriptome analysis, in vitro validation, and protein–protein docking studies. *BMC Genomics*, *26*(1), 42. https://doi.org/10.1186/s12864-024-10918-7

Vela-Corcia, D., Colino-Palomino, A. M., de Vicente, A., Pérez García, A., & Romero, D. (2025). Characterization of BvlzGluc, a Novel Antifungal β-Glucanase from *Bacillus velezensis* , with Potential Agricultural and Industrial Applications. *BioRxiv*, 2025.01.23.634490. https://doi.org/10.1101/2025.01.23.634490

Venice, F., Ghignone, S., Salvioli di Fossalunga, A., Amselem, J., Novero, M., Xianan, X., Sędzielewska Toro, K., Morin, E., Lipzen, A., Grigoriev, I. V., Henrissat, B., Martin, F. M., & Bonfante, P. (2020). At the nexus of three kingdoms: the genome of the mycorrhizal fungus *Gigaspora margarita* provides insights into plant, endobacterial and fungal interactions. *Environmental Microbiology*, *22*(1), 122–141. https://doi.org/10.1111/1462-2920.14827

Vernié, T., Rich, M., Pellen, T., Teyssier, E., Garrigues, V., Chauderon, L., Medioni, L., van Beveren, F., Libourel, C., Keller, J., Girou, C., Lefort, C., Le Ru, A., Martinez, Y., Reinhardt, D., Kodama, K., Shimazaki, S., Morel, P., Kyozuka, J., … Delaux, P. M. (2025). Conservation of symbiotic signaling since the most recent common ancestor of land plants. *Proceedings of the National Academy of Sciences of the United States of America*, *122*(1), e2408539121. https://doi.org/10.1073/PNAS.2408539121/SUPPL_FILE/PNAS.2408539121.SD02.XLSX

Vieira, C. K., Marascalchi, M. N., Rozmoš, M., Benada, O., Belova, V., & Jansa, J. (2025). Arbuscular mycorrhizal fungal highways – What, how and why? *Soil Biology and Biochemistry*, *202*, 109702. https://doi.org/10.1016/j.soilbio.2024.109702

Vila, T., Nazir, R., Rozental, S., dos Santos, G. M. P., Calixto, R. O. R., Barreto-Bergter, E., Wick, L. Y., & van Elsas, J. D. (2016). The Role of Hydrophobicity and Surface Receptors at Hyphae of *Lyophyllum* sp. Strain Karsten in the Interaction with *Burkholderia terrae* BS001 – Implications for Interactions in Soil. *Frontiers in Microbiology*, *7*(OCT), 189737. https://doi.org/10.3389/fmicb.2016.01689

Vlamakis, H., Chai, Y., Beauregard, P., Losick, R., & Kolter, R. (2013). Sticking together: building a biofilm the *Bacillus subtilis* way. *Nature Reviews Microbiology*, *11*(3), 157–168. https://doi.org/10.1038/nrmicro2960

Voxeur, A., Habrylo, O., Guénin, S., Miart, F., Soulié, M.-C., Rihouey, C., Pau-Roblot, C., Domon, J.-M., Gutierrez, L., Pelloux, J., Mouille, G., Fagard, M., Höfte, H., & Vernhettes, S. (2019). Oligogalacturonide production upon *Arabidopsis thaliana – Botrytis cinerea* interaction. *Proceedings of the National Academy of Sciences*, *116*(39), 19743–19752.

https://doi.org/10.1073/pnas.1900317116

Wahlen, L. (Kaatz), Mantei, J. R., DiOrio, J. P., Jones, C. M., & Pasmore, M. E. (2018). Production and analysis of a *Bacillus subtilis* biofilm comprised of vegetative cells and spores using a modified colony biofilm model. *Journal of Microbiological Methods*, *148*, 181–187. https://doi.org/10.1016/j.mimet.2018.04.011

Wang, D.-J., Ding, M.-Z., Hou, Z.-J., Zhang, Y., Shang, W., Duan, T.-X., Xu, Q.-M., & Cheng, J.-S. (2025a). Carbon Metabolism Modification in *Bacillus subtilis* for Improving Fengycin Production and Investigating Antifungal Activity of Its Homologous Components. *ACS Synthetic Biology*, *14*(7), 2644–2656. https://doi.org/10.1021/acssynbio.5c00101

Wang, F., Shi, N., Jiang, R., Zhang, F., & Feng, G. (2016). *In situ* stable isotope probing of phosphate-solubilizing bacteria in the hyphosphere. *Journal of Experimental Botany*, *67*(6), 1689–1701. https://doi.org/10.1093/jxb/erv561

Wang, L., Zhang, L., George, T. S., & Feng, G. (2023a). A core microbiome in the hyphosphere of arbuscular mycorrhizal fungi has functional significance in organic phosphorus mineralization. *New Phytologist*, *238*(2), 859–873. https://doi.org/10.1111/nph.18642

Wang, L., Zhang, L., George, T. S., & Feng, G. (2025b). Hyphosphere core taxa link plant-arbuscular mycorrhizal fungi combinations to soil organic phosphorus mineralization. *Soil Biology and Biochemistry*, *201*, 109647. https://doi.org/10.1016/j.soilbio.2024.109647

Wang, R., Liu, C., Bie, X., Dai, Y., Feng, X., Wang, R., Wang, M., Xu, S., & Chen, Y. (2024a). Pecan-medicinal crops intercropping improved soil fertility and promoted interactions between soil microorganisms and metabolites. *Chemical and Biological Technologies in Agriculture*, *11*(1), 162. https://doi.org/10.1186/s40538-024-00693-8

Wang, S., Xu, M., Han, Y., & Zhou, Z. (2024b). Exploring Mechanisms of Antifungal Lipopeptide Iturin A from *Bacillus* against *Aspergillus niger*. *Journal of Fungi*, *10*(3), 172. https://doi.org/10.3390/jof10030172

Wang, Y., Zhang, C., Liang, J., Wang, L., Gao, W., Jiang, J., & Chang, R. (2020a). Surfactin and fengycin B extracted from *Bacillus pumilus* W-7 provide protection against potato late blight via distinct and synergistic mechanisms. *Applied Microbiology and Biotechnology*, *104*(17), 7467–7481. https://doi.org/10.1007/s00253-020-10773-y

Wang, Y., Zhang, C., Liang, J., Wu, L., Gao, W., & Jiang, J. (2020b). Iturin A Extracted From *Bacillus subtilis* WL-2 Affects *Phytophthora infestans* via Cell Structure Disruption, Oxidative Stress, and Energy Supply Dysfunction. *Frontiers in Microbiology*, *11*, 536083. https://doi.org/10.3389/fmicb.2020.536083

Wang, Z., Zeng, J., Deng, J., Hou, X., Zhang, J., Yan, W., & Cai, Q. (2023b). Pathogen-Derived Extracellular Vesicles: Emerging Mediators of Plant-Microbe Interactions. *Molecular Plant-Microbe Interactions®*, *36*(4), 218–227.

https://doi.org/10.1094/MPMI-08-22-0162-FI

Wawra, S., Fesel, P., Widmer, H., Timm, M., Seibel, J., Leson, L., Kesseler, L., Nostadt, R., Hilbert, M., Langen, G., & Zuccaro, A. (2016). The fungal-specific β-glucan-binding lectin FGB1 alters cell-wall composition and suppresses glucan-triggered immunity in plants. *Nature Communications*, *7*(1), 13188. https://doi.org/10.1038/ncomms13188

Weersma, R. K., Zhernakova, A., & Fu, J. (2020). Interaction between drugs and the gut microbiome. *Gut*, *69*(8), 1510–1519. https://doi.org/10.1136/gutjnl-2019-320204

Weete, J. D., Abril, M., & Blackwell, M. (2010). Phylogenetic Distribution of Fungal Sterols. *PLoS ONE*, *5*(5), e10899. https://doi.org/10.1371/journal.pone.0010899

Wewer, V., Brands, M., & Dörmann, P. (2014). Fatty acid synthesis and lipid metabolism in the obligate biotrophic fungus *Rhizophagus irregularis* during mycorrhization of *Lotus japonicus* . *The Plant Journal*, *79*(3), 398–412. https://doi.org/10.1111/tpj.12566

Whiteside, M. D., Werner, G. D. A., Caldas, V. E. A., van't Padje, A., Dupin, S. E., Elbers, B., Bakker, M., Wyatt, G. A. K., Klein, M., Hink, M. A., Postma, M., Vaitla, B., Noë, R., Shimizu, T. S., West, S. A., & Kiers, E. T. (2019). Mycorrhizal Fungi Respond to Resource Inequality by Moving Phosphorus from Rich to Poor Patches across Networks. *Current Biology*, *29*(12), 2043-2050.e8. https://doi.org/10.1016/j.cub.2019.04.061

Wilkes, T. I., Warner, D. J., Edmonds-Brown, V., & Davies, K. G. (2020). Species-Specific Interactions of Bacillus Innocula and Arbuscular Mycorrhizal Fungi Symbiosis with Winter Wheat. *Microorganisms*, *8*(11), 1795. https://doi.org/10.3390/microorganisms8111795

Wilkinson, S. W., Magerøy, M. H., López Sánchez, A., Smith, L. M., Furci, L., Cotton, T. E. A., Krokene, P., & Ton, J. (2019). Surviving in a Hostile World: Plant Strategies to Resist Pests and Diseases. *Annual Review of Phytopathology*, *57*(1), 505–529. https://doi.org/10.1146/annurev-phyto-082718-095959

Wipf, D., Krajinski, F., van Tuinen, D., Recorbet, G., & Courty, P. (2019). Trading on the arbuscular mycorrhiza market: from arbuscules to common mycorrhizal networks. *New Phytologist*, *223*(3), 1127–1142. https://doi.org/10.1111/nph.15775

Wise, C., Falardeau, J., Hagberg, I., & Avis, T. J. (2014). Cellular Lipid Composition Affects Sensitivity of Plant Pathogens to Fengycin, an Antifungal Compound Produced by *Bacillus subtilis* Strain CU12. *Phytopathology®*, *104*(10), 1036–1041. https://doi.org/10.1094/PHYTO-12-13-0336-R

Wu, L., Wu, H., Chen, L., Yu, X., Borriss, R., & Gao, X. (2015). Difficidin and bacilysin from *Bacillus amyloliquefaciens* FZB42 have antibacterial activity against *Xanthomonas oryzae* rice pathogens. *Scientific Reports*, *5*(1), 12975. https://doi.org/10.1038/srep12975

Xiao, X., Chen, H., Chen, H., Wang, J., Ren, C., & Wu, L. (2008). Impact of *Bacillus subtilis* JA, a biocontrol strain of fungal plant pathogens, on arbuscular

mycorrhiza formation in *Zea mays* . *World Journal of Microbiology and Biotechnology*, *24*(7), 1133–1137. https://doi.org/10.1007/s11274-007-9584-3

Xie, J., Sun, X., Xia, Y., Tao, L., Tan, T., Zhang, N., Xun, W., Zhang, R., Kovács, Á. T., Xu, Z., & Shen, Q. (2024). Bridging the Gap: Biofilm-mediated establishment of *Bacillus velezensis* on *Trichoderma guizhouense* mycelia. *Biofilm*, *8*, 100239. https://doi.org/10.1016/j.bioflm.2024.100239

Xie, L., Lehvävirta, S., Timonen, S., Kasurinen, J., Niemikapee, J., & Valkonen, J. P. T. (2018). Species-specific synergistic effects of two plant growth—promoting microbes on green roof plant biomass and photosynthetic efficiency. *PLOS ONE*, *13*(12), e0209432. https://doi.org/10.1371/journal.pone.0209432

Xie, X., & Fan, X. (2025). Fungal small RNA hijacking: a new layer of cross-kingdom communications in arbuscular mycorrhizal symbiosis. *New Phytologist*, *246*(3), 814–817. https://doi.org/10.1111/nph.70085

Xie, X., Mori, N., Yoneyama, K., Nomura, T., Uchida, K., Yoneyama, K., & Akiyama, K. (2019). Lotuslactone, a non-canonical strigolactone from *Lotus japonicus* . *Phytochemistry*, *157*, 200–205. https://doi.org/10.1016/j.phytochem.2018.10.034

Xiong, J., Ashraf, U., Ye, J., & Cao, S. (2024). Extracellular Vesicles in Pathogenic Infection, Transmission, and Immunity. *Engineering*, *43*, 228–240. https://doi.org/10.1016/j.eng.2024.06.011

Xu, M., Li, G., Guo, Y., Gao, Y., Zhu, L., Liu, Z., Tian, R., Gao, C., Han, P., Wang, N., Guo, F., Bao, J., Jia, C., Feng, H., & Huang, L. (2022). A fungal microRNA-like RNA subverts host immunity and facilitates pathogen infection by silencing two host receptor-like kinase genes. *New Phytologist*, *233*(6), 2503–2519. https://doi.org/10.1111/nph.17945

Xu, M., Shi, Y., Fan, D.-L., Kang, Y.-J., Yan, X.-L., & Wang, H.-W. (2023a). Co-Culture of White Rot Fungi *Pleurotus ostreatus* P5 and *Bacillus amyloliquefaciens* B2: A Strategy to Enhance Lipopeptide Production and Suppress of *Fusarium* Wilt of Cucumber. *Journal of Fungi*, *9*(11), 1049. https://doi.org/10.3390/jof9111049

Xu, Y., Chen, Z., Li, X., Tan, J., Liu, F., & Wu, J. (2023b). The mechanism of promoting rhizosphere nutrient turnover for arbuscular mycorrhizal fungi attributes to recruited functional bacterial assembly. *Molecular Ecology*, *32*(9), 2335–2350. https://doi.org/10.1111/mec.16880

Xu, Y., Li, J., Qiao, C., Yang, J., Li, J., Zheng, X., Wang, C., Cao, P., Li, Y., & Chen, Q. (2024). Rhizosphere bacterial community is mainly determined by soil environmental factors, but the active bacterial diversity is mainly shaped by plant selection. *BMC Microbiology*, *24*(1), 450. https://doi.org/10.1186/s12866-024-03611-y

Xu, Z., Premarathna, M., Liu, J., & Seneviratne, G. (2025). Current knowledge on the dual species interaction and biofilm between *Aspergillus* and *Bacillus*: exploiting molecular understanding toward applications. *Critical Reviews in Microbiology*, 1–13. https://doi.org/10.1080/1040841X.2025.2482658

Xun, W., Liu, Y., Li, W., Ren, Y., Xiong, W., Xu, Z., Zhang, N., Miao, Y., Shen, Q., & Zhang, R. (2021). Specialized metabolic functions of keystone taxa sustain soil microbiome stability. *Microbiome*, *9*(1), 35. https://doi.org/10.1186/s40168-020-00985-9

Yadav, R., Ror, P., Rathore, P., & Ramakrishna, W. (2020). Bacteria from native soil in combination with arbuscular mycorrhizal fungi augment wheat yield and biofortification. *Plant Physiology and Biochemistry*, *150*, 222–233. https://doi.org/10.1016/j.plaphy.2020.02.039

Yamamoto, S., Shiraishi, S., & Suzuki, S. (2015). Are cyclic lipopeptides produced by *Bacillus amyloliquefaciens* S13-3 responsible for the plant defence response in strawberry against *Colletotrichum gloeosporioides* ? *Letters in Applied Microbiology*, *60*(4), 379–386. https://doi.org/10.1111/lam.12382

Yang, S., Ji, Y., Xue, P., Li, Z., Chen, X., Shi, J., & Jiang, C. (2024a). Insights into the antifungal mechanism of *Bacillus subtilis* cyclic lipopeptide iturin A mediated by potassium ion channel. *International Journal of Biological Macromolecules*, *277*, 134306. https://doi.org/10.1016/j.ijbiomac.2024.134306

Yang, Y., Xie, P., Nan, Y., Yuan, J., Gong, D., Li, Y., Bi, Y., & Prusky, D. B. (2024b). The low-affinity calcium channel protein AaFig1 is essential for the growth and development, infection structure differentiation, and pathogenicity of *Alternaria alternata*. *Postharvest Biology and Technology*, *210*, 112756. https://doi.org/10.1016/j.postharvbio.2024.112756

Ye, M., Tang, X., Yang, R., Zhang, H., Li, F., Tao, F., Li, F., & Wang, Z. (2018). Characteristics and Application of a Novel Species of *Bacillus* : *Bacillus velezensis*. *ACS Chemical Biology*, *13*(3), 500–505. https://doi.org/10.1021/acschembio.7b00874

Yoneyama, K., & Brewer, P. B. (2021). Strigolactones, how are they synthesized to regulate plant growth and development? *Current Opinion in Plant Biology*, *63*, 102072. https://doi.org/10.1016/j.pbi.2021.102072

Yssel, A., Reva, O., & Tastan Bishop, O. (2011). Comparative structural bioinformatics analysis of *Bacillus amyloliquefaciens* chemotaxis proteins within *Bacillus subtilis* group. *Applied Microbiology and Biotechnology*, *92*(5), 997–1008. https://doi.org/10.1007/s00253-011-3582-y

Yu, K., Pieterse, C. M. J., Bakker, P. A. H. M., & Berendsen, R. L. (2019). Beneficial microbes going underground of root immunity. *Plant, Cell & Environment*, *42*(10), 2860–2870. https://doi.org/10.1111/pce.13632

Yu, X., Feng, B., He, P., & Shan, L. (2017). From Chaos to Harmony: Responses and Signaling upon Microbial Pattern Recognition. *Annual Review of Phytopathology*, *55*(1), 109–137. https://doi.org/10.1146/annurev-phyto-080516-035649

Yuan, M., Ngou, B. P. M., Ding, P., & Xin, X.-F. (2021). PTI-ETI crosstalk: an integrative view of plant immunity. *Current Opinion in Plant Biology*, *62*, 102030. https://doi.org/10.1016/j.pbi.2021.102030

Yun, H. S., Sul, W. J., Chung, H. S., Lee, J., & Kwon, C. (2023). Secretory membrane

traffic in plant–microbe interactions. *New Phytologist*, *237*(1), 53–59. https://doi.org/10.1111/nph.18470

Zakharova, A. A., Efimova, S. S., Malev, V. V., & Ostroumova, O. S. (2019). Fengycin induces ion channels in lipid bilayers mimicking target fungal cell membranes. *Scientific Reports*, *9*(1), 16034. https://doi.org/10.1038/s41598-019-52551-5

Zeng, T., Holmer, R., Hontelez, J., te Lintel-Hekkert, B., Marufu, L., de Zeeuw, T., Wu, F., Schijlen, E., Bisseling, T., & Limpens, E. (2018). Host- and stage-dependent secretome of the arbuscular mycorrhizal fungus *Rhizophagus irregularis*. *The Plant Journal*, *94*(3), 411–425. https://doi.org/10.1111/tpj.13908

Zeng, T., Rodriguez-Moreno, L., Mansurkhodzaev, A., Wang, P., van den Berg, W., Gasciolli, V., Cottaz, S., Fort, S., Thomma, B. P. H. J., Bono, J., Bisseling, T., & Limpens, E. (2020). A lysin motif effector subverts chitin-triggered immunity to facilitate arbuscular mycorrhizal symbiosis. *New Phytologist*, *225*(1), 448–460. https://doi.org/10.1111/nph.16245

Zhang, C., He, J., Dai, H., Wang, G., Zhang, X., Wang, C., Shi, J., Chen, X., Wang, D., & Wang, E. (2021). Discriminating symbiosis and immunity signals by receptor competition in rice. *Proceedings of the National Academy of Sciences*, *118*(16), e2023738118. https://doi.org/10.1073/pnas.2023738118

Zhang, C., van der Heijden, M. G. A., Dodds, B. K., Nguyen, T. B., Spooren, J., Valzano-Held, A., Cosme, M., & Berendsen, R. L. (2024a). A tripartite bacterial-fungal-plant symbiosis in the mycorrhiza-shaped microbiome drives plant growth and mycorrhization. *Microbiome*, *12*(1), 13. https://doi.org/10.1186/s40168-023-01726-4

Zhang, J., Pan, L., Xu, W., Yang, H., He, F., Ma, J., Bai, L., Zhang, Q., Zhou, Q., & Gao, H. (2024b). Extracellular vesicles in plant-microbe interactions: Recent advances and future directions. *Plant Science*, *341*, 111999. https://doi.org/10.1016/j.plantsci.2024.111999

Zhang, J., Sun, J., Chiu, C. H., Landry, D., Li, K., Wen, J., Mysore, K. S., Fort, S., Lefebvre, B., Oldroyd, G. E. D., & Feng, F. (2024c). A receptor required for chitin perception facilitates arbuscular mycorrhizal associations and distinguishes root symbiosis from immunity. *Current Biology*, *34*(8), 1705-1717.e6. https://doi.org/10.1016/j.cub.2024.03.015

Zhang, L., Feng, G., & Declerck, S. (2018a). Signal beyond nutrient, fructose, exuded by an arbuscular mycorrhizal fungus triggers phytate mineralization by a phosphate solubilizing bacterium. *The ISME Journal*, *12*(10), 2339–2351. https://doi.org/10.1038/s41396-018-0171-4

Zhang, L., Xu, M., Liu, Y., Zhang, F., Hodge, A., & Feng, G. (2016). Carbon and phosphorus exchange may enable cooperation between an arbuscular mycorrhizal fungus and a phosphate-solubilizing bacterium. *New Phytologist*, *210*(3), 1022–1032. https://doi.org/10.1111/nph.13838

Zhang, L., Zhou, J., George, T. S., Limpens, E., & Feng, G. (2022). Arbuscular

mycorrhizal fungi conducting the hyphosphere bacterial orchestra. *Trends in Plant Science*, *27*(4), 402–411. https://doi.org/10.1016/j.tplants.2021.10.008

Zhang, M., & Kong, X. (2022). How plants discern friends from foes. *Trends in Plant Science*, *27*(2), 107–109. https://doi.org/10.1016/j.tplants.2021.11.001

Zhang, N., Fan, Y., Li, C., Wang, Q., Leksawasdi, N., Li, F., & Wang, S. (2018b). Cell permeability and nuclear DNA staining by propidium iodide in basidiomycetous yeasts. *Applied Microbiology and Biotechnology*, *102*(9), 4183–4191. https://doi.org/10.1007/s00253-018-8906-8

Zhang, N., Yang, D., Wang, D., Miao, Y., Shao, J., Zhou, X., Xu, Z., Li, Q., Feng, H., Li, S., Shen, Q., & Zhang, R. (2015). Whole transcriptomic analysis of the plant-beneficial rhizobacterium *Bacillus amyloliquefaciens* SQR9 during enhanced biofilm formation regulated by maize root exudates. *BMC Genomics*, *16*(1), 685. https://doi.org/10.1186/s12864-015-1825-5

Zhang, P., Liang, J., Yi, X., Setlow, P., & Li, Y. (2014). Monitoring of Commitment, Blocking, and Continuation of Nutrient Germination of Individual *Bacillus subtilis* Spores. *Journal of Bacteriology*, *196*(13), 2443–2454. https://doi.org/10.1128/JB.01687-14

Zhang, X., Jia, S., He, Y., Wen, J., Li, D., Yang, W., Yue, Y., Li, H., Cheng, K., & Zhang, X. (2024d). Wall-associated kinase GhWAK13 mediates arbuscular mycorrhizal symbiosis and *Verticillium* wilt resistance in cotton. *New Phytologist*, *242*(5), 2180–2194. https://doi.org/10.1111/nph.19468

Zhang, X., Tan, X., & Wang, E. (2025). Networks of the symbiosis-immunity continuum in plants. *Cell Host & Microbe*, *33*(8), 1256–1275. https://doi.org/10.1016/j.chom.2025.06.009

Zhao, X., Li, R., Lu, C., Baluška, F., & Wan, Y. (2015). Di-4-ANEPPDHQ, a fluorescent probe for the visualisation of membrane microdomains in living *Arabidopsis thaliana* cells. *Plant Physiology and Biochemistry*, *87*, 53–60. https://doi.org/10.1016/j.plaphy.2014.12.015

Zhou, F., Emonet, A., Dénervaud Tendon, V., Marhavy, P., Wu, D., Lahaye, T., & Geldner, N. (2020a). Co-incidence of Damage and Microbial Patterns Controls Localized Immune Responses in Roots. *Cell*, *180*(3), 440-453.e18. https://doi.org/10.1016/j.cell.2020.01.013

Zhou, H., Dong, K., Du, Q., Wei, Q., Wu, J., Deng, J., & Wang, F. (2024). Biofilm-forming of *Bacillus tequilensis* DZY 6715 enhanced suppression the *Camellia oleifera* anthracnose caused by *Colletotrichum fructicola* and its mechanism. *Scientia Horticulturae*, *338*, 113676. https://doi.org/10.1016/j.scienta.2024.113676

Zhou, J., Chai, X., Zhang, L., George, T. S., Wang, F., & Feng, G. (2020b). Different Arbuscular Mycorrhizal Fungi Cocolonizing on a Single Plant Root System Recruit Distinct Microbiomes. *MSystems*, *5*(6). https://doi.org/10.1128/mSystems.00929-20

Zhou, J., Loeppmann, S., Yang, H., Gube, M., Shi, L., Pausch, J., & Dippold, M. A. (2025). Linking microbial community dynamics to rhizosphere carbon flow

depend on arbuscular mycorrhizae and nitrogen fertilization. *Biology and Fertility of Soils*, *61*(4), 791–804. https://doi.org/10.1007/s00374-025-01897-2

Zhou, Y., Wang, H., Xu, S., Liu, K., Qi, H., Wang, M., Chen, X., Berg, G., Ma, Z., Cernava, T., & Chen, Y. (2022). Bacterial-fungal interactions under agricultural settings: from physical to chemical interactions. *Stress Biology*, *2*(1), 22. https://doi.org/10.1007/s44154-022-00046-1

Zhou, Y., Yang, Z., Liu, J., Li, X., Wang, X., Dai, C., Zhang, T., Carrión, V. J., Wei, Z., Cao, F., Delgado-Baquerizo, M., & Li, X. (2023). Crop rotation and native microbiome inoculation restore soil capacity to suppress a root disease. *Nature Communications*, *14*(1), 8126. https://doi.org/10.1038/s41467-023-43926-4

Zhu, C., Liu, J.-H., Zhao, J.-H., Liu, T., Chen, Y.-Y., Wang, C.-H., Zhang, Z.-H., Guo, H.-S., & Duan, C.-G. (2022). A fungal effector suppresses the nuclear export of AGO1–miRNA complex to promote infection in plants. *Proceedings of the National Academy of Sciences*, *119*(12), e2114583119. https://doi.org/10.1073/pnas.2114583119

Zhu, M., Wang, Q., Mu, H., Han, F., Wang, Y., & Dai, X. (2023a). A fitness trade-off between growth and survival governed by Spo0A-mediated proteome allocation constraints in *Bacillus subtilis*. *Science Advances*, *9*(39), eadg9733. https://doi.org/10.1126/sciadv.adg9733

Zhu, X.-M., Li, L., Bao, J.-D., Wang, J.-Y., Daskalov, A., Liu, X.-H., Del Poeta, M., & Lin, F.-C. (2023b). The biological functions of sphingolipids in plant pathogenic fungi. *PLOS Pathogens*, *19*(11), e1011733. https://doi.org/10.1371/journal.ppat.1011733

Zihalirwa Kulimushi, P., Argüelles Arias, A., Franzil, L., Steels, S., & Ongena, M. (2017). Stimulation of Fengycin-Type Antifungal Lipopeptides in *Bacillus amyloliquefaciens* in the Presence of the Maize Fungal Pathogen *Rhizomucor variabilis*. *Frontiers in Microbiology*, *8*(MAY), 252373. https://doi.org/10.3389/fmicb.2017.00850

Zipfel, C., & Oldroyd, G. E. D. (2017). Plant signalling in symbiosis and immunity. *Nature*, *543*(7645), 328–336. https://doi.org/10.1038/nature22009